PHYTOCHEMICAL INVESTIGATIONS OF
Goniothalamus tapis AND *G. tapisoides,* AND
KINETIC MECHANISM STUDIES OF GONIOTHALAMIN

ROSALIND KIM PEI THENG

FACULTY OF SCIENCE
UNIVERSITY OF MALAYA
KUALA LUMPUR

2020

PHYTOCHEMICAL INVESTIGATIONS OF *Goniothalamus tapis* AND *G. tapisoides*, AND KINETIC MECHANISM STUDIES OF GONIOTHALAMIN

ROSALIND KIM PEI THENG

THESIS SUBMITTED IN FULFILMENT OF THE REQUIREMENTS FOR THE DEGREE OF DOCTOR OF PHILOSOPHY

DEPARTMENT OF CHEMISTRY
FACULTY OF SCIENCE
UNIVERSITY OF MALAYA
KUALA LUMPUR

2020

UNIVERSITY OF MALAYA
ORIGINAL LITERARY WORK DECLARATION

Name of Candidate: **ROSALIND KIM PEI THENG**

Registration/Matric No: **SHC120115**

Name of Degree: **DOCTOR OF PHILOSOPHY**

Title of Project Paper/Research Report/Dissertation/Thesis ("this Work"):

PHYTOCHEMICAL INVESTIGATIONS OF *Goniothalamus tapis* AND *G. tapisoides*, AND KINETIC MECHANISM STUDIES OF GONIOTHALAMIN

Field of Study:

NATURAL PRODUCT & PHYSICAL ORGANIC CHEMISTRY

I do solemnly and sincerely declare that:

(1) I am the sole author/writer of this Work;
(2) This Work is original;
(3) Any use of any work in which copyright exists was done by way of fair dealing and for permitted purposes and any excerpt or extract from, or reference to or reproduction of any copyright work has been disclosed expressly and sufficiently and the title of the Work and its authorship have been acknowledged in this Work;
(4) I do not have any actual knowledge nor do I ought reasonably to know that the making of this work constitutes an infringement of any copyright work;
(5) I hereby assign all and every rights in the copyright to this Work to the University of Malaya ("UM"), who henceforth shall be owner of the copyright in this Work and that any reproduction or use in any form or by any means whatsoever is prohibited without the written consent of UM having been first had and obtained;
(6) I am fully aware that if in the course of making this Work I have infringed any copyright whether intentionally or otherwise, I may be subject to legal action or any other action as may be determined by UM.

Candidate's Signature   Date:

Subscribed and solemnly declared before,

Witness's Signature   Date:

Name:

Designation:

PHYTOCHEMICAL INVESTIGATIONS OF *Goniothalamus tapis* AND *G. tapisoides*, AND KINETIC MECHANISM STUDIES OF GONIOTHALAMIN

ABSTRACT

Phytochemical studies on two species of Annonaceae; *Goniothalamus tapis* and *Goniothalamus tapisoides* have been carried out. Isolation and purification of the crude extract of stem bark of *G. tapis* and *G. tapisoides* yielded seventeen compounds. *G. tapis* gave nine compounds; goniothalamin **1**, isoaltholactone **41**, 3-acetylisoaltholactone **151**, cheliensisin A **22**, garvensintriol **4**, goniopyyprone **26**, 7-*epi*-goniofufurone **49**, stigmasterol **133** and β-sitosterol **134**. Out of nine compounds, 3-acetyl-isoaltholactone **151** was identified as a new styryl-lactone. The skeleton is similar as the major compound, isoaltholactone **41**. But 3-acetylisoaltholactone **151** have different functional group compared to hydroxyl group in isoaltholactone **41**, which is acetyl group. As for *G. tapisoides*, eight compounds were acquired; goniodiol **3**, 7-*epi*-goniodiol **10**, 8-*epi*-9-deoxygoniopypyrone **24**, goniomicin A **147**, goniomicin E **152**, goniomicin F **153**, goniomicin G **154** and goniomicin H **155**. Compounds **152**, **153**, **154** and **155** were identified as new styryl-lactones. The structure of all compound was elucidated using various spectroscopic methods; 1D-NMR (1H, 13C, DEPT), 2D-NMR (COSY, HSQC, HMBC, NOESY), UV, IR and mass spectrometry. Goniothalamin **1** is a major compound isolated from dichloromethane extract of *G. tapisoides*. A spectrophotometric kinetic study of hydrolysis of **1** has been carried out in alkaline and acidic medium at various temperature to determine the reaction mechanism of the hydroxide ion-catalyzed reaction. Alkaline hydrolysis undergoes monotonic reaction and pseudo-first-order rate constant (k_{obs}). It showed linear relationship with the increase of concentration of NaOH, giving goniomicin A **147** as a product. Hydrolysis of **1** in alkaline medium involved the ring opening of the lactone moiety. As to acidic medium, hydroxonium ions will catalysed the

cleavage of lactone ring and the intermediate product further undergoes dehydration to form a product with three consecutive double bonds. The products of both alkaline and acidic hydrolysis were characterized by 1D-NMR, 2D-NMR and mass spectrometry.

Keywords: *Goniothalamus tapis*, *Goniothalamus tapisoides*, styryl-lactones, goniothalamin, kinetic study, hydrolysis

KAJIAN FITOKIMIA KE ATAS *Goniothalamus tapis* DAN *G. tapisoides*, DAN PENYELIDIKAN KINETIK MEKANISME BAGI GONIOTHALAMIN

ABSTRAK

Kajian fitokimia telah dijalankan ke atas dua spesis Annonaceae; *Goniothalamus tapis* dan *Goniothalamus tapisoides*. Lima belas sebatian tulen telah dipisahkan dan dengan menggunakan pelbagai kaedah kromatografi seperti kromatografi turus, kromatografi lapisan nipis, kromatografi lapisan nipis persediaan dan kromatografi cecair prestasi tinggi. Pemisahan dan penulenan ke atas ekstrak diklorometana dan methanol bagi kulit batang *G. tapis* dan *G. tapisoides* membawa kepada pemencilan tujuh belas sebatian. Sembilan sebatian diasingkan daripada ekstrak *G. tapis* bernama; goniothalamin **1**, isoaltholactone **41**, 3-acetylisoaltholactone **151**, cheliensisin A **22**, garvensintriol **4**, goniopyyprone **26**, 7-*epi*-goniofufurone **49**, stigmasterol **133** dan β-sitosterol **134**. 3-acetylisoaltholactone **151** adalah salah satu stiril-lakton baru daripada kesemua sembilan sebatian tersebut. Struktur rangka bagi sebatian **151** adalah mirip dengan sebatian utama, iaitu isoaltholactone **41**. Kedua-dua sebatian tersebut mempunyai kumpulan berfungsi yang berlainan. 3-acetylisoaltholactone **151** mempunyai kumpulan asetil manakala isoaltholactone **41** terdapat kumpulan hidrosil. Selain daripada itu, struktur rangka bagi kedua-dua sebatian adalah serupa. Sementara itu, lapan sebatian diasingkan daripada ekstrak *G. tapisoides*, iaitu goniodiol **3**, 7-*epi*-goniodiol **10**, 8-*epi*-9-deoxygoniopypyrone **24**, goniomicin A **147**, goniomicin E **152**, goniomicin F **153**, goniomicin G **154** dan goniomicin H **155**. Lima sebatian; **152**, **153**, **154** dan **155** dikenal pasti sebagai stiril-lakton baharu. Sturktur sebatian dikenalpastikan dengan menggunakan pelbagai teknik spektroskopi; 1D-NMR (1H, 13C, DEPT), 2D-NMR (COSY, HSQC, HMBC, NOESY), UV, IR, spektrometri jisim dan perbandingan dengan kajian-kajian lepas. Goniothalamin **1** merupakan sebatian utama yang diasingkan daripada ekstrak diklorometana *G.*

tapisoides. Penyelidikan kinetik spektrometrik telah dijalankan ke atas **1** untuk mendedahkan proses hidrolisis **1** dalam media alkali dan asid pada suhu yang berlainan. Penyelidikan ini adalah untuk mengaji mekanisme reaksi bagi tindak balas pemangkinan ion hidroksida. Hidrolisis alkali melibatkan tindak balas monotonik dan pemalar kadar tertib pertama (k_{obs}). Didapati bahawa kadar tindak balas adalah berkadar terus dengan peningkatan kepekatan natrium hidroksida, dengan penghasilan produk goniomicin A **147**. Hidrolisis alkali melibatkan pembukaan cincin lakton. Manakala dalam media asid, ion hidronium memangkinkan tindak balas pembukaan cincin lakton dan bahantara terbentuk. Bahantara itu seterusnya menghasilkan produk yang mempunyai tiga ikatan kembar secara berterusan dengan melalui dehidrasi. Produk hidrolisis alkali dan asid dikenalpastikan dengan teknik 1D-NMR, 2D-NMR dan spektrometri jisim.

Kata kunci: *Goniothalamus tapis*, *Goniothalamus tapisoides*, stiril-lakton, goniomicin, goniothalamin, penyelidikan kinetik, hidrolisis

ACKNOWLEDGEMENTS

TABLE OF CONTENTS

LIST OF SCHEMES

LIST OF FIGURES

LIST OF TABLES

LIST OF SYMBOLS AND ABBREVIATIONS

Å	:	Armstrong
β	:	Beta
γ	:	Gamma
δ	:	Chemical shift
λ	:	Wavelength (lambda)
ε	:	Molar absorptivity
δ_{app}	:	Apparent molar absorptivity
^1H	:	Proton NMR
A	:	Alpha
Ar	:	Aromatic
br s	:	Broad singlet
s	:	Singlet
d	:	Doublet
dd	:	Doublet of doublet
ddd	:	Doublet of doublet of doublet
dt	:	Doublet of triplet
t	:	Triplet
m	:	Multiplet
q	:	Quartet
CC	:	Column chromatography
$CDCl_3$	:	Deuterated chloroform
CD_3OD	:	Deuterated methanol
CH_3	:	Methyl group
COSY	:	Correlation Spectroscopy

g	:	Gram
GCMS	:	Gas Chromatography Mass Spectrometry
HMBC	:	Heteronuclear Multiple Bond Correlation
HSQC	:	Heteronuclear Single Quantum Correlation
HPLC	:	High Performance Liquid Chromatography
Hz	:	Hertz
IR	:	Infrared
J	:	Coupling constant
L	:	Litre
m	:	Metre
nm	:	Nanometer
μM	:	Micromolar
m/z	:	Mass to charge ratio
MeOH	:	Methanol
MHz	:	Mega Hertz
MS	:	Mass spectrum
ml	:	Mililitre
NMR	:	Nuclear Magnetic Resonance
NOESY	:	Nuclear Overhauser Effect Spectroscopy
ppm	:	Parts per million
RE	:	Relative Error
TLC	:	Thin Layer Chromatography
UV	:	Ultraviolet
^{13}C	:	Carbon-13 NMR
2D NMR	:	Two Dimensional Nuclear Magnetic Resonance

CHAPTER 1 : INTRODUCTION

1.1 General

The term "natural products" is often referred to secondary metabolites of natural origins produced by a living organism. Natural products have been used by human for the treatment of many diseases and illnesses since thousands of years. In countries such as China, Greece, Tibet and India (Gurib-Fakim, 2006) the usage of natural products are still prevalent. In the early 1900s, before the ''Synthetic Era'', 80% of all medicines were obtained from roots, barks and leaves. In 2013, approximately 25% of all drugs prescribed originated from plants. (Schwartsmann, 2000; McChesney et al., 2007; Rout et al., 2009 July-Sep; Krause & Tobin, 2013)

As Rudyard Kipling wrote (1910), "Anything green that grew out of the mould was an excellent herb to our fathers of old." Throughout these years, natural products have been recognized as an important source of drugs and leads. Approximately 60% of anticancer compounds and 75% of drugs for infectious diseases that are either natural products or natural product derivatives. (Newman et al., 2003; Cragg et al., 2005; McChesney et al., 2007)

In the field of medicinal chemistry, natural products are known as secondary metabolites with molecular weight less than 2000 amu produced by living organisms. Secondary metabolites are not a necessity in primary metabolic processes, such as metabolism, photosynthesis, and reproduction. But it plays a vital role in the adaptation of plants to the environment. (Bourgaud et al., 2001) It exists for the purpose of competitive weapons, defence system, metal transporting agents, agents of symbiosis, sexual hormones, and differentiation effectors. (Arnold L Demain & Fang, 2000) For example, plants will produce phytoalexins when attacked by bacteria and fungi. (Gurib-Fakim, 2006, pp. 13-14)

Therefore, secondary metabolites are crucial for plant survival. Plants will produce secondary metabolites that evolve naturally to overcome the needs and challenges of the natural environment. Secondary metabolites keep evolving as nature are continually carrying out its own version of combinational chemistry for over 3 billion years during which bacteria have inhabited the earth (Verdine, 1996; Holland, 1997). For the useful metabolites, the biosynthetic genes were retained, and genetic modifications further improved the process. Combinatorial chemistry occurred by nature is much more sophisticated than that in the laboratory (Verdine, 1996; Holland, 1997; L. Zhang & Demain, 2005). As a consequences, a lot of new secondary metabolites are derived with different stereochemistry and functional group (L. Zhang & Demain, 2005; Gurib-Fakim, 2006, pp. 13-14).

Phytochemical studies on medicinal plants is to discover the potential of secondary metabolites as drugs or leads against diseases. Today, almost 80% of antimicrobial, cardiovascular, immunosuppressive, and anticancer drugs are of plant origin (Gordaliza, 2009; Pan et al., 2013). A great amount and different variety of secondary metabolites have been found naturally. In 1995, Mendelsohn & Balick has reported that the total numbers of secondary metabolites have been estimated to be over 500,000 in the world (Mendelsohn & Balick, 1995; L. Zhang & Demain, 2005). Up till the year of 2005, there are about 200,000 secondary metabolites have been identified (Tulp & Bohlin, 2005).

Malaysia ranks 12th on the list of 17 mega-diverse countries in the world, it had been recognized as one of the highly diversified flora and fauna country ("National Policy on Biological Diversity," 1998). Malaysia is endowed with over 15,000 species of flowering plants, 1,500 species of terrestrial vertebrates, and 150,000 of invertebrates (Sajise et al., 2010). From about 10,000 species of higher plants and 2,000 species of lower plants available in Peninsular Malaysia, approximately 16% are claimed to be used for medicinal

purposes (Lattif et al., 1984).

Natural product are widely used as medicine, almost half of the best-selling pharmaceuticals are natural or natural products related (Arnold L. Demain & Vaishnav, 2011). For example Taxol (paclitaxel), a diterpene alkaloid used as anti-cancer drug. Taxol were firstly discovered from the bark of the Pacific yew tree (*Taxus brevifolia*). But the amount of Taxol in the tree is not much, therefore, it is now produced by plant cell culture or semi synthesis.

An important aspect in the investigation of potential leads or medicines is the study of the kinetic mechanism and stability of the drug in various system in terms of pH and temperature. After a drug is consumed into our body, a series of reaction might occur due to the pH changes. Amongst which, the most important one being hydrolysis. Hydrolysis could be triggered in an alkaline or an acidic environment.

In view of the importance of discovering new bioactive compounds that have therapeutical potential and also to understand their behaviour upon changes in the pH (environment), this particular study will concentrate on isolation of chemical constituents of *G. tapis* and *G. tapisoides*. In addition, the influences of pH and temperature on the hydrolysis kinetics of the bioactive goniothalamin isolated from both plants mentioned above.

1.2   The family Annonaceae

Annonaceae (custard-apple family) is the most species-rich family of Magnoliales, comprising about 108 genera and 2400 species in predominantly tropical and subtropical lowland forests (Chatrou et al., 2012). Annonaceae is a pantropical family that well developed in tropical regions mainly at low elevations in moist forests. They are generally

distributed throughout the tropical areas of Africa America, and Asia. Except for two related North American genera (*Asimina* and *Deeringothamnus*).

The largest number of genera and species are found in Asia, with approximately 60 genera and 1000 species. Within Asia, Indo-Malaysia has the greatest concentration of genera and species compared to other areas. Around 40 genera and 450 species are known from Africa and Madagascar. In the American continent, existence of about 740 species and 30 genera represent that the genus have better diversity in this region compared to Africa and Madagascar (W. C. Chen, 1995).

1.3   Classification of Annonaceae

Kingdom: Plantae

Phylum: Tracheophyta

Class: Magnoliopsida

Order: Magnoliales

Family: Annonaceae (Custard-apple family)
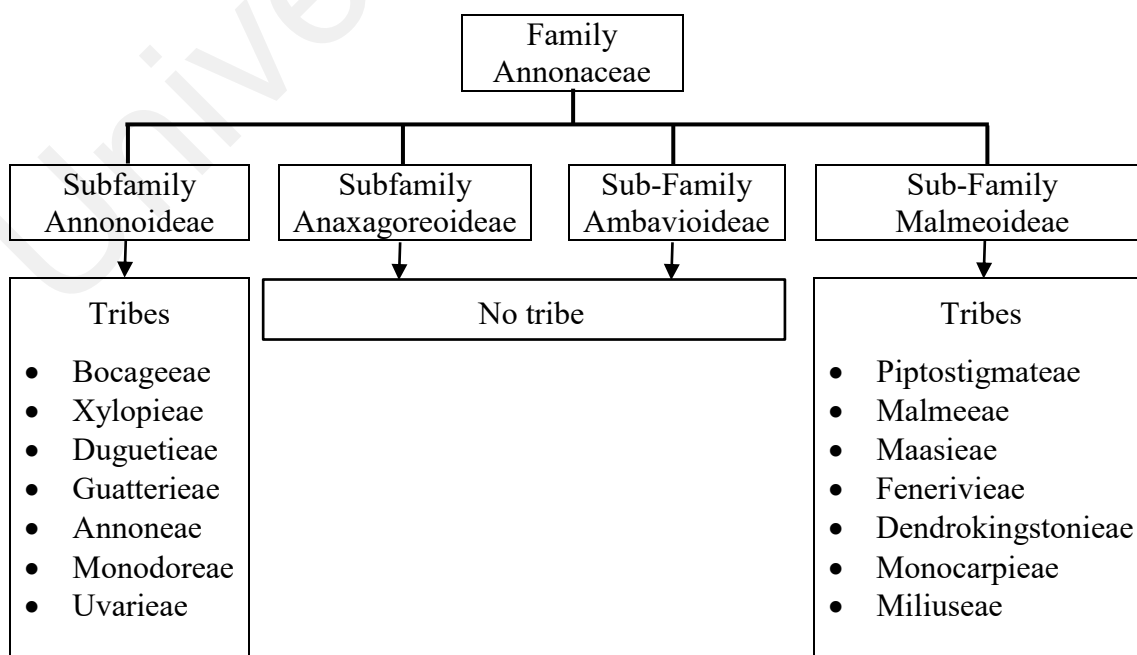
Scheme 1.1: Classification of family Annonaceae.

The phylogeny-based classification of family Annonaceae comprises of four subfamilies and 14 tribes as shown in **Scheme 1.1** (Chatrou et al., 2012).

Two subfamilies (Anaxagoreoideae & Ambavioideae) and fourteen tribes are further categorized into 108 genera as stated in **Table 1.1**. Classification and determination of a subfamily, tribe and genus is dependent on the combination of characters, for instance that of the petal and the fruit. Genus *Goniothalamus* is fall in the tribe Annoneae, subfamily Annonoideae.

Table 1.1: Genera of Annonaceae.

Tribes & Subfamily	Genera	
Bocageeae	• *Bocagea* • *Cardiopetalum* • *Cymbopetalum* • *Froesiodendron*	• *Hornschuchia* • *Mkilua* • *Porcelia* • *Trigynaea*
Xylopieae	• *Artabotrys*	• *Xylopia*
Duguetieae	• *Duckeanthus* • *Duguetia* • *Fusaea*	• *Letestudoxa* • *Pseudartabotrys*
Guatterieae	• *Guatteria*	
Annoneae	• *Annona* • *Anonidium* • *Asimina* • *Boutiquea*	• *Diclinanona* • *Disepalum* • *Goniothalamus* • *Neostenanthera*
Monodoreae	• *Asteranthe* • *Hexalobus* • *Isolona* • *Mischogyne* • *Monocyclanthus*	• *Monodora* • *Ophrypetalum* • *Sanrafaelia* • *Uvariastrum* • *Uvariopsis*
Uvarieae	• *Afroguatteria* • *Cleistochlamys* • *Dasymaschalon* • *Desmos* • *Dielsiothamnus* • *Exellia* • *Fissistigma* • *Friesodielsia*	• *Gilbertiella* • *Melodorum* • *Monanthotaxis* • *Pyramidanthe* • *Schefferomitra* • *Sphaerocoryne* • *Toussaintia* • *Uvaria*
Anaxagoreoideae	• *Anaxagorea*	

Ambavioideae	• *Ambavia*	• *Lettowianthus*
	• *Cananga*	• *Meiocarpidium*
	• *Cleistopholis*	• *Mezzettia*
	• *Cyathocalyx*	• *Tetrameranthus*
	• *Drepananthus*	
Piptostigmateae	• *Annickia*	• *Piptostigma*
	• *Greenwayodendron*	• *Polyceratocarpus*
	• *Mwasumbia*	
Malmeeae	• *Bocageopsis*	• *Oxandra*
	• *Cremastosperma*	• *Pseudephedranthus*
	• *Ephedranthus*	• *Pseudomalmea*
	• *Klarobelia*	• *Pseudoxandra*
	• *Malmea*	• *Ruizodendron*
	• *Mosannona*	• *Unonopsis*
	• *Onychopetalum*	
Maasieae	• *Maasia*	
Fenerivieae	• *Fenerivia*	
Dendrokingstonieae	• *Dendrokingstonia*	
Monocarpieae	• *Monocarpia*	
Miliuseae	• *Alphonsea*	• *Phoenicanthus*
	• *Desmopsis*	• *Platymitra*
	• *Enicosanthum*	• *Polyalthia*
	• *Fitzalania*	• *Popowia*
	• *Haplostichanthus*	• *Pseuduvaria*
	• *Marsypopetalum*	• *Sageraea*
	• *Meiogyne*	• *Sapranthus*
	• *Miliusa*	• *Stelechocarpus*
	• *Mitrephora*	• *Stenanona*
	• *Neo-uvaria*	• *Tridimeris*
	• *Oncodostigma*	• *Trivalvaria*
	• *Orophea*	• *Woodiellantha*
	• *Phaeanthus*	

1.4   The genus *Goniothalamus* (Blume) Hook. F. & Thomson

The genus *Goniothalamus* is one of the largest genera of palaeotropical Annonaceae in the tribe Annoneae. About 160 species of shrubs and small to large trees have been identified (Wiart, 2007). Over 120 species are distributed in lowland and sub montane tropical south-east Asia; the centre of diversity lies in Sumatra, Peninsular Malaysia and Borneo (Saunders, 2003), (Saunders, 2002). In most of the species of *Goniothalamus*, the

flowers or inflorescences are strictly axillary. It consist of one whorl of three sepals, and two whorls of three petals each. The outer petals are always larger than inner whorl and are typically cream, yellow or red at maturity (Saunders, 2002).

1.5   *Goniothalamus tapis* Miq.

Goniothalamus tapis is a tree of 8 m tall and 12 cm in diameter. The bark is grey in color and scaly with yellowish pink inner bark. The leaves are thinly coriaceous, from elliptic lanceolate to oblong with apex abruptly acuminate blunt and base shortly acute. The area of leaves are 9.5–19.0 cm × 3.5–6.0 cm with bright green above and pale yellow green below, sometimes glaucous beneath. This species is distributed throughout Peninsular Malaysia, Sarawak and Sumatra (Ahmad et al., 2010).

Figure 1.1: *Goniothalamus tapis* with voucher specimen number KL5744.

Figure 1.2: Bark of *Goniothalamus tapis*.

1.6 *Goniothalamus tapisoides* Mat Salleh

G. tapisoides is a small tree about 5 m in height, it known as 'selada' by the Malays or 'semukau' by the Iban. It is a small tree around 5 m in height. It is endemic to Borneo, especially the sourthern part of Sarawak.

1.7 Problem statement

These two species from *Goniothalamus* genus are used as traditional medicine in Malaysia and Indonesia. The roots of *G. tapis* is used to treat typhoid fever in Java, Indonesia (Efdi et al., 2010). *G. tapisoides* is used to relieve stomach-ache and to cure poisonous animal bites in Sarawak, Malaysia (Ahmad et al., 2010). Thus, it is important to discover the chemical constituents of these plants.

In addition, interesting to found that past studies on several *Goniothalamus* species consists of numerous types of bioactive constituents. The first study on *G. tapis* was done in year 1990, the roots was collected from Kelantan, and there is only one compound reported (Colegate et al., 1990). Ten years later, the leaves of the species were

investigated, three compounds were reported (Ee et al., 2000). At year 2010, the stem bark of the same species from West Sumatran rainforest were studied and various compounds were reported as stated in Table 2.1 (Efdi et al., 2010).

On the other hand, research has been done on the dichloromethane crude of the stem bark of *G. tapisoides* during the author's master study (Kim et al., 2012). This is continuous work to further investigate the bioactive constituents in the plant.

According to literature, goniothalamin is found in almost fifty percent of all *Goniothalamus* genus that had been studied and reported. It is one of the most well investigated compound, extensive studied have been conducted to study the cytotoxic activity of **1**, and it showed promising activity against wide range of cancer cell lines (Wach et al., 2010; Chiu et al., 2011; Seyed et al., 2014). It also exhibited antibacterial (Mosaddik & Haque, 2003), antifungal (Martins et al., 2009) and mosquito larvicidal activities (Kabir et al., 2003).

Therefore it is important to investigate its stability at various pH and temperature as it can be a candidate as lead compound. It is vital that biological and clinical studies are conducted on the drug compound to assure that it is not degraded in those conditions. This is because drugs usually undergo hydrolysis upon introduction into human body. In this case, complete degradation of the drug in aqueous solution as a function of acidic and alkali medium in various temperature should be determined before goniothalamin can be evaluated further for its potential use as a therapeutic agent.

1.8   Objectives of the study

The objectives of the present PhD study were as follows:

i.   to isolate chemical constituents from two Malaysian *Goniothalamus* species; *G. tapis* and *G. tapisoides*,

ii. to elucidate the structure of isolated compounds using spectroscopic methods such as 1D-NMR (1H, 13C and DEPT-135), 2D-NMR (COSY, HMBC, HSQC, NOESY), ultraviolet (UV), infrared (FTIR) and LCMS-IT-TOF analysis,

iii. to carry out kinetic mechanism study of degradation on goniothalamin **1** in alkaline and acidic medium, and also at different temperature.

CHAPTER 2 : GENERAL CHEMICAL ASPECTS

2.1   Introduction

Phytochemical studies on genus *Goniothalamus* is known to its yield of large number of bioactive styryl-lactones and acetogenins. This genus also produces a wide range of compounds, for example, terpenes, alkaloids and flavonoids are secondary metabolites have been isolated from this genus. In this chapter, the general aspects of the styryl-lactones in terms of their classification and biogenesis will be briefly discussed.

2.2   Traditional medicinal uses of *Goniothalamus* species

The genus *Goniothalamus* have been reported to be used for various medicinal purposes. The root decoction of *G. macrophyllus* is taken orally by indigenous people in Peninsular Malaysia for anti-aging purpose. The mixed decoction with *Eurycoma longifolia* is taken orally as male tonic (Ong et al., 2012). Other than that, different part of *G. macrophyllus* are used to treat numerous ailments such as body pains, rheumatism, and skin diseases.

The root of *G. tapis* is used to cure stomach-ache and also as abortifacient. The roots or stem bark of *G. tapisoides* can also be used for abortifacient and stomach-ache, by adding it into warm water and taken orally. Besides that, the crushed roots or stem bark of *G. tapisoides* are used to cure poisonous animal or insect bites by applied it on the affected area (Ahmad et al., 2010).

The seeds of *G. amuyon* is known to have its traditional medicinal uses in different country. In Taiwan, the seeds are used to treat scabies. In Philippines, the seeds are evoked with oil make an effective liniment to treat rheumatism (Wiart, 2007).

2.3 Phytochemical studies from *Goniothalamus* species

Extensive work on the isolation and identification of chemical constituents from *Goniothalamus* species, as well as their biological activities have been reported, as this genus are known for their medicinal value. Out of 160 *Goniothalamus* species, approximately 40 species (25%) were phytochemically investigated. Various types of compounds including styryl-lactones, acetogenins, alkaloids, flavonoids and terpenes have been isolated from the genus. Among all these compounds, styryl-lactones is one of the major type of compounds commonly yielded from the genus *Goniothalamus*.

2.3.1 Styryl-lactones

Styryl-lactones is a group of secondary metabolite found primarily in the *Goniothalamus* species (Annonaceae) that have demonstrated to possess interesting biological properties. Styryl-lactones have been reported to possess cytotoxic (Tian et al., 2006), antimicrobial (Siddig Ibrahim et al., 2009), pesticides (Senthil-Nathan et al., 2008), teratogenic and embryotoxic activities (Sam et al., 1987).

Styryl-lactones are low molecular weight which characterized by a basic skeleton of 13 carbon atoms that consists of a styryl or pseudo-styryl fragment linked to a lactone moiety. In furanone (five-membered) and pyranone (six-membered) have basic C_6–C_3–C_4 skeleton, having γ- or δ- lactone rings. In the heptolide group, the ζ-lactone is directly attached to the aromatic ring. Currently, approximately seventy styryl-lactones are discovered from natural products.

In general, styryl-lactones can be classified into six minor groups based on their structural characteristics of the skeletons as shown in **Figure 2.1**. These groups are; styryl-pyrones, furano-pyrones, furano-furones, pyrano-pyrones, butenolides, and heptolides. The formation of variety class of styryl-lactone skeletons are shown in the biosynthetic pathway in section 2.3.2, **Figure 2.2**.

Pyrone **Furano-pyrone** **Furano-furone**

Pyrano-pyrone **Butenolide** **Heptolide**
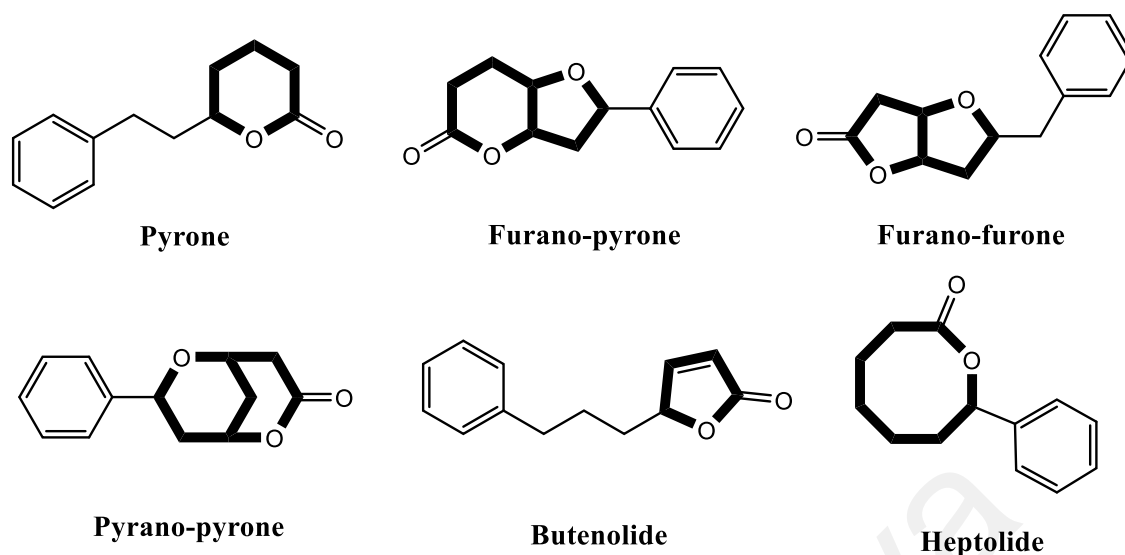
Figure 2.1: Styryl-lactone skeletons isolated from the genus *Goniothalamus.*

2.3.1.1 Styryl-pyrones

Styryl-pyrone skeleton is the most abundance class of styryl-lactone in the genus *Goniothalamus*. Styryl-pyrone moiety can further classified into four types:

Type I is 7,8-olefinic styryl-pyrones. There is a double bond between carbon 7 and 8 ($C_7=C_8$). Example for type I styryl-pyrone is goniothalamin **1**.

Type II is 7,8-epoxide styryl-pyrones. There is an epoxide exists between carbon 7 and 8. Example for type II styryl-pyrone is goniothalamin oxide **2**.

1 **2**

13
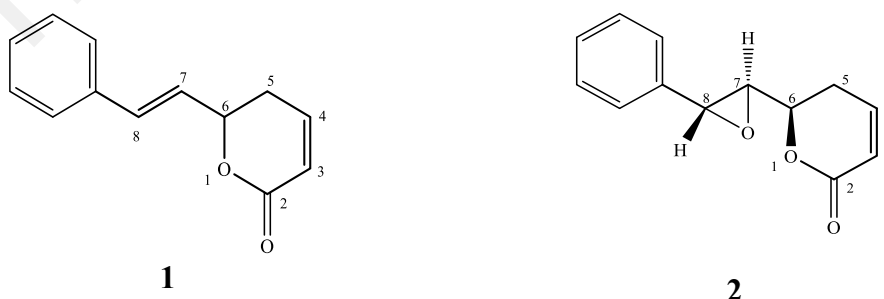
Type III is 7,8-dioxygenated styryl-pyrones. There are –OH group attached to both carbon 7 and 8. Example for type III styryl-pyrone is goniodiol **3**.

Type IV is saturated styryl-pyrones. There is no double bond from carbon 3 to carbon 8. Example for type IV styryl-pyrone is garvensintriol **4**.

3　　　　　　　　　　　**4**
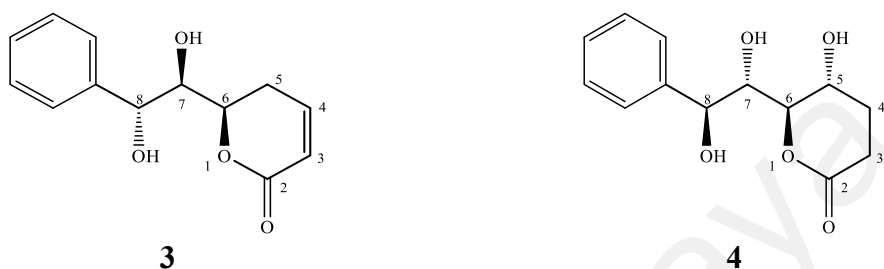
2.3.1.2　Furano-pyrones

The furano-pyrone skeleton represents the second most abundant class of styryl lactones in *Goniothalamus*. Altholactone **40**, is the first member in this group that was first identified from *Polyalthia* (Loder & Nearn, 1977) and eight years later was isolated from the bark of *G. giganteus* and reported with different trivial name, goniothelenol (**Table 2.1**).

40
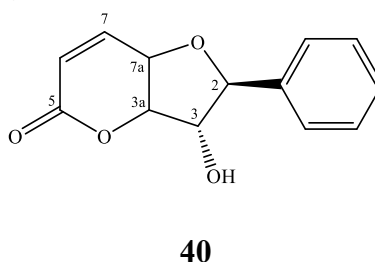
2.3.1.3　Furano-furones

Only three styryl-lactones with this skeleton have been reported. Two stereoisomers, goniofufurone **47** and 7-epi-goniofufurone **49** were isolated from the stem bark of *G. giganteus* (X. P. Fang et al., 1991b). The third furano-furones type of styryl-lactone, namely 8-acetoxy goniofufurone **48** was isolated from the leaves of *G. wynaadensis* recently (Ajithabai et al., 2011).

2.3.1.4 Pyrano-pyrones

Styryl-lactones with this skeleton have to two six-membered ring. Both rings share two carbons at position 1 and position 5.
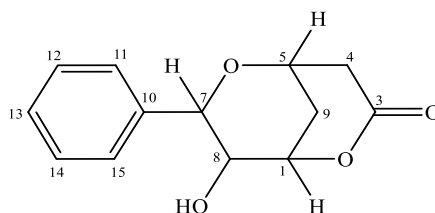
2.3.1.5 Butenolides

The first two butenolide compounds were firstly isolated from *G. giganteus* (X. P. Fang et al., 1991a). Then, they were isolated from the bark of *G. borneensis* (Cao et al., 1998).

2.3.1.6 Heptolides

Styryl-lactone of this group contain an unusual, saturated eight-membered lactone moiety (ζ-lactone). Gonioheptolides-A and gonioheptolides-B were the first two compounds of this class to be isolated from the stem bark of *G. giganteus* (X. P. Fang et al., 1993).

2.3.2   Biosynthetic of styryl-lactones
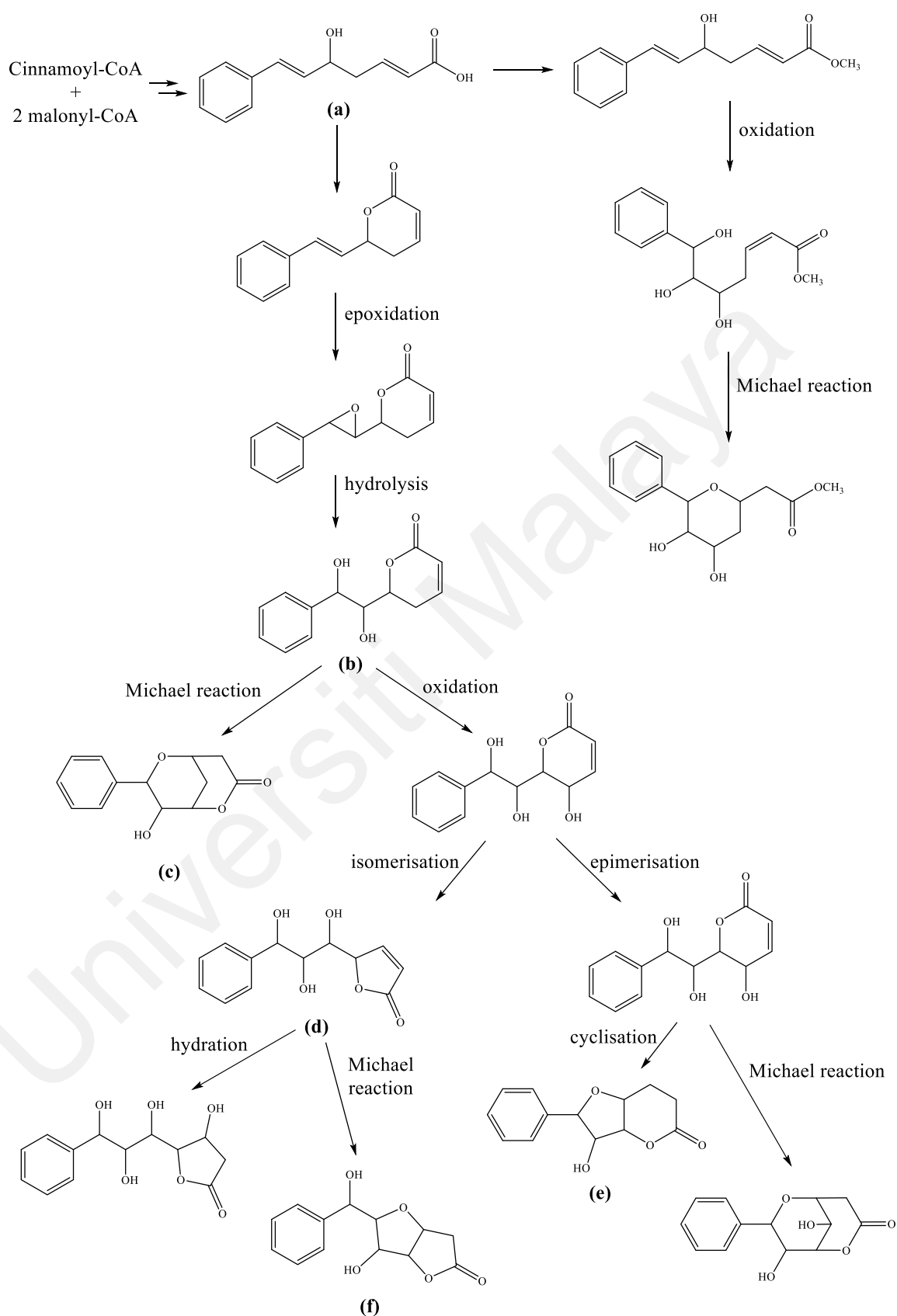
Figure 2.2: Plausible biosynthetic pathways of styryl-lactones.

According to the literature (Suchaichit et al., 2015), a plausible biosynthetic pathway for styryl-lactones has been proposed in **Figure 2.2**. Starting from cinnamoyl-CoA and two malonyl-CoA molecules to give a seven carbon molecule (**a**). A cyclisation and dehydration then occur between C-1 with carboxylic acid and C-5 with hydroxyl group. This forms the basic skeleton of styryl fragment linked to a lactone moiety and it can be further transformed into five types of skeleton (**b-f**) through series of reaction.

Pyrano-pyrones skeleton is produced through Michael reaction. Meanwhile, furano-pyrone skeleton is the result of cyclisation of styryl-pyrones. Butenolide skeleton, on the other hand, is a cyclisation of styryl-pyrones. It could undergo Michael reaction to produce furano-furones.

2.3.3   Chemical constituents isolated from *Goniothalamus* species

Collective data of previous studies on *Goniothalamus* species have desmonstrated styryl lactone as one of the main group of secondary metabolites (Blazquez et al., 1999; de Fatima et al., 2006). Table 2.1 summarises 145 chemical constituents that consists of styryl-lactones, alkaloids, terpenes and other miscellaneous group of compounds. These chemical constituents were isolated from thirty eight *Goniothalamus* species; *G. amuyon, G. andersonii, G. arvensis, G. australis, G. borneensis, G. cardiopetalus, G. cheliensis, G. chenensis, G. dolichocarpus, G. elegants, G. giganteus, G. gitingensis, G. grandifloras, G. griffithii, G. howii, G. kinabaluensis, G. lanceolatus, G. laoticus, G. leiocarpus, G. macrocalyx, G. macrophyllus, G. malayanus, G. marcanii, G. montanus, G. ridleyi, G. scortechinii, G. sesquipedalis, G. tamirensis, G. tapis, G. tapisoides, G. tenuifolis, G. thwaitesii, G. umbrosus, G. undulates, G. uvaroides, G. velutinus, G. wightii* and *G. wynaadensis.*

Up to year 2019, approximately sixty seven styryl-lactones were obtained naturally from *Goniothalamus* species. Among all styryl-lactones, goniothalamin **1** is one of the

commonly exist in the genus. It have been isolated from twenty *Goniothalamus* species, out of fourty *Goniothalamus* species been studied, either from barks/ roots/ leaves or fruits (based on literature data in Table 2.1). Those species consist of **1** are *G. amuyon*, *G. andersonii, G. borneensis, G. cardiopetalus, G. dolichocarpus, G. elegants, G. griffithii, G. howii, G. kinabaluensis, G. macrophyllus, G. ridleyi, G. scortechinii, G. sesquipedalis, G. tamirensis, G. tapisoides, G. umbrosus, G. uvaroides, G. velutinus, G. wightii* and *G. wynaadensis*.

Goniothalamin **1** is first isolated in 1967 from the bark of *Cryptocarya caloneura* (Hlubucek & Robertson, 1967). Later it was isolated from several species of *Goniothalamus* in 1972 (Jewers et al., 1972). It is the first styryl-lactone found in Annonaceae, it has displayed in vitro cytotoxic effect especially by inducing apoptosis on different cancer cell lines; promyelocytic leukemia (HL-60); hepatocarcinoma (Bel7402); human lung carcinoma (A-549); human stomach cancer (SGC-7901) (de Fatima et al., 2006).

Table 2.1: Chemical constituents isolated from *Goniothalamus* species.

Plants	Parts	Compounds	Reference(s)
G. amuyon Merr. (Hengchun, Pingtung Hsien, Taiwan)	Aerial	8-Chlorogoniodiol **5** 8-Methoxygoniodiol **6** (+)-9-Deoxygoniopypyrone **23** Aristolactam FII **115** (6*R*,7*R*,8*R*)-Goniodiol **3** (5*S*,6*R*,7*R*,8*R*)-Goniotriol **7** Digoniodiol **63** Deoxygoniopypyrone A **29** Goniobutenolide A **50** Goniobutenolide B **51** Goniofupyrone A **35** Goniothalamin **1** Goniothalamin epoxide **2** *β*-Sitosterol **134** Stigmasterol **133**	(Lan et al., 2003)
G. amuyon Merr. (Hengchun, Pingtung Hsien, Taiwan)	Leaves	Cinnamic acid **131** (6*R*,7*R*,8*R*)-Goniodiol-7-monoacetate **16** (6*R*,7*R*,8*R*)-Goniodiol-8-monoacetate **17** Goniotriol **7** Liriodenine **114** Lysicamine **117**	(Lan et al., 2003) (Wu et al., 1991) (Wu et al., 1992)

Table 2.1, continued.

Plants	Parts	Compounds	Reference(s)
G. amuyon Merr. (Hengchun, Pingtung Hsien, Taiwan)	Stems	4-Methyl-2,9,10-(2H)-1-azaanthracencetrione **92** Aristolactam BII **107** Goniodiol-7-monoacetate **16** Goniodiol-8-monoacetate **17** Goniothalesacetate **137** Goniothalesdiol A **139** Griffithazanone A **91** Leiocarpin C **19** Liriodenine **114** Velutinam **106**	(Lan et al., 2006)
G. andersonii J. Sinclair		(+)-Goniodiol **3** (+)-Goniothalamin **1**	(Tanaka et al., 2001)
G. andersonii J. Sinclair	Stem bark	Goniothalamin **1** Stigmasterol **133**	(Izaddin et al., 2008)
G. arvensis Scheff. (National Park of Varirata, Papua New Guinea)	Stem bark	(+)-2-*epi*-Altholactone **39** 3-Acetylaltholactone **37** 5-Acetoxyisogoniothalamin oxide **15** Almuheptolide-A **57** Almuheptolide-B **58** Altholactone **40** Arvensin **42** (+)-Etharvendiol **8** Etharvensin **44** (+)-Garvensintriol **4** (+)-Goniofufurone **47** (+)-Goniotharvensin **43** (+)-Isoaltholactone **41**	(Bermejo et al., 1999) (Peris et al., 2000) (Bermejo, 1997) (Bermejo et al., 1997) (Bermejo et al., 1998) (Bermejo et al., 1995)

Table 2.1, continued.

Plants	Parts	Compounds	Reference(s)
G. australis Jessup (Queensland, Australia)	Aerial	(−)-Anonaine **101** Altholactone **40** Aristolactam AII **102** Asimilobine **95** Caldensine **120** Enterocarpam II **109** (+)-Goniofufurone **47** Goniothaline A **122** Goniothaline B **123** Sauristolactam **121**	(Levrier et al., 2013)
G. borneensis Mat Salleh (Sabah, Malaysia)	Bark	Aristolactam AIII **108** Cinnamyl cinnamate **6** Goniobutenolide A **50** Goniobutenolide B **51** Goniofufurone **47** Goniothalactam **105** Goniothalamin **1** (+)-Goniothalenol **40** Goniothalesdiol **141** Goniotriol **7** Pinocembrin **94** Stigmasterol **133**	(Cao et al., 1998)
G. cardiopetalus Hook. f. & Thoms. (Kerala, India)	Stem bark	Altholactone **40** Cardiobutanolide **53** Cardiopetalolactone **140** Goniodiol **3**	(Hisham et al., 2000) (Hisham et al., 2003)

Plants	Parts	Compounds	Reference(s)
G. cardiopetalus Hook. f. & Thoms. (Kerala, India)	Stem bark	Goniofufurone **47** Goniofupyrone **46** Goniopypyrone **26** Goniothalamin **1**	(Hisham et al., 2000) (Hisham et al., 2003)
G. cheliensis Hu (Yunnan Province, China)	Leaves	Aristolactam AII **102** Aristolactam AIII **108** Goniodilactone **62** Goniodiol **3** Goniodiol-7-monoacetate **16** Gonioheptenolactone **61** (+)-Isoaltholactone **41** Leiocarpin A **30** Liriodenine **114** Pinocembrin **94** Stigmasterol **133** Varilactam **104**	(G. J. Zhu et al., 2000) (J. X. Zhu et al., 2006) (J. X. Zhu et al., 2012)
G. cheliensis Hu (Yunnan Province, China)	Roots	(3S)-2-Oxo-5,12-dimethoxy-3-hydroxy-3-methylbenz[f]indoline **77** 7-Acetyl-digoniodiol **63** 8-*epi*-Goniofufurone **49** 8-*epi*-Goniotriol **11** 8-Acetyl-9-deoxygoniopypyrone **31** Acetylgoniofupyrone A **36** Cardiobutanolide **53** Cepharanone B **107** Cheliensisame A **104** Goniodiol **3**	(Jiang et al., 2008) (M.M. Jiang et al., 2011) (Wang et al., 2003) (M. M. Jiang,Y. F. Feng,X. Zhang, et al., 2011)

Plants	Parts	Compounds	Reference(s)
G. cheliensis Hu (Yunnan Province, China)	Roots	*Iso*-goniopypyrone **32** Goniofufurone acetonide **45** Goniolactone A **64** Goniolactone B **65** Goniolactone C **66** Goniolactone D **67** Goniolactone E **73** Goniolactone F **74** Goniolactone G **69** Goniolactone H **70** Goniolactone I **72** Pinocembrin **94**	(Wang et al., 2003) (Wang et al., 2001) (Wang et al., 2002) (M. M. Jiang, Y. F. Feng, H. Gao, et al., 2011) (M. M. Jiang, Y. F. Feng, X. Zhang, et al., 2011)
G. cheliensis Hu (Yunnan Province, China)	Stem	Cheliensisin A **22**	(Zhong et al., 2005)
G. cheliensis Hu (Doi Tung, Chiang Rai Province, Thailand)	Twigs & leaves	8-Acetoxy goniofufurone **48** (−)-(*4S,5S,6R,7S,8S*)-7-acetylgoniochelienlactone **34** (+)-7-O-Acetylgoniodiol **16** 3-methyl-1*H*-benz[*f*]indole-4,9-dione **81** Goniochelienic acid A **82** Goniochelienic acid B **83** Goniochelieninone **80** (+)-(*7S,8S*)-Goniochelienbutenolide A **55** (−)-(*7S,8R*)-Goniochelienbutenolide B **52** (−)-(*4S,5S,6R,7S,8S*)-Goniochelienlactone **33**	(Jaidee et al., 2019)

Table 2.1, continued.

Plants	Parts	Compounds	Reference(s)
G. cheliensis Hu (Doi Tung, Chiang Rai Province, Thailand)	Twigs & leaves	(–)-Goniobutenolide B **51** 7-*epi*-(–)-Goniobutenolide B **56** (+)-Goniodiol **3** Goniodiol-8-monoacetate **17** Isoaltholactone **41** Methyl goniochelienate **84**	(Jaidee et al., 2019)
G. chinensis Merr. & Chun Ha Giang province, Vietnam	Bark	Goniothalamin **1** Aristolactam BII **107** 3-methyl-1*H*-benz[*f*]indole-4,9-dione **81**	(Duc et al., 2016)
G. dolichocarpus Merr.	Stem bark	(+)-5β-hydroxygoniothalamin **12** (+)-Goniothalamin **1** (+)-Goniothalamin epoxide **2**	(Goh et al., 1995)
G. elegants Ast. (Ubonratana district, Khon Kaen, Thailand)	Bark	6-*epi*-Goniothalesdiol A **142** (–)-8-epi-9-deoxygoniopypyrone **24** (+)-Altholactone **40** Aristolactam BII **107** (+)-Cardiobutanolide **53** (+)-Goniodiol **3** (+)-Goniofufurone **47** Goniopedaline **115** (+)-Goniopypyrone **26** (+)-Goniothalamin **1** (+)-Goniothalamin oxide **2** (+)-Goniotriol **7** Velutinam **106**	(Suchaichit et al., 2015)

Table 2.1, continued.

Plants	Parts	Compounds	Reference(s)
G. giganteus Hook. f. & Thoms. (Thailand)	Stem bark	7-*epi*-Goniofufurone **49** 8-Acetylgoniotriol **9** 9-Deoxygoniopypyrone **23** Goniobutenolide A **50** Goniobutenolide B **51** Goniodiol **3** Goniofufurone **47** Goniofupyrone **45** Gonioheptolide A **59** Gonioheptolide B **60** Goniopypyrone **26** Goniothalenol **40** Goniotriol **7**	(X. P. Fang et al., 1991a) (X. P. Fang et al., 1990) (X. P. Fang et al., 1991b) (X. P. Fang et al., 1993) (El-Zayat et al., 1985) (Alkofahi et al., 1989)
G. gitingensis Elmer (Romblon, Philippines)	Leaves	Altholactone **40** Goniopypyrone **26** Isoaltholactone **41** Liriodenine **114**	(Macabeo et al., 2014)
G. grandifloras Boerl. (New Guinea)	Leaves	(+)-Isoaltholactone **41**	(Khan et al., 1998)
G. griffithii Hook f. & Thoms.	Bark	8-Acetylgoniofufurone **48** Goniothalamin **1** Pinocembrine **94** β-Sitosterol **134** Stigmasterol **133**	(Hu et al., 2000)
G. griffithii Hook f. & Thoms.	Leaves	Goniodiol monoacetate **16** Griffithine A β-Sitosterol **134**	(Li et al., 1997)

Table 2.1, continued.

Plants	Parts	Compounds	Reference(s)
G. griffithii Hook f. & Thoms.	Leaves & twigs	(−)-7-O-Acetylgoniodiol **16** Goniothalamin **1** Pinocembrine **94**	(Kampong et al., 2013)
G. griffithii Hook f. & Thoms. (Yunnan Province, China)	Rhizomes	5-Acetylgoniopypyrone **27** 7-Acetylgoniodiol **18** 7-Acetylgoniopypyrone **28** 8-Acetylgoniofufurone **48** 8-Acetylgoniotriol **9** 9-Deoxygoniopypyrone **23** Goniodiol **3** Goniofufurone **47** Goniopypyrone **26** Goniothalamin **1** Goniothalenol **40** Goniotriol **7** Griffithdione **98** (+)-Isoaltholactone **41**	(Y. J. Zhang et al., 1998) (Y. J. Zhang,Zhou, et al., 1999)
G. griffithii Hook f. & Thoms. (Yunnan Province, China)	Roots	Aristolactam AII **102** Aristolactam BII **107** Griffithazanone A **91** Griffithdione **98** Griffithinam **104** Velutinam **106**	(Y. J. Zhang,Kong, et al., 1999)
G. griffithii Hook f. & Thoms. (Yunnan Province, China)	Stems	8-*O*-Acetylgoniotriol **9** 9-Deoxygoniopypyrone **23** Altholactone **40** Goniodiol **3**	(Q. Mu et al., 2003) (S. B. Chen & Yu, 1999)

Table 2.1, continued.

Plants	Parts	Compounds	Reference(s)
G. griffithii Hook f. & Thoms. (Yunnan Province, China)	Stems	Goniofufurone **47** Goniothalamin **1** Goniotharvensin **43** Griffithinam **104** Pinocembrine **94** β-Sitosterol **134** Stigmasterol **133**	(S. B. Chen & Yu, 1999) (Q. Mu et al., 2003) (S. B. Chen & Yu, 1999)
G. howii Merr. & Chun	Barks	Howiinin A **143** Howiinol A **144**	(R. Chen et al., 1998)
G. howii Merr. & Chun	Fruits	Goniothalamin **1**	(L. L. Zhang et al., 1993)
G. kinabaluensis Bân ex Mat Salleh	Roots	5β-Acetoxygoniothalamin **14** 5β-Hydroxygoniothalamin **12** Goniothalamin **1**	(Zakaria et al., 2002)
G. lanceolatus Miq. (Sematan, Sarawak, Malaysia)	Roots	Goniolanceolactam **125** 2-acetyl-3-amino-1,4-naphthoquinone **79**	(Rasol et al., 2018)
G. laoticus (Finet & Gagnep.) Bân (Nakhon Phanom Province, Thailand)	Flowers	(+)-3-Acetylaltholactone **37** 9-Deoxygoniopypyrone **23** (+)-Altholactone **40** Cinnamic acid **131** (+)-Goniofufurone **47** Goniotriol **7** Howiinin A **143** (−)-Nordicentrine **100** β-Sitosterol **134**	(Lekphrom et al., 2009)

Plants	Parts	Compounds	Reference(s)
G. laoticus (Finet & Gagnep.) Bân (Sakon Nakhon Province, Thailand)	Stems	2-*epi*-Altholactone **39** Altholactone **40** Goniopypyrone **26** Griffithazanone A **91** Pinocembrin **94**	(Tip-pyang et al., 2010) (Limpipatwattana & Khumkratok, 2008)
G. leiocarpus (W.T.Wang) P.T Li (Yunnan Province, China)	Stem barks	7-*epi*-Goniodiol **10** Leiocarpin A **30** Leiocarpin B **71** Leiocarpin C **19** Leiocarpin E **68**	(Qing Mu et al., 1999) (Qing Mu et al., 2004)
G. macrocalyx Bân (Ha Giang, Vietnam)	Fruits	3-Deoxycardiobutanolide **54** 7-Acetylaltholactone **37** Macrocalactone **38**	(Trieu et al., 2014)
G. macrophyllus Hook f. & Thoms.		Goniothalamin oxide **2**	(Sam et al., 1987)
G. macrophyllus Hook f. & Thoms.	Stem bark	(+)-Goniothalamin **1** (+)-Goniothalamin epoxide **2** (−)-Pinocembrin **94**	(Ee et al., 2001)
G. macrophyllus Hook f. & Thoms.	Roots & stems	8-*O*-Acetyl-8-*epi*-9-deoxygoniopypyrone **25**	(Fun et al., 2012)
G. macrophyllus Hook f. & Thoms. (Perak, Malaysia)	Roots	Goniolandrene A **149** Goniolandrene B **150** Goniothalamin **1**	(N. Abdullah et al., 2013)
G. malayanus Hook f. & Thoms.	Stem bark	(+)-Isoaltholactone **41**	(Colegate et al., 1990)

Table 2.1, continued.

Plants	Parts	Compounds	Reference(s)
G. marcanii Craib (Loei Province, Thailand)	Stem bark	5-Hydroxy-3-amino-2-aceto-1,4-naphthoquinone **78** Dielsiquinone **85** Marcanine A **86** Marcanine B **87** Marcanine C **88** Marcanine D **89** Marcanine E **90**	(Soonthornchareonnon et al., 1999)
G. marcanii Craib (Nong Khai Province, Thailand)	Leaves & twigs	5-Acetylgoniothalamin **14** 5-Hydroxygoniothalamin **12** Goniopypyrone **26**	(Mahiwan et al., 2013)
G. montanus J. Sinclair	Leaves	(+)-Isoaltholactone **41**	(Colegate et al., 1990)
G. ridleyi King (Kelantan, Malaysia)	Fruit	Goniothalamin **1**	(Ahmad et al., 2015)
	Roots	5-Hydroxygoniothalamin **12**	(Ahmad et al., 2015)
	Stem barks & fruits	5-Acetoxyisogoniothalamin oxide **15**	(Ahmad et al., 2015)
	Stem & root	5-Acetoxygoniothalamin **14** Dehydrogoniothalamin **21**	(Ahmad et al., 2015)
G. ridleyi King (Malaysia)	Stem barks	(+)-Goniothalamin **1** (+)-Goniothalamin epoxide **2** Isoaltholactone **41**	(Ee et al., 1999)
G. scortechinii King (Kelantan, Malaysia)	Fruit peel	Altholactone **40** Goniofufurone **47** Goniopypyrone **26** Goniotriol **7** Pinocembrine **94**	(A. Abdullah et al., 2009)

Plants	Parts	Compounds	Reference(s)
G. scortechinii King	Roots	Scorazanone **93**	(Bin Din et al., 1990)
G. scortechinii King (Satun Province, Thailand)	Roots	8-Chlorogoniodiol **5** Dielsiquinone **85** Goniothalamin **1** Goniothalamin oxide **2** Goniothalaminone A **75** Goniothalaminone B **76**	(Prawat et al., 2012)
G. scortechinii King (Satun Province, Thailand)	Leaves	8-Chlorogoniodiol **5** (–)-8-*epi*-9-Deoxygoniopypyrone **24** (–)-8-*epi*-9-Deoxygoniopypyrone acetate **25** (+)-Altholactone **40** Cryptomeridiol **126** (+)-Goniodiol **3** Goniothalamin **1** Goniothalamin oxide **2**	(Prawat et al., 2012)
G. sesquipedalis (Wall.) Hook f. & Thoms.	Leaves & twigs	β-Sitosterol **134** Goniodiol **3** Goniopedaline **115** Goniotriol **7**	(Talapatra et al., 1988) (Talapatra et al., 1985)
G. sesquipedalis (Wall.) Hook f. & Thoms.	Stem bark	5-Acetoxyisogoniothalamin oxide **15** Goniothalamin **1**	(Hasan et al., 1994) (Hasan et al., 1995)
G. tamirensis Pierre ex Finet & Gagnep (Ha Tinh Province, Vietnam)	Leaves	(+)-8-*epi*-9-Deoxygoniopypyrone **24** (+)-9-Deoxygoniopypyrone **23**	(Tai et al., 2010)

Plants	Parts	Compounds	Reference(s)
G. tamirensis Pierre ex Finet & Gagnep (Nghe-An Province, Vietnam)	Leaves	3,5-Demethoxypiperolide **146** 8-*epi*-9-Deoxygoniopypyrone **24** 8-*epi*-9-Deoxygoniopypyrone acetate **25** 9-Deoxygoniopypyrone **23** (–)-Anonaine **101** Goniodiol **3** Goniotamiric acid **145** Goniothalamin **1** Liriodenine **114**	(Tran et al., 2013)
G. tapis Miq.	Leaves	Arvensin **42** (+)-Isoaltholactone **41** Stigmasterol **133**	(Ee et al., 2000)
G. tapis Miq. (West Sumatran, Indonesia)	Stem bark	3-methyl-1*H*-benz[*f*]indole-4,9-dione **6** Aristolactam AII **102** Aristolactam AIIIa **112** Aristolactam FII **115** Cryptomeridiol **126** Merioesinol **7** Methylpiperolactone **110** Piperolactam B **111** Piperolactam A **113** Scorazone **93**	(Efdi et al., 2010)
G. tapis Miq. (Kelantan, Malaysia)	Roots	(+)-Isoaltholactone **41**	(Colegate et al., 1990)

Table 2.1, continued.

Plants	Parts	Compounds	Reference(s)
G. tapisoides Mat Salleh (Sarawak, Malaysia)	Stem bark	9-Deoxygoniopypyrone **23** Benzamide **127** Cinnamic acid **131** Cryptomeridiol **126** Goniomicin A **147** Goniomicin B **148** Goniomicin C **20** Goniomicin D **8** Goniothalamin **1** Liriodenine **114** Tapisoidin **124**	(Kim et al., 2012)
G. tenuifolius King	Bark	Aristolactam AII **102** Cepharanone B **107** Norcepharadione B **99** Taliscanine **103** Velutinam **106**	(Likhitwitayawuid et al., 1997)
G. tenuifolius King (Phetchaburi Province, Thailand)	Leaves	*trans*-cinnamic acid **131**	(Likhitwitayawuid et al., 2006)
G. thwaitesii Hook. f. & Thoms. (Lalani Botanicals, Sri Lanka)	Aerial	Annulatin **96** Betulinic acid **128** Friedelin **129** Friedelinol **130** Mearnsitrin **97**	(Seidel et al., 2000)
G. umbrosus J. Sinclair (Sabah, Malaysia)	Roots	5-Acetoxygoniothalamin **14** Dehydrogoniothalamin **21** Goniothalamin **1**	(Ahmad & Din, 2002)

Plants	Parts	Compounds	Reference(s)
G. undulatus Ridl. (Phatthalung Povince, Thailand)	Roots	5-Acetoxyisogoniothalamin oxide **15** *O*-Acetylaltholactone **37** Altholactone **40**	(Tantithanaporn et al., 2011)
G. uvaroides King	Roots	5-Acetylgoniothalamin **13** Goniothalamin **1**	(Ahmad et al., 1991)
G. velutinus Airy Shaw	Bark	Aristolactam BII **107** Goniothalamin **1** Goniothalenol **40** Ouregidione **116** Velutinam **106**	(Omar et al., 1992) (Ee, 1998)
G. wightii Hook. f. & Thoms.	Leaves	Goniothalamin **1**	(Harikumar et al., 2008)
G. wynaadensis Bedd. (Kerala, India)	Leaves	8-Acetoxy goniofufurone **48** Altholactone **40** Aristolactam BII **107** Goniopypyrone **26** Goniothalamin **1** β-Sitosterol **134**	(Ajithabai et al., 2011)
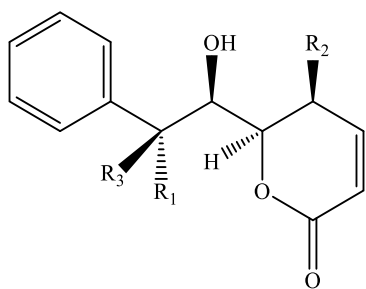
	R₁	R₂	R₃
5	Cl	H	H
6	OMe	H	H
7	OH	OH	H
8	OH	OEt	H
9	OAc	H	H
10	H	H	OH
11	H	OH	OH
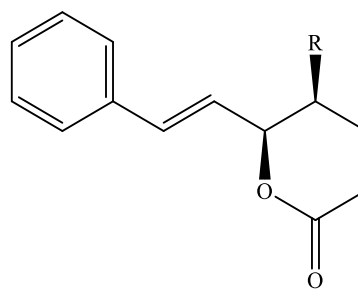
	R
12	OH
13	Ac
14	OAc
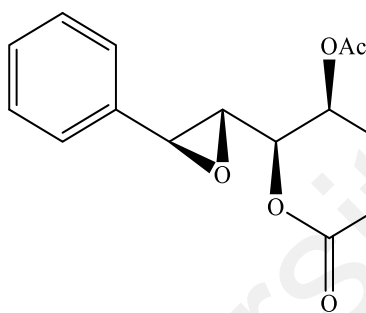
15
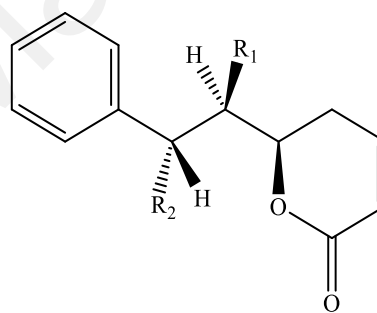
	R₁	R₂
16	OAc	OH
17	OH	OAc
18	Ac	OH
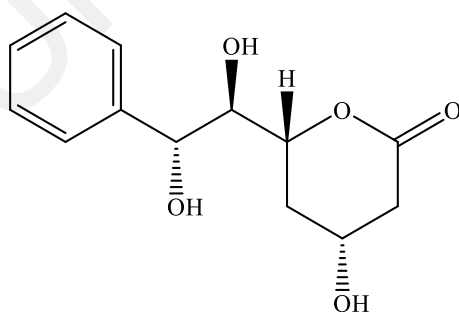
19
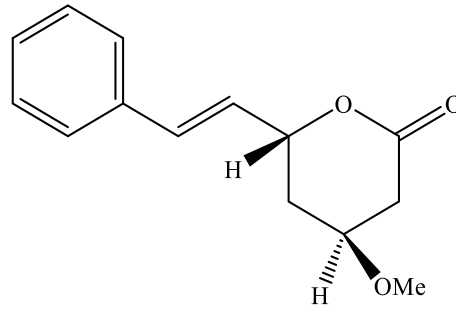
20

Figure 2.3: Chemical constituents isolated from *Goniothalamus* species.
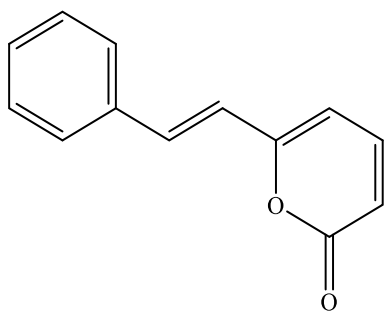
21
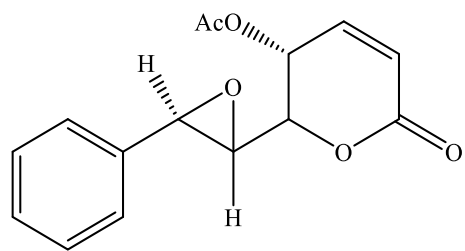
22
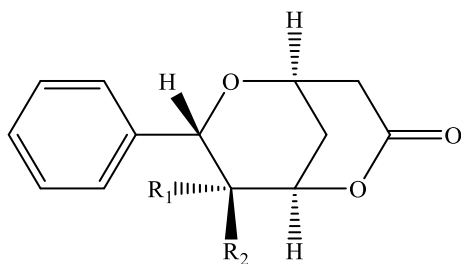
	R₁	R₂
23	OH	H
24	H	OH
25	H	OAc
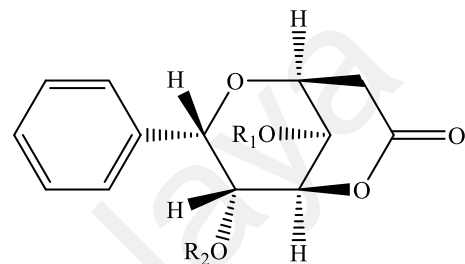
	R₁	R₂
26	H	H
27	Ac	H
28	H	Ac
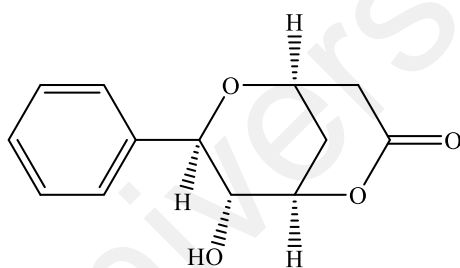
29
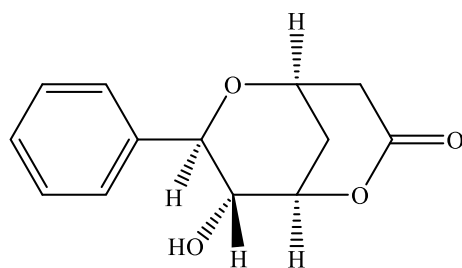
30
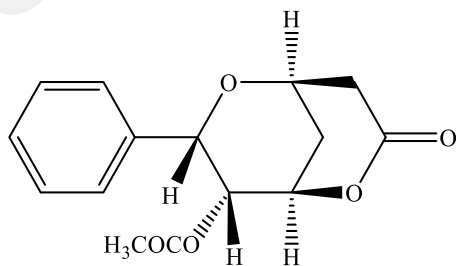
31

32

Figure 2.3, continued.

35
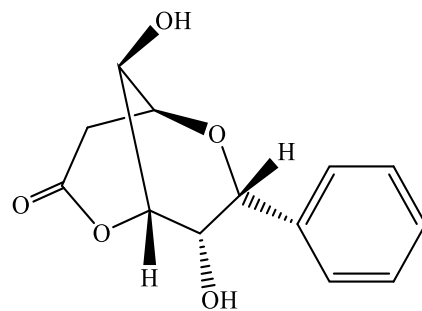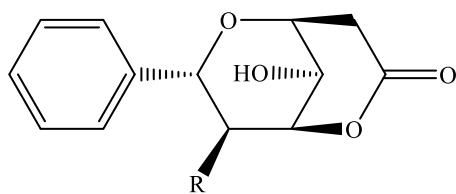
	R
33	OH
34	OAc
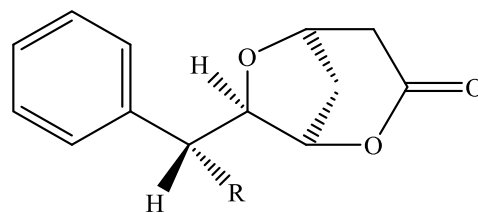
	R
35	OH
36	OAc
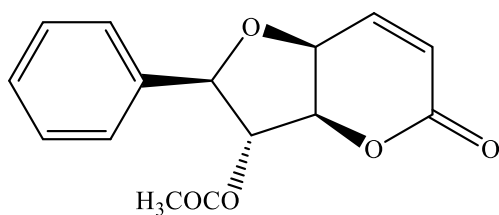
37
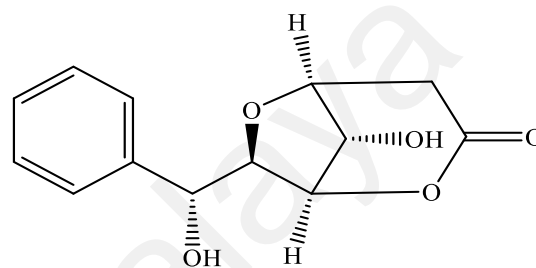
38
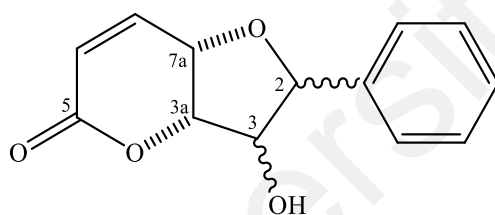
39	2,3-*cis*; 3,3a-*trans*
40	2,3-*trans*; 3,3a-*trans*
41	2,3-*trans*; 3,3a-*cis*
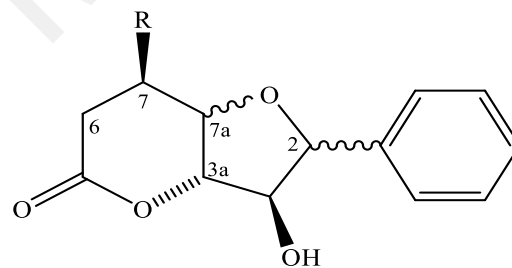
	R	
42	OH	7,7a-*cis*; 7a,3a-*trans*
43	H	7a,3a-*cis*
44	OEt	7,7a-*trans*; 7a,3a-*cis*
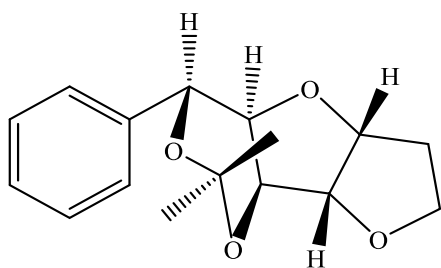
45
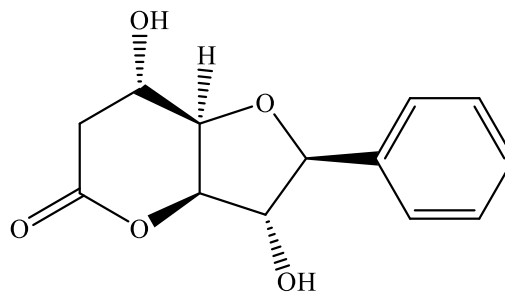
46

Figure 2.3, continued.
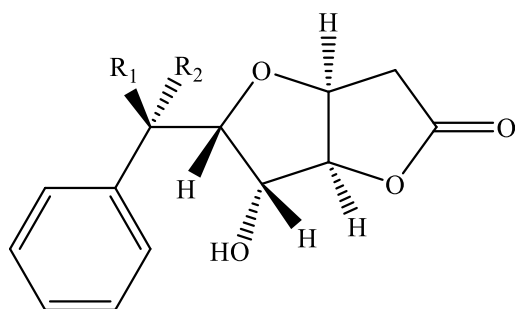
	R₁	R₂
47	H	OH
48	H	OAc
49	OH	H
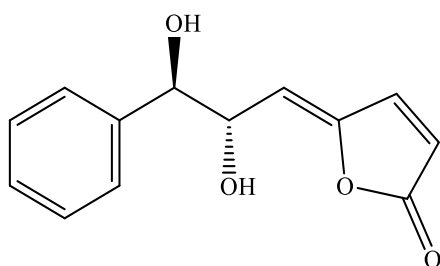
50
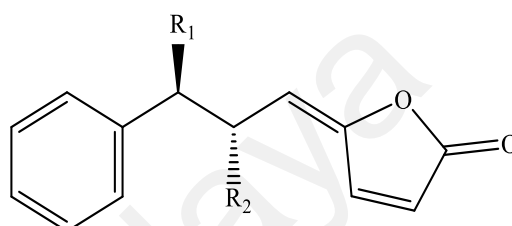
	R₁	R₂
51	OH	OH
52	OAc	OH
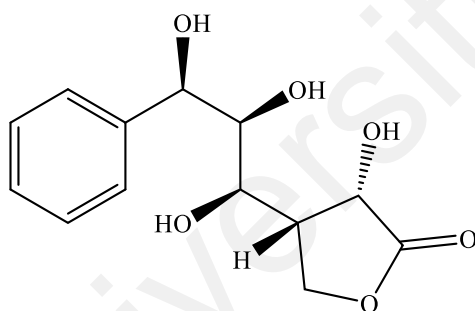
53
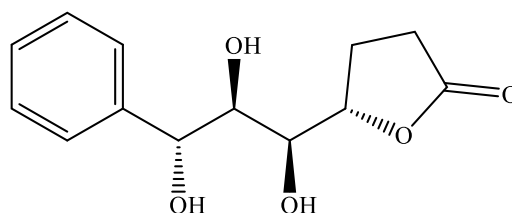
54
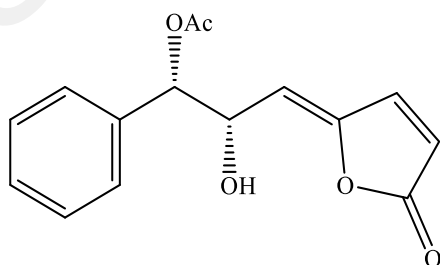
55
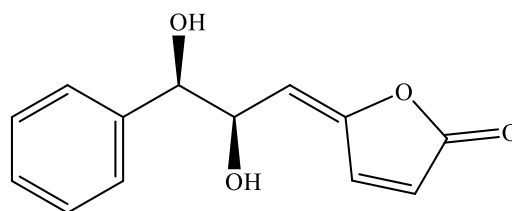
56

Figure 2.3, continued.

37
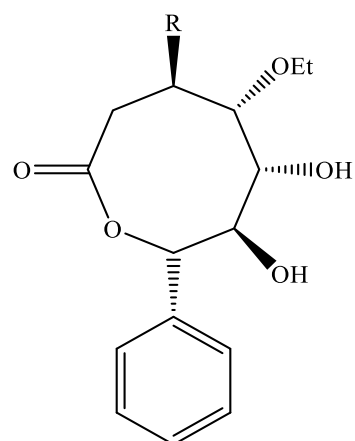
	R
57	OEt
58	H
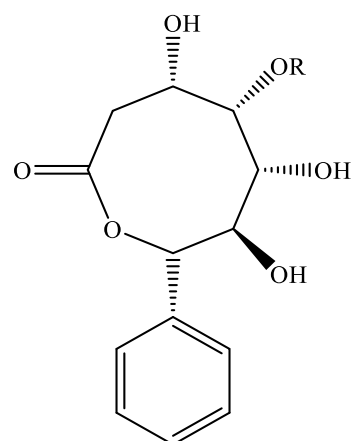
	R
59	Me
60	Et
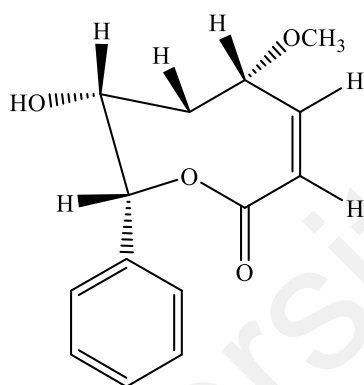
61
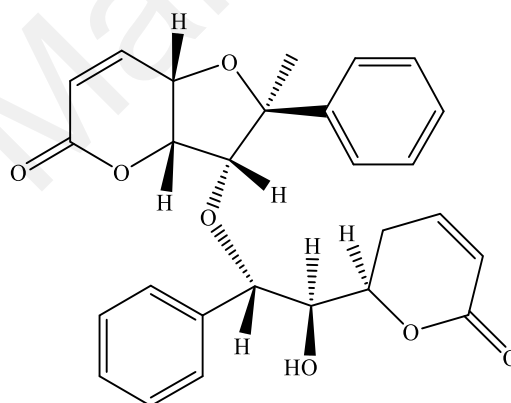
62
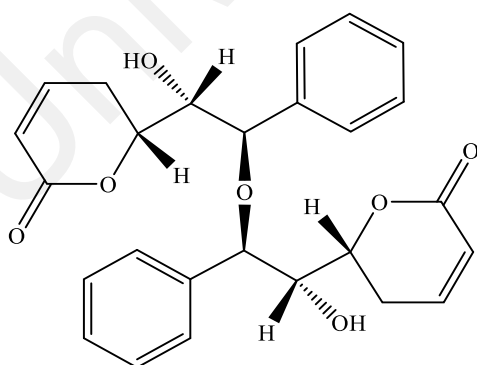
63
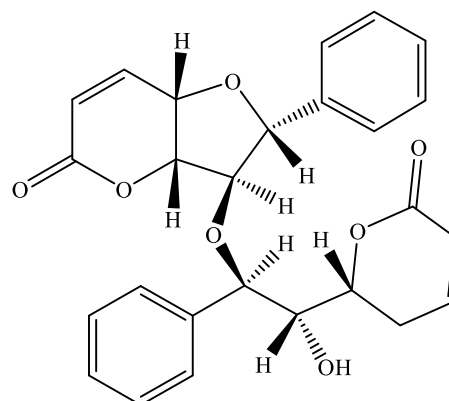
64

Figure 2.3, continued.
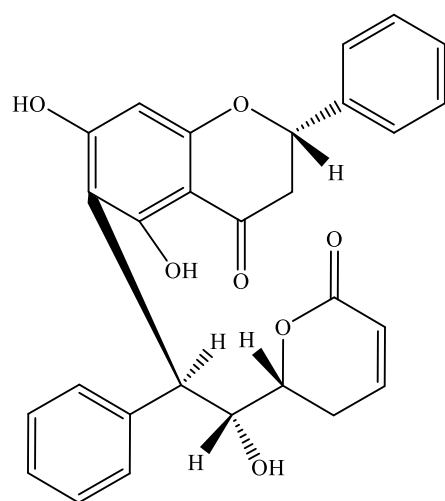
65
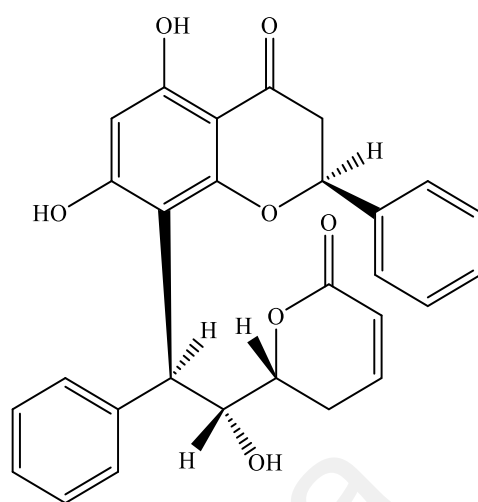
66
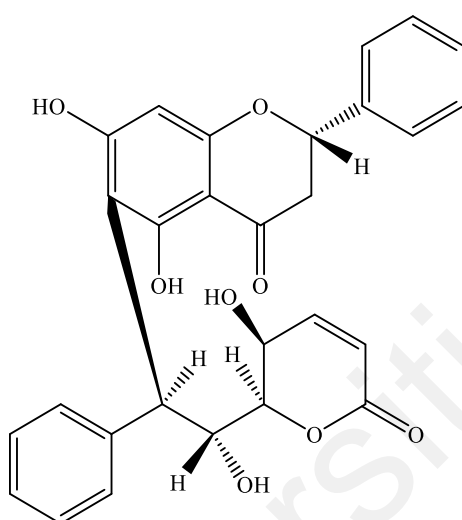
67
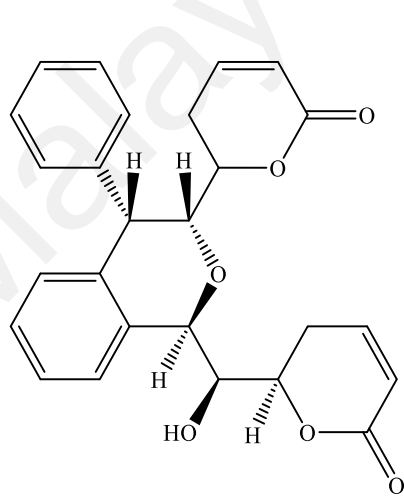
68

69

70
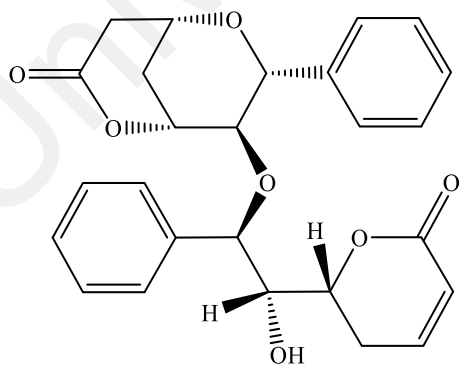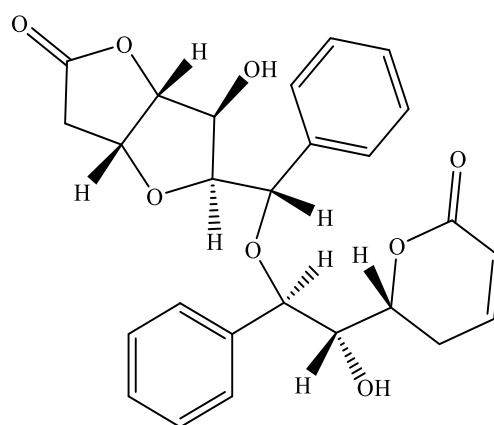
Figure 2.3, continued.
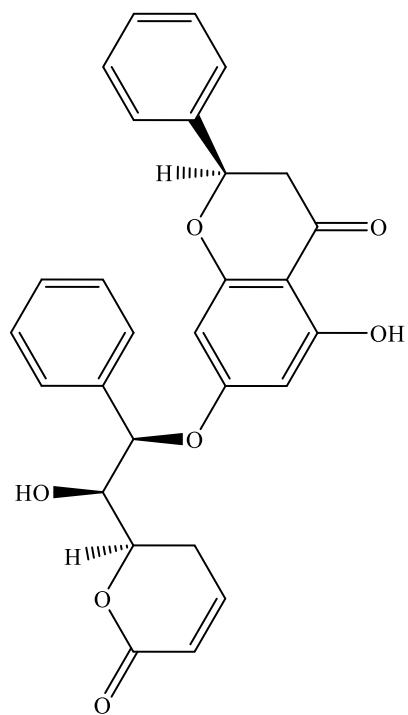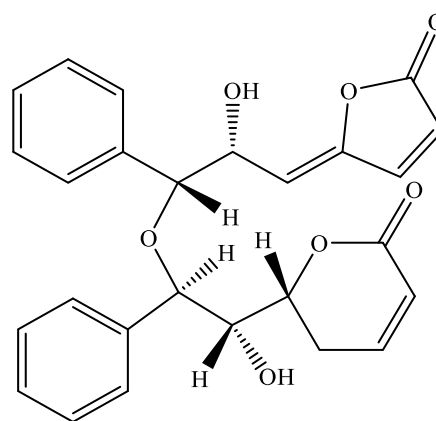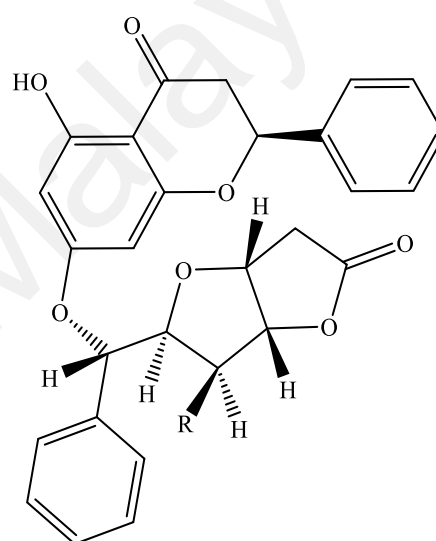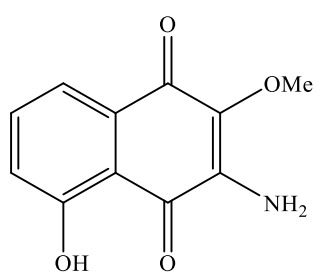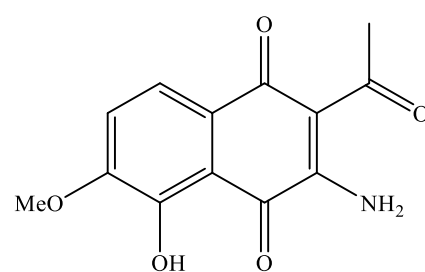
Figure 2.3, continued.
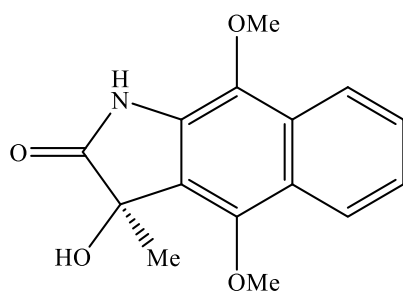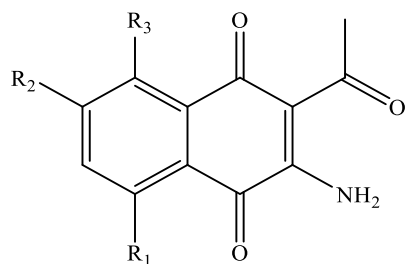
	R_1	R_2	R_3
78	OH	H	H
79	H	H	H
80	H	OMe	OH
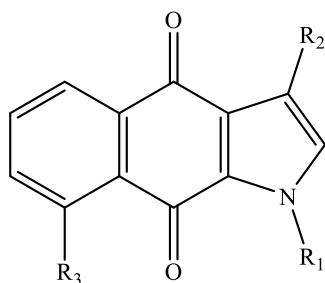
	R_1	R_2	R_3
81	H	Me	H
82	Me	COOH	OH
83	Me	COOH	H
84	H	COOMe	H
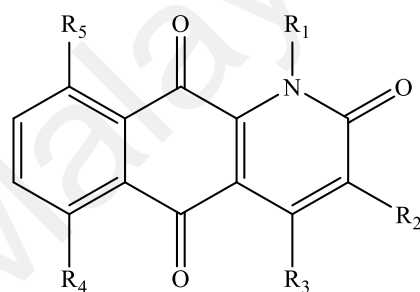
	R_1	R_2	R_3	R_4	R_5
85	H	OMe	Me	H	H
86	H	H	Me	H	H
87	Me	OMe	Me	H	H
88	Me	OMe	EtOH	H	H
89	H	OMe	Me	OH	H
90	Me	OMe	Me	H	OH

	R
91	OH
92	H

Figure 2.3, continued.

94

95

96

97
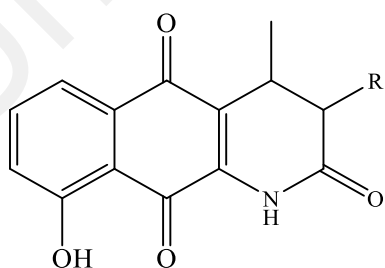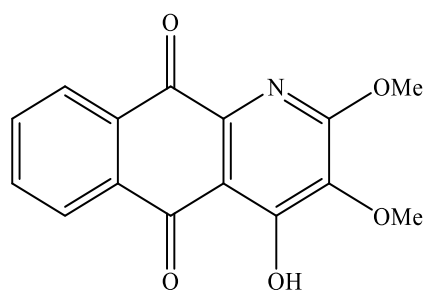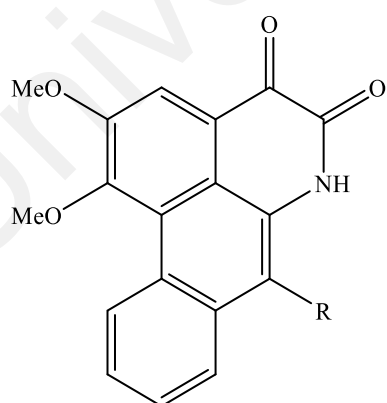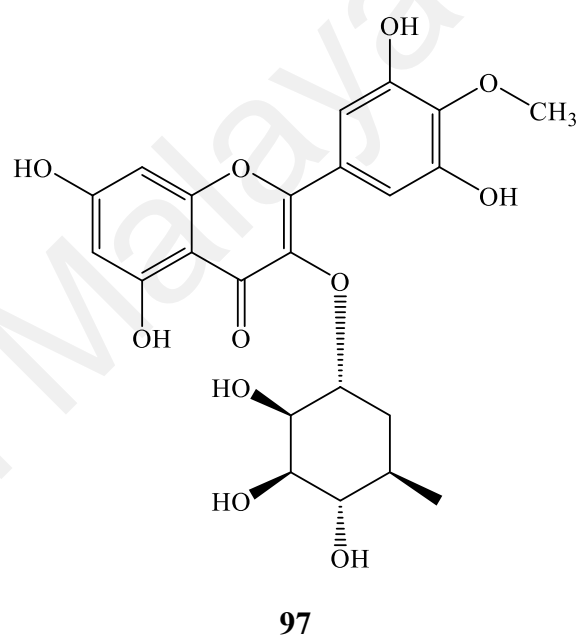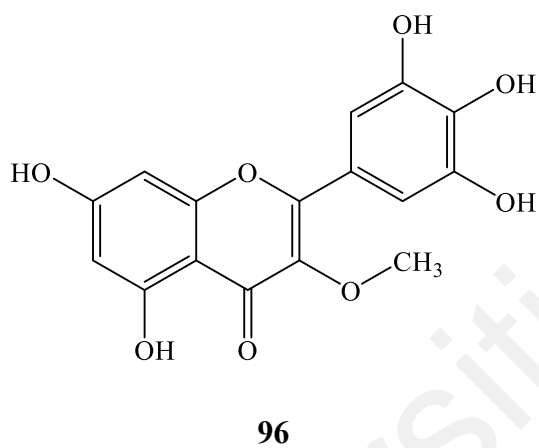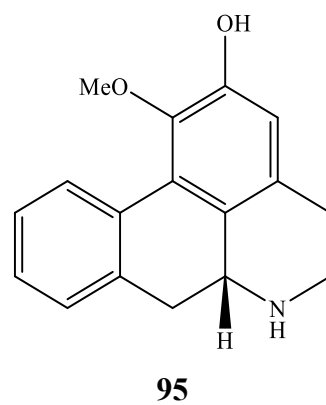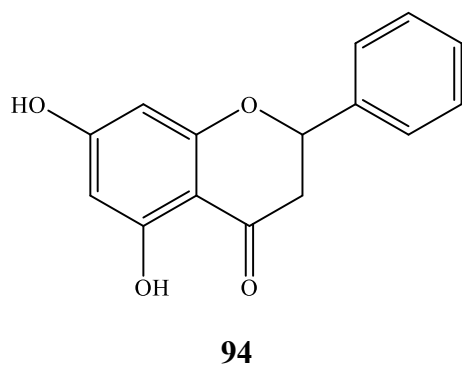
	R
98	Me
99	H
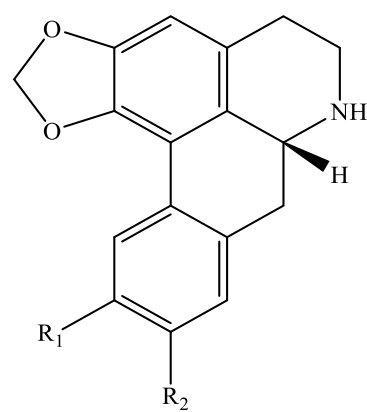
	R₁	R₂
100	OMe	OMe
101	H	H

Figure 2.3, continued.
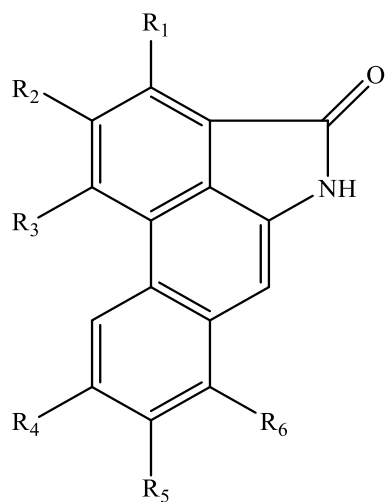
	R$_1$	R$_2$	R$_3$	R$_4$	R$_5$	R$_6$
102	H	OH	OMe	H	H	H
103	H	OMe	OMe	H	H	OMe
104	H	OMe	OH	H	H	OMe
105	H	OMe	OMe	H	OH	H
106	H	OMe	OMe	H	H	OH
107	H	OMe	OMe	H	H	H
108	H	H	OMe	H	OH	H
109	H	OH	OMe	H	H	OMe
110	OMe	OMe	OMe	H	H	H
111	H	OMe	OMe	H	H	H
112	H	OH	OMe	OH	H	H
113	H	OMe	OH	H	H	H
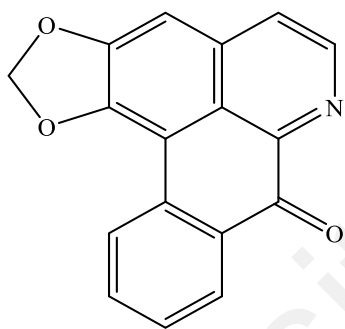
114
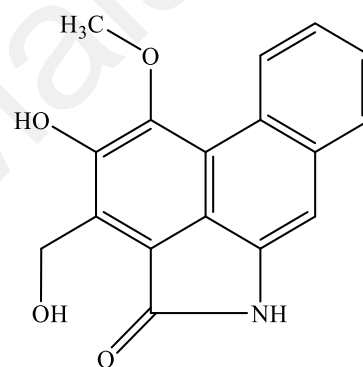
115
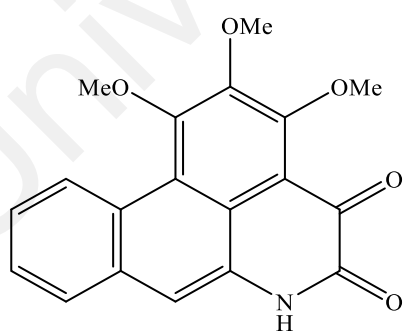
116
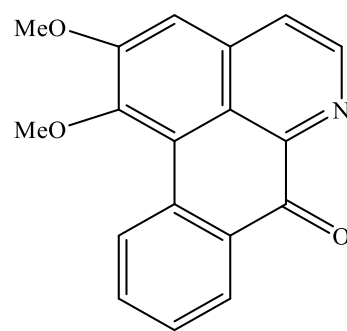
117

Figure 2.3, continued.
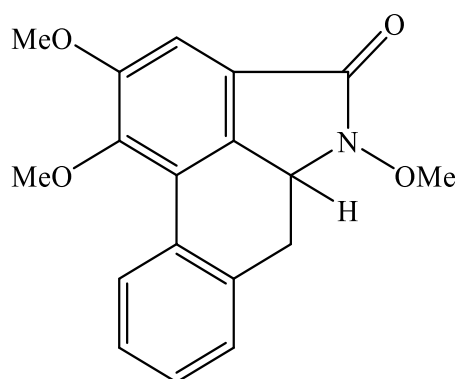
118
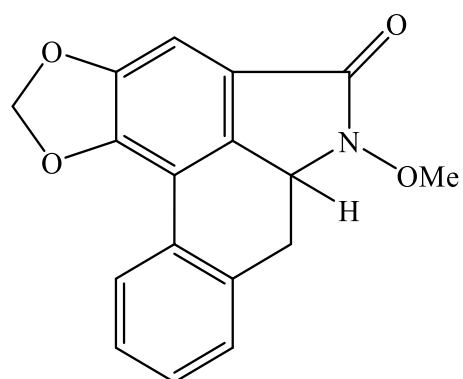
119
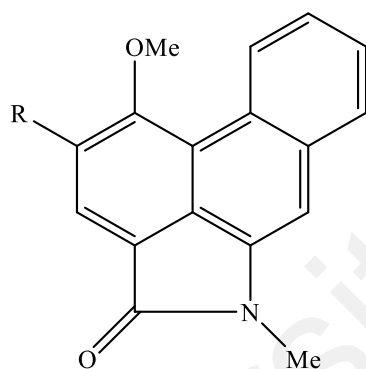
	R
120	OMe
121	OH
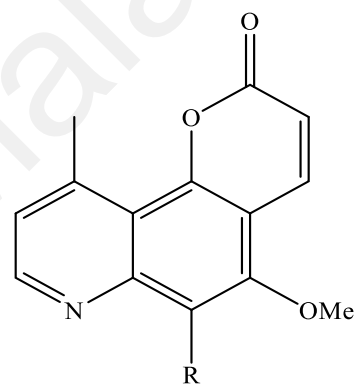
	R
122	OMe
123	OH
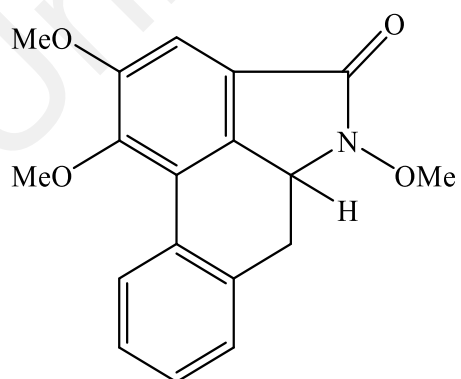
124
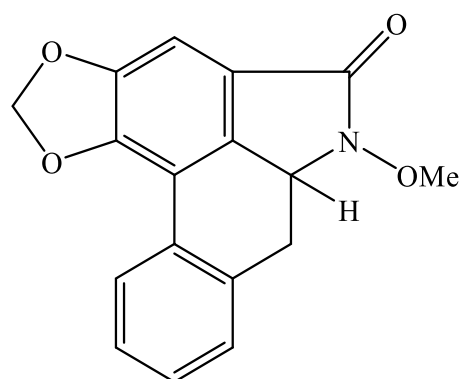
125

Figure 2.3, continued.
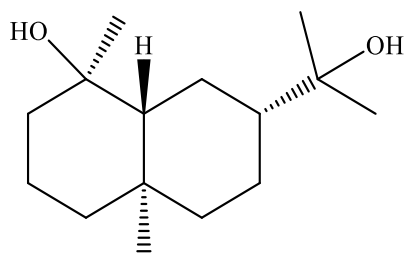
126
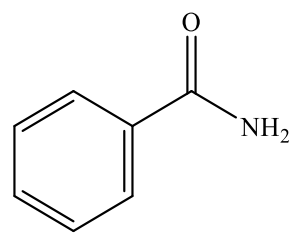
127
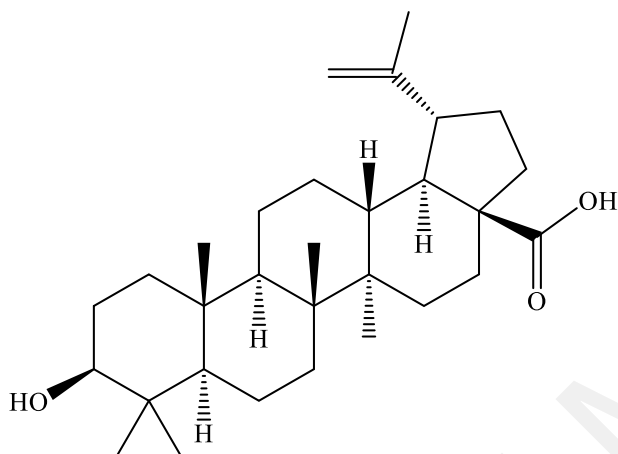
128
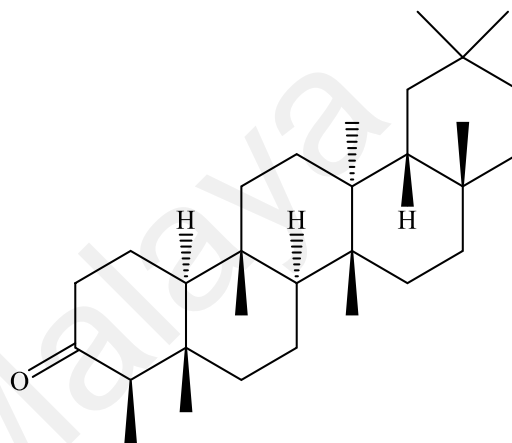
129
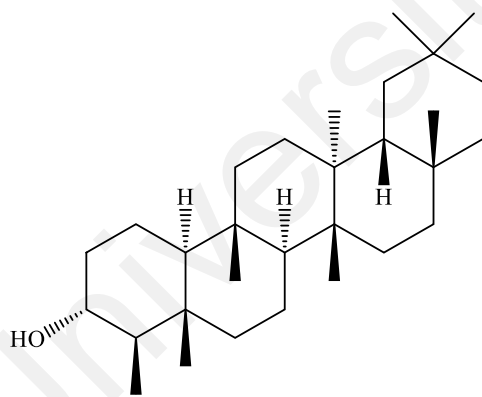
130
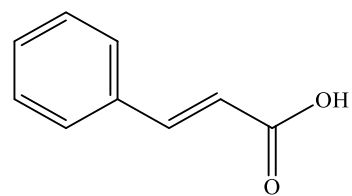
131

132
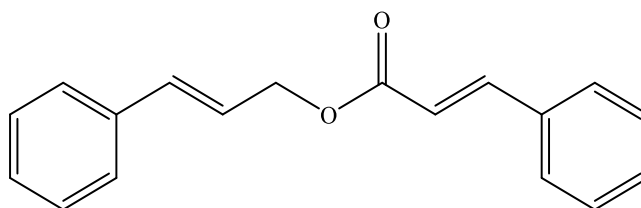
Figure 2.3, continued.
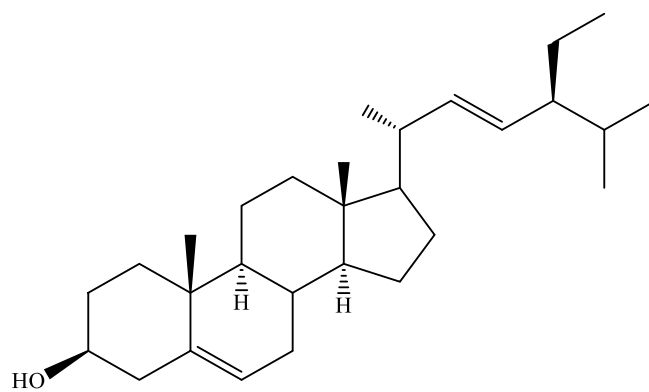
133
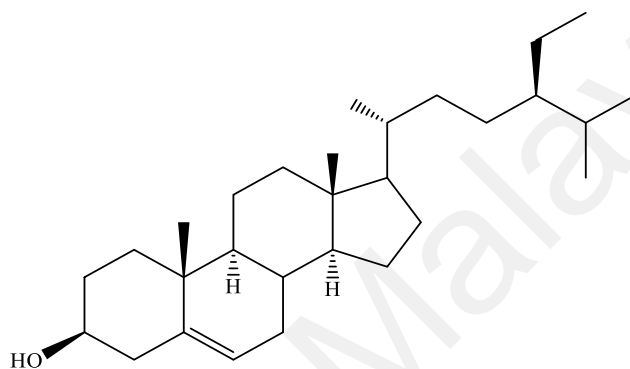
134
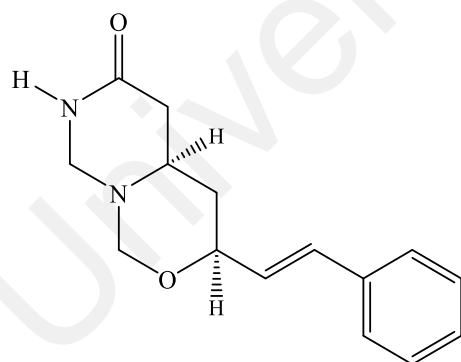
135
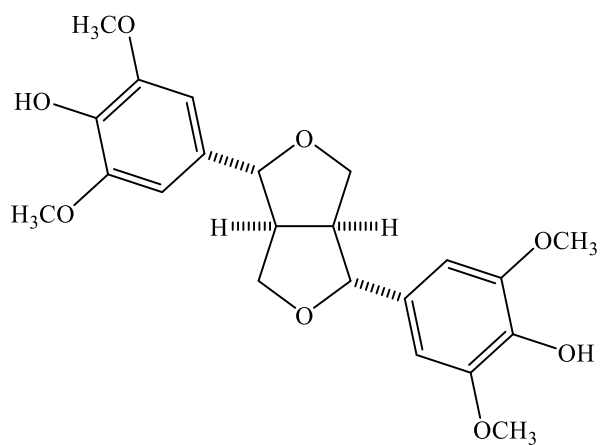
136

Figure 2.3, continued.
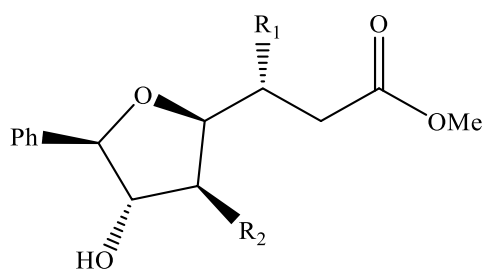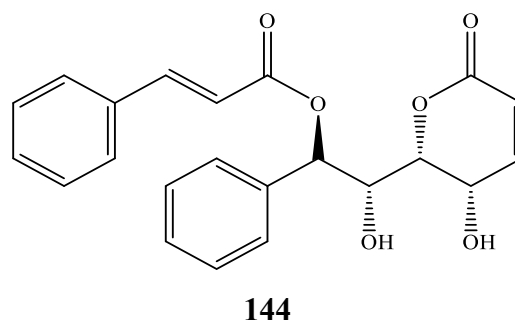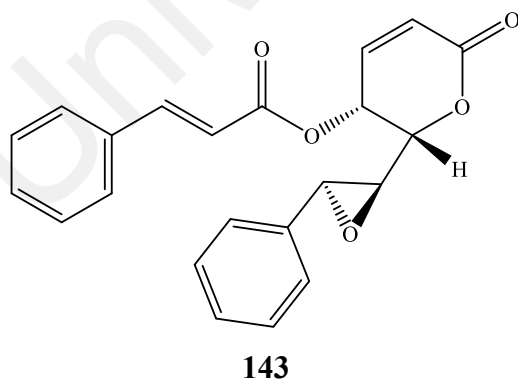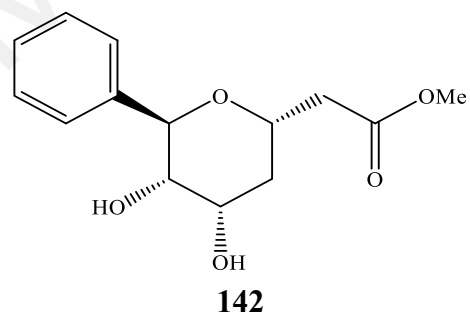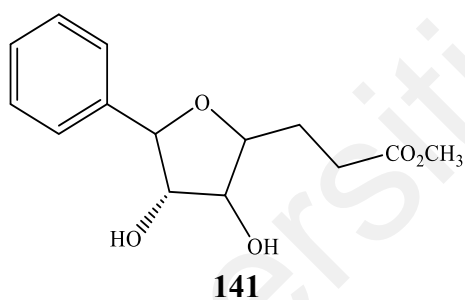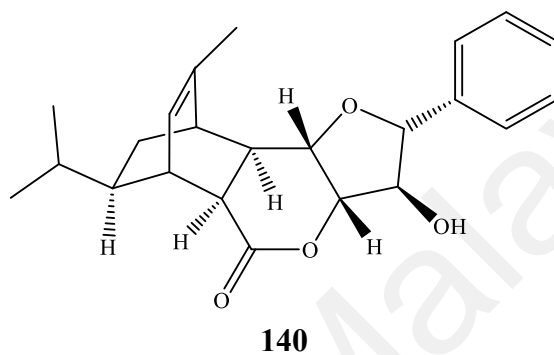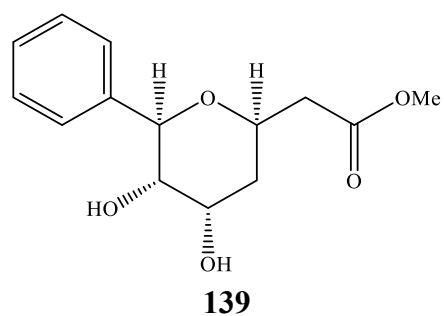
Figure 2.3, continued.
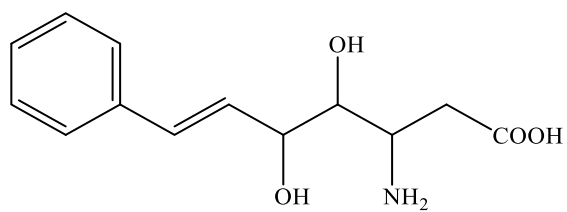
145
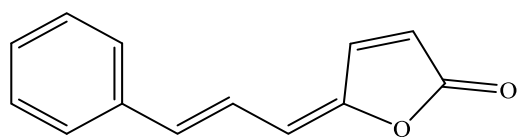
146
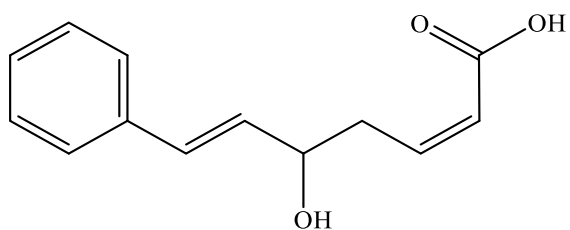
147
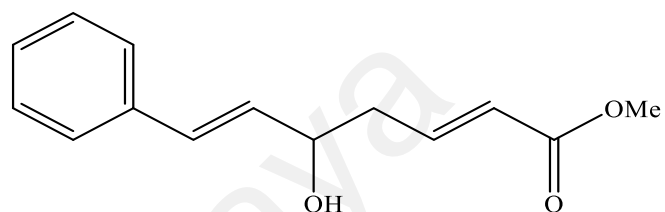
148
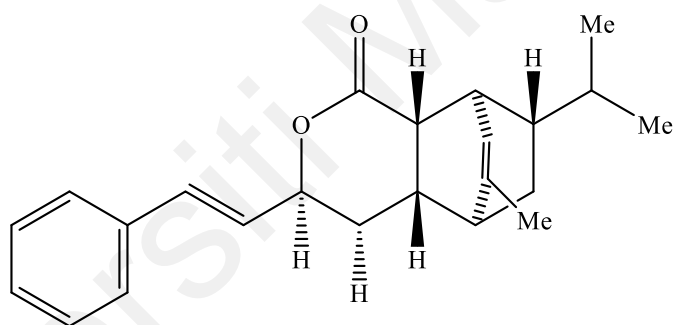
149
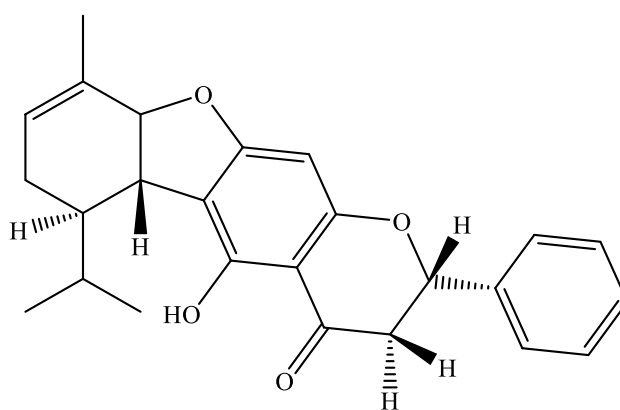
150

Figure 2.3, continued.

CHAPTER 3 : EXPERIMENTAL

3.1 Plant Materials

Goniothalamus tapis

The stem bark of *Goniothalamus tapis* was collected from Kampung Bukit Jering, Jeli, Kelantan, Malaysia on 6th August 2010 by Mr. Din bin Muhammad Nor. The sample (**Figure 1.1**) with voucher specimen number KL5744, was identified by Mr. Teo Leong Eng and deposited in herbarium of the Department of Chemistry, Faculty of Science, University of Malaya.

Goniothalamus tapisoides

The stem bark of *Goniothalamus tapisoides* was collected from Sarawak. The voucher specimen is HUMS 000108. The plant was identified by Prof. Dr. Kamruddin Mat Salleh from National Univeristy of Malaysia (UKM).

3.2 Instrumentation

- NMR spectra were obtained using JEOL LA400 FT NMR, JEOL ECA400 FT NMR Spectrometer System and Bruker AVN400 FT NMR.

- Reverse phase Recycling HPLC using a JAIGEL-ODS-AP-30, SP-120-15 column. HPLC grade methanol, acetonitrile and deionized water were used as mobile phase solvents.

- Mass spectra were obtained from Agilent Technologies 6530 Accurate-Mass Q-TOF LC/MS, with ZORBAX Eclipse XDB-C18 Rapid Resolution HT 4.6 mm i.d. × 50 mm × 1.8 μm column. HPLC grade methanol, acetonitrile and deionized water were used as mobile phase solvents. All solvents and samples were filtered with 0.2 μm nylon membrane filter (WHATMAN) prior to LCMS analysis.

- UV spectra were recorded on a Shimadzu UV-Visible Recording Spectrophoto-meter using AR grade ethanol as solvent with mirror UV cell.

- The infrared (IR) spectra were obtained through Perkin Elmer FT-IR Spectrometer Spectrum RX1.

3.3   Chemical and reagents

All solvents used in extraction and isolation with column chromatography are of AR grade. Those used for bulk extraction were distilled prior to use. The solvents used were hexane, dichloromethane, methanol, ethyl acetate and ammonia solution. Deuterated solvents (eg. $CDCl_3$, CD_3OD, C_5D_5N) were used to dissolve sample for the purpose to acquire 1D- and 2D- NMR spectra.

3.3.1   Preparation of detecting reagent

The identification for the isolated compounds with different type of skeleton were detected by various reagent. The reagents were vanillin and anisaldehyde-sulphuric acid. the procedure for the preparation of the used reagent were described below:

3.3.1.1   Vanillin-Sulphuric Acid

Vanillin (1.0 g) in concentrated H_2SO_4 (10 ml) was added upon cooling to 90 ml of ethanol before spraying onto the colours had occurred. The TLC plate was then heated at ~50ºC until full development of the colours had occurred. The occurrence of blue, purple, grey or brown spots indicated the presence of styryl-lactones.

3.3.1.2   Anisaldehyde-Sulphuric Acid

Anisaldehyde (0.5 ml) was added in glacial acetic acid (50 ml) and 1 ml concentrated H_2SO_4. After the reagent was sprayed onto the TLC plate, the TLC plate was then heated to ~105ºC until maximum visualization of spots had occurred. The occurrence of purple,

blue, red, grey or green spots indicated the presence of phenols, sugars, steroids, and terpenes.

3.4 Isolation techniques

The crude extracts of dichloromethane and methanol of the barks of *G. tapis* and *G. tapisoides* was further investigate using various separation techniques such as Thin Layer Chromatography (TLC), Column Chromatography (CC), and Recycling High-Performance Liquid Chromatography (Recycling HPLC) to obtain pure compounds.

3.4.1 Thin Layer Chromatography (TLC)

Aluminium supported silica gel 60 F254 plates were used to visualize the spots of the isolated compounds. UV Light Model UVGL-58 Mineralight Lamp 230 V~50/60 Hz was used to examine spots or bands on the TLC after spraying with the specified reagents.

3.4.2 Column Chromatography (CC)

Silica gel 60, 230-400 mesh ASTM (Merck 9385) was used for column chromatography on hexane and dichloromethane crude extracts. A slurry of silica gel 60 (approximately 30:1 silica gel to sample ratio) in hexane solvent system was poured into a glass column of appropriate size with gentle tapping to remove trapped air bubbles.

The other two mediums used for column chromatography were C-18 reversed phase silica gel and Sephadex LH-20. These two mediums were used for methanol crude extract which have more polar compounds. C-18 reversed phase silica gel (approximately 30:1 silica gel to sample ratio) was dissolved in methanol and water solvent mixtures and loaded into the column. While Sephadex LH-20 was soaked in methanol:water (10:90) solvent to allow it to swell. A long glass column with narrow width is preferable, because Sephadex LH-20 is designed to separate mixtures of molecules based on the size and

molecular structure. When these mediums were used, the silica gel or Sephadex LH-20 was slowly loaded into the column to avoid formation of air bubbles.

The crude extract was initially dissolved in a minimum amount of solvent and loaded on top of the packed column. The extract was eluted with an appropriate solvent system at a certain flow rate. Fractions were collected in either conical flasks or test tubes and evaporated for the next step. Fractions with similar compounds were then combined after TLC monitoring.

3.4.3   Recycling HPLC

Recycling HPLC model used is JAIGEL-ODS-AP-30 series, the column is a large scale preparative column (30.0 mm × 250 mm), packed with highly pure silica gel bonded octadecylsilyl (ODS or C-18) groups. All samples are dissolved in the minimum amount of solvent and injected into the isocratic column. The solvent used to dissolve the sample is the solvent system of the mobile phase. This is to avoid any polarity differences, as small changes of solvent polarity might greatly affect the speed of compound being eluted and peaks might shift and overlap with the neighbouring peaks.

The flow rate and solvent system of the mobile phase is fixed throughout the experiment. The samples was eluted or recycled with an appropriate solvent system at a certain flow rate to acquire the ideal separation. The intensity of peaks is based on UV absorbance of the samples. Separated peaks were collected and sent for proton NMR spectroscopy.

3.5   Extraction, isolation and purification of the secondary metabolites

The experimental details of extraction, isolation and purification of secondary metabolites from the stem barks of *G. tapis* and *G. tapisoides* were described in section 3.5.1 and 3.5.2 respectively.

3.5.1 Extraction, isolation and purification of *G. tapis*

The experimental details of extraction, isolation and purification of secondary metabolites from the stem barks of *G. tapis* will be described in this section 3.5.1.

3.5.1.1 Extraction of *G. tapis*

The extraction of dried and milled stem bark was carried out by the cold percolation method. Dried ground bark (1.5 kg) was macerated with hexane (3 × 4 L, each 48 hours) at room temperature. The hexane extract was then evaporated using rotary-evaporator and a yellow gummy extract (20.6 g) was obtained. The plant material was then subjected to dichloromethane and methanol extraction successively (3 × 4 L, each 48 hours) at room temperature. The extracts were then evaporated using a rotary-evaporator. The dichloromethane crude (87.2 g) was obtained as brown gummy residue while the methanol extract (220.5 g) was obtained as a brown amorphous powder.

3.5.1.2 Purification of compounds from dichloromethane extract of *G. tapis*

20 g of dichloromethane (CH_2Cl_2) crude extract of *G. tapis* was subjected to column chromatography fractionation over silica gel (230-400 mesh) to give 9 fractions (F1-F9). The fractionation was based on the gradient elution method. The amount of silica gel used was based on the ratio 1 g of crude extract to 30 g of silica gel. Each fraction was tested on thin layer chromatography (TLC) and subjected to repeated column chromatography (CC) until a single spot on the TLC was obtained. Compounds were isolated from some fractions as shown in **Scheme 3.1**.

Fraction 2 (Hex/CH_2Cl_2, 10:90, 0.586 g) was further fractionated by CC over silica gel, eluting gradient with gradient solvent system 90:10 to 80:20 of hexane: ethyl acetate (EA) to furnish a mixture of **133** and **134** (20.4 mg), and a compound **1** (3.5 mg). Fraction 4 (CH_2Cl_2/MeOH, 99.5:0.5, 1.322 g) was also purified by CC eluted with gradient solvent system 70:30 to 20:80 of hexane: EA to yield **41** (62.9 mg), **22** (3.9 mg) and **151** (2.1 mg).

Fraction 8 (CH$_2$Cl$_2$/MeOH, 97.5:2.5, 0.527 g) was subjected to silica gel CC, using gradient solvent system 99.5:0.5 to 98.5:1.5 of CH$_2$Cl$_2$:MeOH to yield **49** (3.7 mg) and **26** (3.3 mg).

```
                      ┌────────────────────────────────┐
                      │  DCM crude of G. tapis (20 g)   │
                      └────────────────────────────────┘
```

F1	F3	F5	F7	F9
Hex : DCM	100% DCM	DCM : MeOH	DCM : MeOH	DCM : MeOH
(5 : 5)		(99 : 1)	(98 : 2)	(97 : 3)

F2	F4	F6	F8
Hex : DCM	DCM : MeOH	DCM : MeOH	DCM : MeOH
(1 : 9)	(99.5 : 0.5)	(98.5 : 1.5)	(97.5 : 2.5)

Goniothalamin **1** (3.5 mg)
Stigmasterol **133** &
β-sitosterol **134** (20.4 mg)

Goniopypyrone **26** (3.3 mg)
7-*epi*-Goniofufurone **49** (3.7 mg)

Cheliensisin A **22** (3.9 mg)
Isoaltholactone **41** (62.9 mg)
3-acetylisoaltholactone **151** (2.1 mg)
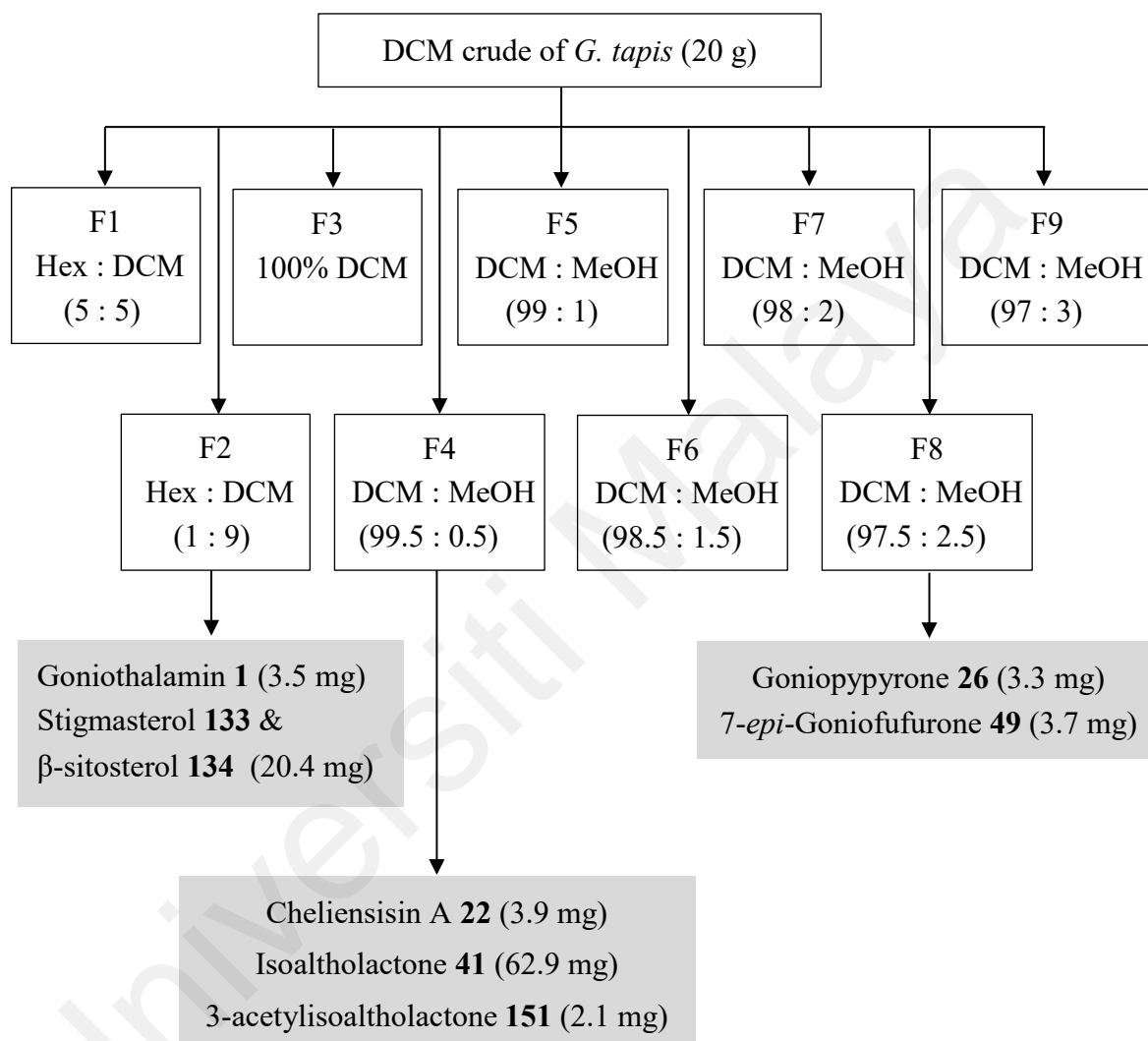
Scheme 3.1: Isolation and purification of compounds from the CH$_2$Cl$_2$ crude extract of the bark of *G. tapis*.

3.5.1.3   Purification of compounds from methanol extract of *G. tapis*

3 g of methanol crude extract was subjected to column chromatography (CC) fractionation over C-18 reversed phase silica gel. The fractionation was based on the gradient elution method. Nine fractions were acquired.

Fraction 3 (0.164 g) was then subjected to column chromatography over Sephadex LH-20. Isocratic elution method was used in this medium, because the isolation is based on molecular structure. The same solvent system as in the first CC fractionation was used, which is 60 H_2O: 40 MeOH. A styryl-lactone was isolated, which is **4** (3.1 mg) as shown in **Scheme 3.2**.

```
                    Methanol crude of G. tapis (3 g)
                                   |
   ┌──────────┬──────────┬──────────┬──────────┬──────────┐
   ▼          ▼          ▼          ▼          ▼
┌──────┐   ┌──────┐   ┌──────┐   ┌──────┐   ┌──────┐
│  F1  │   │  F3  │   │  F5  │   │  F7  │   │  F9  │
│H₂O:MeOH│ │H₂O:MeOH│ │H₂O:MeOH│ │H₂O:MeOH│ │100% MeOH│
│(8 : 2)│  │(6 : 4)│  │(4 : 6)│  │(2 : 8)│  │      │
└──────┘   └──────┘   └──────┘   └──────┘   └──────┘
      │          │          │          │
      ▼          ▼          ▼          ▼
   ┌──────┐   ┌──────┐   ┌──────┐   ┌──────┐
   │  F2  │   │  F4  │   │  F6  │   │  F8  │
   │H₂O:MeOH│ │H₂O:MeOH│ │H₂O:MeOH│ │H₂O:MeOH│
   │(7 : 3)│  │(5 : 5)│  │(3 : 7)│  │(1 : 9)│
   └──────┘   └──────┘   └──────┘   └──────┘
                   │
                   ▼
         Garvensintriol 4 (3.1 mg)
```

Chart: Methanol crude of *G. tapis* (3 g) branches into F1 H_2O: MeOH (8 : 2), F3 H_2O: MeOH (6 : 4), F5 H_2O: MeOH (4 : 6), F7 H_2O: MeOH (2 : 8), F9 100% MeOH; and second row F2 H_2O: MeOH (7 : 3), F4 H_2O: MeOH (5 : 5), F6 H_2O: MeOH (3 : 7), F8 H_2O: MeOH (1 : 9); with Garvensintriol **4** (3.1 mg).

Scheme 3.2: Isolation and purification of compounds from the MeOH crude extract of the bark of *G. tapis*.

3.5.2 Extraction, isolation and purification of *G. tapisoides*

The experimental details of extraction, isolation and purification of secondary metabolites from the stem barks of *G. tapisoides* will be described in this section.

3.5.2.1 Extraction of *G. tapisoides*

The extraction of dried and milled stem bark was carried out by the cold percolation method. Dried ground bark (1.0 kg) was macerated with hexane (3 × 4 L, each 48 hours) at room temperature. The hexane extract was then evaporated using rotary-evaporator and

a yellow amorphous powder extract (25.2 g) was obtained. The plant material was then subjected to dichloromethane and methanol extraction successively (3 × 4 L, each 48 hours) at room temperature. The extracts were then evaporated using a rotary-evaporator. The dichloromethane (43.3 g) and methanol (24.5 g) crudes were obtained as brown gummy residue.

3.5.2.2   Purification of compounds from dichloromethane fraction of *G. tapisoides*

After few CC fractionations of Fraction 7 (CH$_2$Cl$_2$/MeOH, 98:2, 0.627 g) eluted from dichloromethane crude of *G. tapisoides*. A sample (120 mg) with three compounds mixture was acquired. It doesn't separated by the method CC fractionation, therefore, it was subjected into recycling HPLC. The recycling HPLC isolation was based on the isocratic elution method, with 60 MeOH : 40 H$_2$O and flow rate is 5 ml/min.

As shown in Figure 3.1, during the first cycle, three narrow peaks appeared closely and overlapping with one another. In order to separate them into three individual peaks, the sample is allowed to pass through the column for two more round. The compounds were collected when the peaks appeared to be single and isolated. This is to ensure collected compound from every single fraction is pure and clean.
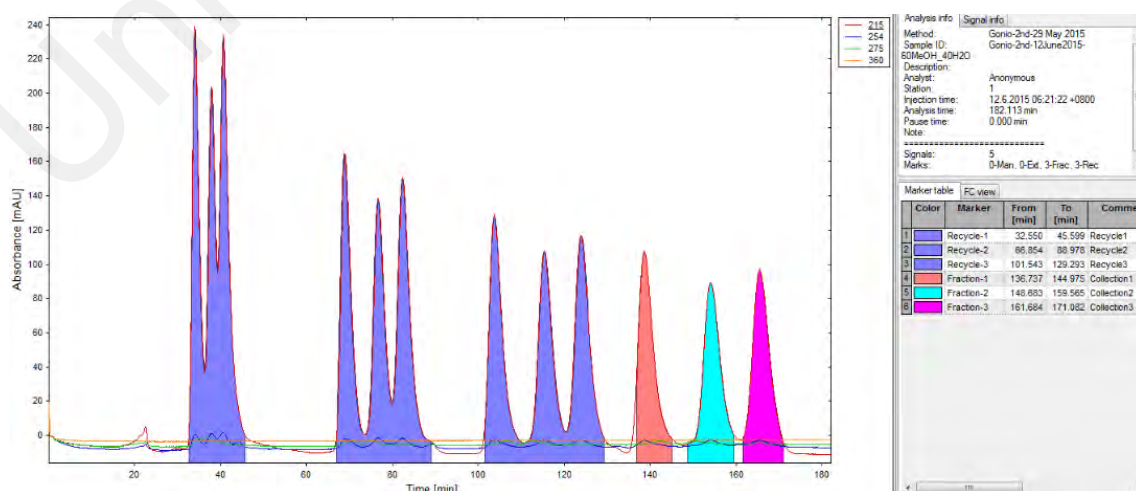
Figure 3.1: Recycling HPLC chromatogram for fraction eluted from F7.

The first compound collected was goniodiol **3**, it was eluted starting from 136.74 minutes to 144.98 minutes. Second collection occurred at 148.68 – 159.57 minutes, compound acquired was 8-*epi*-9-deoxygoniopypyrone **24**. The third compound, 7-*epi*-goniodiol **10**, was earned from the last collection at 161.68 – 171.08 minutes.

3.5.2.3   Purification of compounds from methanol extract of *G. tapisoides*

3 g of methanol crude extract was subjected to column chromatography fractionation over C-18 reversed phase silica gel. The isolation was based on the gradient elution method. Nine fractions were acquired. Each fraction was tested on reversed phase thin layer chromatography (TLC) and subjected into repeated column chromatography (CC) over Sephadex LH-20 until a single spot on the TLC was obtained. Compounds were isolated from some fractions as shown in **Scheme 3.3**.

All fractions were then subjected to CC over Sephadex LH-20. Isocratic elution method was used in this medium, because the isolation is based on molecular structure. The solvent system of further CC is based on the solvent system of the fractions being eluted.

Fraction 1 (0.108 g) was subjected to CC with solvent system 80:20 of H_2O:MeOH was used to yield **152** (3.7 mg). Fraction 2 (0.126 g) was also purified by CC elution with solvent system 70:30 of H_2O:MeOH to yield **154** (2.9 mg) and **155** (3.4 mg). Fraction 4 (0.187 g) was further fractionated through CC with solvent system 50:50 of H_2O:MeOH to yield **153** (13.8 mg). Compound **147** was acquired from purification of fraction 6 (0.094 g), with CC elution of solvent system of 30 H_2O:70 MeOH.

```
                    ┌─────────────────────────────────────┐
                    │  Methanol crude of G. tapisoides (3 g) │
                    └─────────────────────────────────────┘
```

F1	F3	F5	F7	F9
H₂O: MeOH (8 : 2)	H₂O: MeOH (6 : 4)	H₂O: MeOH (4 : 6)	H₂O: MeOH (2 : 8)	100% MeOH

F2	F4	F6	F8
H₂O: MeOH (7 : 3)	H₂O: MeOH (5 : 5)	H₂O: MeOH (3 : 7)	H₂O: MeOH (1 : 9)

Goniomicin F **153** (13.8 mg)

Goniomicin G **154** (4.2 mg)
Goniomicin H **155** (3.1 mg)

Goniomicin A **147** (3.3 mg)

Goniomicin E **152** (3.7 mg)

Scheme 3.3: Isolation and purification of compounds from the MeOH crude extract of the bark of *G. tapisoides*.

3.6 Physical data of the isolated compounds

Isoaltholactone **41**

Molecular formula	: $C_{13}H_{12}O_4$
UV	: 215 nm
IR v_{max}	: 3372, 3028, 1732, 1638 cm^{-1}
$[\alpha]_D^{25}$	: +63.51° (*c* 0.012 M; MeOH)
Mass spectrum *m/z*	: 232.2574 [M+H]$^+$ (calcd. for $C_{13}H_{13}O_4$, 233.2578)
^{1}H-NMR δ ppm	: see **Figure 4.1**
^{13}C-NMR δ ppm	: see **Figure 4.2**

3-acetylisoaltholactone **151**

Molecular formula	: $C_{15}H_{14}O_5$
UV	: 216 nm
IR v_{max}	: 1677, 1369 cm^{-1}
$[\alpha]_D^{25}$	: +8.04° (*c* 0.007 M; MeOH)
Mass spectrum *m/z*	: 275.1596 [M+H]$^+$ (calcd. for $C_{15}H_{15}O_5$, 275.1593)
^{1}H-NMR δ ppm	: see **Figure 4.3**
^{13}C-NMR δ ppm	: see **Figure 4.4**

7-*epi*-Goniofufurone **49**

Molecular formula	: $C_{13}H_{14}O_5$
UV	: 205 nm
IR v_{max}	: 3404, 1755, 1634, 1185 cm^{-1}
$[\alpha]_D^{25}$	: +6.85° (*c* 0.006 M; MeOH)
Mass spectrum *m/z*	: 251.0697 [M+H]$^+$ (calcd. for $C_{13}H_{15}O_5$, 251.0693)
^{1}H-NMR δ ppm	: see **Figure 4.9**
^{13}C-NMR δ ppm	: see **Figure 4.10**

Goniothalamin **1**

Molecular formula	: $C_{13}H_{12}O_2$
UV	: 207, 255 and 284 nm
IR v_{max}	: 1725, 1249, 751 cm^{-1}
$[\alpha]_D^{25}$	: +81.66° (*c* 0.018 M; MeOH)
Mass spectrum *m/z*	: 201.0144 [M+H]$^+$ (calcd. for $C_{13}H_{13}O_2$, 201.0143)
^{1}H-NMR δ ppm	: see **Figure 4.11**
^{13}C-NMR δ ppm	: see **Figure 4.12**

Cheliensisin A **22**

Molecular formula	: $C_{15}H_{14}O_5$
UV	: 215 nm
IR v_{max}	: 1735, 1720, 1620, 1020, 820 cm^{-1}
$[\alpha]_D^{25}$	: +23.51º (*c* 0.007 M; MeOH)
Mass spectrum *m/z*	: 275.2136 [M+H]$^+$ (calcd. for $C_{15}H_{15}O_5$, 275.2161)
^{1}H-NMR δ ppm	: see **Figure 4.13**
^{13}C-NMR δ ppm	: see **Figure 4.14**

Goniodiol **3**

Molecular formula	: $C_{13}H_{14}O_4$
UV	: 215 nm
IR v_{max}	: 3403, 1702, 1389 cm^{-1}
$[\alpha]_D^{25}$	: +28.71º (*c* 0.012 M; MeOH)
Mass spectrum *m/z*	: 216.2096 [M – H$_2$O]$^-$ (calcd. for $C_{13}H_{12}O_3$, 216.2101)
^{1}H-NMR δ ppm	: see **Figure 4.15**
^{13}C-NMR δ ppm	: see **Figure 4.16**

7-*epi*-goniodiol **10**

Molecular formula	: $C_{13}H_{14}O_4$
UV	: 215 nm
IR v_{max}	: 3410, 1714, 1402 cm^{-1}
$[\alpha]_D^{25}$	: +36.42º (*c* 0.015 M; MeOH)
Mass spectrum *m/z*	: 216.2054 [M – H$_2$O]$^-$ (calcd. for $C_{13}H_{12}O_3$, 216.2052)
^{1}H-NMR δ ppm	: see **Figure 4.17**
^{13}C-NMR δ ppm	: see **Figure 4.18**

Garvensintriol **4**

Molecular formula	: $C_{13}H_{16}O_5$
UV	: 220, 250 nm
IR v_{max}	: 3393, 2905, 1755 cm^{-1}
$[\alpha]_D^{25}$	: +8.62º (*c* 0.005 M; MeOH)
Mass spectrum *m/z*	: 234.2374 [M – H$_2$O]$^-$ (calcd. for $C_{13}H_{14}O_4$, 234.2372)
^{1}H-NMR δ ppm	: see **Figure 4.19**
^{13}C-NMR δ ppm	: see **Figure 4.20**

Goniopypyrone **26**

Molecular formula	: $C_{13}H_{14}O_5$
UV	: 208 nm
IR v_{max}	: 3398, 2978, 1745 cm^{-1}
$[\alpha]_D^{25}$	: +10.34º (*c* 0.007 M; MeOH)
Mass spectrum *m/z*	: 249.0717 [M – H]$^-$ (calcd. for $C_{13}H_{13}O_5$, 249.0718)
^{1}H-NMR δ ppm	: see **Figure 4.21**
^{13}C-NMR δ ppm	: see **Figure 4.22**

8-*epi*-9-deoxygoniopypyrone **24**

Molecular formula	: $C_{13}H_{14}O_4$
UV	: 210 nm
IR v_{max}	: 3395, 3283, 1734 cm^{-1}
$[\alpha]_D^{25}$	: +13.11º (*c* 0.000 M; MeOH)
Mass spectrum *m/z*	: 233.0174 [M – H]$^-$ (calcd. for $C_{13}H_{14}O_4$, 233.0171)
^{1}H-NMR δ ppm	: see **Figure 4.23**
^{13}C-NMR δ ppm	: see **Figure 4.24**

Goniomicin A **147**

Molecular formula	: $C_{13}H_{14}O_3$
UV	: 206, 252 nm
IR v_{max}	: 3350, 1665, 1327 cm^{-1}
$[\alpha]_D^{25}$	: +15.34º (c 0.020 M; MeOH)
Mass spectrum m/z	: 200.0078 $[M - H_2O]^-$ (calcd. for $C_{13}H_{12}O_2$, 200.0073)
^{1}H-NMR δ ppm	: see **Figure 4.25**
^{13}C-NMR δ ppm	: see **Figure 4.26**

Goniomicin E **152**

Molecular formula	: $C_{13}H_{19}NO_5$
UV	: 205 nm
IR v_{max} cm^{-1}	: 1717, 1609 cm^{-1}
$[\alpha]_D^{25}$	: +5.38º (c 0.012 M; MeOH)
Mass spectrum m/z	: 270.1355 $[M+H]^+$ (calcd. for $C_{13}H_{20}NO_5$, 270.1359)
^{1}H-NMR δ ppm	: see **Figure 4.27**
^{13}C-NMR δ ppm	: see **Figure 4.28**

Goniomicin F **153**

Molecular formula	: $C_{13}H_{17}NO_3$
UV	: 207 and 255 nm
IR v_{max} cm^{-1}	: 3568, 1702 cm^{-1}
$[\alpha]_D^{25}$	: +10.87º (c 0.023 M; MeOH)
Mass spectrum m/z	: 235.1447 [M] (calcd. for $C_{13}H_{17}NO_3$, 235.1451)
^{1}H-NMR δ ppm	: see **Figure 4.34**
^{13}C-NMR δ ppm	: see **Figure 4.35**

Goniomicin G **154**

Molecular formula	: $C_{13}H_{18}O_6$
UV	: 204 nm
IR v_{max} cm^{-1}	: 3606, 1710 cm^{-1}
$[\alpha]_D^{25}$	: –4.09º (*c* 0.010 M; MeOH)
Mass spectrum *m/z*	: 252.1249 [M – H$_2$O]$^-$ (calcd. for $C_{13}H_{16}O_5$, 252.1246)
^{1}H-NMR δ ppm	: see **Figure 4.40**
^{13}C-NMR δ ppm	: see **Figure 4.41**

Goniomicin H **155**

Molecular formula	: $C_{13}H_{16}O_5$
UV	: 206 nm
IR v_{max} cm^{-1}	: 3556, 1720 cm^{-1}
$[\alpha]_D^{25}$	: +3.70º (*c* 0.009 M; MeOH)
Mass spectrum *m/z*	: 252.1233 [M] (calcd. for $C_{13}H_{16}O_5$, 252.1235)
^{1}H-NMR δ ppm	: see **Figure 4.47**
^{13}C-NMR δ ppm	: see **Figure 4.48**

Stigmasterol **133**

Molecular formula	: $C_{29}H_{48}O$
UV	: 257 nm
IR v_{max}	: 3374, 2941, 1642 cm^{-1}
Mass spectrum *m/z*	: 413.3
^{1}H-NMR δ ppm	: see **Figure 4.54**
^{13}C-NMR δ ppm	: see **Figure 4.55**

β-sitosterol **134**

Molecular formula	: $C_{29}H_{50}O$
UV	: 257 nm
IR v_{max}	: 3374, 2941, 1642 cm^{-1}
Mass spectrum *m/z*	: 415.2
^{1}H-NMR δ ppm	: see **Figure 4.54**
^{13}C-NMR δ ppm	: see **Figure 4.55**

CHAPTER 4 : RESULTS AND DISCUSSION

4.1 Secondary metabolites isolated from stem barks of *G. tapis* and *G. tapisoides*

Chemical screening of the stem bark of *G. tapisoides* and *G. tapis*, belonging to the Annonaceae family were studied in detail for their chemical constituents. The dicholoromethane and methanol extracts of stem bark from these two species were subjected to various sepration techniques discussed in Chapter 3, successfully yielded seventeen compounds.

Nine compounds consists of styryl-lactones and steroids were isolated from the dichloromethane and methanol extract of the bark of *G. tapis*. Seven styryl-lactones; isoaltholactone **41**, 3-acetyl-isoaltholactone **151**, 7-*epi*-goniofufurone **49**, goniothalamin **1**, cheliensisin A **22**, garvensintriol **4**, and goniopyyprone **26**. Two steroids were stigmasterol **133** and β-sitosterol **134**.

As for *G. tapisoides*, eight compounds were isolated from the bark excract. Three styryl-lactones were isolated from dichloromethane crude, namely goniodiol **3**, 7-*epi*-goniodiol **10** and 8-*epi*-9-deoxygoniopypyrone **24**. Another five styryl-lactones were isolated from methanol crude; goniomicin A **147**, goniomicin E **152**, goniomicin F **153**, goniomicin G **154** and goniomicin H **155**.

The structural elucidations of these seventeen compounds shall be discussed in details through spectroscopic methods, principally NMR experiments. The elucidated compounds have been arranged according to their skeletal types and presented in **Table 4.1**. Complete ^{1}H, ^{13}C, DEPT-135, HSQC and HMBC spectral data were given for new compounds and also by comparison with literature data for the known compounds.

Table 4.1: Chemical constituents of the bark extracts of *G. tapis* and *G. tapisoides*.

Compounds	Plants	Types	Pages
Isoalthoalctone **41**	*G. tapis*	Furano-pyrone	67
3-acetylisoaltolactone **148**	*G. tapis*	Furano-pyrone	70
7-*epi*-goniofufurone **49**	*G. tapis*	Furano-furone	75
Goniothalamin **1**	*G. tapis*	Styryl-pyrone	78
Cheliensisin A **22**	*G. tapis*	Styryl-pyrone	81
Goniodiol **3**	*G. tapisoides*	Styryl-pyrone	84
7-*epi*-Goniodiol **10**	*G. tapisoides*	Styryl-pyrone	87
Garvensintriol **4**	*G. tapis*	Styryl-pyrone	90
Goniopypyrone **26**	*G. tapis*	Pyrano-pyrone	93
8-*epi*-9-deoxygoniopypyrone **24**	*G. tapisoides*	Pyrano-pyrone	96
Goniomicin A **147**	*G. tapisoides*	Styryl-lactone	99
Goniomicin E **152**	*G. tapisoides*	Styryl-lactone	102
Goniomicin F **153**	*G. tapisoides*	Styryl-lactone	108
Goniomicin G **154**	*G. tapisoides*	Styryl-lactone	113
Goniomicin H **155**	*G. tapisoides*	Styryl-lactone	119
Stigmasterol **133**	*G. tapis*	Steroid	126
β-sitosterol **134**	*G. tapis*	Steroid	126

4.1.1   Isoaltholactone 41
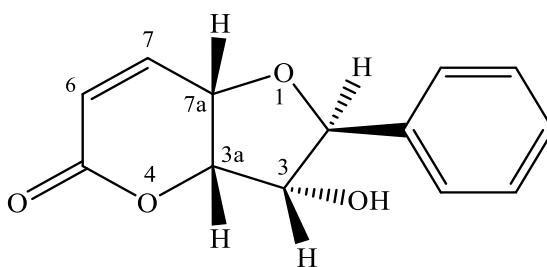
Compound **41** was isolated as yellow amorphous with $[\alpha]_D^{25}= +63.51$. The LCMS-IT-TOF spectrum showed a positive molecular ion peak $[M+H]^+$ at m/z 232.2574 (calcd. for $C_{13}H_{13}O_4$, 233.2578) spectrum, corresponding to a molecular formula of $C_{13}H_{12}O_4$. It showed broad and strong bands in IR spectrum at 3372 cm^{-1} due to the presence of hydroxyl group.

In the ^{1}H NMR spectrum, a multiplet signal at δ 7.31-7.36 characteristics for five aromatic protons (H-2' to H-6') of *mono*-substituted phenyl ring. The two olefinic proton with *cis* configuration split into doublet of triplet at δ 6.15 (J = 10.2, 1.2 Hz) and doublet of doublet of doublet at δ 6.82 (J = 10.2, 4.4, 1.2 Hz) are belonged to H-6 and H-7, respectively. Four deshielded oxymethine proton signals at δ 5.01 (*br t*, J = 6.0, 5.8 Hz), δ 4.85 (*br t*, J = 5.8, 4.4 Hz), δ 4.76 (*d*, J = 7.6 Hz), and δ 4.23 (J = 6.0 Hz) were assignable to H-3a, H-7a, H-2 and H-3 of the furan ring which correlated with the methine carbon at δ 78.7, δ 67.9, δ 83.4, and δ 78.2 in the HSQC spectrum.

In the ^{13}C NMR spectrum, a most downfield signal is observed at δ 161.8 which correspond to a highly deshielded carbonyl carbon of lactone. Among all the carbons in furan ring, C-2 is the most deshielded carbon, because it bonded to aromatic ring.

The assignments of all the proton and carbon signals of compound **41** were confirmed by comparison with the literature values (Colegate et al., 1990). Thus, compound **41** was identified as isoaltholactone, which was first isolated from *Goniothalamus malayanus*.

Table 4.2: ^{1}H (400 MHz), ^{13}C (100 MHz) NMR spectroscopic data (in CDCl$_3$) of isoaltholactone **41**.

Position	^{1}H-NMR δ_H (ppm), J (Hz)		^{13}C-NMR δ_C (ppm)	
	Experimental	Literature	Experimental	Literature
1	-	-	-	-
2	4.76 (1H, *d*) *J*=7.6	4.76 (1H, *d*) *J*=7.5	83.4	83.3
3	4.23 (1H, *br t*) *J*=6.0	4.28 (1H, *m*)	78.2	78.4
3-OH	3.73 (*br s*)	2.86 (*d*, *J*=8.86)	-	-
3a	5.01 (1H, *br t*) *J*=6.0, 5.8	5.07 (1H, *br t*) *J*=5.5, 5.5	78.7	78.5
4	-	-	-	-
5	-	-	161.8	161.8
6	6.15 (1H, *dt*) *J*=10.2, 1.2	6.22 (1H, *dd*) *J*=10.0, 0.8	123.0	123.0
7	6.82 (1H, *ddd*) *J*=10.2, 4.4, 1.2	6.89 (1H, *dd*) *J*=10.0, 4.5	142.1	141.7
7a	4.85 (1H, *br t*) *J*=5.8, 4.4	4.89 (1H, *br t*) *J*=5.5, 4.5	67.9	67.7
1'	-	-	138.7	138.4
2', 6'			125.9	125.7
3', 5'	7.31-7.36 (5H, *m*)	7.48 (5H, *m*)	128.7	128.7
4'			128.4	128.3

Figure 4.1: ^{1}H (400 MHz) NMR spectrum of isoaltholactone **41**.
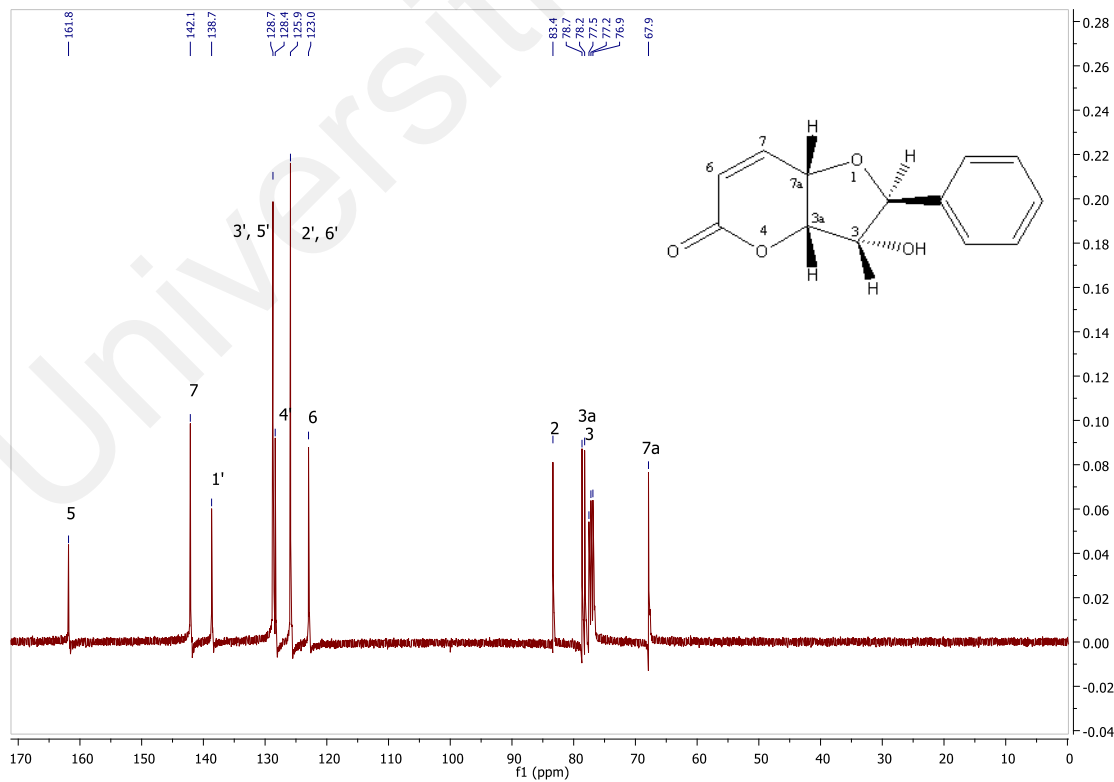
Figure 4.2: ^{13}C (100 MHz) NMR spectrum of isoaltholactone **41**.

4.1.2　3-Acetylisoaltholactone 151
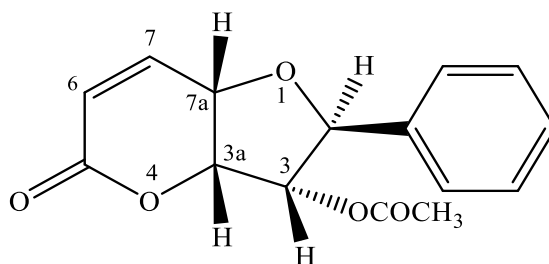
151

Compound **151** was isolated as yellow amorphous with $[\alpha]_D^{25}= +8.04$. The LCMS-IT-TOF spectrum showed a positive molecular ion peak $[M+H]^+$ at m/z 275.1596 (calcd. for $C_{15}H_{15}O_5$ 275.1593), which corresponded to a molecular formula of $C_{15}H_{14}O_5$. It showed IR absorptions bands at 1677 and 1369 cm^{-1} due to the stretching of C=O and C-O, respectively.
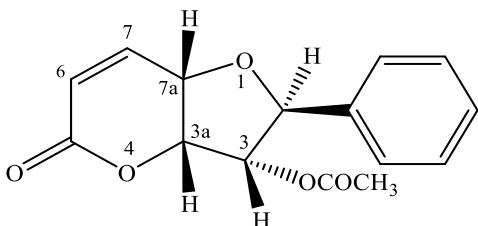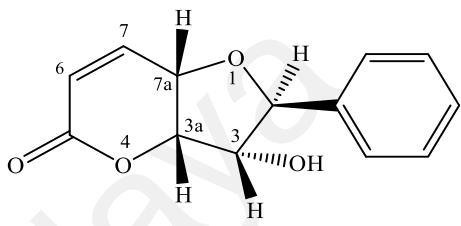
In the ^{1}H NMR spectrum showed the presence two olefinic proton with *cis* configuration split into doublet at δ 6.20 (*J* = 10.0 Hz) and doublet of doublet at δ 6.83 (*J* = 10.0, 4.0 Hz) which corresponding to H-6 and H-7, respectively. A multiplet signal at δ 7.22-7.58 characteristics for five aromatic protons (H-2' to H-6') of *mono*-substituted phenyl ring. Four deshielded oxymethine proton signals at δ 5.01 (*d*, *J* = 6.3 Hz), δ 5.16 (*t*, *J* = 6.3 Hz), δ 5.28 (*t*, *J* = 5.9 Hz), and δ 4.99 (*br d*, *J* = 4.0 Hz) were assignable to H-2, H-3, H-3a and H-7a. Assignments of these four protons were established by the ^{1}H-^{1}H COSY spectrum. These oxymethine carbons resonated in the range of δ 68.3-81.2.

A singlet signal at δ 2.11 was observed in ^{1}H NMR spectrum, revealed the presence of a methyl group. The methyl protons showed correlations with most deshielded carbonyl carbon, δ 169.9 in HMBC spectrum, indicated this compound has an acetyl group.

The assignments of all the proton and carbon signals of compound **151** were confirmed by HSQC, COSY and HMBC experimetns. This compound was compared with the

literature values (Colegate et al., 1990) of the major compound, isoaltholactone **41**. Thus, compound **151** was identified as 3-acetylisoaltholactone, which a new ne compound isolated from *G. tapis*.

Table 4.3: ^{1}H (400 MHz), ^{13}C (100 MHz) NMR spectroscopic data (in CDCl$_3$) of 3-acetylisoaltholactone **151** and isoaltholactone **41**.

Position	3-acetylisoaltholactone		Isoaltholactone	
	^{1}H-NMR δ_H (ppm), J (Hz)	^{13}C-NMR δ_C (ppm)	^{1}H-NMR δ_H (ppm), J (Hz)	^{13}C-NMR δ_C (ppm)
1	-	-	-	-
2	5.01 (1H, *d*) *J*=6.3	81.2	4.76 (1H, *d*) *J*=7.5	83.3
3	5.16 (1H, *t*) *J*=6.3	77.8	4.28 (1H, *m*)	78.4
3-OH	-	-	2.86 (*d*, *J*=8.86)	-
3-OAc	- 2.11 (3H, *s*)	169.9 20.7	-	-
3a	5.28 (1H, *t*) *J*=5.9	76.0	5.07 (1H, *br t*) *J*=5.5, 5.5	78.5
4	-	-	-	-
5	-	160.9	-	161.8
6	6.20 (1H, *d*) *J*=10.0	122.9	6.22 (1H, *dd*) *J*=10.0, 0.8	123.0
7	6.83 (1H, *dd*) *J*=10.0, 4.0	141.8	6.89 (1H, *dd*) *J*=10.0, 4.5	141.7
7a	4.99 (1H, *br d*) *J*=4.0	68.3	4.89 (1H, *br t*) *J*=5.5, 4.5	67.7
1'		137.6	-	138.4
2', 6'		125.8		125.7
3', 5'	7.22-7.58 (5H, *m*)	128.9	7.48 (5H, *m*)	128.7
4'		128.7		128.3
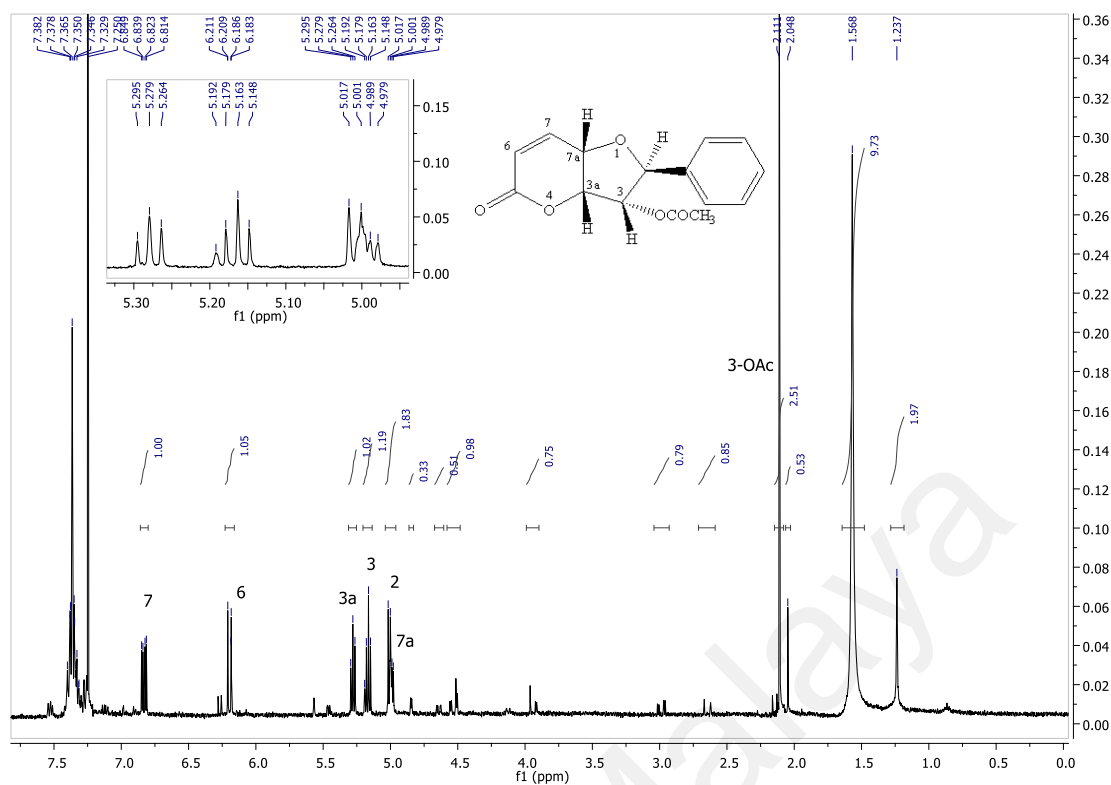
Figure 4.3: ^{1}H (400 MHz) NMR spectrum of 3-acetylisoaltholactone **151**.
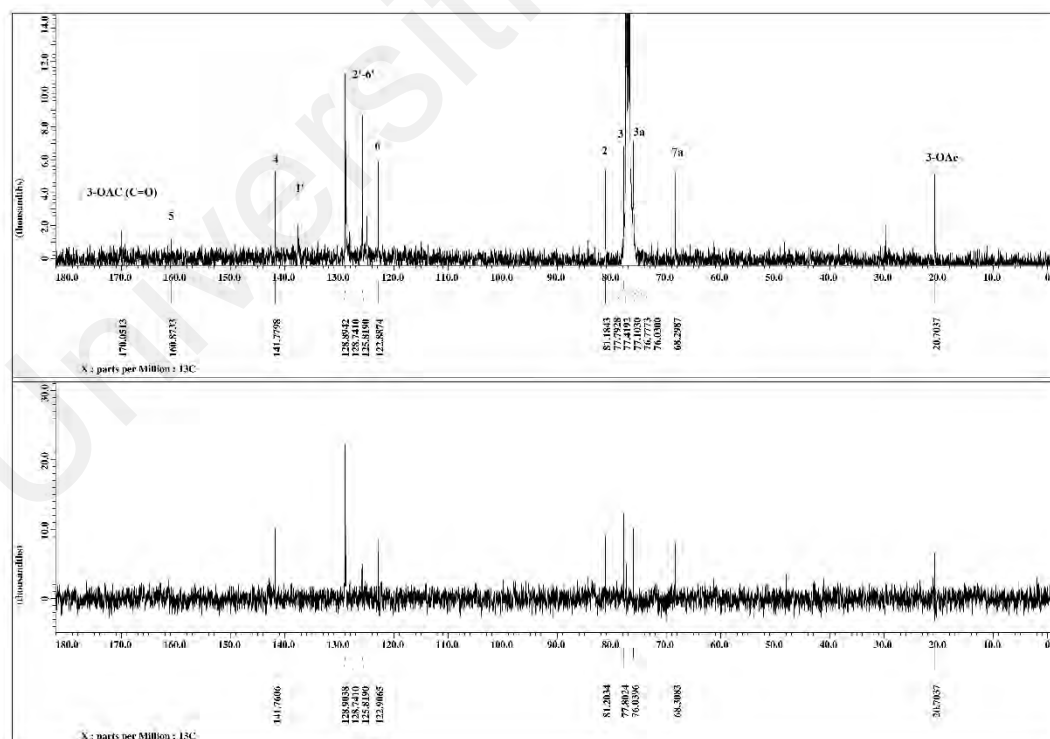
Figure 4.4: ^{13}C (100 MHz) and DEPT-135 NMR spectra of 3-acetylisoaltholactone **151**.
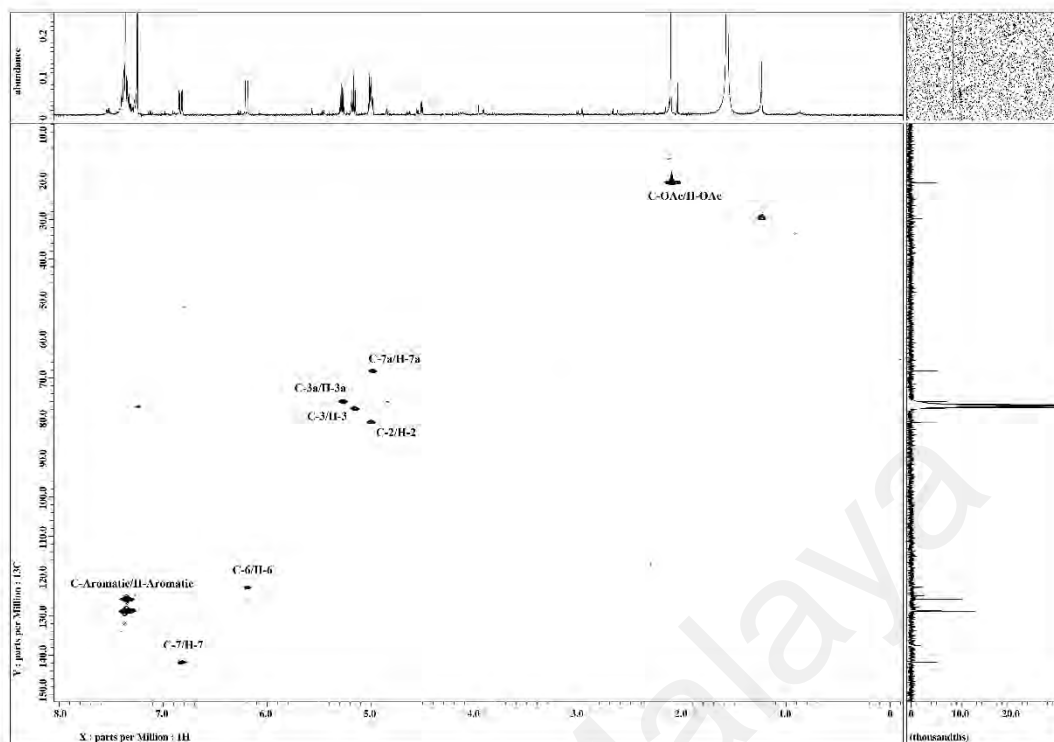
Figure 4.5: HSQC spectrum of 3-acetylisoaltholactone **151**.
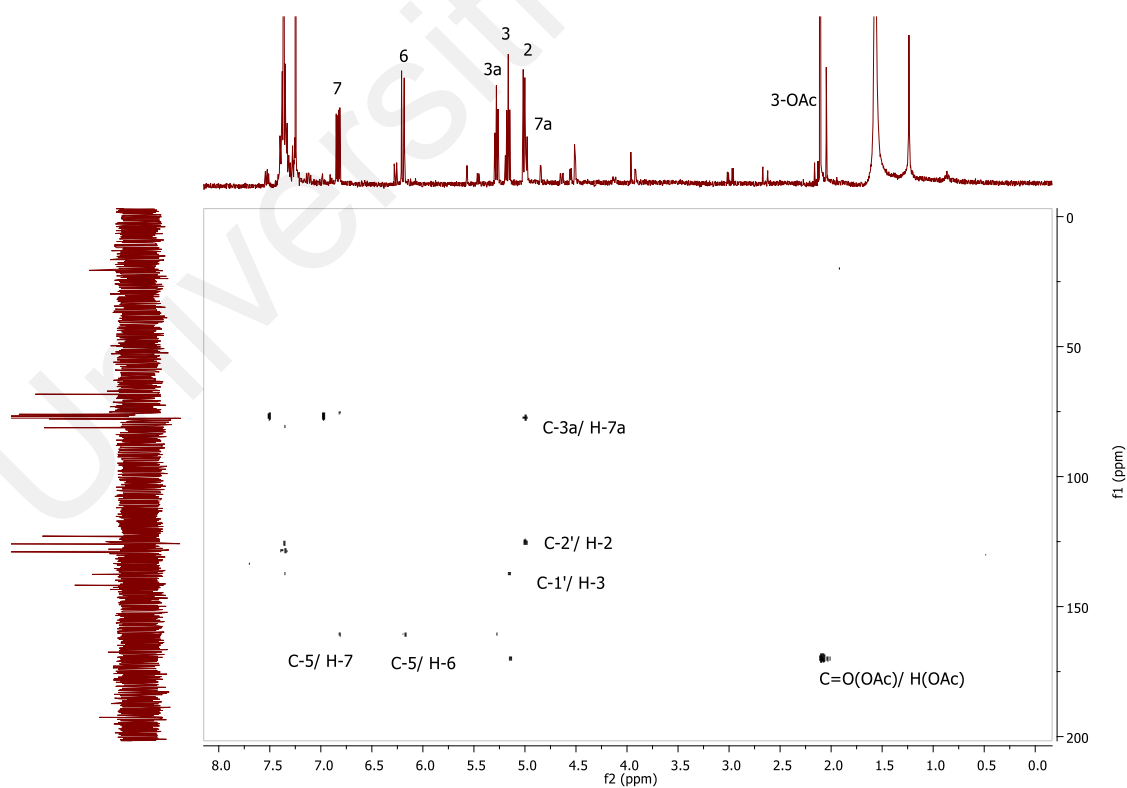
Figure 4.6: HMBC spectrum of 3-acetylisoaltholactone **151**.

73
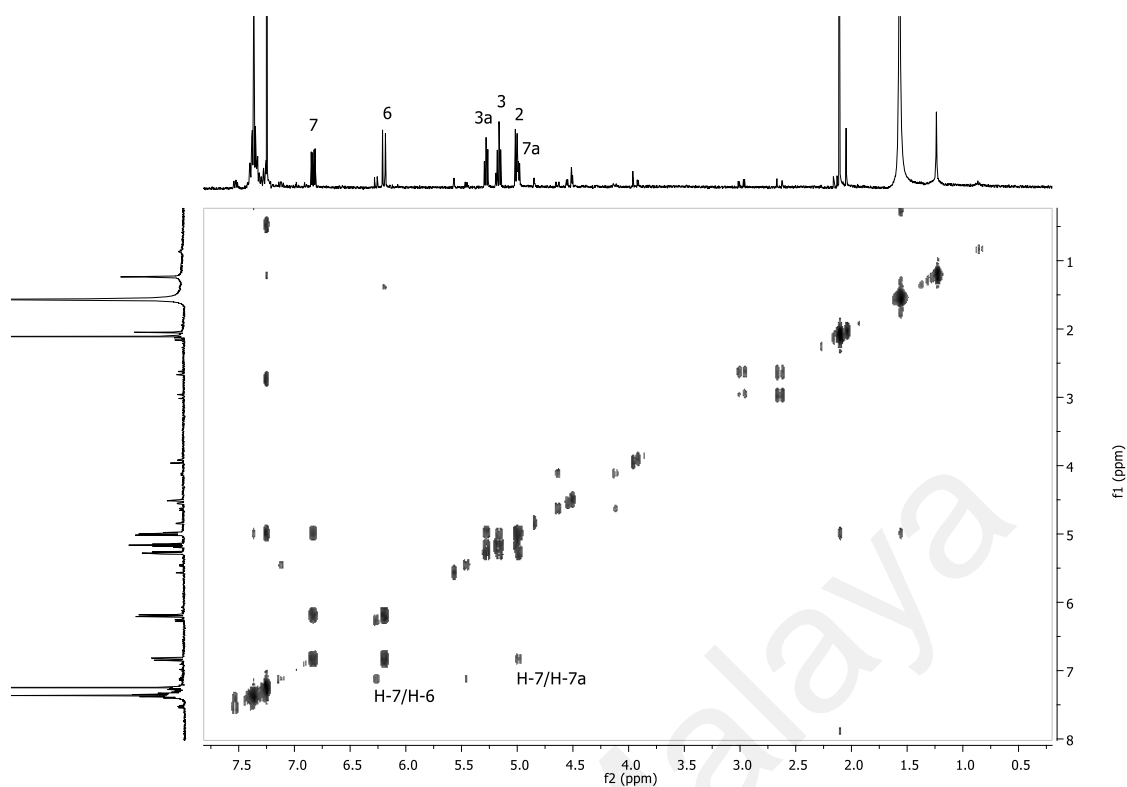
Figure 4.7: COSY spectrum of 3-acetylisoaltholactone **151**.
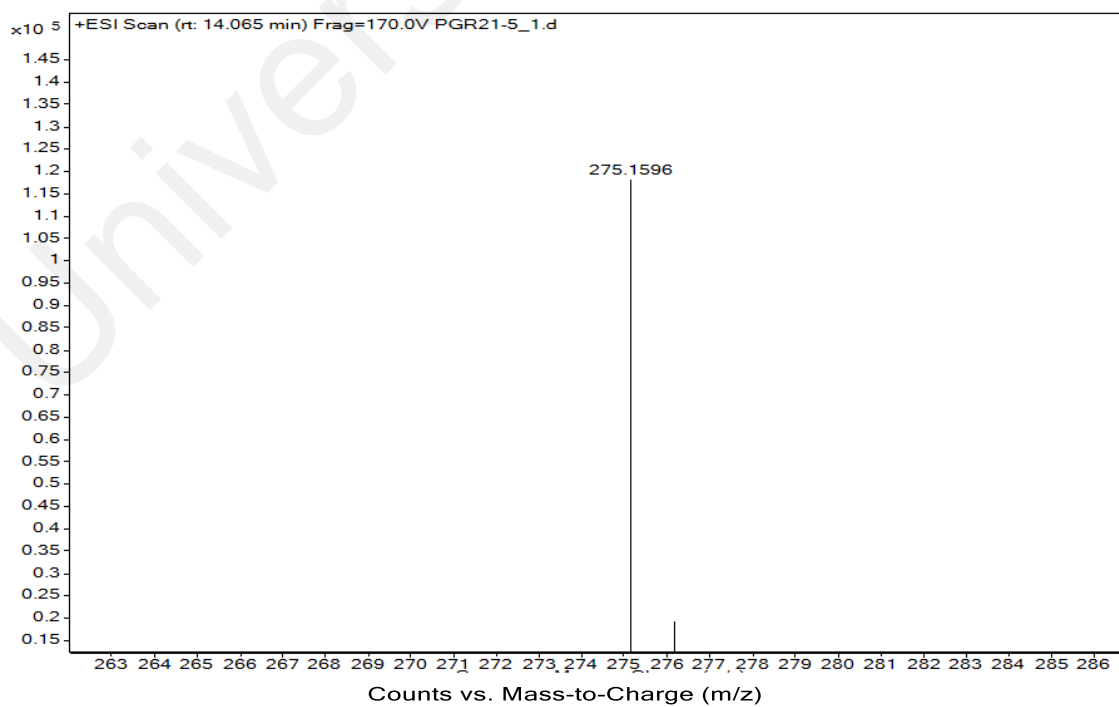
Figure 4.8: LCMS spectrum of 3-acetylisoaltholactone **151**.

4.1.3   7-*epi*-Goniofufurone 49
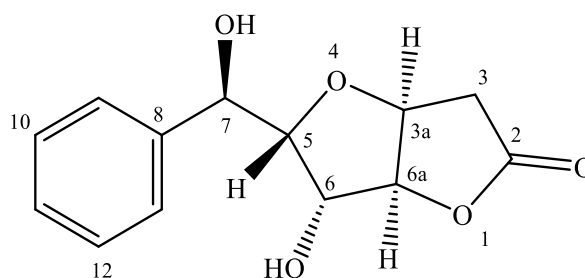
Compound **49** was isolated as yellow amorphous with $[\alpha]_D^{25}= +6.85$. The LCMS-IT-TOF spectrum showed a positive ion peak $[M+H]^+$ at m/z 251.0697 (calcd. for $C_{13}H_{15}O_5$, 251.0693), which corresponded to a molecular formula of $C_{13}H_{14}O_5$. The IR spectrum showed strong absorptions bands of O-H stretching at 3404 cm^{-1} and C=O stretching at 1755 cm^{-1}. The UV spectrum with absorptions bands at 205 nm.

The ^1H NMR spectrum showed a multiplet δ 7.25-7.42 referring to five aromatic protons (H-9 to H-13) from a *mono*-substituted phenyl ring. Five deshielded one-proton signal at δ 4.84 (*dt*), δ 3.98 (*dd*), δ 4.25 (*d*), δ 4.80 (*dd*) and δ 4.70 (*d*) were indicative of oxygen bearing methine protons belonged to H-3a, H-5, H-6, H-6a and H-7, respectively. A methylene group at position 3 resonated at δ 2.75 (*m,* 2H).

The ^{13}C NMR spectrum showed thirteen carbons; one methylene, ten methine and two quaternary carbon. Two quaternary carbon peaks at δ 174.9 and δ 139.1 were assigned to C-2 and C-8 respectively. Two methine carbons, C-5, C-6a resonated more downfield at δ 90.2 and δ 90.0 respectively. This may due to the deshielding effect by the neighbouring oxygen atom and hydroxyl group. The other three methine carbons resonated at the range of δ 75.0 – δ 77.6. Finally the aromatic carbon peaks showed signal at δ 127.4 attributed to the two aromatic carbons of C-11 and C-15, meanwhile the peak at δ 128.7 corresponding to the two aromatic carbons of C-12 and C-14 and *para* aromatic carbon

peak appeared at δ 127.4 which was assigned for C-13. The carbonyl carbon of the lactone appeared at δ 174.9.

Comparison of the obtained spectral data with the literature values (X. P. Fang et al., 1991b) confirmed that **49** was 7-*epi*-goniofufurone, which is furano-furone skeleton.

Table 4.4: [1]H (400 MHz), ^{13}C (100 MHz) NMR spectroscopic data (in CD₃OD) of 7-*epi*-goniofufurone **49**.

Position	¹H-NMR δ_H (ppm), J (Hz)		¹³C-NMR δ_C (ppm)	
	Experimental	Literature [a]	Experimental	Literature [a]
1	-	-	-	-
2	-	-	174.9	176.10
3	2.75 (2H, *m*)	2.77 (1H, *dd*) J=18.6, 6.9 2.71 (1H, *d*) J=18.6	36.0	36.68
3a	4.84 (1H, *dt*) J=4.2, 2.0	5.12 (1H, *dd*) J=6.0, 4.0	77.6	78.09
4	-	-	-	-
5	3.98 (1H, *dd*) J=7.0, 5.6	4.24 (1H, *dd*) J=4.0, 3.5	90.2	85.81
6	4.25 (1H, *d*) J=5.6	4.43 (1H, *br t*) J=4.5, 3.5	75.0	75.35
6a	4.80 (1H, *dd*) J=4.2, 0.8	4.90 (1H, *dd*) J=4.0	90.0	89.14
7	4.70 (1H, *d*) J=7.0	5.09 (1H, *br t*) J=5.0, 4.0	76.8	72.23
8	-	-	139.1	142.82
9, 13	7.25-7.42 (5H, *m*)	7.24-7.45 (5H, *m*)	127.4	127.8
10, 12			128.7	128.8
11			127.4	128.2

[a] In CDCl₃.
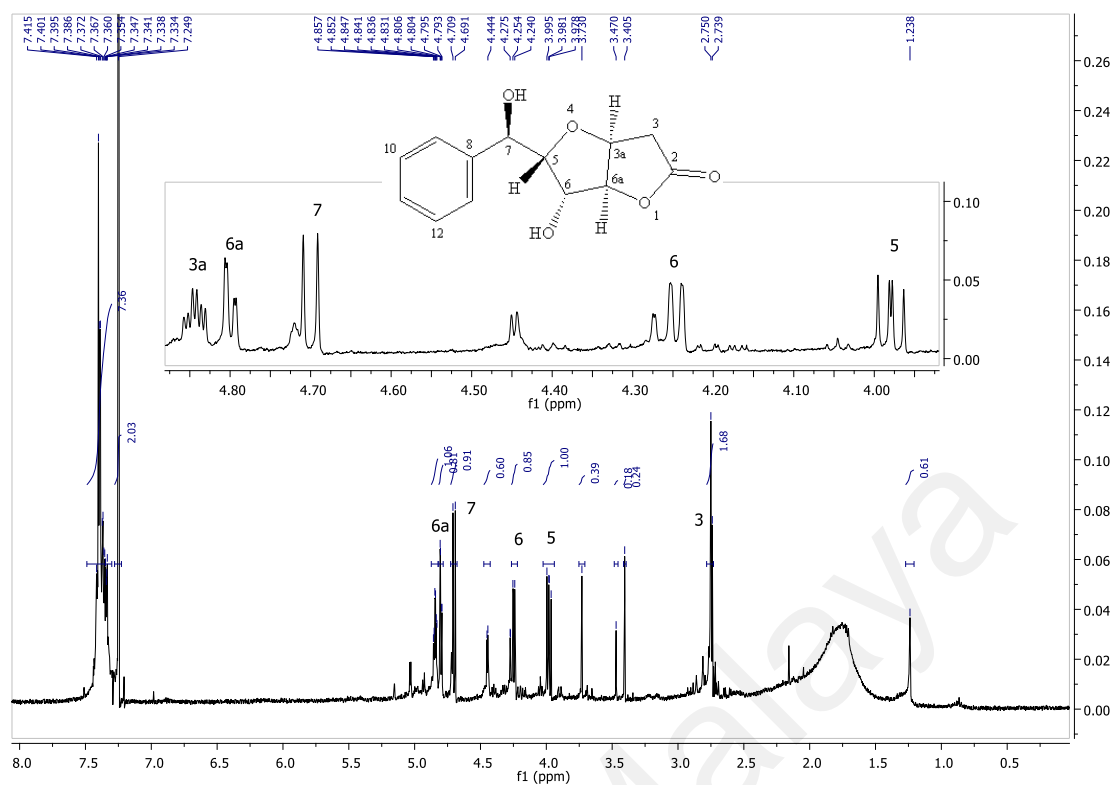
Figure 4.9: ^{1}H (400 MHz) NMR spectrum of 7-*epi*-goniofufurone **49**.
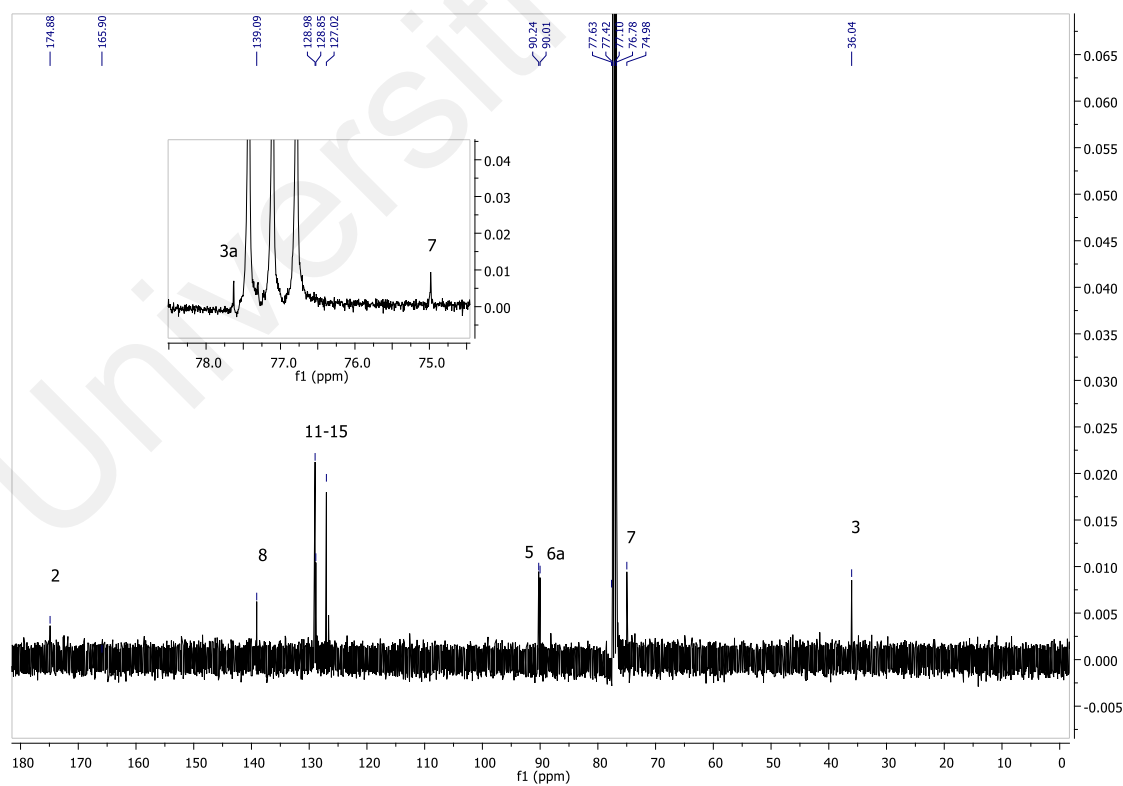
Figure 4.10: ^{13}C (100 MHz) NMR spectrum of 7-*epi*-goniofufurone **49**.

4.1.4 Goniothalamin 1
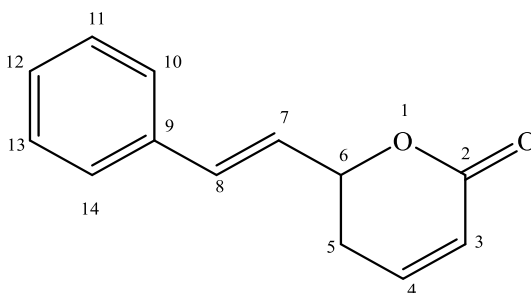
Compound **1** was isolated as colourless crystal with $[\alpha]_D^{25}= +81.66$. The molecular formula of $C_{13}H_{12}O_2$ was deduced from its positive LCMS-IT-TOF spectrum (m/z 201.0144 [M+H]$^+$; calcd. for $C_{13}H_{13}O_2$, 201.0143). It showed strong bands in IR spectrum at 1725, 1249, 751 cm^{-1} corresponding to the resonance of α, β-unsaturated δ-lactone moiety.

The ^{1}H NMR spectrum showed a multiplet δ 7.25-7.40 referring to five aromatic protons (H-10 to H-14) of a *mono*-substituted phenyl ring. The two olefinic proton peaks at δ 6.72 (*d*, *J*=16.0 Hz) and δ 6.27 (*dd*, *J*=16.0 and 6.4 Hz) with a *trans* configuration belonged to H-8 and H-7, respectively. An allylic methylene signal observed as a multiplet at δ 2.51-2.55 (*m*) could be assigned to H-5 and a proton on a carbon bearing the oxygen of the lactone group appeared as a multiplet at δ 5.06-5.12 (*m*) belonged to H-6. The two proton of the allyl group resonating at δ 6.08 (*dd*, *J*=12.0, 4.0 Hz) and δ 6.92 (*ddd*, *J*=12.0, 4.0 Hz) belonged to H-3 and H-4 respectively.

The ^{13}C NMR spectrum showed thirteen carbons; one methylene, ten methine and two quaternary carbon. The olefinic carbons C-7 and C-8 resonated at δ 125.7 and δ 133.2 respectively. A methylene carbon C-5 gave a peak at δ 30.0 meanwhile a methine carbon C-6 showed the peak at δ 78.1 due to the deshielding effect by the neighbouring oxygen atom. The signals for C-3 and C-4 resonated at δ 121.8 and δ 144.8 respectively. Finally for aromatic carbon peak occured at δ 126.8 which attributed to the two aromatic carbons

of C-10 and C-14, meanwhile the peak at δ 128.8 corresponding to the two aromatic carbons of C-11 and C-13. Another aromatic carbon peak appeared at δ 128.5 which could be assigned for C-12. The carbonyl carbon of the lactone appeared at δ 164.0.

Comparison of the spectral data with the literature values confirmed that **1** was indeed the styryl-lactone, goniothalamin (de Fatima et al., 2005).

Table 4.5: ^{1}H (400 MHz), ^{13}C (100 MHz) NMR spectroscopic data (in CDCl$_3$) of goniothalamin **1**.

Position	^{1}H-NMR δ$_H$ (ppm), J (Hz)		^{13}C-NMR δ$_C$ (ppm)	
	Experimental	Literature	Experimental	Literature
1	-	-	-	-
2	-	-	164.0	163.6
3	6.08 (1H, *dd*) J=12.0, 4.0	6.08 (1H, *d*) J=9.5	121.8	121.4
4	6.92, (1H, *dt*) J=12.0, 4.0	6.92 (1H, *dt*) J=4.0	144.8	144.5
5	2.51-2.55 (2H, *m*)	2.52-2.56 (2H, *m*)	30.0	29.8
6	5.06-5.12 (1H, *m*)	5.10 (1H, *q*)	78.1	77.8
7	6.27 (1H, *dd*) J=16.0, 4.0	6.27 (1H, *dd*) J=15.9, 6.2	125.7	125.5
8	6.72 (1H, *d*) J=16.0	6.72 (1H, *d*) J=15.9	133.2	132.8
9	-	-	135.8	135.5
10, 14	7.25-7.40 (5H, *m*)	7.25-7.41 (5H, *m*)	126.8	126.5
11, 13			128.8	128.5
12			128.5	128.1
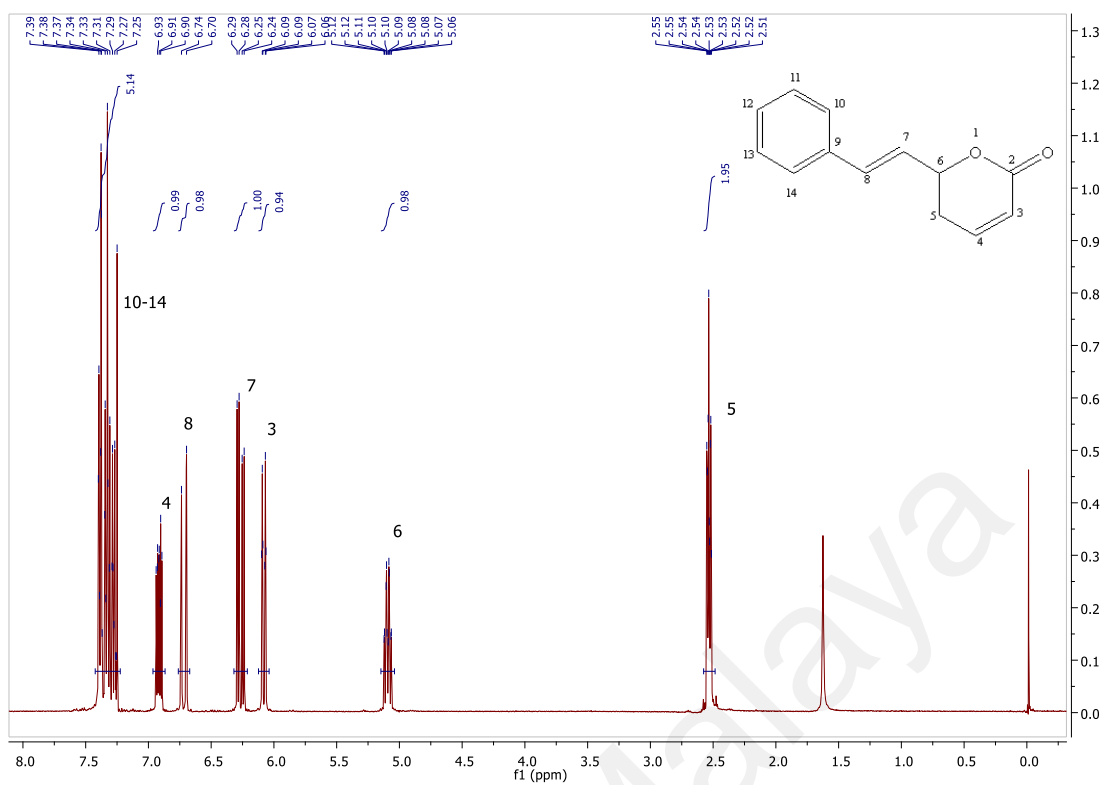
Figure 4.11: ^{1}H (400 MHz) NMR spectrum of goniothalamin **1**.
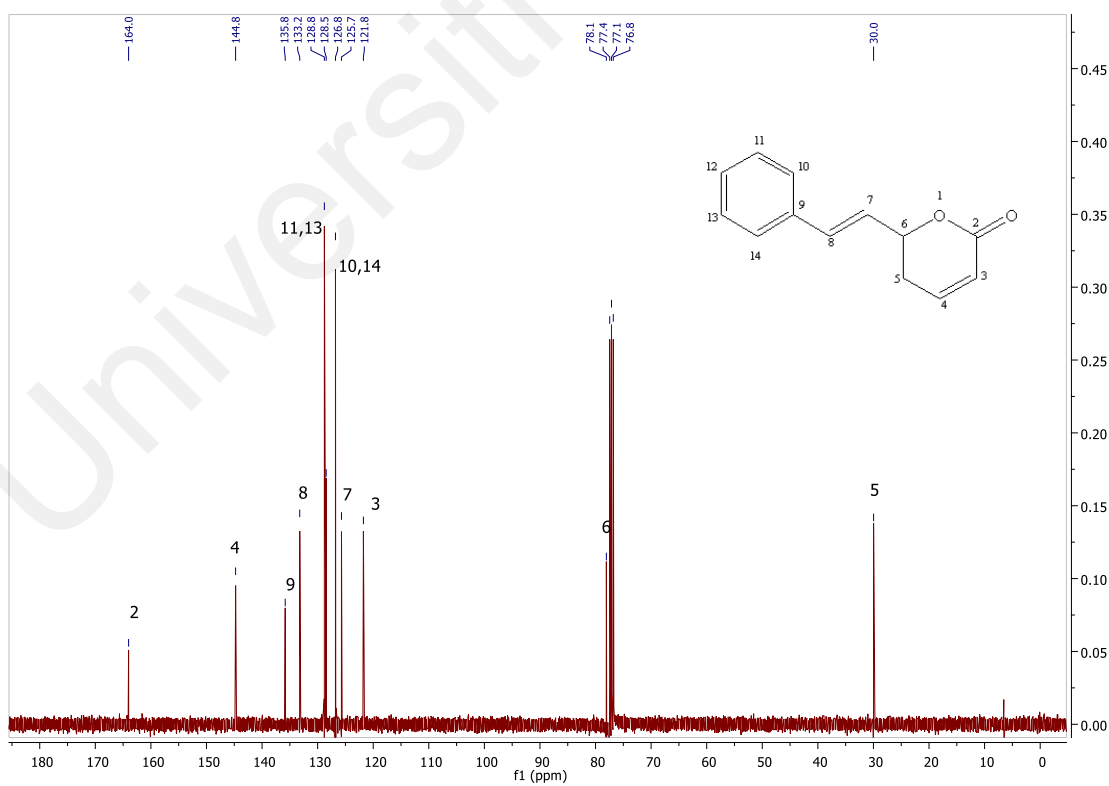
Figure 4.12: ^{13}C (100 MHz) NMR spectrum of goniothalamin **1**.

4.1.5   Cheliensisin A 22
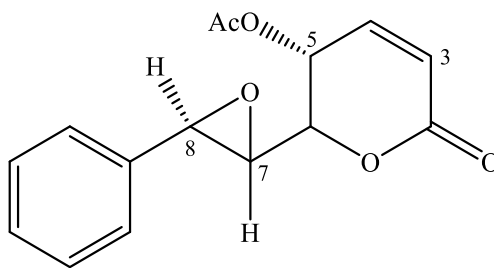
Compound **22** was isolated as yellow amorphous with $[\alpha]_D^{25}= +23.51$. The positive LCMS-IT-TOF analysis exhibited an ion peak $[M+H]^+$ at m/z 275.2136 (calcd. for $C_{15}H_{15}O_5$, 275.2161), corresponded to a molecular formula of $C_{15}H_{14}O_5$. It showed strong bands in IR spectrum at 1020, 820 cm^{-1} corresponding to the epoxide group.

In the ^1H NMR spectrum, a multiplet signal at δ 7.27-7.36 characteristics for five aromatic protons (H-10 to H-14) of *mono*-substituted phenyl ring. The two olefinic proton split into doublet at δ 6.24 (J = 10.1 Hz) and doublet of doublet at δ 7.08 (J = 10.1, 5.7 Hz) with *cis* configuration belonged to H-3 and H-4 respectively. Four deshielded one proton signal at δ 5.40 (*dd*, J = 5.7, 2.8 Hz, H-5), δ 4.41 (*dd*, J = 5.9, 2.8 Hz, H-6), δ 3.33 (*dd*, J = 5.9, 1.8 Hz, H-7), and δ 4.00 (J = 1.8 Hz, H-8) were indicative of oxygen bearing methine protons. Two less deshielded methine protons is in conjunction with the epoxide group. The position of four oxymethine were assigned based on ^1H-^1H COSY and HMBC experiments.

The presence of a carbonyl carbon with chemical shift δ 169.9 and a methyl group with chemical shift δ 20.6 indicate the presence of acetoxy (-OAc) group. Two carbons; C-7 and C-8 with chemical shift δ 58.2 and δ 57.6 respectively due to the deshielding effect of epoxide oxygen.

Comparison of the spectral data with the literature values confirmed that compound **22** was indeed the styryl-lactone, cheliensisin A (Li et al., 1998).

Table 4.6: ^{1}H (400 MHz), ^{13}C (100 MHz) NMR spectroscopic data (in CDCl$_3$) of cheliensisin A **22**.

Position	^{1}H-NMR δ_H (ppm), J (Hz)		^{13}C-NMR δ_C (ppm)	
	Experimental	Literature	Experimental	Literature
1	-	-	-	-
2	-	-	161.4	161.1
3	6.24 (1H, *d*) *J*=10.1	6.21 (1H, *d*) *J*=9.7	125.1	125.0
4	7.08, (1H, *dd*) *J*=10.1, 5.7	7.05 (1H, *dd*) *J*=9.7, 5.7	140.4	140.2
5	5.40 (1H, *dd*) *J*=5.7, 2.8	5.37 (1H, *dd*) *J*=5.7, 2.9	62.6	62.1
6	4.41 (1H, *dd*) *J*=5.9, 2.8	4.40 (1H, *dd*) *J*=5.9, 1.9	78.1	77.9
7	3.33 (1H, *dd*) *J*=5.9, 1.8	3.31 (1H, *dd*) *J*=5.9, 1.9	58.2	58.1
8	4.00 (1H, *d*) *J*=1.8	4.00 (1H, *d*) *J*=1.8	57.6	57.4
C=O (OAc)	-	-	169.9	169.6
-CH$_3$	2.07 (3H, *s*)	2.04 (3H, *s*)	20.6	20.4
9	-	-	135.6	135.6
10, 14	7.27-7.36 (5H, *m*)	7.25-7.35 (5H, *m*)	125.8	125.7
11, 13			128.7	128.6
12			128.8	128.7
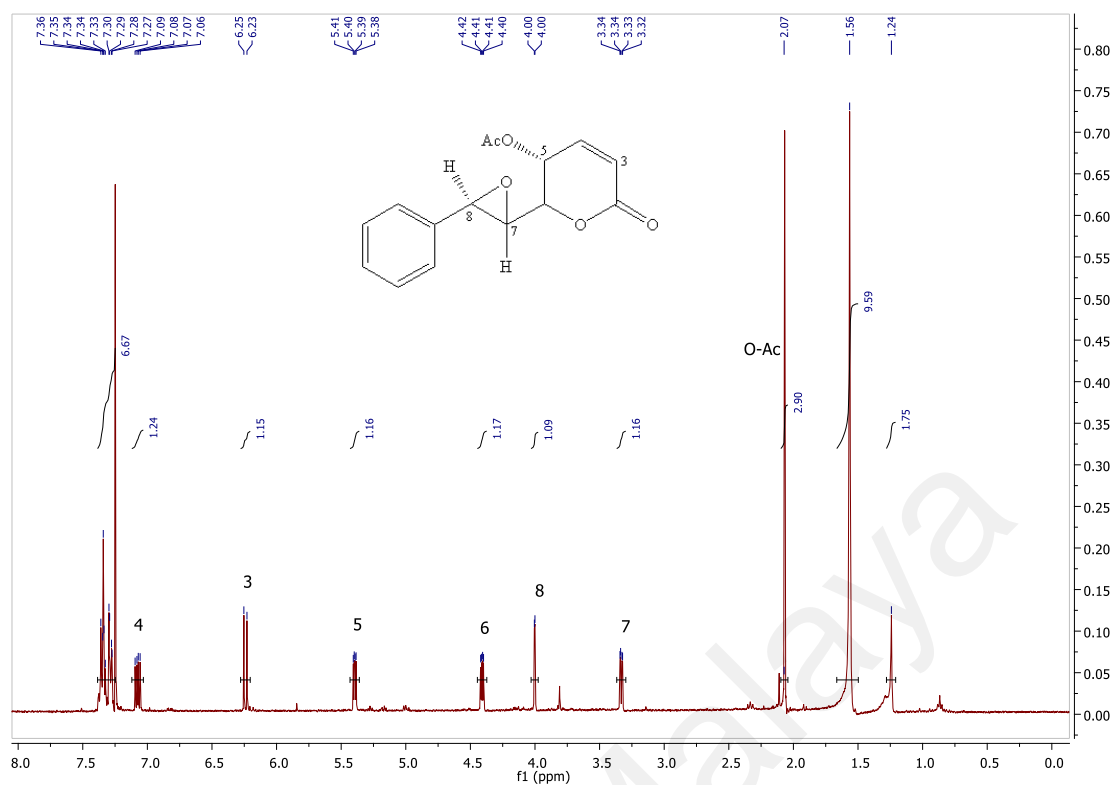
Figure 4.13: ^{1}H (400 MHz) NMR spectrum of cheliensisin A **22**.
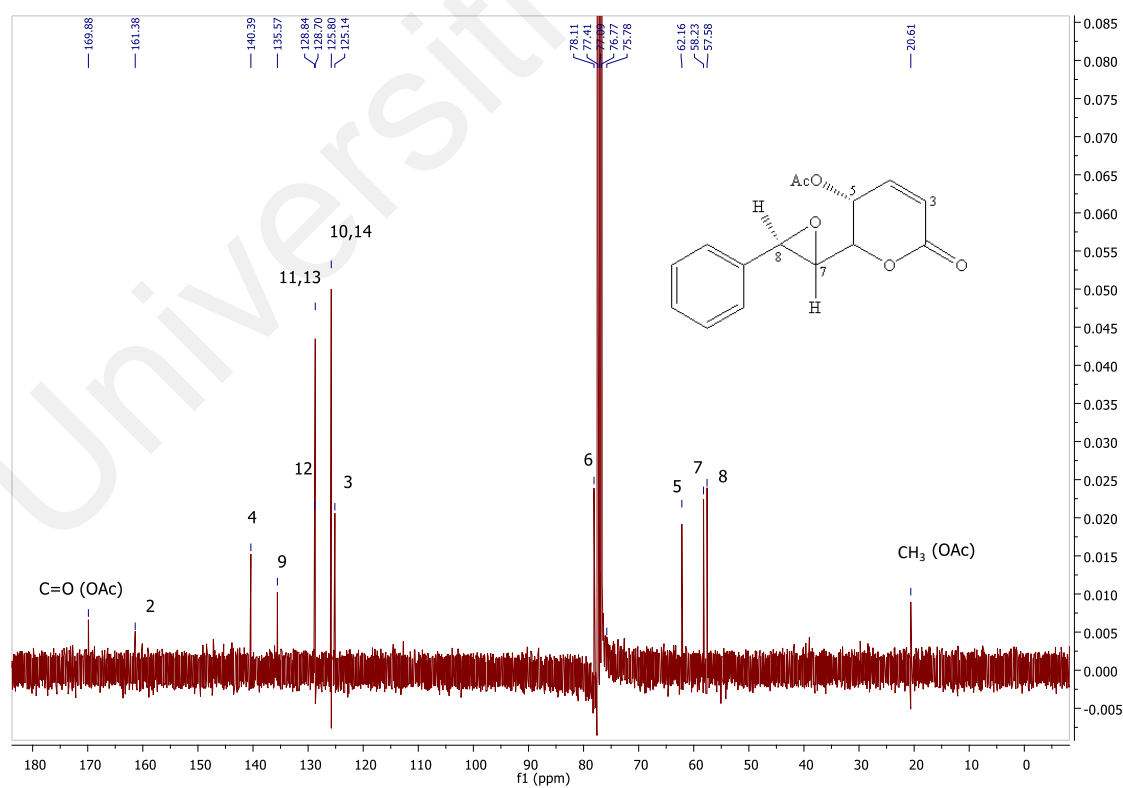
Figure 4.14: ^{13}C (100 MHz) NMR spectrum of cheliensisin A **22**.

4.1.6 Goniodiol 3
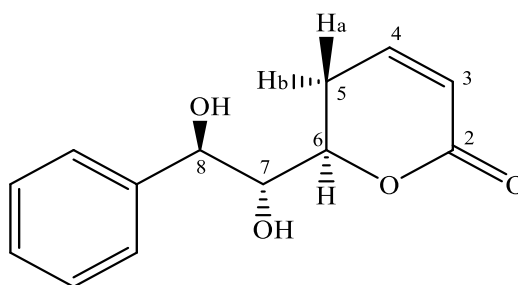
Compound **3** was isolated as yellow amorphous with $[\alpha]_D^{25} = +28.71$. The LCMS-IT-TOF spectrum showed a negative molecular ion peak $[M - H_2O]^-$ at m/z 216.2096 (calcd. for $C_{13}H_{12}O_3$, 216.2101), which corresponded to a molecular formula of $C_{13}H_{14}O_4$. It showed absorption bands in IR spectrum at 3403, 1702, 1389 cm^{-1} corresponding to the hydroxyl, carbonyl and aromatic group.

In the ^{1}H NMR spectrum, a multiplet signal at δ 7.30-7.35 characteristics for five aromatic protons (H-10 to H-14) of *mono*-substituted phenyl ring. The two olefinic proton split into doublet of doublet at δ 5.99 ($J = 10.1, 0.9$ Hz) and doublet of doublet of doublet at δ 6.92 ($J = 10.1, 6.4, 2.3$ Hz) with *cis* configuration belonged to H-3 and H-4, respectively. The spectrum exhibited two one-proton signals at δ 2.80 and δ 2.16 which assignable for the methylene proton adjacent to the double bond.

Three deshielded one proton signal at δ 4.79 (*ddd*, $J = 12.8, 3.9, 2.3$ Hz, H-6), δ 3.71 (*dd*, $J = 7.3, 2.3$ Hz, H-7), and δ 4.94 (*d*, $J = 7.3$ Hz, H-8), were indicative of oxygen bearing methine protons. The coupling constant of H-6/H-7 and H-7/H-8 were 2.3 Hz and 7.3 Hz. These protons were assigned based on ^{1}H-^{1}H COSY and HMBC experiments.

The ^{13}C NMR spectrum showed thirteen carbons; one methylene, ten methine and two quaternary carbon. The olefinic carbons C-3 and C-4 resonated at δ 120.7 and δ 146.3 respectively. A methylene carbon C-5 gave a peak at δ 26.2 meanwhile three methine carbon C-6, C-7 and C-8 showed the peak at δ 76.9, δ 75.1 and δ 73.8, respectively, due

to the deshielding effect by the neighbouring oxygen atom. Finally for aromatic carbon peak occurred at δ 126.8 which attributed to the two aromatic carbons of C-10 and C-14, meanwhile the peak at δ 128.8 corresponding to the two aromatic carbons of C-11 and C-13. Another aromatic carbon peak appeared at δ 128.8 which could be assigned for C-12. The carbonyl carbon of the lactone appeared at δ 163.8.

Comparison of the spectral data with the literature values confirmed that compound **3** was indeed a styryl-pyrones type of styryl-lactone, goniodiol (X.-P. Fang et al., 1991).

Table 4.7: ^{1}H (400 MHz), ^{13}C (100 MHz) NMR spectroscopic data (in CDCl$_3$) of goniodiol **3**.

Position	^{1}H-NMR δ_H (ppm), J (Hz)		^{13}C-NMR δ_C (ppm)	
	Experimental	Literature	Experimental	Literature
1	-	-	-	-
2	-	-	163.8	163.9
3	5.99 (1H, *dd*) *J*=10.1, 0.9	5.98 (1H, *dd*) *J*=9.8, 2.9	120.7	120.4
4	6.92, (1H, *ddd*) *J*=10.1, 6.4, 2.3	6.91 (1H, *dd*) *J*=9.8, 6.4, 2.3	146.3	146.3
5	2.80 (H-a, *m*) 2.16 (H-b, *dddd*) *J*=18.5, 6.4, 3.9, 0.9	2.78 (H-a, *dddd*) *J*=18.5, 12.8, 2.9, 2.3 2.16 (H-b, *ddd*) *J*=18.5, 6.4, 3.7	26.2	26.0
6	4.79 (1H, *ddd*) *J*=12.8, 3.9, 2.3	4.77 (1H, *ddd*) *J*=12.8, 3.7, 2.2	76.9	76.8
7	3.71 (1H, *dd*) *J*=7.3, 2.3	3.71 (1H, *t*) *J*=8.0, 7.0, 2.2	75.1	73.56
8	4.94 (1H, *d*) *J*=7.3	4.93 (1H, *dd*) *J*=7.0, 5.0	73.8	75.0
7-OH	-	2.34 (1H, *d*) *J*=8.0	-	-
8-OH	-	2.67 (1H, *d*) *J*=5.0	-	-
9	-	-	140.8	140.8
10, 14	7.32-7.40 (5H, *m*)	7.29-7.41 (5H, *m*)	126.6	126.5
11, 13			128.9	128.6
12			128.4	128.1
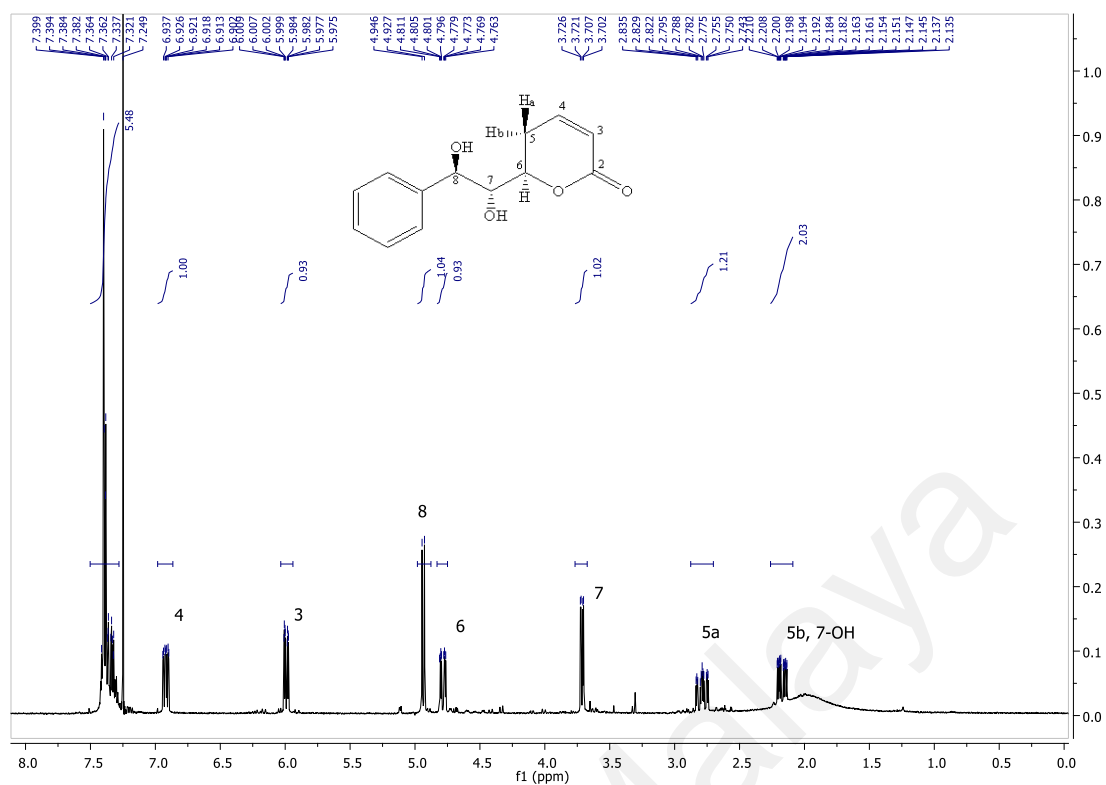
Figure 4.15: ^{1}H (400 MHz) NMR spectrum of goniodiol **3**.
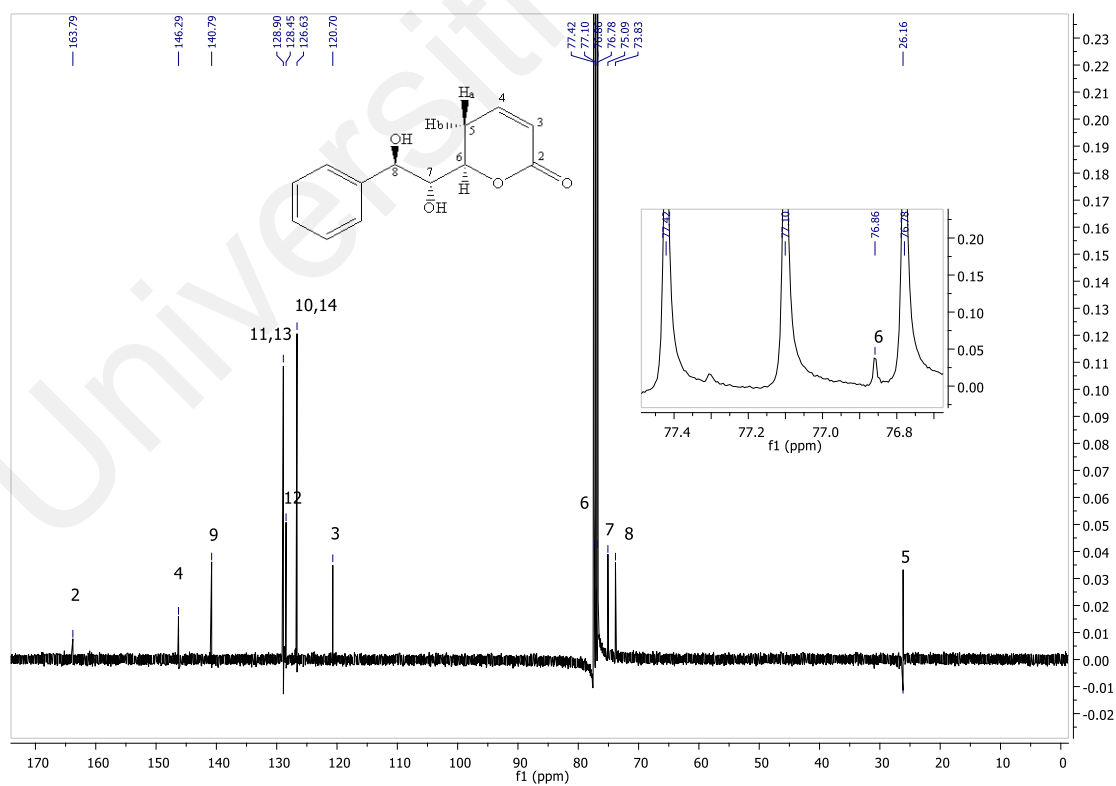
Figure 4.16: ^{13}C (400 MHz) NMR spectrum of goniodiol **3**.

4.1.7   *7-epi*-Goniodiol 10
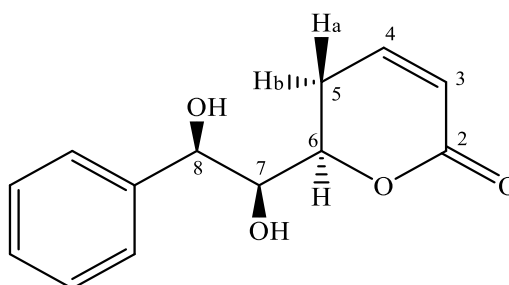
Compound **10** was obtained as yellow amorphous with $[\alpha]_D^{25}= +36.42$. The LCMS-IT-TOF spectrum showed a negative molecular ion peak $[M - H_2O]^-$ at m/z 216.2054 (calcd. for $C_{13}H_{12}O_3$, 216.2052), which corresponded to a molecular formula of $C_{13}H_{14}O_4$. It showed absorption bands in IR spectrum at 3410, 1714, 1402 cm^{-1} corresponding to the hydroxyl, carbonyl and aromatic group.

The ^{1}H NMR of **10** is very similar to that of goniodiol **3**. However, a difference was detected at the chemical shift of H-7 which is more deshielded. H-7 appeared as doublet of doublet at 3.93 ppm with the coupling constant of 5.8 Hz and 4.6 Hz. This suggest that **10** differs from **3** in the configuration at C-7. Meanwhile, H-6 is less deshielded in **10**, it resonated at 4.37-4.42 ppm as doublet of doublet of doublet, with the coupling constant of 12.0 Hz, 5.8 Hz and 4.6 Hz.

Other than that, ^{13}C NMR spectra data also suggested that **10** possessed the same styryl-pyrones type of skeleton as **3**. The ^{1}H NMR spectrum showed that $J_{7/8}$ was 4.6 Hz, and compared with corresponding coupling constant in goniodiol **3**, indicated compound **10** is C-7 epimers.

Comparison of the spectral data with the literature values confirmed that compound **10** was indeed 7-*epi*-goniodiol (Kumaraswamy & Satish Kumar, 2013).

Table 4.8: ^1H (400 MHz), ^{13}C (100 MHz) NMR spectroscopic data (in $CDCl_3$) of 7-*epi*-goniodiol **10**.

Position	^{1}H-NMR δ_H (ppm), J (Hz)		^{13}C-NMR δ_C (ppm)	
	Experimental	Literature	Experimental	Literature
1	-	-	-	-
2	-	-	163.8	163.8
3	5.96-5.99 (1H, *ddd*) J=9.8, 2.8, 1.2	6.00 (1H, *dd*) J=9.7, 1.0	121.1	120.9
4	6.88-6.93, (1H, *ddd*) J=9.8, 6.0, 2.4	6.91-6.93 (1H, *m*)	145.6	145.6
5	2.55-2.59 (1H, *dt*) J=11.6, 2.4 2.59-2.64 (1H, *dt*) J=12.0, 2.8	2.59-2.61 (1H, *m*) 2.49 (1H, *ddd*) J=18.5, 5.2, 4.9	25.0	24.9
6	4.37-4.42 (1H, *ddd*) J=12.0, 5.8, 4.6	4.38-4.42 (1H, *m*)	77.3	77.3
7	3.93 (1H, *dd*) J=5.8, 4.6	3.93-3.95 (1H, *m*)	76.3	76.1
8	4.88 (1H, *d*) J=4.6	4.90 (1H, *d*) J=4.1	72.0	71.9
7-OH	-	2.34 (1H, *d*) J=8.0	-	-
8-OH	-	2.67 (1H, *d*) J=5.0	-	-
9	-	-	140.1	140.1
10, 14	7.37-7.42 (5H, *m*)	7.31-7.38 (5H, *m*)	126.5	126.4
11, 13			128.9	128.7
12			128.5	128.7
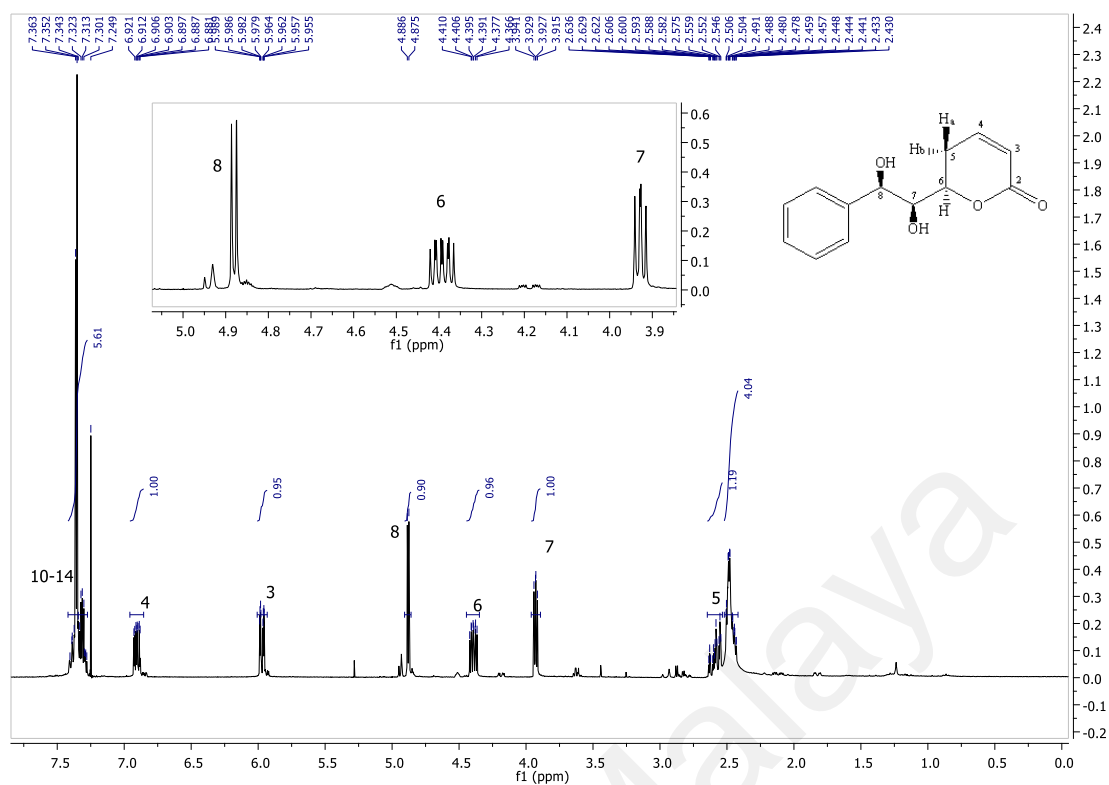
Figure 4.17: ^{1}H (400 MHz) NMR spectrum of 7-*epi*-goniodiol **10**.
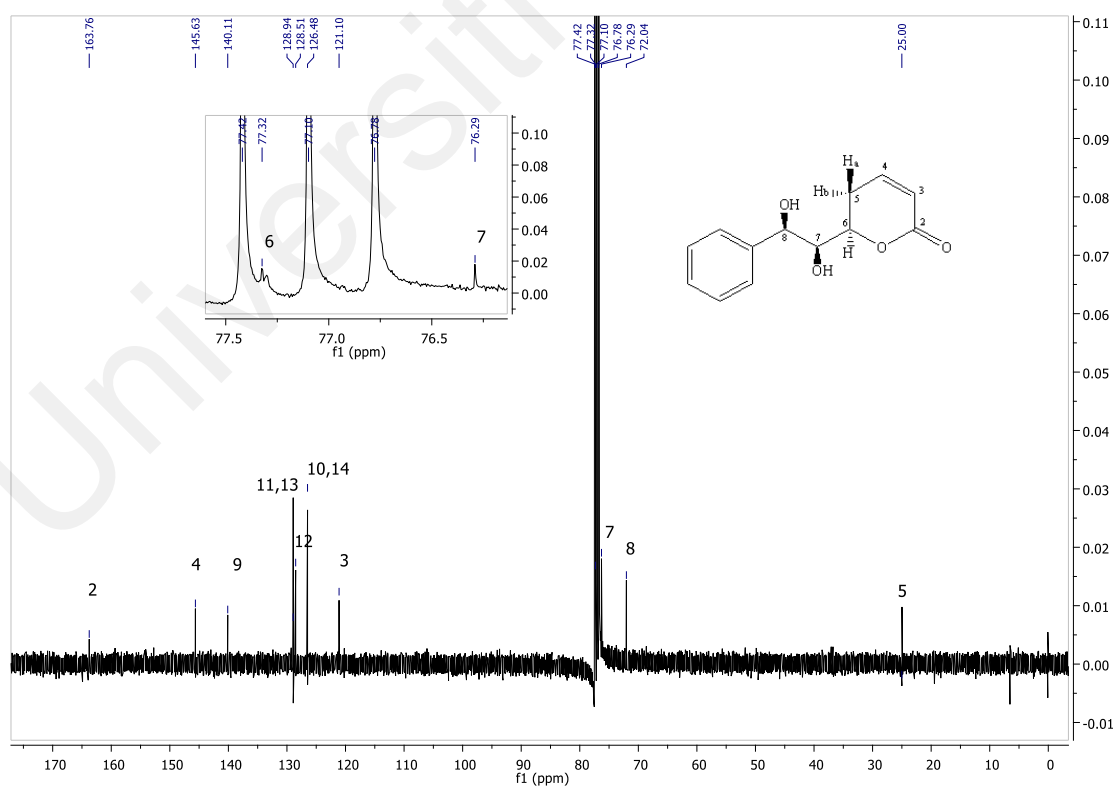
Figure 4.18: ^{13}C (100 MHz) NMR spectrum of 7-*epi*-goniodiol **10**.

4.1.8 Garvensintriol 4
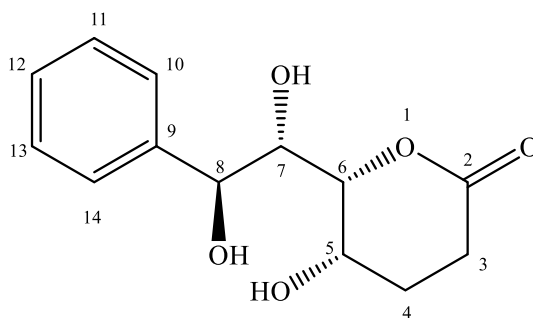
Compound **4** was isolated as yellow amorphous with $[\alpha]_D^{25} = +8.62$. The LCMS-IT-TOF spectrum showed a negative molecular ion peak $[M - H_2O]^-$ at m/z 234.2374 (calcd. for $C_{13}H_{14}O_4$, 234.2372), which corresponded to a molecular formula of $C_{13}H_{16}O_5$. It showed absorption bands in IR spectrum at 3393 and 1755 cm^{-1} corresponding to the hydroxyl and carbonyl group.

In the ^{1}H NMR spectrum, a multiplet signal at δ 7.23-7.40 characteristics for five aromatic protons (H-10 to H-14) of *mono*-substituted phenyl ring. Two methylene protons resonated at δ 2.42-2.47 (*m*) and δ 1.97-2.03 (*m*) belonged to H-3 and H-4, respectively. Four deshielded one proton signal at δ 4.22 (*td*, *J* = 7.4, 3.6 Hz, H-5), δ 4.05 (*dd*, *J* = 7.4, 4.6 Hz, H-6), δ 4.00 (*dd*, *J* = 8.4, 4.6 Hz, H-7) and δ 4.70 (*d*, *J* = 8.4 Hz, H-8), were indicative of oxygen bearing methine protons. These protons were assigned based on ^{1}H-^{1}H COSY and HMBC experiments.

The ^{13}C NMR spectrum showed thirteen carbons; two methylene, nine methine and two quaternary carbon. Two methylene carbon C-3 and C-4 showed the peak at δ 30.0 and δ 25.0, respectively. The other four methine carbon resonated in the range δ 72 – 82 is due to the deshielding effect by the neighbouring oxygen atom. Finally for aromatic carbon peak occurred at δ 128.0 which attributed to the two aromatic carbons of C-10 and C-14, meanwhile the peak at δ 125.7 corresponding to the two aromatic carbons of C-11 and C-13. Another aromatic carbon peak appeared at δ 127.2 which could be assigned for

C-12. The carbonyl carbon of the lactone appeared at δ 176.1, it is slightly more deshielded due to the absent of double bond at adjacent carbon.

Comparison of the spectral data with the literature values confirmed that compound **4** was garvensintriol, with styryl-pyrones skeleton, that been isolated from *Goniothalamus arvensis* previously (Bermejo et al., 1998).

Table 4.9: ^{1}H (400 MHz), ^{13}C (100 MHz) NMR spectroscopic data (in CD_3OD) of garvensintriol **4**.

Position	^{1}H-NMR δ_H (ppm), J (Hz)		^{13}C-NMR δ_C (ppm)	
	Experimental	Literature [a]	Experimental	Literature [a]
1	-	-	-	-
2	-	-	176.1	177.0
3	2.42-2.47 (2H, *m*)	2.49 (H-a, *dtd*) J=17.9, 1.8, 1.4 2.59 (H-b, *ddd*) J=17.9, 5.3, 5.1	30.0	28.2
4	1.97-2.03 (2H, *m*)	2.05 (H-a, *m*) J=17.8, 7.9, 5.3, 1.4 2.25 (H-b, *m*) J=17.8, 7.4, 5.1, 1.8	25.0	24.0
5	4.22 (1H, *td*) J=7.4, 3.6	4.62 (1H, *td*) J=7.9, 7.4, 4.6	80.5	75.8
6	4.05 (1H, *dd*) J=7.4, 4.6	3.77 (1H, *dd*) J=4.6, 1.8	72.6	81.8
7	4.00 (1H, *dd*) J=8.4, 4.6	3.84 (1H, *dd*) J=5.8, 1.8	79.9	72.1
8	4.70 (1H, *d*) J=8.4	4.96 (1H, *d*) J=5.8	82.2	73.8
7-OH	-	-	-	-
8-OH	-	-	-	-
9	-	-	141.8	140.2
10, 14	7.23-7.40 (5H, *m*)	7.30-7.39 (5H, *m*)	128.0	128.8
11, 13			125.7	126.1
12			127.2	128.2

[a] In $CDCl_3$.
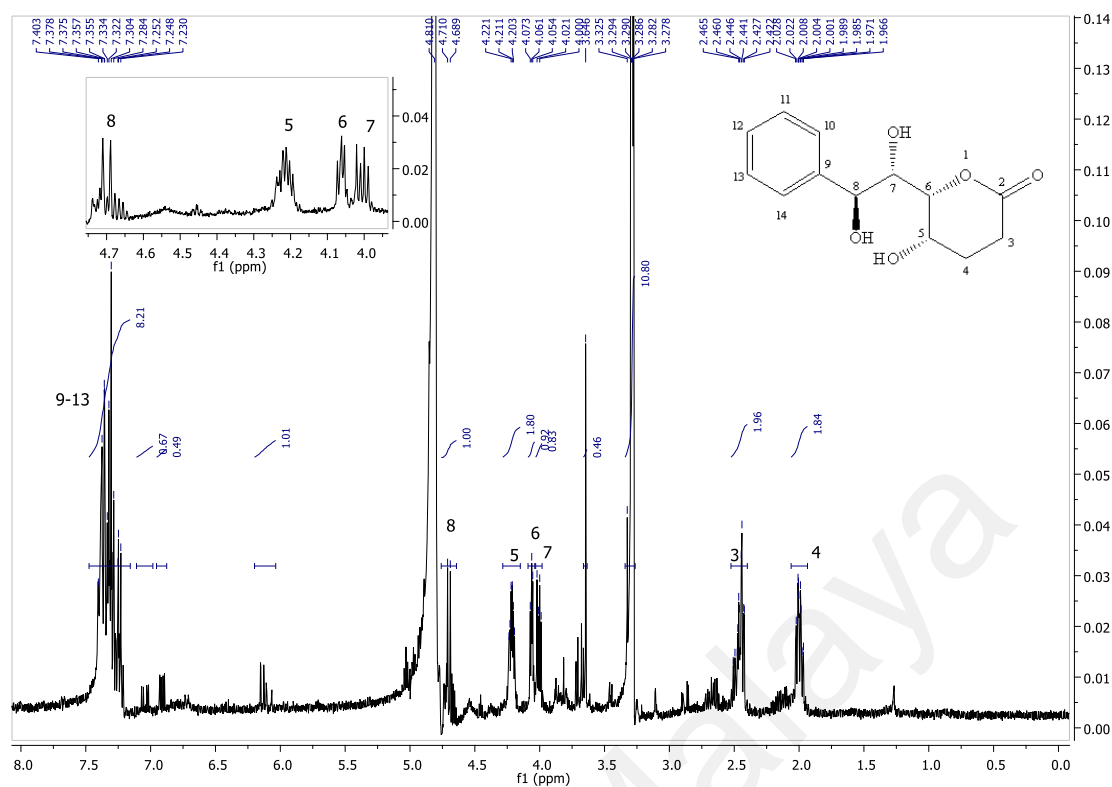
Figure 4.19: ¹H (400 MHz) NMR spectrum of garvensintriol **4**.
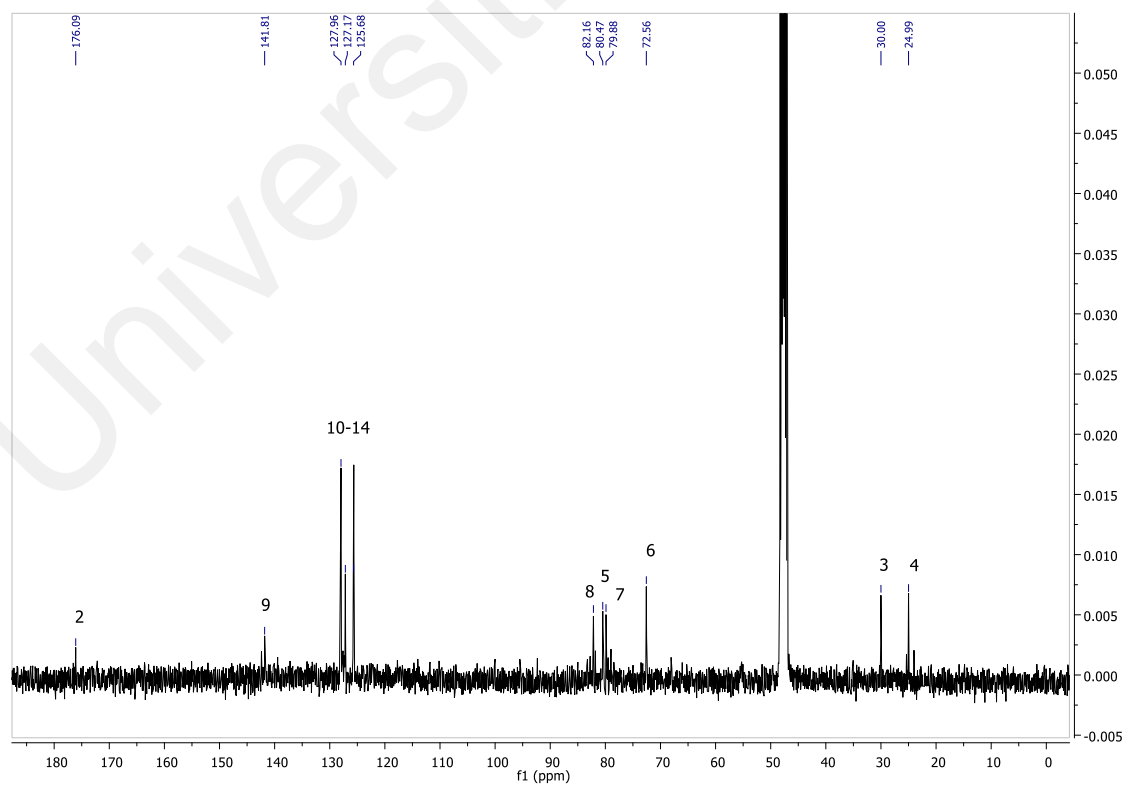
Figure 4.20: ¹³C (100 MHz) NMR spectrum of garvensintriol **4**.

4.1.9   Goniopypyrone 26
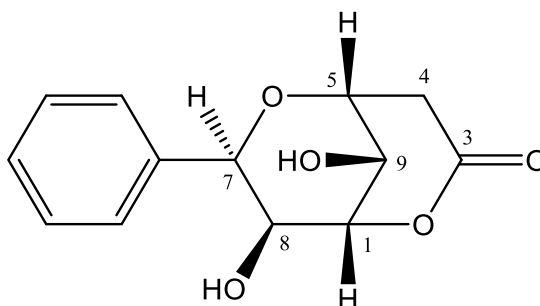
Compound **26** was obtained as yellow amorphous with $[\alpha]_D^{25}$= +10.34. The LCMS-IT-TOF spectrum showed a negative ion peak $[M - H]^-$ at m/z 249.0717 (calcd. for $C_{13}H_{13}O_5$, 249.0718), which corresponded to a molecular formula of $C_{13}H_{14}O_5$. It showed absorption bands in IR spectrum at 3398 and 1745 cm^{-1} corresponding to the hydroxyl and carbonyl group.

In the ^{1}H NMR spectrum, a multiplet signal at δ 7.32-7.52 characteristics for five aromatic protons (H-10 to H-14) of *mono*-substituted phenyl ring. Two protons at position 4 are non-equivalent methylene protons at δ 2.99 (*d*, *J*=19.6 Hz) and δ 3.09 (*dd*, *J*=19.6, 4.8 Hz).

Five deshielded oxymethine proton signals at δ 4.67 (*m*, H-1), δ 4.24 (*d*, *J* = 3.6 Hz, H-5), δ 4.45 (*d*, *J* = 9.8 Hz, H-7), δ 4.11 (*dd*, *J* = 9.8, 2.0 Hz, H-8) and δ 4.33 (*d*, *J* = 4.4 Hz, H-9), were belonged to H-1, H-5, H-7 and H-8, respectively. These protons were assigned based on ^{1}H-^{1}H COSY and HMBC experiments.

The ^{13}C NMR spectrum showed thirteen carbons; one methylene, ten methine and two quaternary carbon. A methylene carbon C-4 showed the peak at δ 35.3. The other four methine carbon resonated in the range δ 65 – 78 is due to the deshielding effect by the neighbouring oxygen atom. Finally for aromatic carbon peak occurred at δ 127.8 which attributed to the two aromatic carbons of C-11 and C-15, meanwhile the peak at δ 127.9

corresponding to the two aromatic carbons of C-12 and C-14. Another aromatic carbon

peak appeared at δ 127.7 which could be assigned for C-13. The carbonyl carbon of the

lactone appeared at δ 167.9.

Comparison of the obtained spectral data with the literature values confirmed that **26**

was goniopypyrone with pyrano-pyrones skeleton (Mahiwan et al., 2013).

Table 4.10: [1]H (400 MHz), ^{13}C (100 MHz) NMR spectroscopic data (in CD$_3$OD and (CD$_3$)$_2$CO) of goniopypyrone **26**.

Position	^{1}H-NMR δ_H (ppm), J (Hz)		^{13}C-NMR δ_C (ppm)	
	Experimental [a]	Literature [b]	Experimental [c]	Literature [b]
1	4.67 (1H, *m*)	4.65 (1H, *m*)	78.6	78.7
2	-	-	-	-
3	-	-	167.9	169.7
4	3.09 (1H, *dd*) J=19.6, 4.8 2.99 (1H, *d*) J=19.6	3.10 (1H, *dd*) J=19.4, 5.1 2.97 (1H, *dd*) J=19.4, 1.5	35.3	35.0
5	4.24 (1H, *d*) J=4.0	4.22 (1H, *m*)	70.1	69.9
6	-	-	-	-
7	4.45 (1H, *d*) J=9.8	4.43 (1H, *d*) J=9.9	73.7	73.8
8	4.11 (1H, dd) J=9.8, 2.0	4.09 (1H, *dd*) J= 9.9, 2.6	68.4	68.0
9	4.33 (1H, *d*) J=4.0	4.30 (1H, *dd*) J=4.6, 1.5	65.7	65.2
5-OH	-	4.58 (*br s*)	-	-
7-OH	-	5.48 (*br s*)		
10	-	-	140.1	139.0
11, 15	7.32-7.52 (5H, *m*)	7.33-7.49 (5H, *m*)	127.8	127.7
12, 14			127.9	127.9
13			127.7	127.8

[a] In CD$_3$OD.

[b] In CDCl$_3$.

[c] In (CD$_3$)$_2$CO.
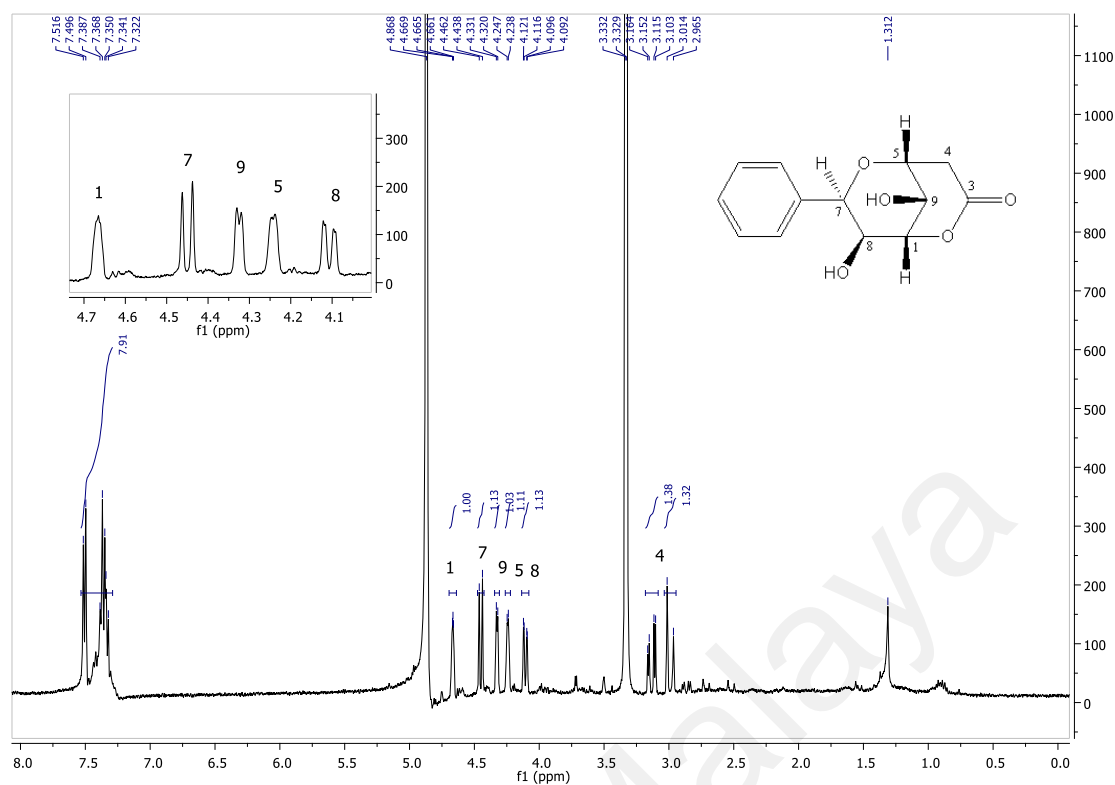
Figure 4.21: ¹H (400 MHz) NMR spectrum of goniopypyrone **26**.
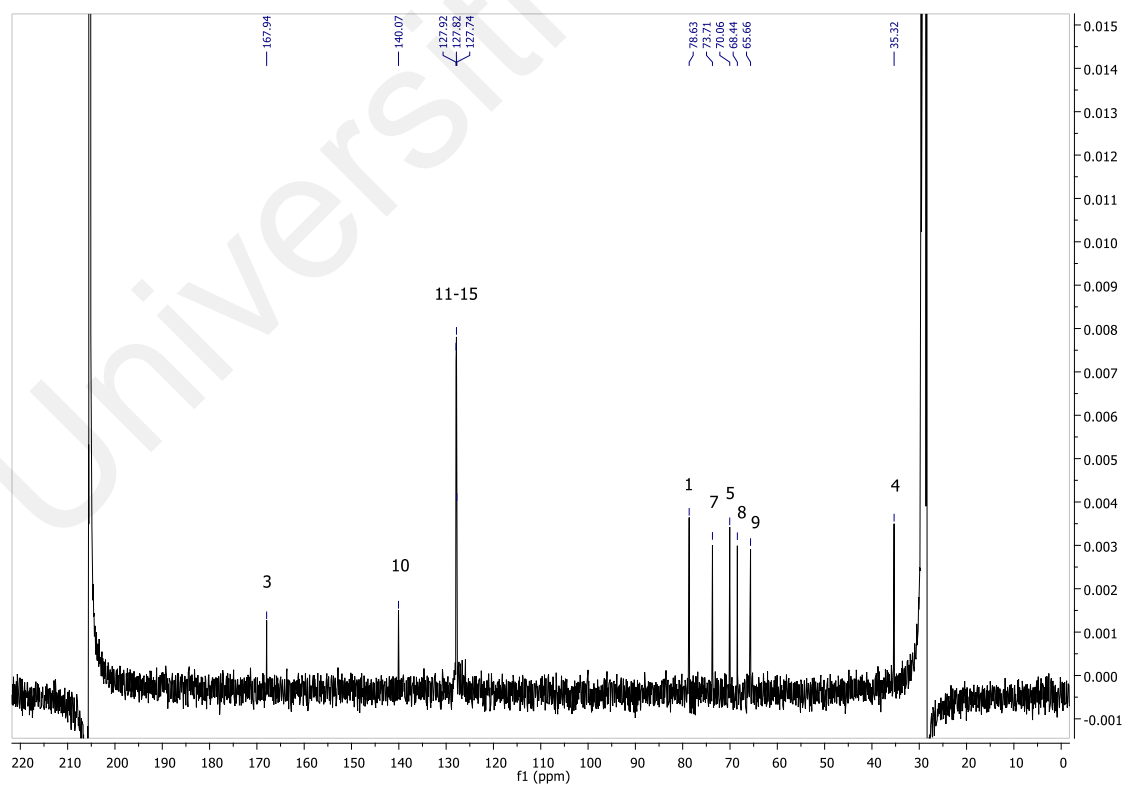
Figure 4.22: ¹³C (100 MHz) NMR spectrum of goniopypyrone **26**.

4.1.10 8-*epi*-9-deoxygoniopypyrone 24
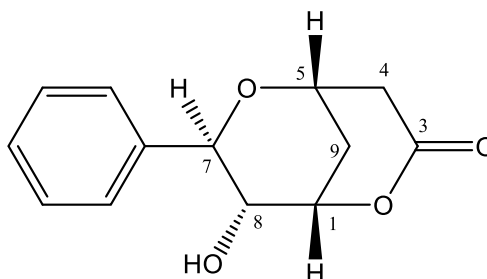
Compound **24** was isolated as yellow amorphous with $[\alpha]_D^{25} = +13.11$. The molecular formula of $C_{13}H_{14}O_4$ was deduced from its negative LCMS-IT-TOF spectrum (m/z 233.0174 $[M - H]^-$; calcd. for $C_{13}H_{13}O_4$, 233.0171). The IR spectrum showed strong absorptions bands of O-H stretching at 3395 cm^{-1} and C=O stretching at 1734 cm^{-1}. The UV spectrum with absorptions bands at 210 nm.

The ^{1}H NMR spectrum showed a multiplet δ 7.33-7.43 referring to five aromatic protons (H-11 to H-15) from a *mono*-substituted phenyl ring. Four deshielded one-proton signal at δ 4.95 (*m*), δ 4.48 (*dq*), δ 4.43 (*d*) and δ 3.62 (*ddd*) were indicative of oxygen bearing methine protons belonged to H-1, H-5, H-7 and H-8, respectively. Two protons at position 4 are non-equivalent methylene protons at δ 2.88 (*dd*, *J*=19.7, 5.0 Hz) and δ 2.99 (*dq*, *J*=19.7, 1.8 Hz).

The ^{13}C NMR spectrum showed thirteen carbons; two methylene, nine methine and two quaternary carbon. Two quaternary carbon peaks at δ 169.1 and δ 137.9 were assigned to C-3 and C-10 respectively. Four carbons, C-1, C-5, C-7 and C-8, resonated in between δ 65.9 – δ 76.8 is due to the deshielding effect by the neighbouring oxygen atom. Finally the aromatic carbon peaks showed signal at δ 127.4 attributed to the two aromatic carbons of C-11 and C-15, meanwhile the peak at δ 128.7 corresponding to the two aromatic carbons of C-12 and C-14 and *para* aromatic carbon peak appeared at δ

127.4 which was assigned for C-13. The carbonyl carbon of the lactone appeared at δ
169.1.

Comparison of the obtained spectral data with the literature values confirmed that **24**
was 8-*epi*-9-deoxygoniopypyrone, which is also with pyrano-pyrone skeleton (Tai et al.,
2010).

Table 4.11: ^{1}H (400 MHz), ^{13}C (100 MHz) NMR spectroscopic data (in CDCl$_3$) of 8-*epi*-
9-deoxy-goniopypyrone **24**.

Position	^{1}H-NMR δ_H (ppm), J (Hz)		^{13}C-NMR δ_C (ppm)	
	Experimental	Literature	Experimental	Literature
1	4.95 (1H, *m*)	4.93 (1H, *br s*)	76.8	76.8
2	-	-	-	-
3	-	-	169.1	169.1
4	2.99 (1H, *dq*) J=19.7, 1.5 2.88 (1H, *dd*) J=19.7, 5.0	2.99 (1H, *d*) J=19.5 2.88 (1H, *dd*) J=19.5, 5.5	36.7	36.6
5	4.48 (1H, *dq*) J=2.8, 1.5	4.47 (1H, *br s*)	65.9	65.8
6	-	-	-	-
7	4.43 (1H, *d*) J=9.9	4.46 (1H, *d*) J=10.0	74.5	74.3
8	3.62 (1H, *ddd*) J=9.9, 8.2, 2.3	3.59 (1H, *ddd*) J=10.0, 8.5, 2.0	72.7	72.6
9	2.24 (2H, *m*)	2.23 (2H, *m*)	30.0	29.9
8-OH	2.28 (1H, *d*) J=8.2	2.43 (1H, *d*) J=8.5	-	-
10	-	-	137.9	137.9
11, 15	7.33-7.43 (5H, *m*)	7.35-7.42 (5H, *m*)	127.4	127.4
12, 14			128.7	128.6
13			127.4	128.7
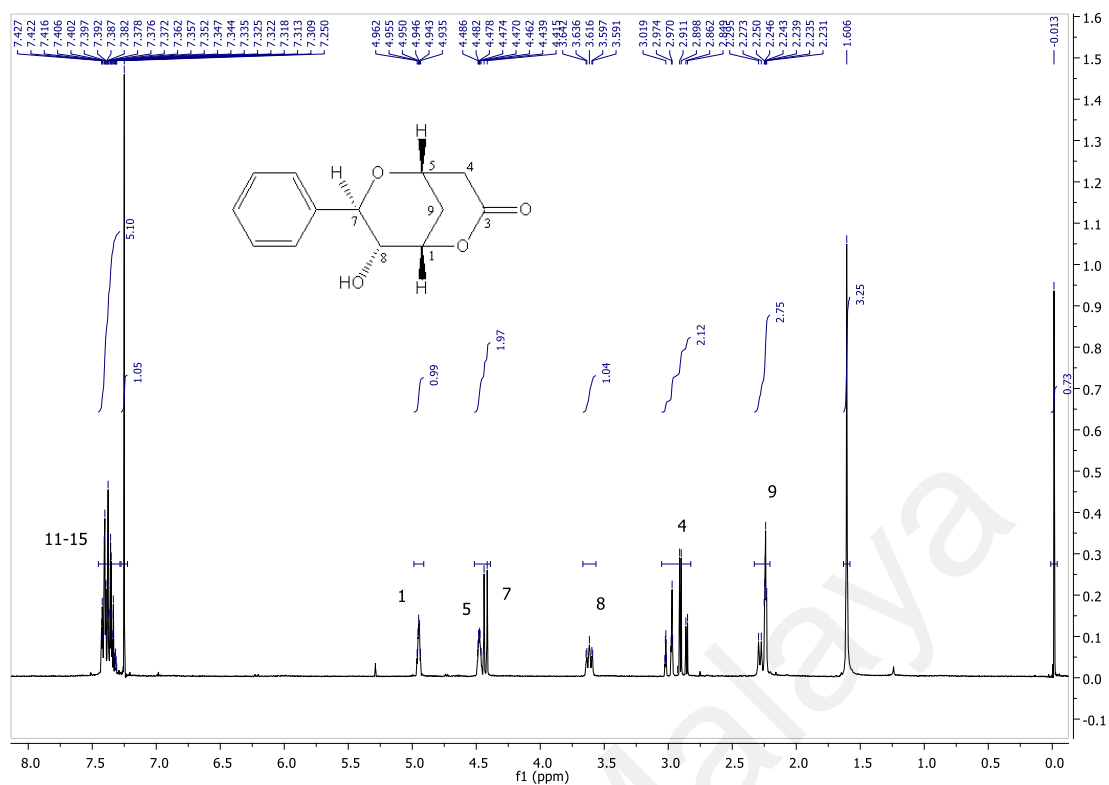
Figure 4.23: ^{1}H (400 MHz) NMR spectrum of 8-*epi*-9-deoxygoniopypyrone **24**.
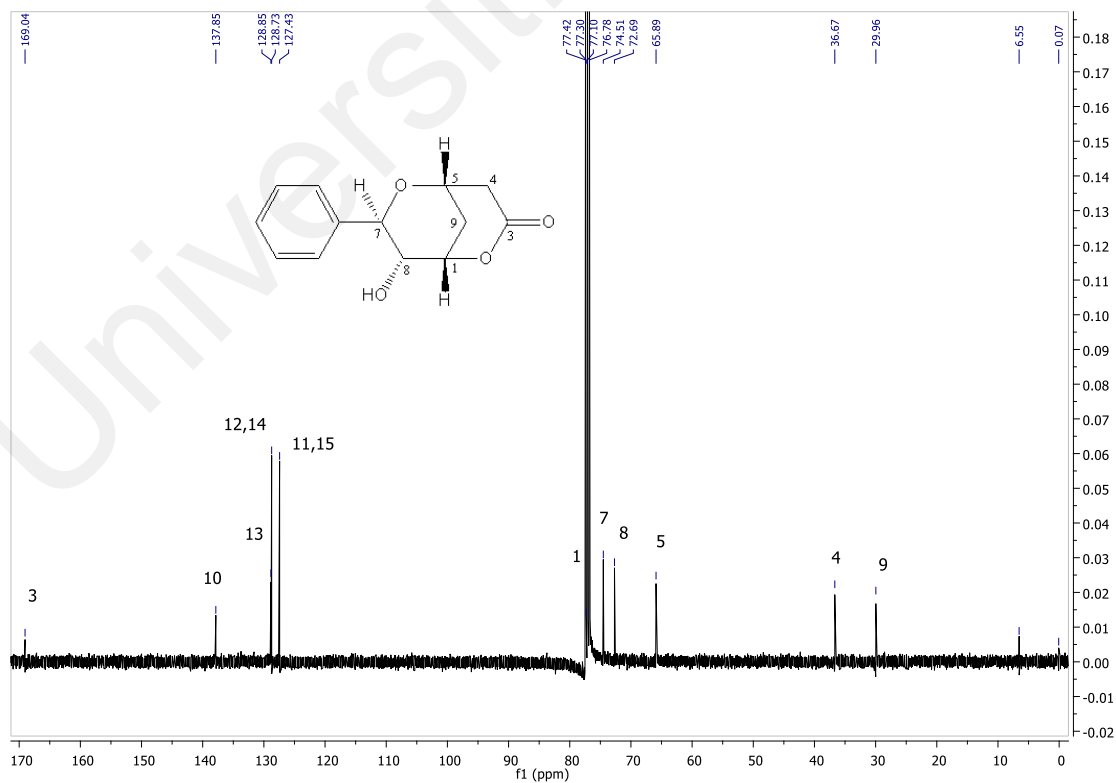
Figure 4.24: ^{13}C (100 MHz) NMR spectrum of 8-*epi*-9-deoxygoniopypyrone **24**.

98

4.1.11 Goniomicin A 147
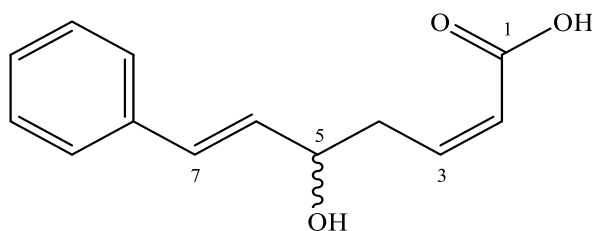
Compound **147** was isolated as yellowish amorphous solid with $[\alpha]_D^{25} = +15.34$. The LCMS-IT-TOF spectrum showed a negative molecular ion peak $[M - H_2O]^-$ at m/z 200.0078 (calcd. for $C_{13}H_{12}O_2$, 200.0073), which corresponded to a molecular formula of $C_{13}H_{14}O_3$. The IR spectrum showed strong absorptions bands of O-H stretching at 3350 cm^{-1}, C=O stretching at 1665 cm^{-1} and C-O stretching at 1327 cm^{-1} (Smith & Dent, 2005). The UV spectrum revealed maximum at 206 and 252 nm.

The ^1H NMR spectrum showed the aromatic protons at δ 7.18-7.38 referring to five aromatic protons (H-9 to H-13) of a *mono*-substituted phenyl ring. Four olefinic protons peaks at δ 6.58, δ 6.27, δ 6.17 and δ 5.95 which belonged to H-7, H-6, H-3 and H-2 were observed. H-7 and H-6 were in *trans* configuration, while H-3 and H-2 were in *cis* configuration. The others configurations were determined by a proton signal at δ 4.33 (*q*, *J*=6.2 Hz) was indicative of oxygen bearing methine proton H-5. Two allylic protons resonated at δ 2.92 (*m*) belonged to H-4.

The ^{13}C and DEPT-135 spectra further confirmed the presence of thirteen carbons; one methylene, ten methines and two quaternary carbon peaks appeared at δ 170.2 and δ 137.0 which were most probably belonged to C-1 and C-8 respectively. Four olefinic carbons; C-2, C-3, C-6 and C-7, resonated at δ123.6, δ 140.9, δ 131.8 and δ 129.8 respectively. C-3 resonated most downfield compared to the other olefinic carbons due to the α-β unsaturated resonance effect of carbonyl group at position C-1. The methylene carbon C-4 gave a peak at δ 36.2 meanwhile C-5 showed a peak at δ 71.5 which were due to the

deshielding effect by the neighbouring oxygen atom. Finally the five aromatic protons gave signals centred at δ 126.1-128.2 (C-9 to C-13).

The HMBC correlations of H-2, H-3 to C-1 suggested that the double bond was linked to C-1. The correlations of the two olefinic protons H-6, H-7 to C-5 and C-8 indicated the aromatic ring was connected to C-7.

Compound **147** was identified as goniomicin A, this compound has been isolated from dichloromethane crude of the stem of *G. tapisoides*.

Table 4.12: [1]H (400 MHz), ^{13}C (100 MHz) NMR spectroscopic data (in CD₃OD) of goniomicin A **147**.

Position	^{1}H-NMR δ_H (ppm), J (Hz)		^{13}C-NMR δ_C (ppm)	
	Experimental	Literature [a]	Experimental	Literature [a]
1	-	-	170.2	169.6
2	5.95 (1H, *td*) J=11.8, 1.6	5.96 (1H, *d*) J=11.9	123.6	125.3
3	6.17 (1H, *td*) J=11.8, 7.6	6.12 (1H, *ddd*) J=11.9, 8.5, 3.5	140.9	140.6
4	2.92 (2H, *m*)	2.76 (1H, *m*) 2.81 (1H, *m*)	36.2	36.6
5	4.33 (2H, *q*) J=6.2	4.41 (1H, *q*) J=6.6	71.5	71.5
6	6.27 (1H, *dd*) J=16.2, 6.2	6.20 (1H, *dd*) J=16.0, 6.6	131.8	131.9
7	6.58 (1H, *d*) J=16.2	6.59 (1H, *d*) J=16.0	129.8	129.9
8	-	-	137.0	136.7
9, 13	7.18-7.38 (5H, *m*)	7.19-7.34 (5H, *m*)	126.1	126.5
10, 12			128.2	128.6
11			127.2	127.6

[a] In CDCl₃.
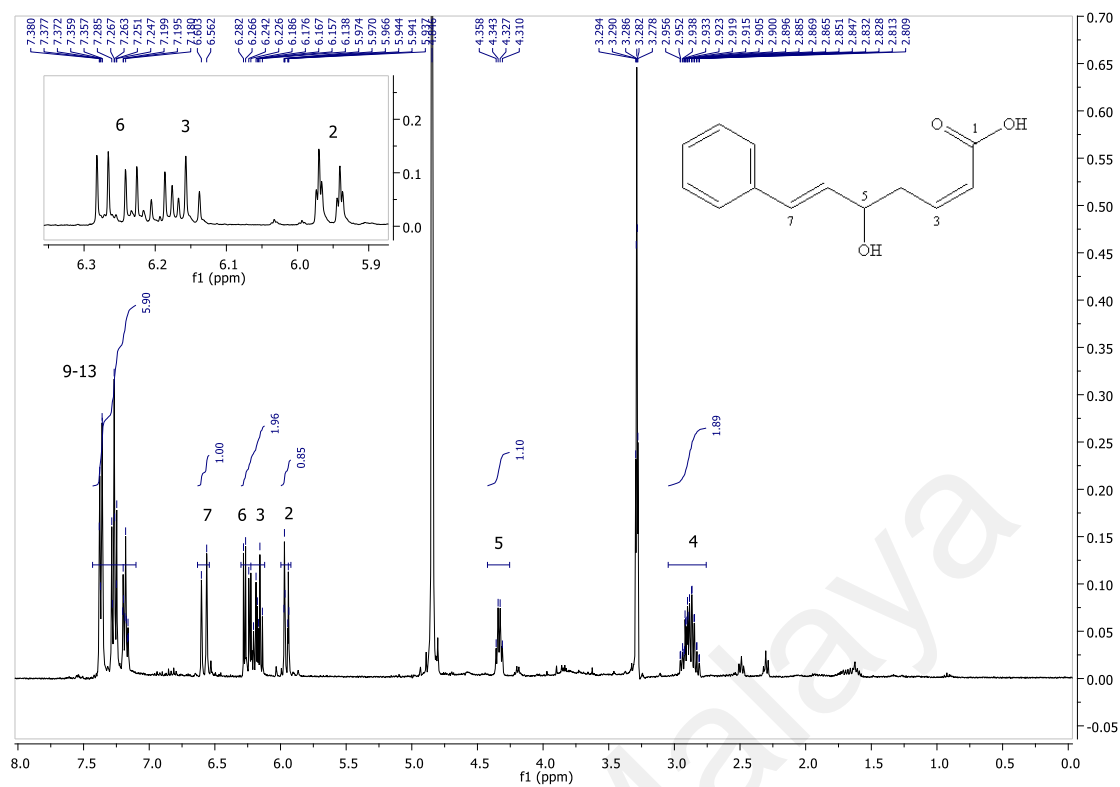
Figure 4.25: ^{1}H (400 MHz) NMR spectrum of goniomicin A **147**.
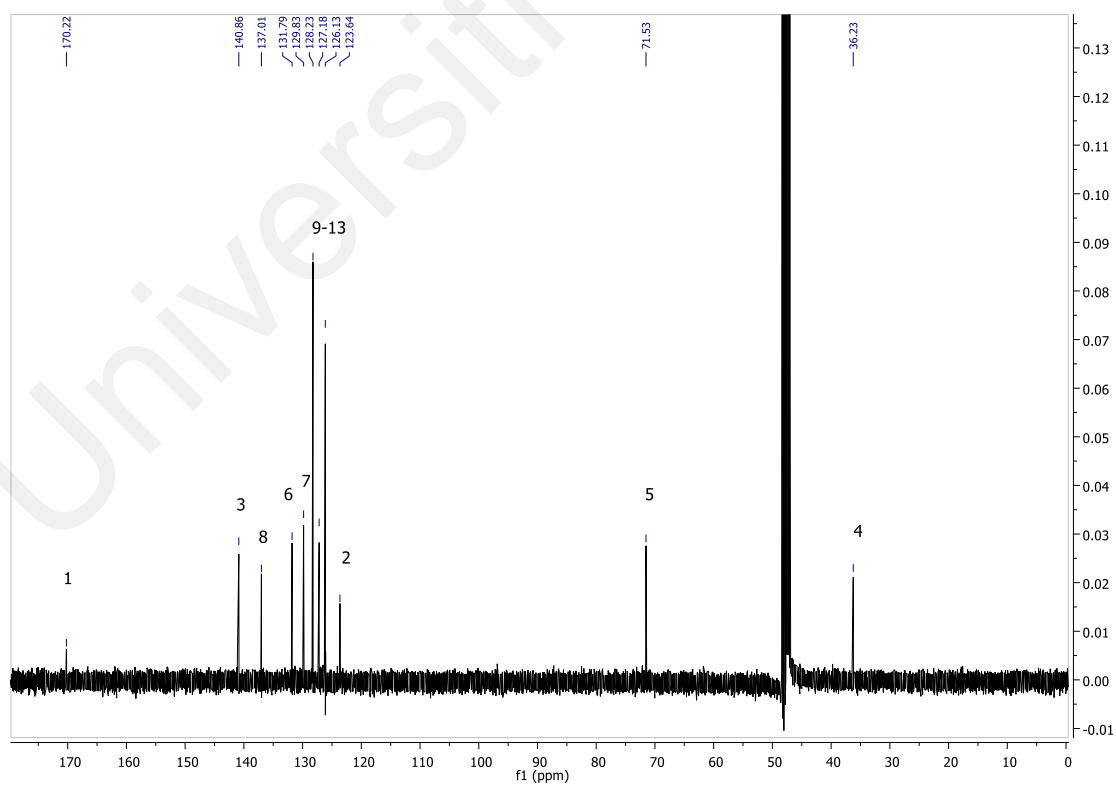
Figure 4.26: ^{13}C (100 MHz) NMR spectrum of goniomicin A **147**.

4.1.12 Goniomicin E 152
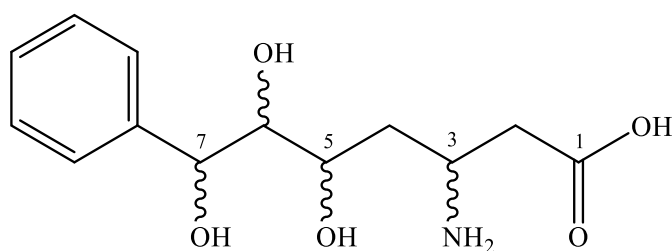
152

Compound **152** was isolated as amorphous solid with $[\alpha]_D^{25} = +5.38$. The LCMS-IT-TOF mass spectrum showed a positive ion peak $[M+H]^+$ at *m/z* 270.1355 (calcd. for $C_{13}H_{20}NO_5$ 270.1359), corresponding to a molecular formula of $C_{13}H_{19}NO_5$. The IR spectrum showed strong absorptions bands of N-H bending at 1609 cm^{-1} and C=O stretching at 1717 cm^{-1}.

The ^1H NMR spectrum showed a multiplet δ 7.21-7.40 referring to five aromatic protons (H-9 to H-13) from a *mono*-substituted phenyl ring. Four deshielded one-proton signal at δ 3.56 (*m*), δ 4.12 (*ddd*), δ 3.41 (*dd*) and δ 4.65 (*d*) were belonged to H-3, H-5, H-6 and H-7, respectively. H-3 was nitrogen bearing methine proton meanwhile H-5, H-6 and H-7 were oxygen bearing methine protons. Four non-equivalent methylene protons of position 2 and 4 resonated at δ 2.33 (*dd*), δ 2.50 (*dd*), δ 1.64 (*ddd*) and δ 2.00 (*ddd*) respectively.

The ^{13}C NMR spectrum showed thirteen carbons; two methylenes, nine methines and two quaternary carbons. Two quaternary carbons resonated at δ 175.1 and δ 142.8 were assigned to C-1 and C-8 respectively. Two methylene carbons, C-2 and C-4 gave peaks at δ 38.3 and δ 35.9 respectively. A methine carbon slightly deshielded and resonated at δ 48.6 is due to the deshielding effect by the neighbouring nitrogen atom. The other three methine carbons, C-5, C-6 and C-7 resonated at δ 68.6, δ 76.3 and δ 74.2 respectively, which is due to the deshielding effect by the neighbouring oxygen atom.

Finally the aromatic carbon peaks showed signal at δ 126.9 attributed to the two aromatic carbons of C-9 and C-13, meanwhile the peak at δ 127.8 corresponding to the two aromatic carbons of C-10 and C-12 and *para* aromatic carbon peak appeared at δ 127.2 which was assigned for C-11. The carbonyl carbon of the lactone appeared at δ 175.1.

Therefore, **152** was identified as 3-amino-5,6,7-trihydroxy-7-phenylheptanoic acid, named as goniomicin E.

Table 4.13: [1]H (400 MHz), ^{13}C (100 MHz) NMR and HMBC spectral data (in CD₃OD) of goniomicin E **152**.

Position	^{1}H-NMR δ_H (ppm), J (Hz)	^{13}C-NMR δ_C (ppm)	HMBC (H→C)
1	-	175.1	-
2	2.33 (1H, *dd*) *J*=16.8, 8.4 2.50 (1H, *dd*) *J*=16.8, 4.4	38.3	C-1, C-3, C-4
3	3.56 (1H, *m*)	48.6	-
4	1.64 (1H, *ddd*) *J*=14.8, 5.2, 3.2 2.00 (1H, *ddd*) *J*=18.8, 10.6, 8.4	35.9	C-3, C-5
5	4.12 (1H, *ddd*) *J*=10.6, 2.8, 1.8	68.6	-
6	3.41 (1H, *dd*) *J*=7.6, 1.8	76.3	C-4, C-7
7	4.65 (1H, *d*) *J*=7.6	74.2	C-5, C-6, C-9, C-13
8	-	142.8	-
9, 13		126.9	C-7
10, 12	7.21-7.40 (5H, *m*)	127.8	C-8
11		127.2	C-9, C-13

Figure 4.27: ^{1}H (400 MHz) NMR spectrum of goniomicin E **152**.
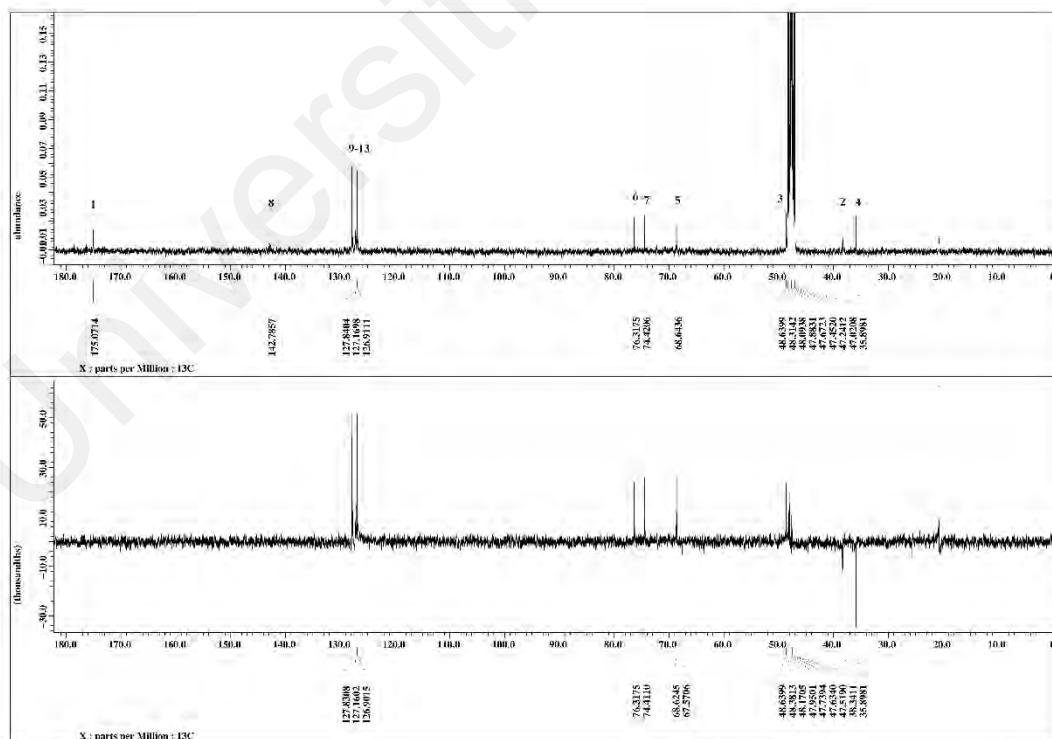
Figure 4.28: ^{13}C (100 MHz) and DEPT-135 NMR spectra of goniomicin E **152**.
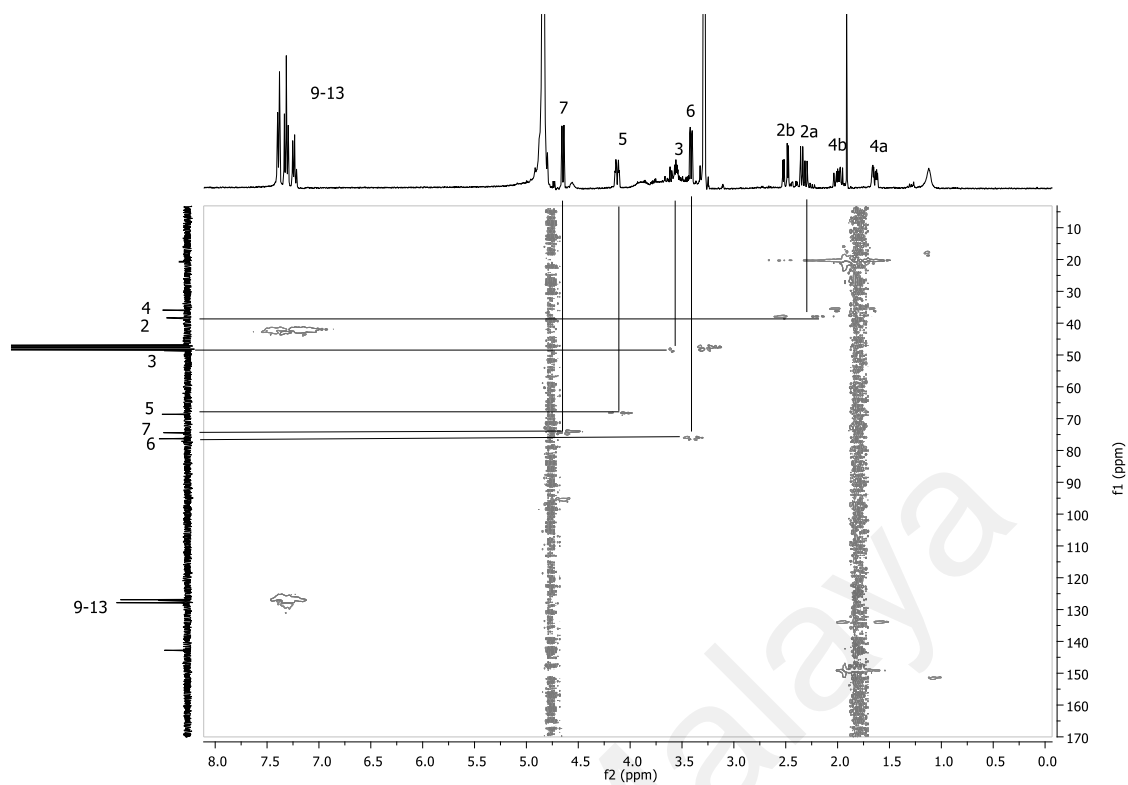
Figure 4.29: HSQC spectrum of goniomicin E **152**.
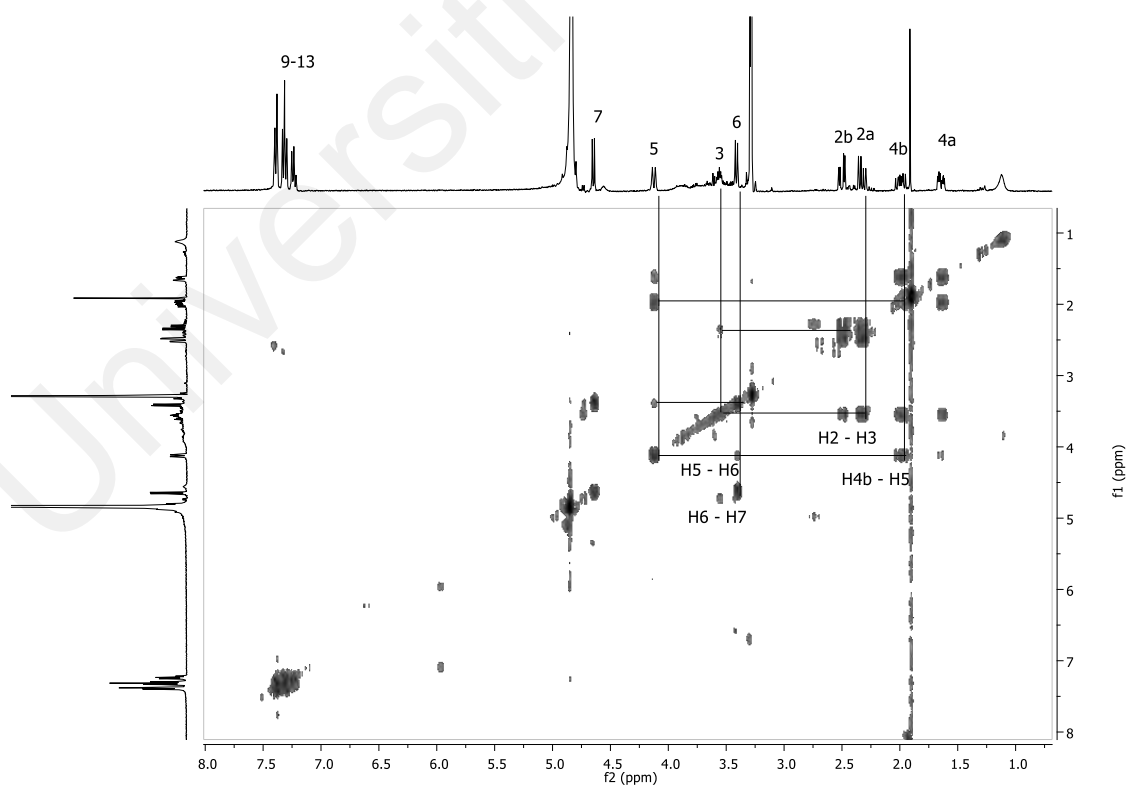
Figure 4.30: COSY spectrum of goniomicin E **152**.
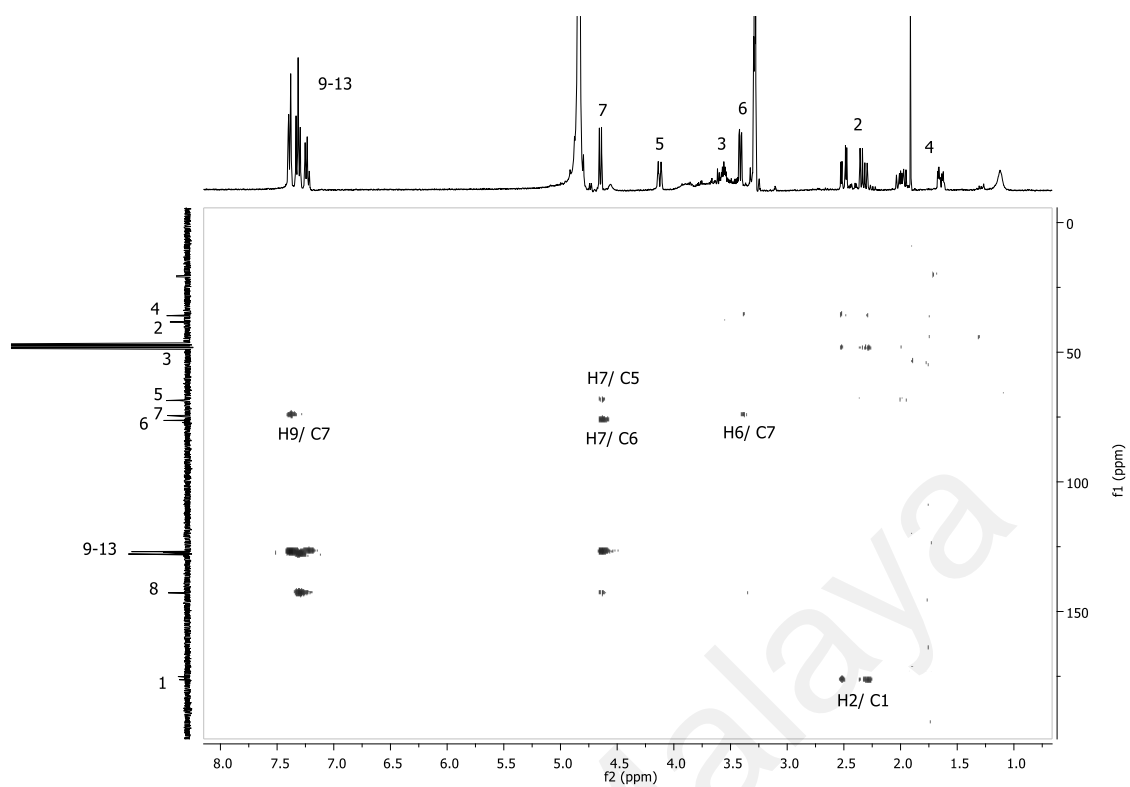
Figure 4.31: HMBC spectrum of goniomicin E **152**.
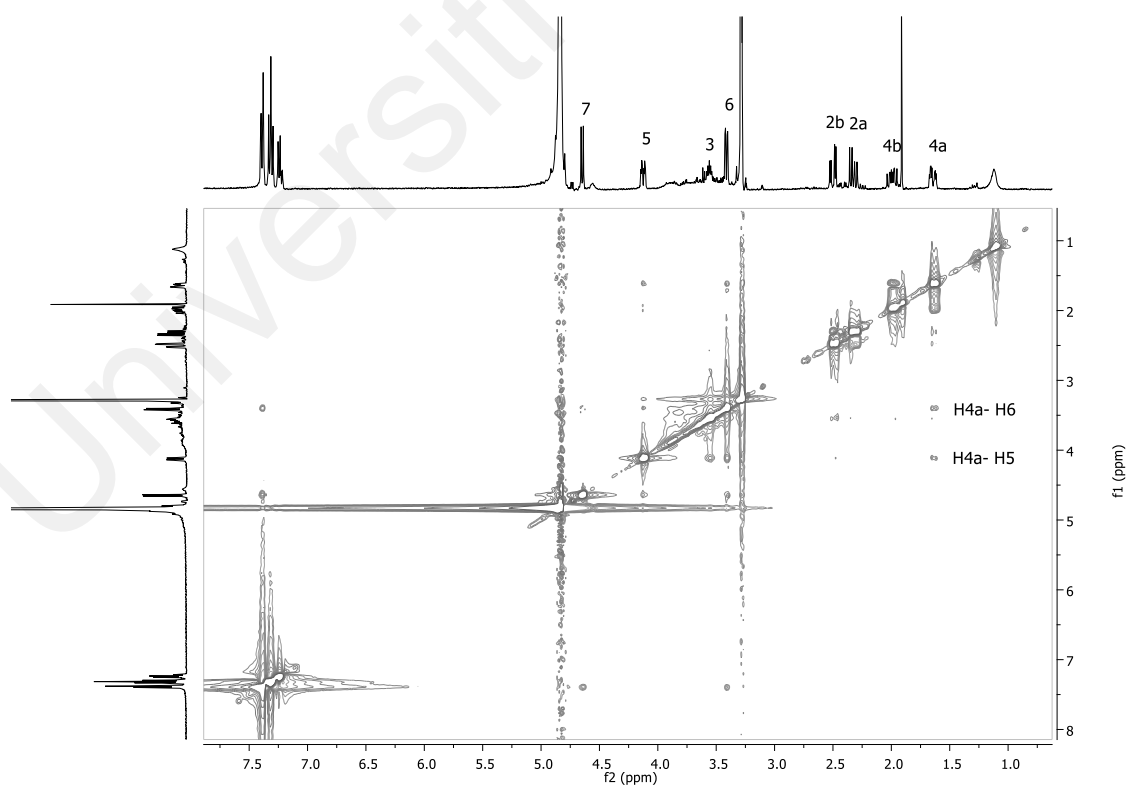
Figure 4.32: NOESY spectrum of goniomicin E **152**.
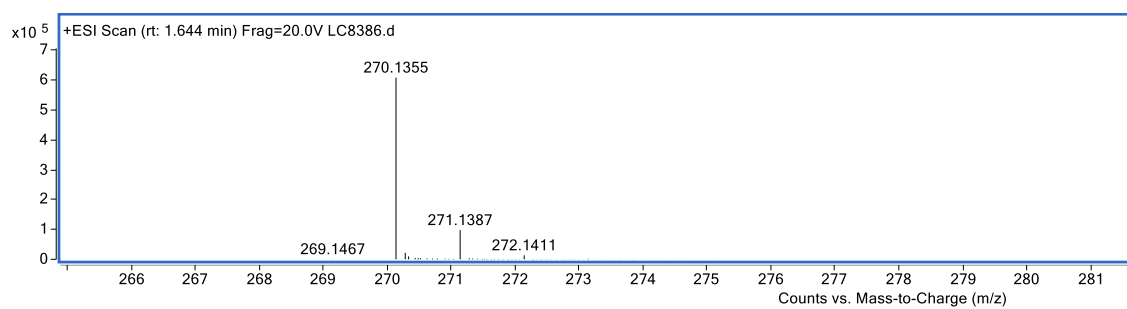
Figure 4.33: LCMS spectrum of goniomicin E **152**.

4.1.13 Goniomicin F 153

153
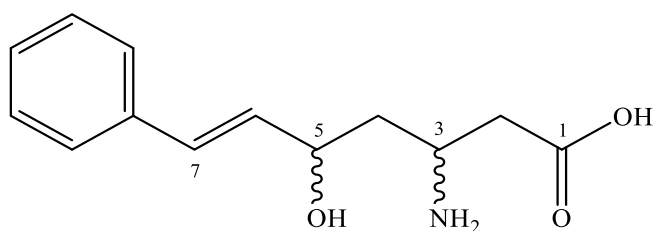
Compound **153** was isolated as colourless crystal with $[\alpha]_D^{25} = +10.87$. The LCMS-IT-TOF mass spectrum showed a peak at *m/z* 235.1447 [M] (calcd. for $C_{13}H_{17}NO_3$ 235.1451), corresponding to a molecular formula of $C_{13}H_{17}NO_3$. The IR spectrum showed strong absorptions band of O-H stretching at 3568 cm⁻¹ and C=O stretching at 1702 cm⁻¹.

The ¹H NMR spectrum showed a multiplet δ 7.18-7.39 referring to five aromatic protons (H-9 to H-13) from a *mono*-substituted phenyl ring. Two olefinic protons peaks at δ 6.61 and δ 6.23 in *trans* configuration which belonged to H-7 and H-6 were observed. An allylic proton resonated at δ 4.43 (*m*) is an oxygen bearing methine proton belonged to H-5. There are two methylene signals at δ 2.35-2.58 and δ 1.82 that assignable to H-2 and H-4 respectively. A downfield shift of H-3 with chemical shift δ 3.60 (*m*) were due to the neighbouring nitrogen.

The ¹³C NMR spectrum showed thirteen carbons; two methylene, nine methine and two quaternary carbon. The olefinic carbons C-6 and C-7 resonated at δ 131.5 and δ 130.1 respectively. Two methylene carbons, C-2 and C-4 gave a peak at δ 38.3 and δ 39.0 respectively. Meanwhile two methine carbon C-3 and C-5 showed the peak at δ 48.8 and δ 70.6 due to the deshielding effect by the neighbouring nitrogen and oxygen atom respectively.

Finally the aromatic carbon peaks showed signal at δ 126.2 attributed to the two aromatic carbons of C-9 and C-13, meanwhile the peak at δ 128.3 corresponding to the

two aromatic carbons of C-10 and C-12 and *para* aromatic carbon peak appeared at δ 127.4 which was assigned for C-11. The carbonyl carbon of the lactone appeared at δ 176.2.

Therefore, **153** was identified as (*E*)-3-amino-5-hydroxy-7-phenylheptane-6-enoic acid, named as goniomicin F.

Table 4.14: ^{1}H (400 MHz), ^{13}C (100 MHz) NMR and HMBC spectral data (in CD$_3$OD) of **153**.

Position	^{1}H-NMR δ_H (ppm), J (Hz)	^{13}C-NMR δ_C (ppm)	HMBC (H→C)
1	-	176.2	-
2	2.35-2.42 (1H, *dd*) J=16.0, 8.0 2.52-2.58 (1H, *dd*) J=20.0, 4.0	38.3	C-1, C-3, C-4
3	3.60 (1H, *m*)	48.8	C-1
4	1.82 (2H, *m*)	39.0	C-2, C-3, C-5, C-6
5	4.43 (1H, *m*)	70.6	C-3, C-4, C-7
6	6.23 (1H, *dd*) J=16.0, 4.0	131.5	C-4, C-5, C-8
7	6.61 (1H, *d*) J=16.0	130.1	C-5, C-8, C-9, C-13
8	-	136.8	-
9, 13	7.18-7.39 (5H, *m*)	126.2	C-7
10, 12		128.3	C-8
11		127.4	C-9, C-13
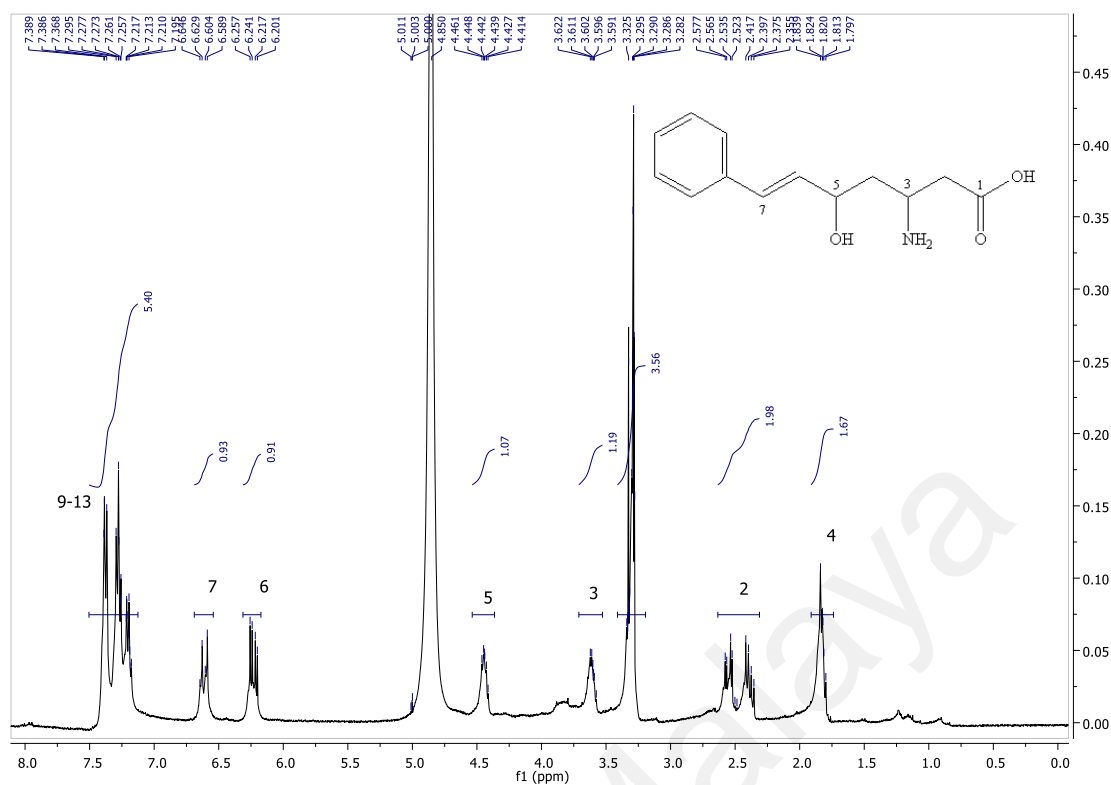
Figure 4.34: ^{1}H (400 MHz) NMR spectrum of goniomicin F **153**.
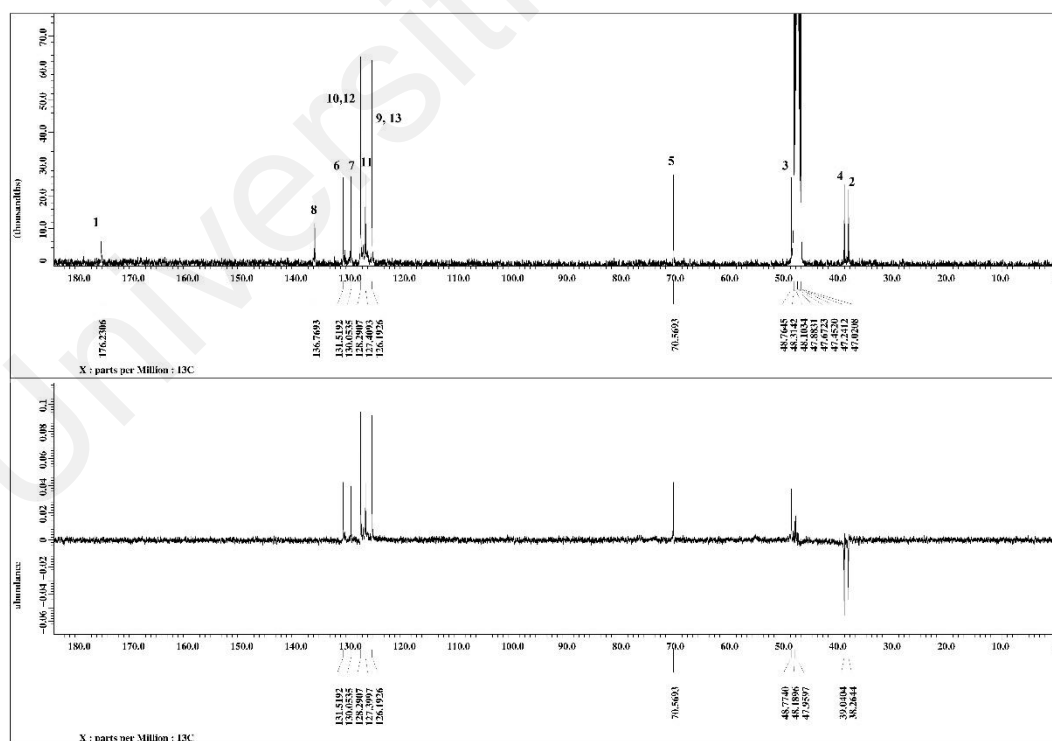
Figure 4.35: ^{13}C (100 MHz) and DEPT-135 NMR spectra of goniomicin F **153**.

110
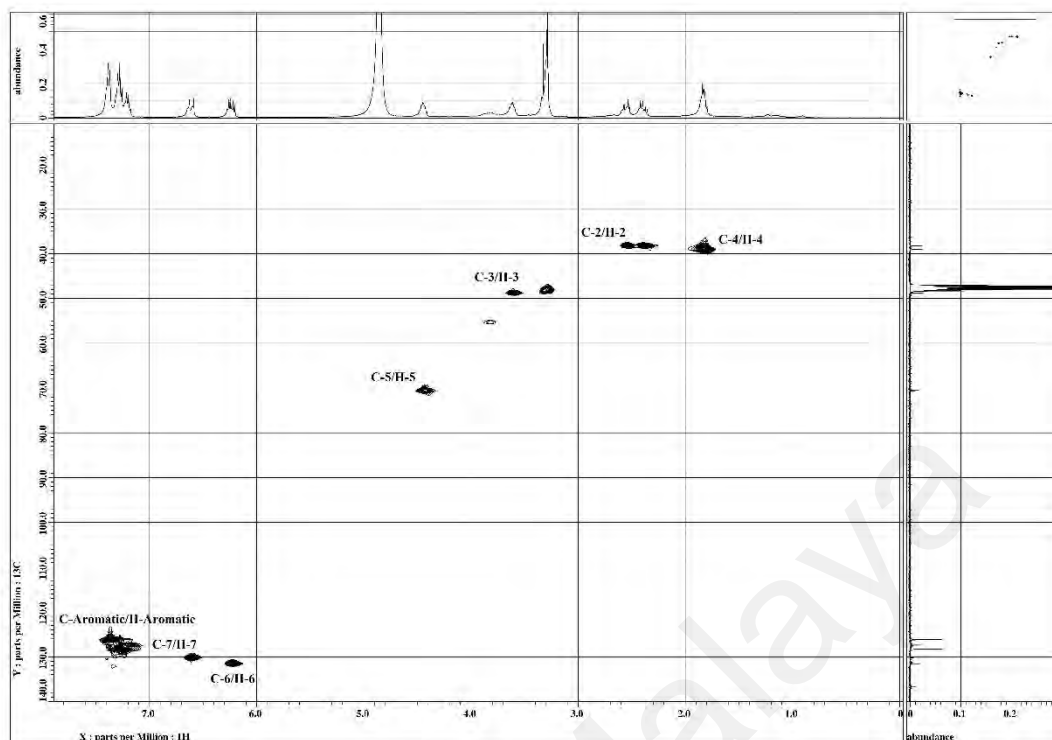
Figure 4.36: HSQC spectrum of goniomicin F **153**.
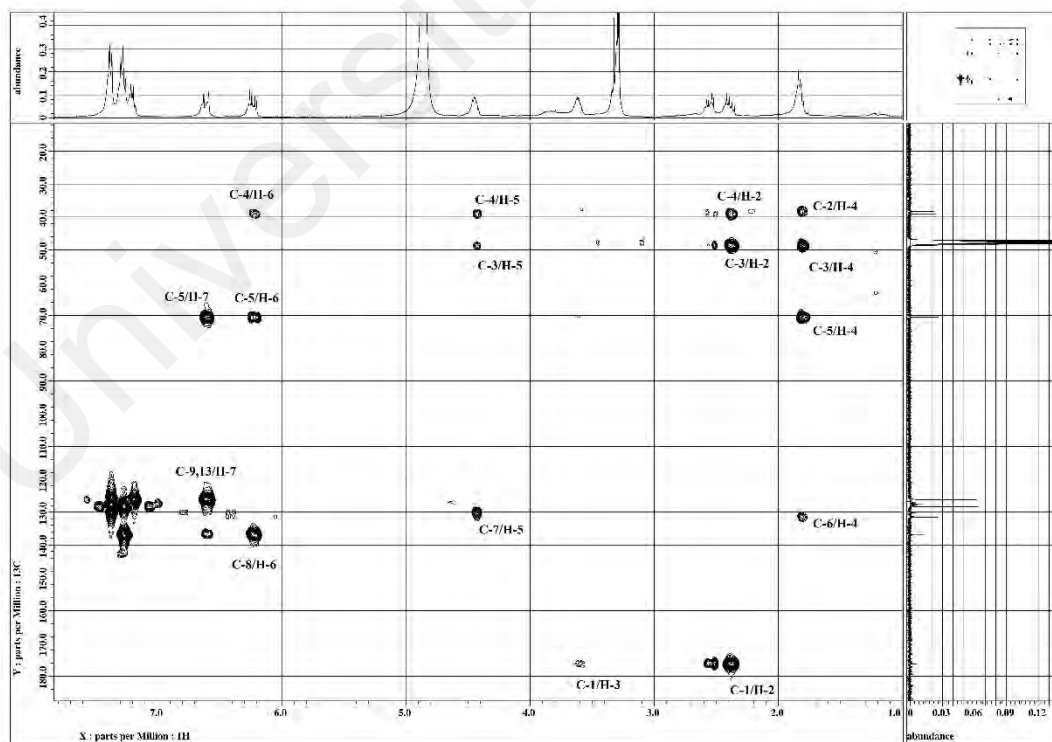
Figure 4.37: HMBC spectrum of goniomicin F **153**.
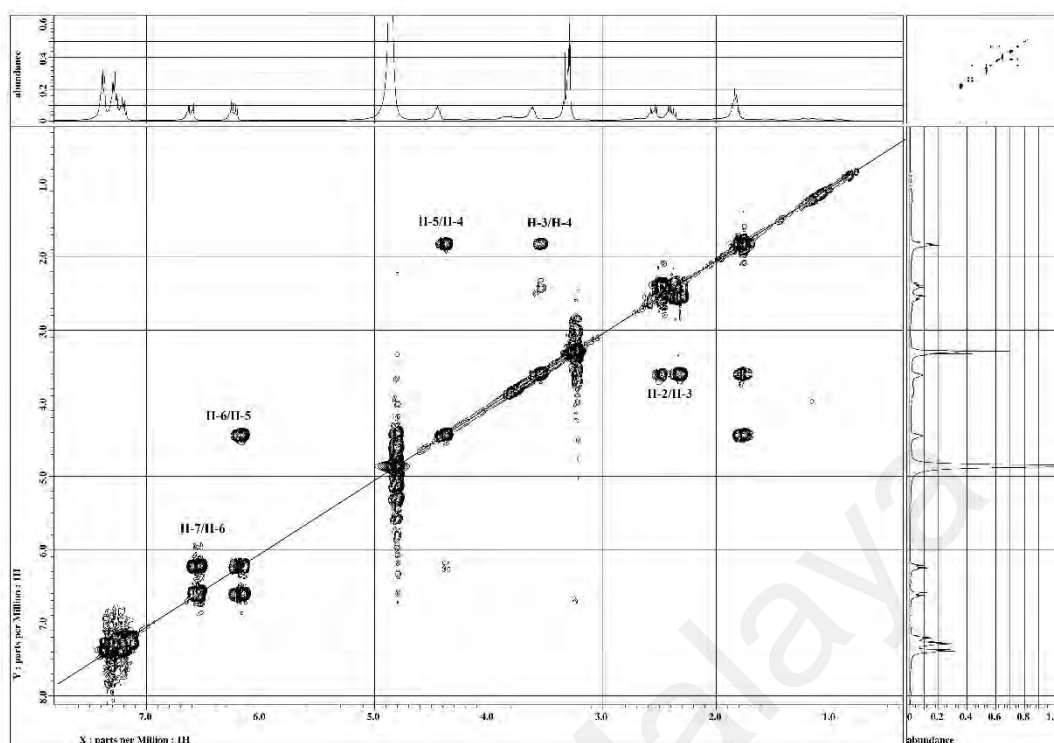
Figure 4.38: COSY spectrum of goniomicin F **153**.

Counts vs. Mass-to-Charge (m/z)
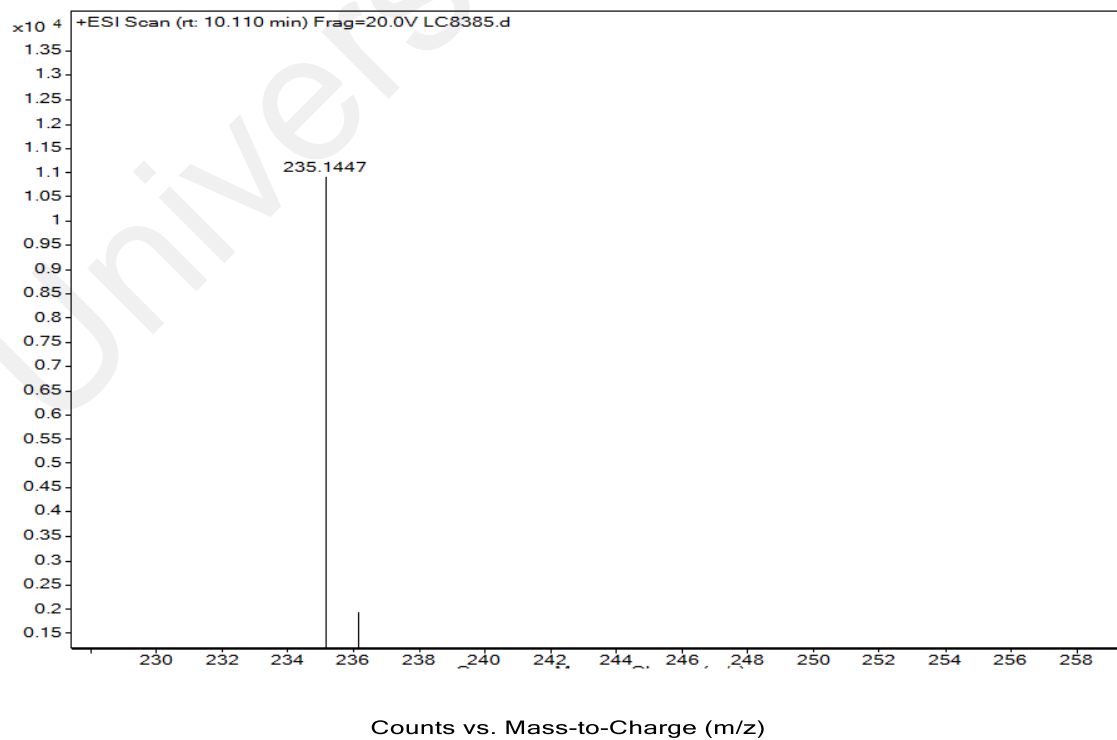
Figure 4.39: LCMS spectrum of goniomicin F **153**.

4.1.14 Goniomicin G 154
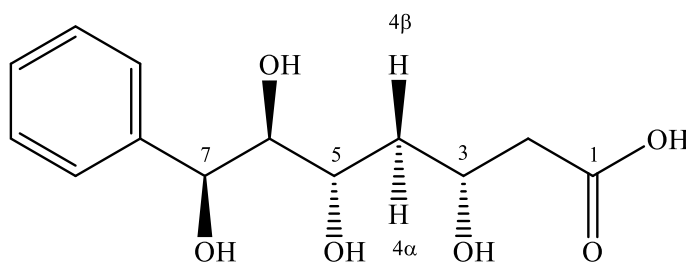
154

Compound **154** was isolated as colorless amorphous solid with $[\alpha]_D^{25} = -4.09$. The LCMS-IT-TOF spectrum showed a negative ion peak $[M - H_2O]^-$ at m/z 252.1249 (calcd. for $C_{13}H_{16}O_5$ 252.1246), corresponding to a molecular formula of $C_{13}H_{18}O_6$. The IR spectrum showed strong absorptions bands of O-H stretching at 3606 cm^{-1} and C=O stretching at 1710 cm^{-1}.

The ^{1}H NMR spectrum showed a multiplet δ 7.23-7.38 referring to five aromatic protons (H-9 to H-13) from a *mono*-substituted phenyl ring. Four deshielded one-proton signal at δ 3.98 (*m*), δ 3.68 (*ddd*), δ 3.25 (*dd*) and δ 4.07 (*d*) were indicative of oxygen bearing methine protons; H-3, H-5, H-6 and H-7, respectively. Four non-equivalent methylene protons at positions 2 and 4 resonated at δ 2.36 (*dd*), δ 2.50 (*dd*), δ 1.51 (*dd*) and δ 2.10 (*ddd*), respectively.

The ^{13}C NMR spectrum showed thirteen carbons; two methylene, nine methine and two quaternary carbon. Two quaternary carbon peaks at δ 174.7 and δ 139.7 were assigned to C-1 and C-8 respectively. Two methylene carbons, C-2 and C-4 gave a peak at δ 41.6 and δ 39.1 respectively. Four methine carbons, C-3, C-5, C-6 and C-7 resonated at δ 72.7, δ 72.3, δ 76.5 and δ 82.4, respectively, which is due to the deshielding effect by the neighbouring oxygen atom.

Finally the aromatic carbons showed a signal at δ 127.6 attributed to the two aromatic carbons of C-9 and C-13, meanwhile the peak at δ 127.7 corresponded to the two aromatic carbons of C-10 and C-12 and the *para* aromatic carbon (C-11) gave a peak at δ 127.5. The carbon of the lactone appeared at δ 174.7.

The relative configuration of **154** was established by the NOESY spectrum. H-6 correlated with H-7, while H-4α correlated with H-6. This implied that H-6 and H-7 is assignable as α. Interestingly, H-5 did not show any correlation with H-6, but it showed correlation with H-4b. H-3 also gave correlation signal with H-4β. Thus, this indicated that H-3 also assumed a β spatial orientation.

Therefore, **154** was identified as 3,5,6,7-tetrahydroxy-7-phenylheptanoic acid, named as goniomicin G.

Table 4.15: ^{1}H (400 MHz), ^{13}C (100 MHz) NMR and HMBC spectral data (in CD$_3$OD) of **154**.

Position	^{1}H-NMR δ$_H$ (ppm), J (Hz)	^{13}C-NMR δ$_C$ (ppm)	HMBC (H→C)
1	-	174.7	-
2α 2β	2.36 (1H, *dd*) *J*=14.4, 5.2 2.50 (1H, *dd*) *J*=14.4, 8.0	41.6	C-1, C-3, C-4
3	3.98 (1H, *m*)	72.7	C-1
4α 4β	1.51 (1H, *q*) *J*=12.2 2.10 (1H, *ddd*) *J*=12.2, 5.2, 2.0	39.1	C-2, C-3, C-5, C-6
5	3.68 (1H, *ddd*) *J*=13.6, 8.8, 4.8	72.3	C-3, C-4, C-7
6	3.25 (1H, *dd*) *J*=9.2, 9.2	76.5	C-4, C-5, C-8
7	4.07 (1H, *d*) *J*=5.6	82.4	C-5, C-8, C-9, C-13
8	-	139.7	-
9, 13		127.6	C-7
10, 12	7.23-7.38 (5H, *m*)	127.7	C-8
11		127.5	C-9, C-13
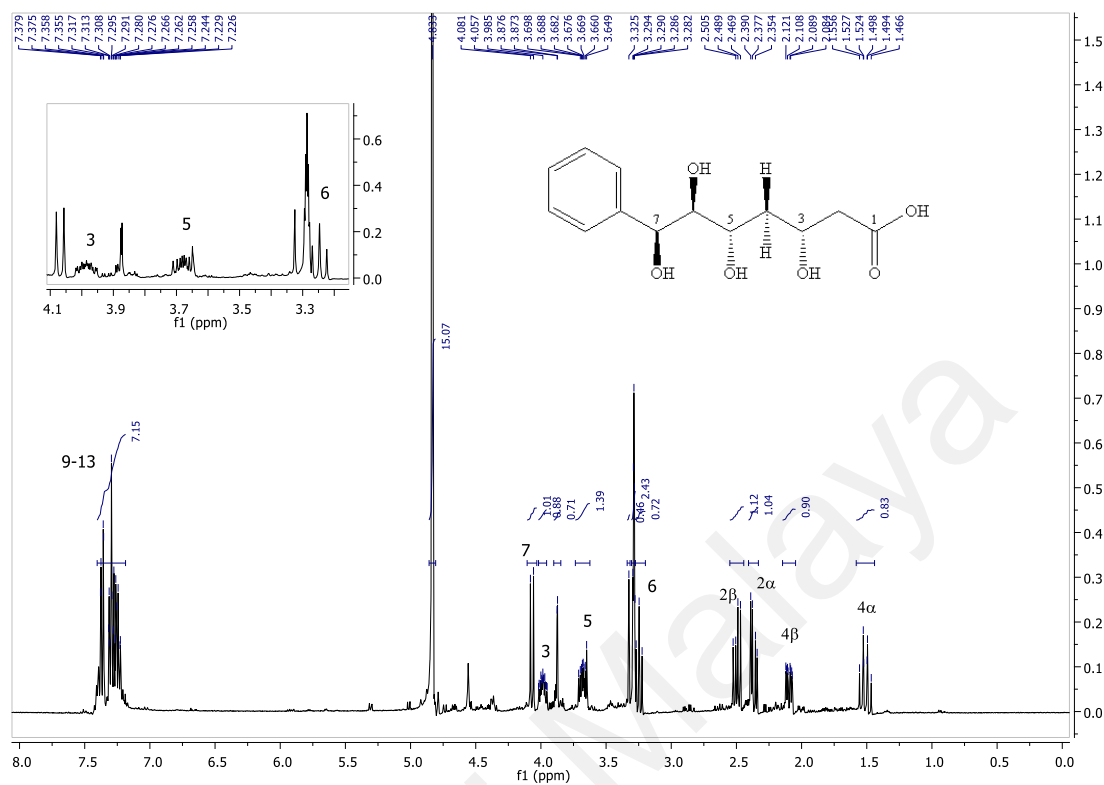
Figure 4.40: ^{1}H (400 MHz) NMR spectrum of goniomicin G **154**.
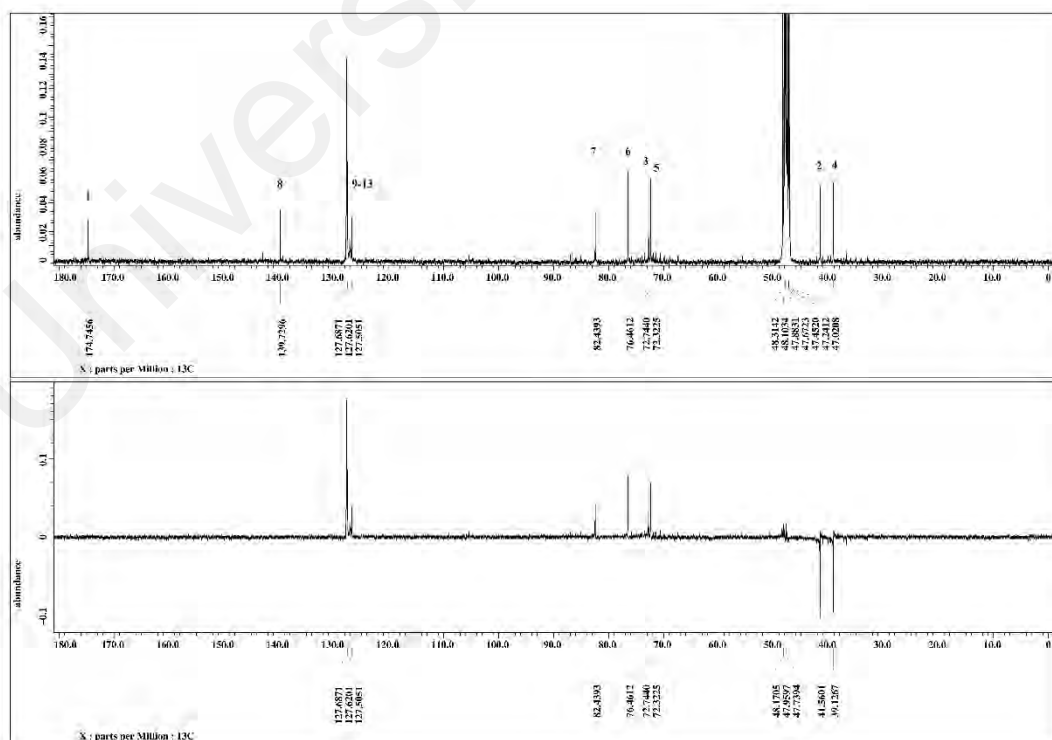
Figure 4.41: ^{13}C (100 MHz) and DEPT-135 NMR spectrum of goniomicin G **154**.
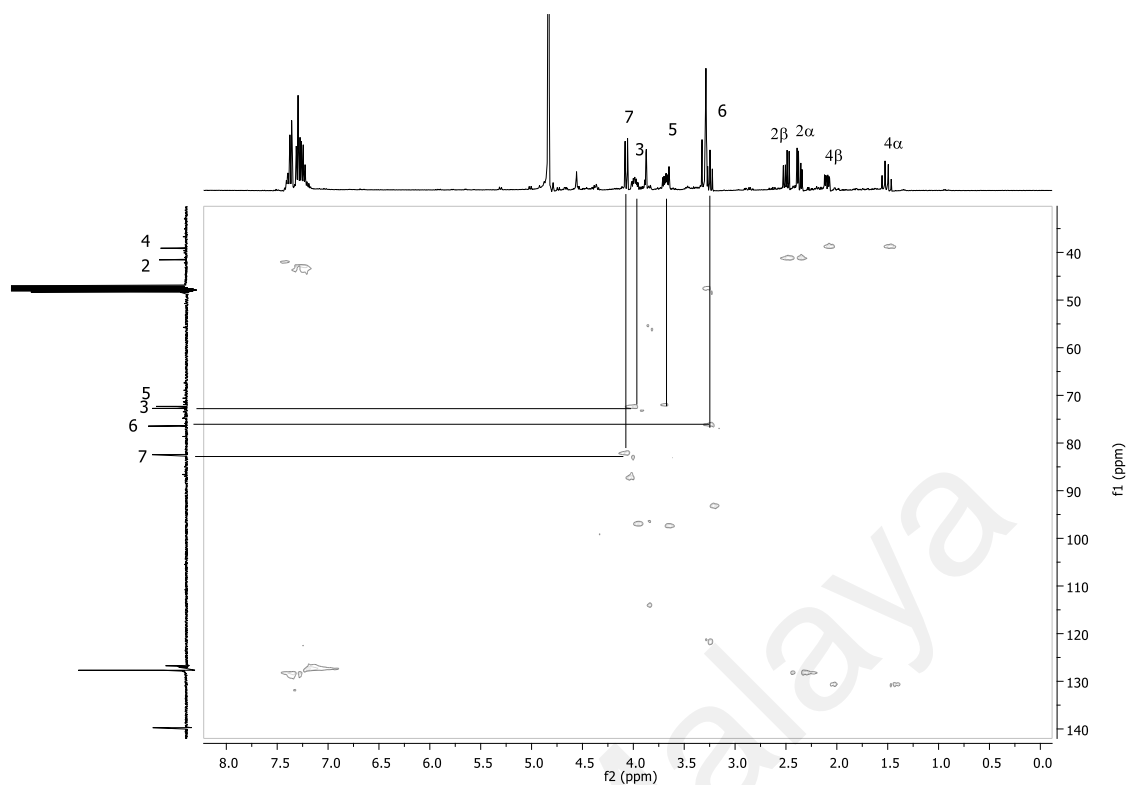
Figure 4.42: HSQC spectrum of goniomicin G **154**.
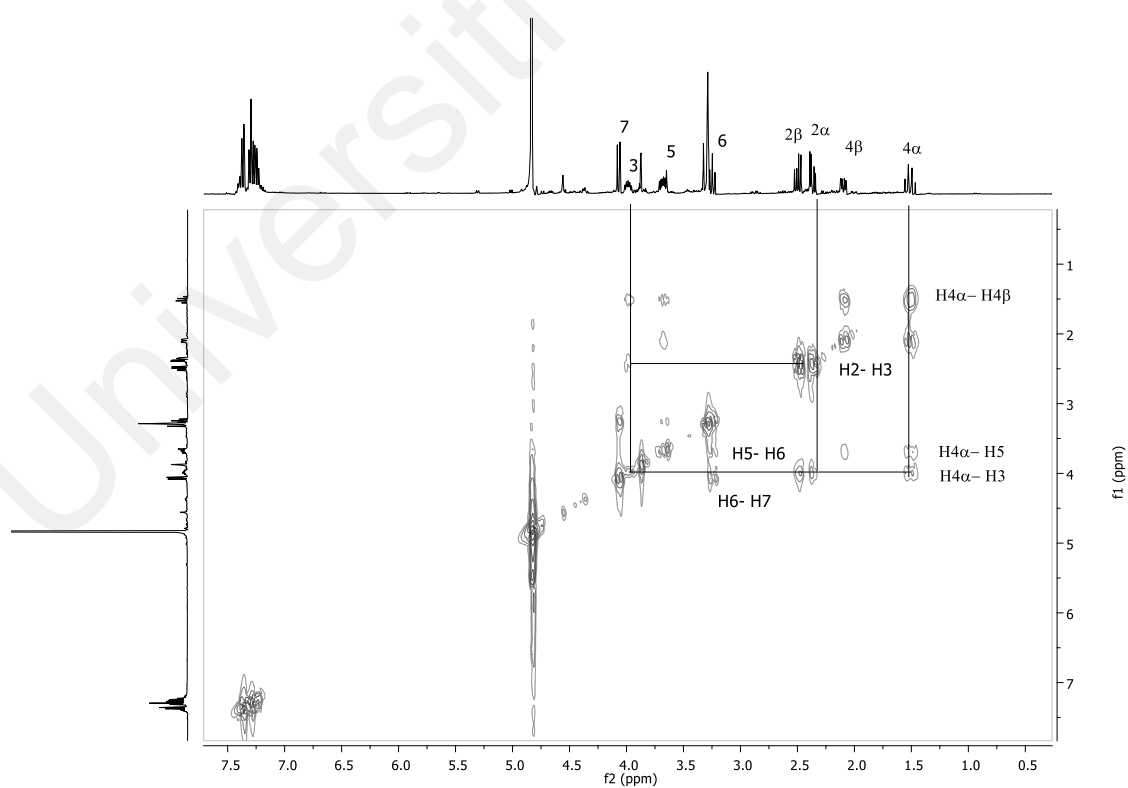
Figure 4.43: COSY spectrum of goniomicin G **154**.
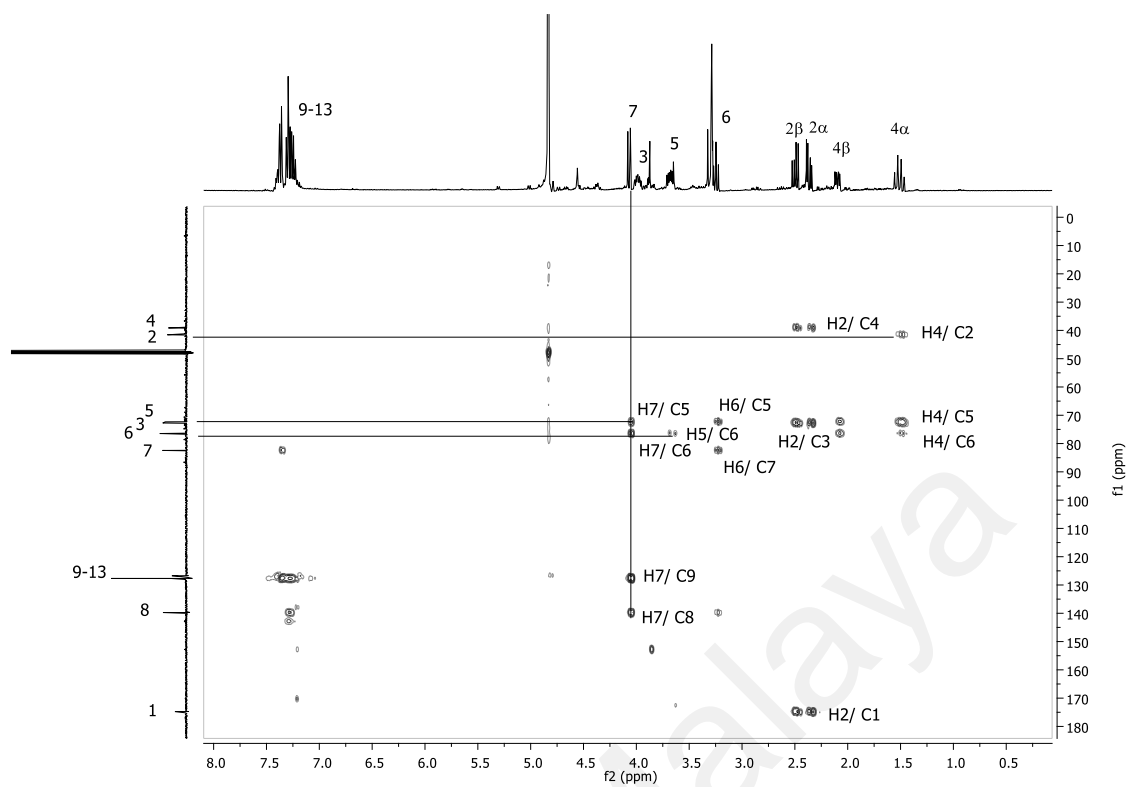
Figure 4.44: HMBC spectrum of goniomicin G **154**.
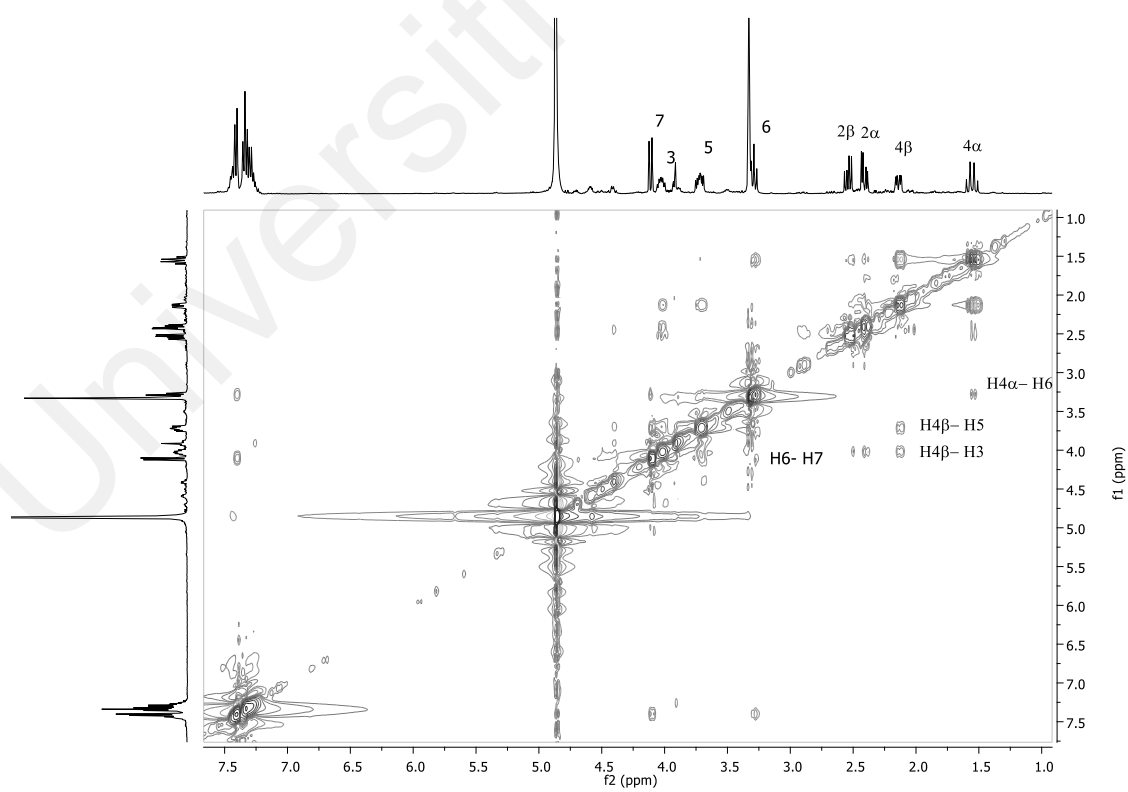
Figure 4.45: NOESY spectrum of goniomicin G **154**.
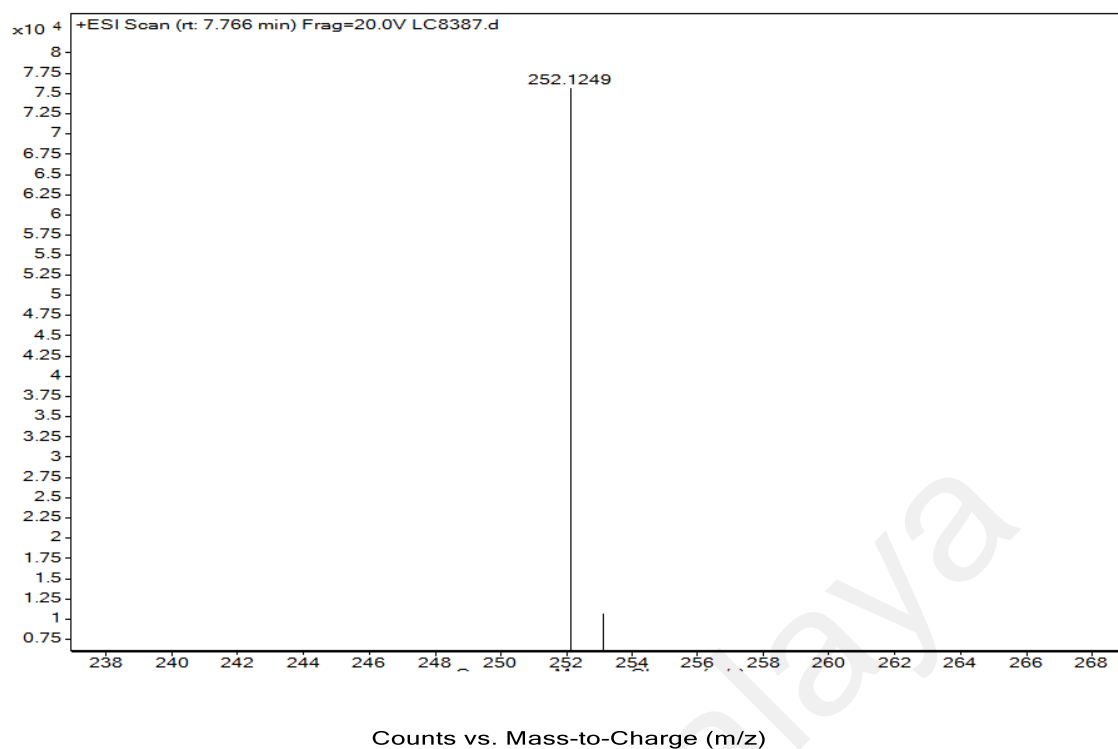
Figure 4.46: LCMS spectrum of goniomicin G **154**.

4.1.15 Goniomicin H 155
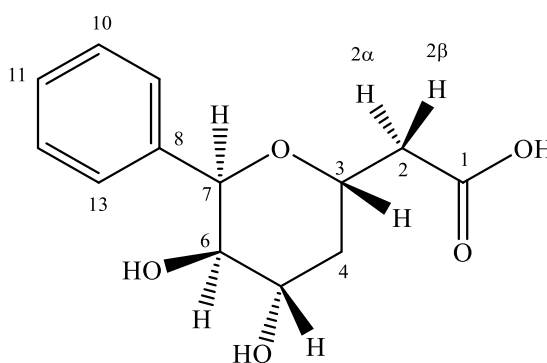
155

Compound **155** was isolated as colorless amorphous solid with $[\alpha]_D^{25} = +3.70$. The LCMS-IT-TOF mass spectrum showed a peak at *m/z* 252.1233 [M] (calcd. for $C_{13}H_{16}O_5$ 252.1235), corresponding to a molecular formula of $C_{13}H_{16}O_5$. The IR spectrum showed strong absorptions bands of O-H stretching at 3556 cm^{-1} and C=O stretching at 1720 cm^{-1}.

The ^{1}H NMR spectrum showed a multiplet δ 7.22-7.58 referring to five aromatic protons (H-9 to H-3) from a *mono*-substituted phenyl ring. Four deshielded one-proton signal at δ 5.15 (*d*; 3.2 Hz), δ 3.76 (*dd*; 6.0, 3.2 Hz), δ 4.06 (*m*) and δ 4.30 (*dd*; 9.4,5.2 Hz) were indicative of oxygen bearing methine protons belonged to H-7, H-6, H-5 and H-3, respectively. Four non-equivalent methylene protons of position 4 and 2 resonated at δ 1.56 (*dt*), δ 2.46 (*ddd*), δ 2.49 (*dd*) and δ 2.95 (*dd*), respectively.

The ^{13}C NMR spectrum showed thirteen carbons; two methylenes, nine methines and two quaternary carbons. Two quaternary carbon peaks at δ 175.5 and δ 139.5 were assigned to C-8 and C-9 respectively. Four carbons; C-3, C-5, C-6 and C-7, resonated in between δ 67.8 – δ 72.6 is due to the deshielding effect by the neighbouring oxygen atom. Finally the aromatic carbon peaks showed signal at δ 127.2 attributed to the two aromatic carbons of C-9 and C-13, meanwhile the peak at δ 127.6 corresponding to the two

aromatic carbons of C-10 and C-12 and *para* aromatic carbon peak appeared at δ 126.6 which was assigned for C-11. The carbonyl carbon of the lactone appeared at δ 175.5.

The HMBC cross peaks of H-6/C-2 suggested the presence of a tetrahydropyranal central skeleton of **155**, which is similar to goniothalesdiol A **139** (Lan et al., 2006). Besides that, the correlations between H-2 and C-10 indicated the aromatic ring was connected to C-7. In addition, COSY spectrum also showed the coupling correlations through H-2 to H-7.

The relative configuration of **155** was established by the NOESY spectrum. Two protons, H-6 and H-2α shown correlation with H-7. Therefore, H-7 is arbitrarily assigned as α together with H-2α. Since that H-7 showed correlations with H-6, the latter can be also assigned as α. H-5 in return, did not shown any correlation with H-6. But it correlated with H-4β, therefore this indicated a β configuration of H-5. H-3 observed both H-2β and H-4β. Therefore, this supported that H-3 and H-5 are β.

Compound **155** possess as carboxylic acid functionality as compared to methoxycarbonyl group in goniothalesdiol A. Compound **155** is named goniomicin H.
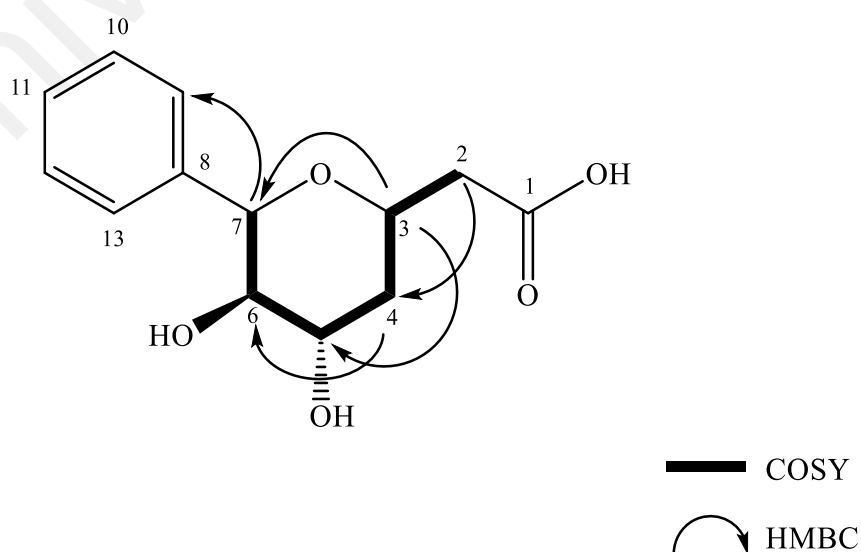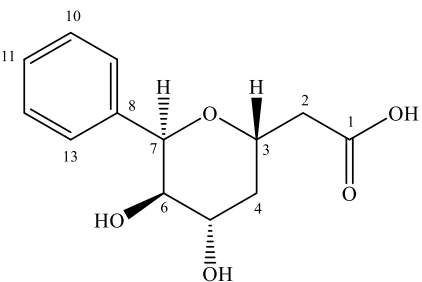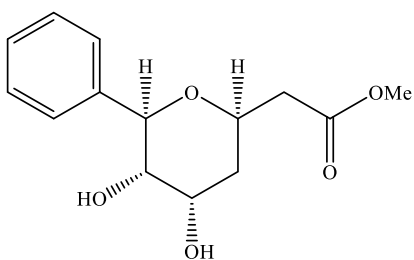
Table 4.16: [1]H (400 MHz), ^{13}C (100 MHz) NMR spectroscopic data (in CD$_3$OD) of goniomicin H **155** and goniothalesdiol A **139**.

	Goniomicin H **155**		Goniothalesdiol A **139**	
Position	^{1}H-NMR [a] δ$_H$ (ppm), J (Hz)	^{13}C-NMR [a] δ$_C$ (ppm)	^{1}H-NMR [b] δ$_H$ (ppm), J (Hz)	^{13}C-NMR [c] δ$_C$ (ppm)
1	-	175.5	-	172.3
1-OCH$_3$	-	-	-	51.8
2α	2.95 (1H, *dd*) J=14.4, 9.4	40.1	2.61 (1H, *dd*) J=15.2, 6.4	40.3
2β	2.49 (1H, *dd*) J=14.4, 5.2		2.75 (1H, *dd*) J=15.2, 7.2	
3	4.30 (1H, *dd*) J=9.4, 5.2	68.6	4.38 (1H, *dddd*) J=8.4, 7.2, 6.4, 4.8	68.6
4α	1.56 (1H, *dt*) J=14.0, 5.6	32.8	1.77 (1H, *ddd*) J=13.6, 4.8, 2.4	39.8
4β	2.46 (1H, *ddd*) J=14.0, 5.2, 4.0		2.35 (1H, *ddd*) J=13.6, 8.4, 5.6	
5	4.06 (1H, *m*)	67.8	4.47 (1H, *ddd*) J=5.6, 3.6, 2.4	72.8
6	3.76 (1H, *dd*) J=6.0, 3.2	72.6	3.68 (1H, *dd*) J=8.0, 3.6	85.7
7	5.15 (1H, *d*) J=3.2	71.4	4.87 (1H, *d*) J=8.0	73.4
8	-	139.5	-	147.7
9, 13	7.22-7.58 (5H, *m*)	127.2	7.40	126.2
10, 12		127.6	7.31	128.4
11		126.6	7.28	127.8

[a] In CD$_3$OD.
[b] In (CD$_3$)$_2$CO.
[c] In CDCl$_3$.
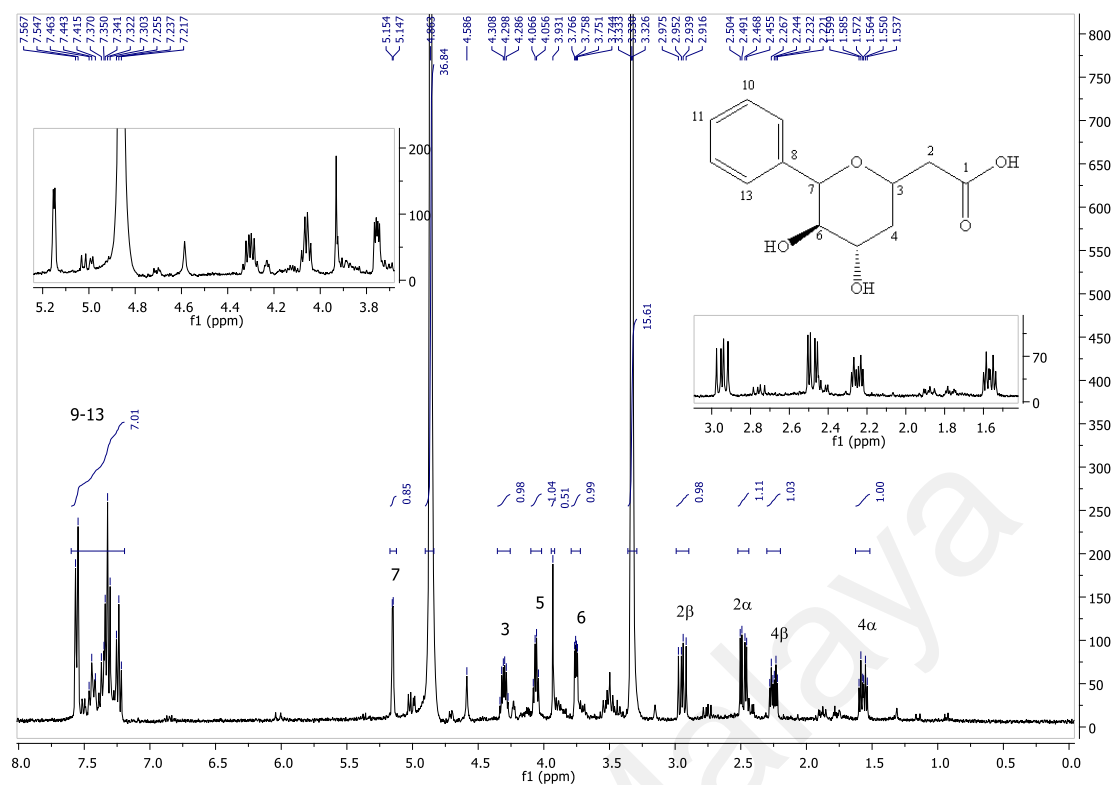
Figure 4.47: ^{1}H (400 MHz) NMR spectrum of goniomicin H **155**.
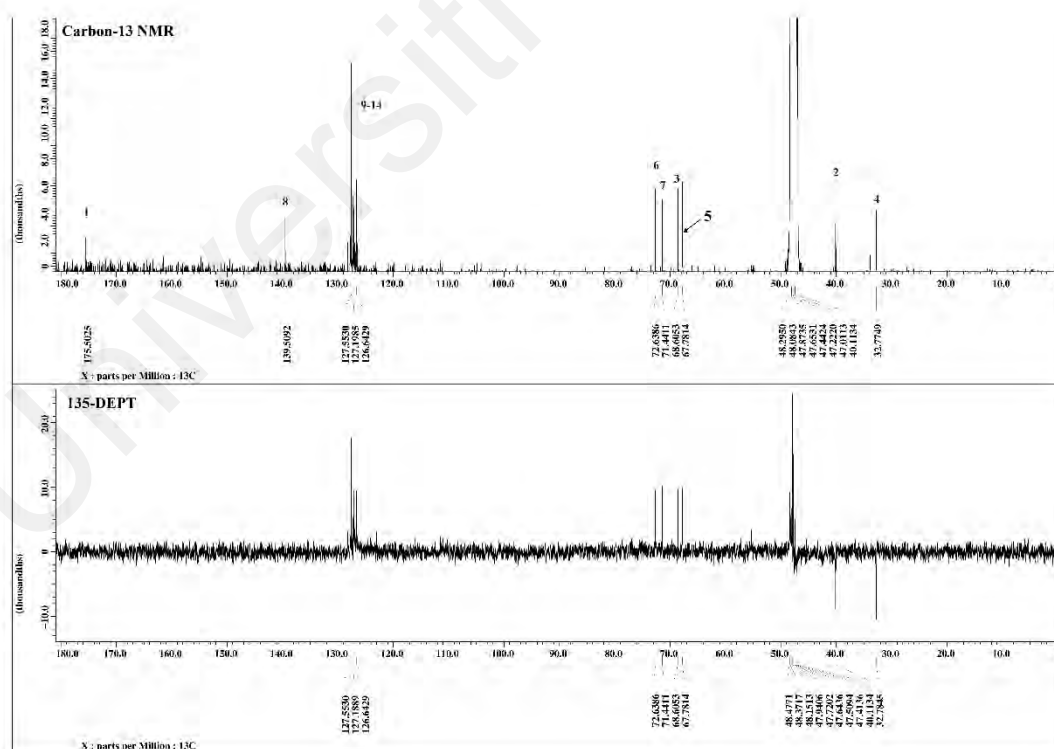
Figure 4.48: ^{13}C (100 MHz) and DEPT-135 NMR spectra of goniomicin H **155**.
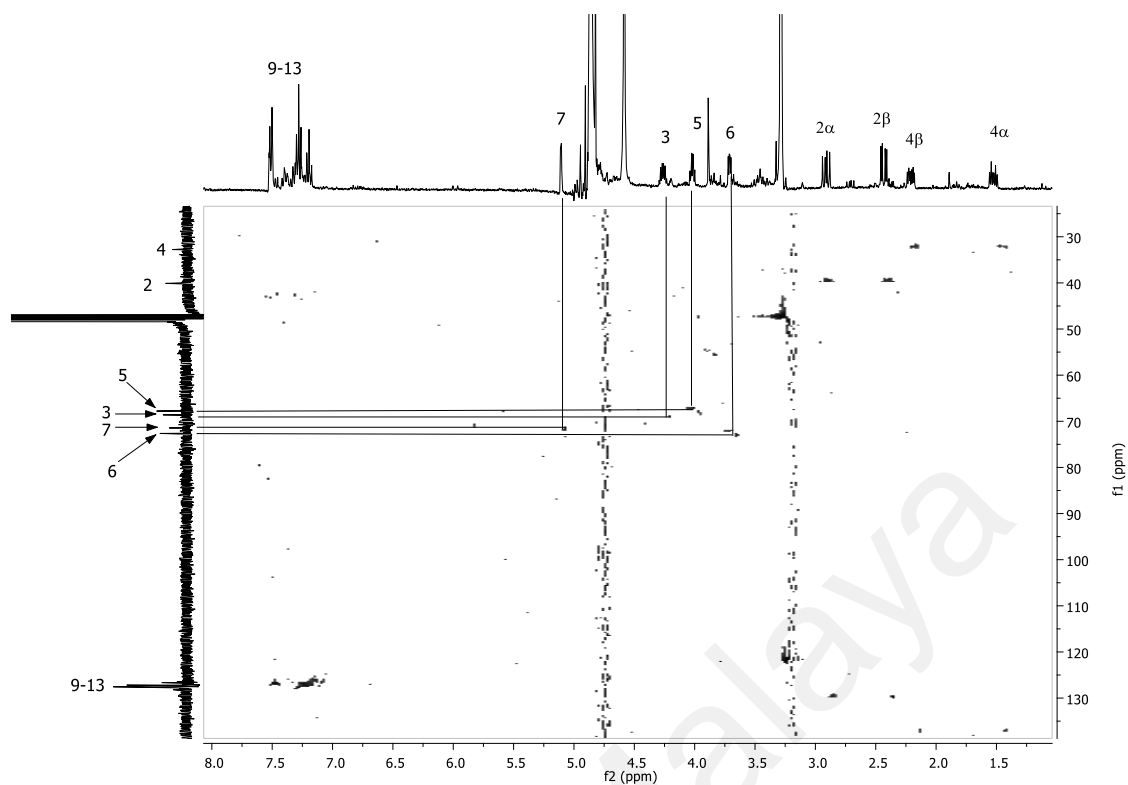
Figure 4.49: HSQC spectrum of goniomicin H **155**.
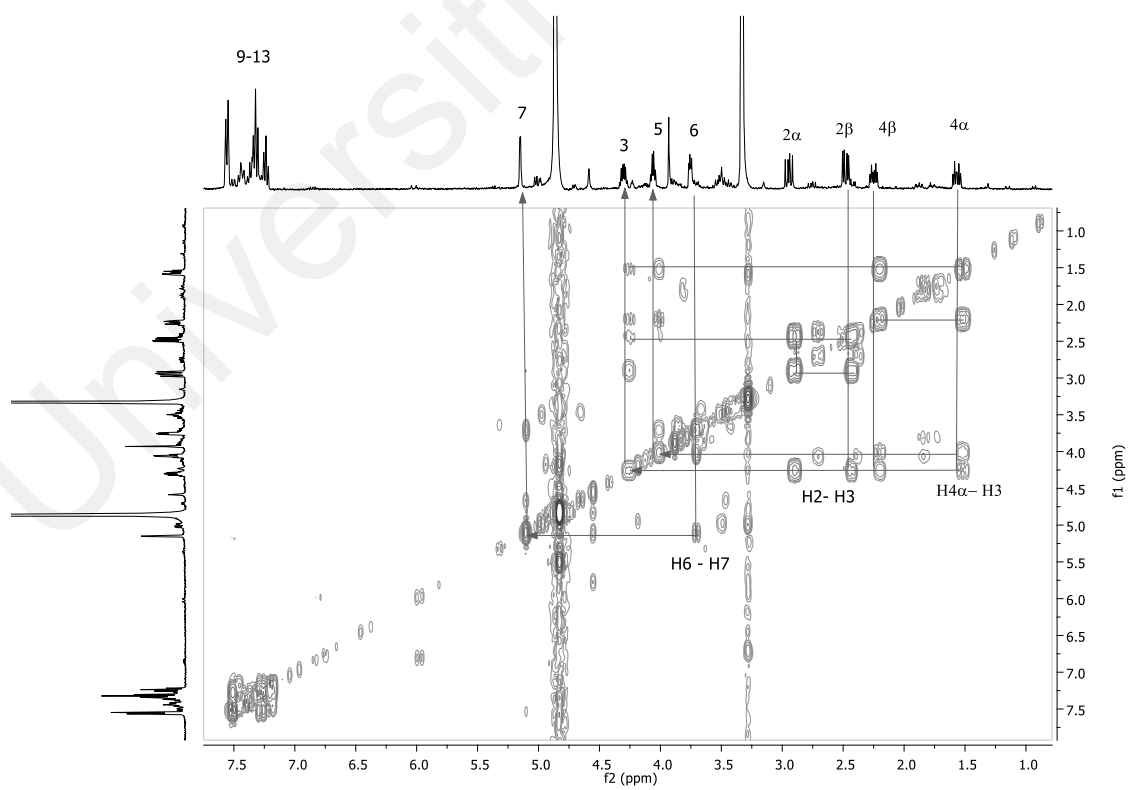
Figure 4.50: COSY spectrum of goniomicin H **155**.
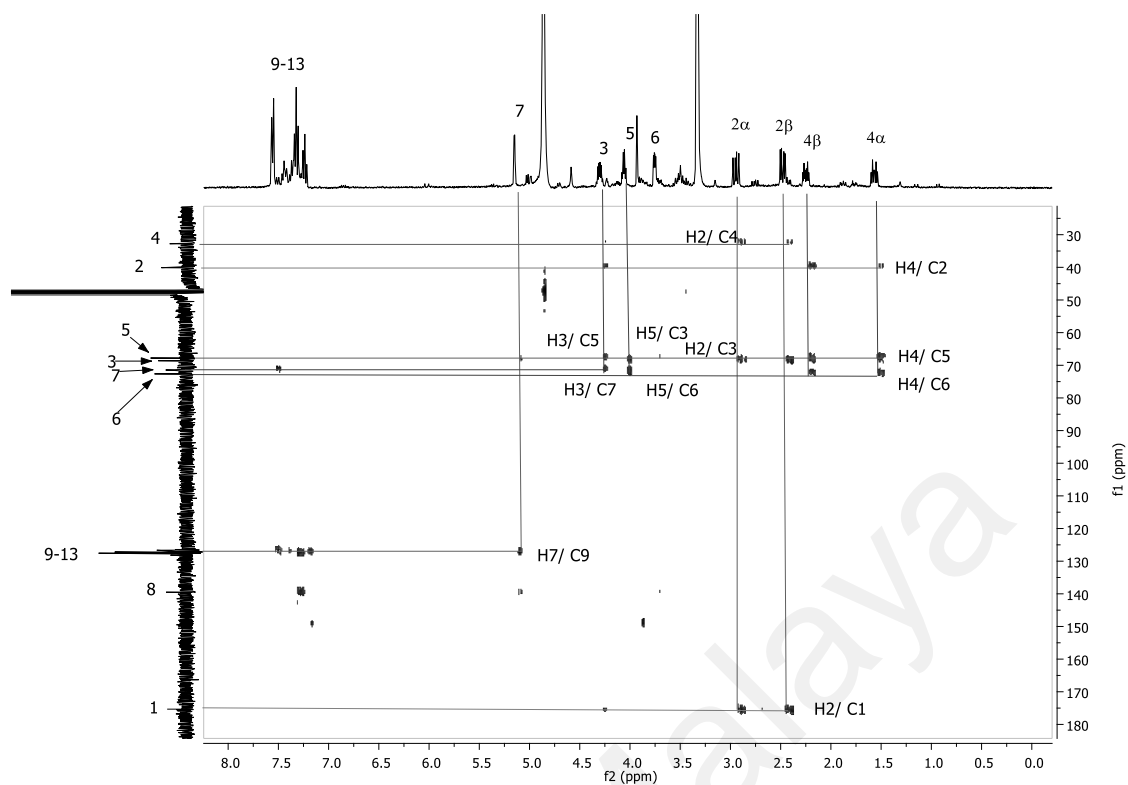
Figure 4.51: HMBC spectrum of goniomicin H **155**.
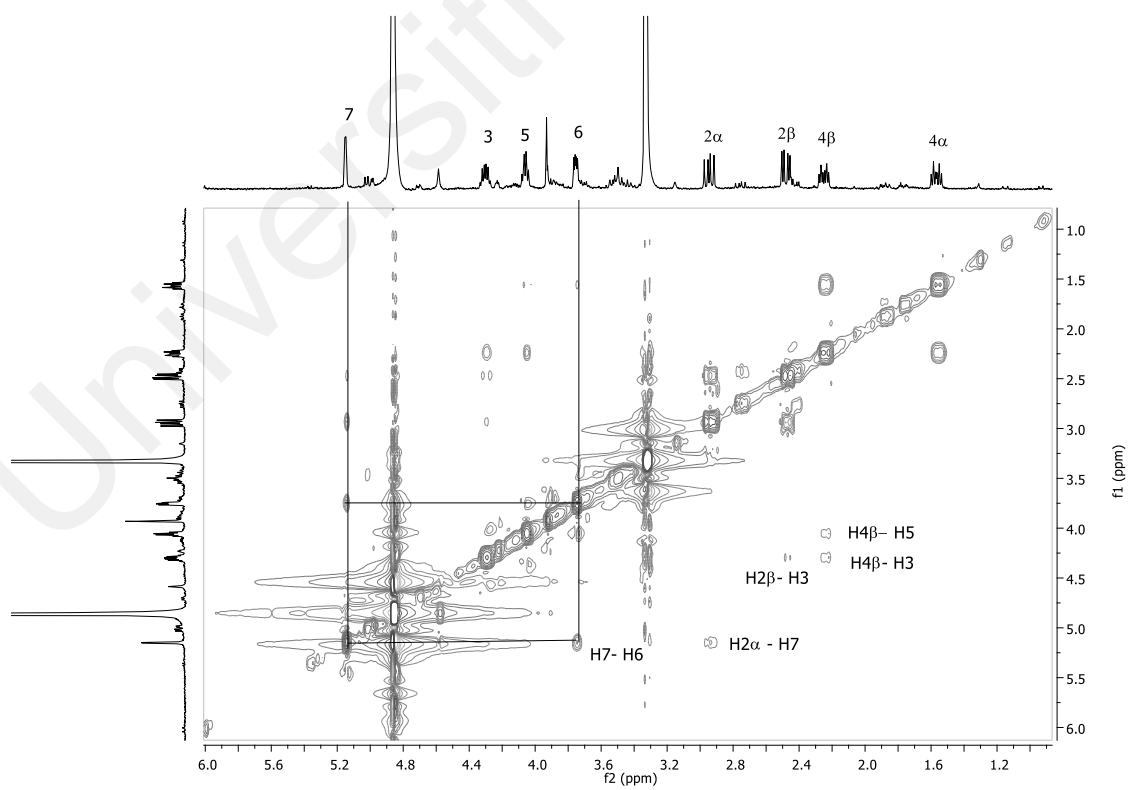
**Figure 4.52:** NOESY spectrum of goniomicin H **155**.
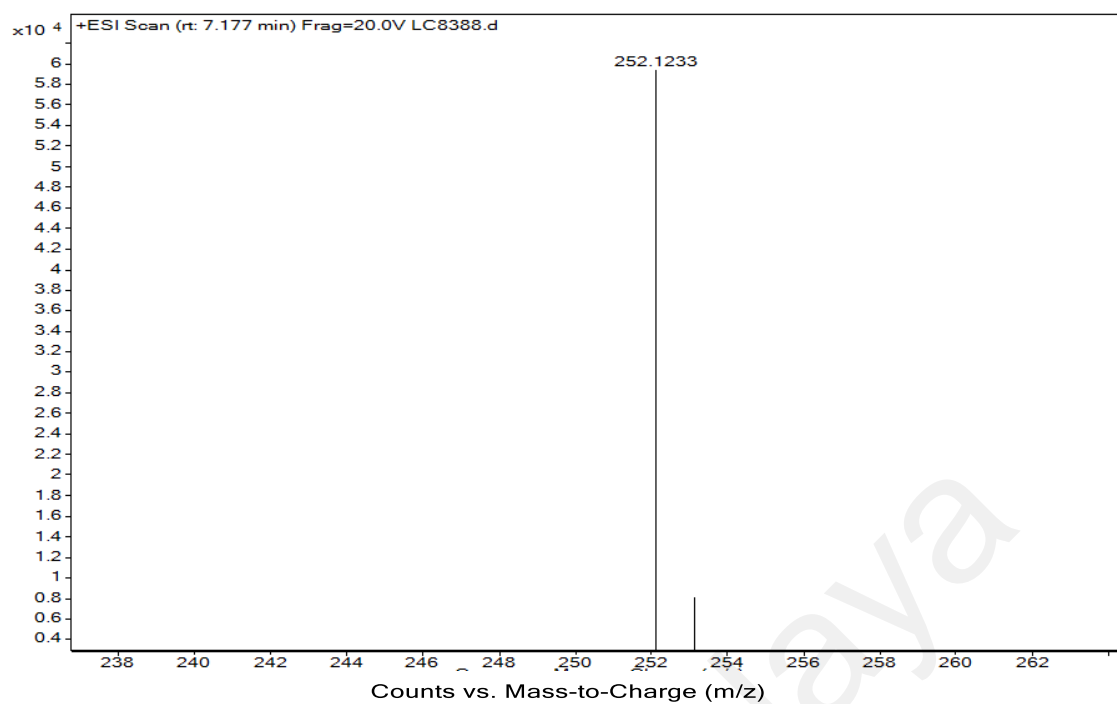
Figure 4.53: LCMS spectrum of goniomicin H **155**.

4.1.16 Stigmasterol 133 & β-sitosterol 134

133

134
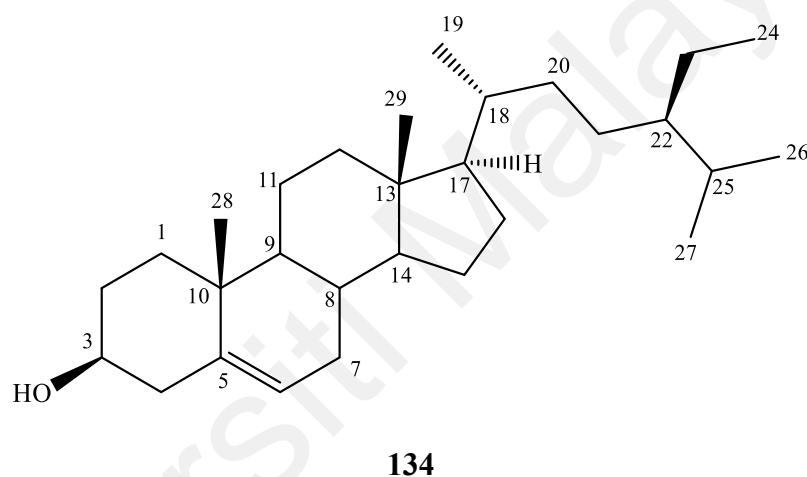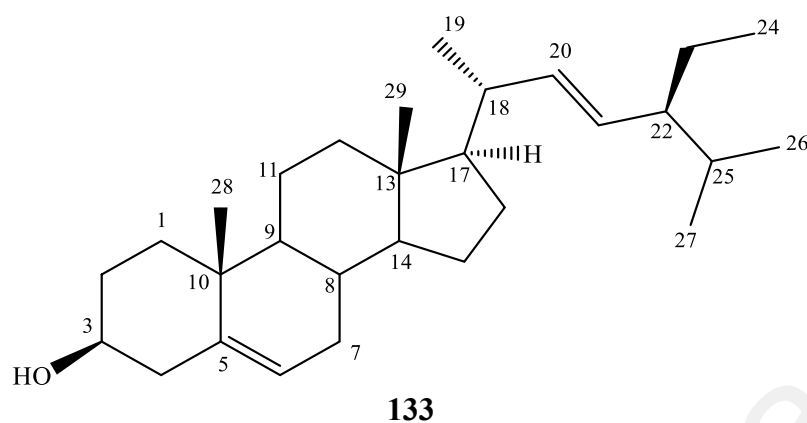
These two pure compound were acquired as mixture in the form of colourless oil. The molecular formula for stigmasterol **133** is $C_{29}H_{48}O$, while β-sitosterol **134** is $C_{29}H_{50}O$. These two compounds were deduced from the LCMS spectrum, two peaks at 413.3 and 415.2 assignable for **133** and **134** respectively.

According to literature, stigmasterol **133** and β-sitosterol **134** are always exists in a mixture form. The only difference for these two compounds is the presence double bond in between C-20 and C-21 in **133**, while there is a single bond in **134**. Compound **133** have three olefinic protons resonated at δ 5.00 (*dd*), δ 5.14 (*dd*) and δ 5.34 (*d*) were assigned to H-20, H-21 and H-6 respectively. While compound **134** have a olefinic proton at position 6 that also resonated at δ 5.34 (*d*).

The ^{13}C NMR spectrum showed four olefinic carbons; C-5, C-6, C-20 and C-21, resonated most downfield at δ 140.8, δ 121.8, δ 138.4 and δ 129.3 respectively. All methylene carbon peaks showed signal in the range 12 – 56 ppm, except for C-3, resonated at δ 71.9 due to the deshielding effect by the neighbouring oxygen atom.

Comparison of the obtained NMR spectral data with the literature values confirmed that **133** and **134** were stigmasterol and β-sitosterol respectively (Chaturvedula & Prakash, 2012).

Table 4.17: ^{1}H (400 MHz), ^{13}C (100 MHz) NMR spectroscopic data (in CDCl$_3$) of stigmasterol **133**.

Position	^{1}H-NMR δ$_H$ (ppm), J (Hz)		^{13}C-NMR δ$_C$ (ppm)	
	Experimental	Literature	Experimental	Literature
1	-	-	37.3	37.6
2	-	-	32.0	32.1
3	3.52 (1H, *m*)	3.51 (1H, *tdd*) J=4.5, 4.2, 3.8 Hz	71.9	72.1
4	-	-	42.4	42.4
5	-	-	140.8	141.1
6	5.34 (1H, *d*) J=5.2 Hz	5.31 (1H, *t*) J=6.1 Hz	121.8	121.8
7	-	-	32.0	31.8
8	-	-	32.0	31.8
9	-	-	50.2	50.2
10	-	-	36.6	36.6
11	-	-	21.3	21.5
12	-	-	39.9	39.9
13	-	-	42.4	42.4
14	-	-	56.8	56.8
15	-	-	24.4	24.4
16	-	-	29.0	29.3
17	-	-	56.1	56.2
18	-	-	40.6	40.6

Table 4.17, continued.

Position	^{1}H-NMR δ$_H$ (ppm), J (Hz)		^{13}C-NMR δ$_C$ (ppm)	
	Experimental	Literature	Experimental	Literature
19	0.91(3H, *d*) *J*=6.4 Hz	0.91 (3H, *d*) *J*=6.2 Hz	21.3	21.7
20	5.00 (1H, *dd*) *J*=8.6, 15.2 Hz	4.98 (1H, *m*)	138.4	138.7
21	5.14 (1H, *dd*) *J*=8.6, 15.2 Hz	5.14 (1H, *m*)	129.3	129.6
22	-	-	45.9	46.1
23	-	-	25.5	25.4
24	0.77-0.84 (3H, *m*)	0.83 (3H, *t*) *J*=7.1 Hz	11.9	12.1
25	-	-	29.2	29.6
26	0.77-0.84 (3H, *m*)	0.82 (3H, *d*) *J*=6.6 Hz	19.9	20.2
27	0.77-0.84 (3H, *m*)	0.80 (3H, *d*) *J*=6.6 Hz	19.5	19.8
28	0.68 (3H, *s*)	0.71 (3H, *s*)	19.1	18.9
29	0.99 (3H, *s*)	1.03 (3H, *s*)	12.1	12.2

Table 4.18: ^{1}H, ^{13}C NMR spectroscopic data (in CDCl$_3$, 400 MHz) of β-sitosterol **134**.

Position	^{1}H-NMR δ$_H$ (ppm), J (Hz)		^{13}C-NMR δ$_C$ (ppm)	
	Experimental	Literature	Experimental	Literature
1	-	-	37.3	37.5
2	-	-	32.0	31.9
3	3.52 (1H, *m*)	3.53 (1H, *tdd*) *J*=4.5, 4.2, 3.8 Hz	71.9	72.0
4	-	-	42.4	42.5
5	-	-	140.8	140.9
6	5.34 (1H, *d*) *J*=5.2 Hz	5.36 (1H, *t*) *J*=6.4 Hz	121.8	121.9
7	-	-	31.7	32.1
8	-	-	31.7	32.1

Table 4.18, continued.

Position	¹H-NMR δ_H (ppm), J (Hz)		¹³C-NMR δ_C (ppm)	
	Experimental	Literature	Experimental	Literature
9	-	-	50.2	50.3
10	-	-	36.3	36.7
11	-	-	21.2	21.3
12	-	-	39.8	39.9
13	-	-	42.3	42.6
14	-	-	56.9	56.9
15	-	-	26.1	26.3
16	-	-	28.3	28.5
17	-	-	56.0	56.3
18	-	-	36.2	36.3
19	0.91 (3H, *d*) *J*=6.4 Hz	0.93 (3H, *d*) *J*=6.5 Hz	19.1	19.2
20	-	-	34.0	34.2
21	-	-	26.1	26.3
22		-	45.9	46.1
23	-	-	23.1	23.3
24	0.77-0.84 (3H, *m*)	0.84 (3H, *t*) *J*=7.2 Hz	12.4	12.2
25	-	-	29.2	29.4
26	0.77-0.84 (3H, *m*)	0.83 (3H, *d*) *J*=6.4 Hz	19.9	20.1
27	0.77-0.84 (3H, *m*)	0.81 (3H, *d*) *J*=6.4 Hz	19.5	19.6
28	0.65 (3H, *s*)	0.68 (3H, *s*)	18.9	19.0
29	0.99 (3H, *s*)	1.01 (3H, *s*)	12.1	12.0

Figure 4.54: ^{1}H (400 MHz) NMR spectrum of stigmasterol **133** and β-sitosterol **134**.

Figure 4.55: ^{13}C (100 MHz) NMR spectrum of stigmasterol **133** and β-sitosterol **134**.
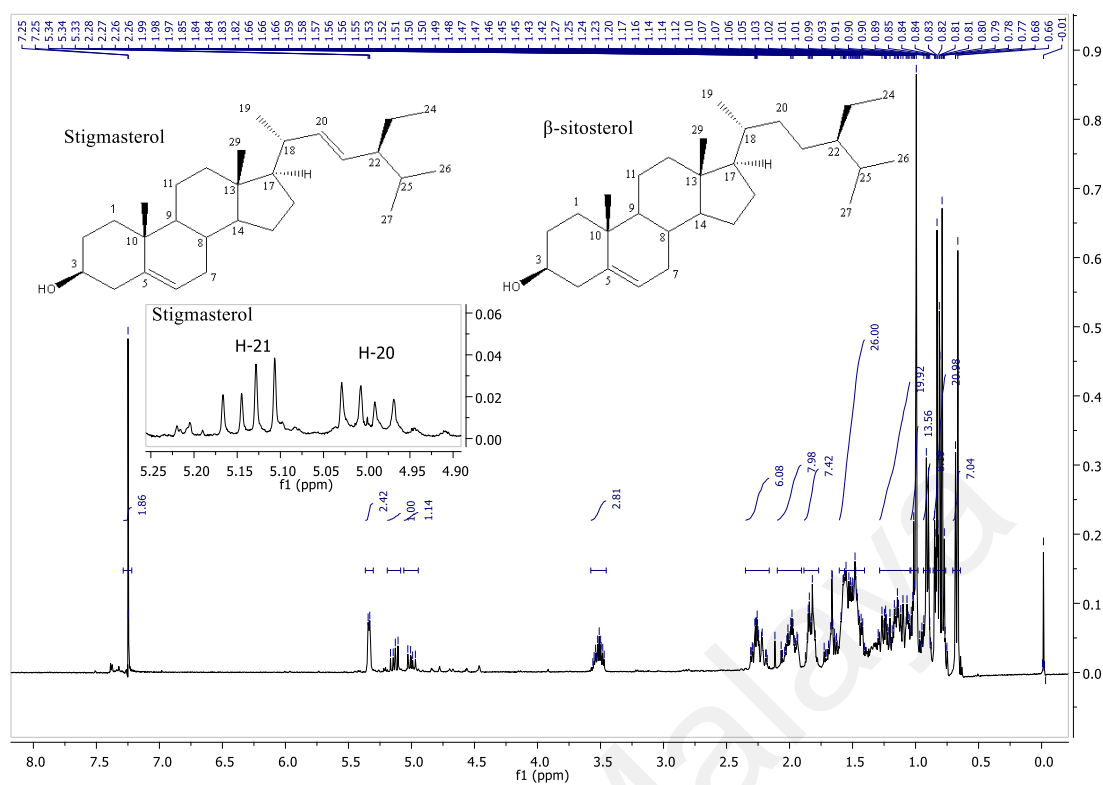
CHAPTER 5 : KINETIC STUDY

5.1   Introduction

Goniothalamin, **1**, the reported bioactive compound, has been isolated from dichloromethane crude of the stem of *Goniothalamus tapisoides*. Based on literature review, a lot of studies have been conducted to study the cytotoxic activity of **1**. It has been recognised as a highly potent compound that provides promising activity against wide range of cancer cell lines (Seyed et al., 2014).

Since goniothalamin is always the major and active compound in many *Goniothalamus* plants, and in tradition medicine practice, oral consumption of *G. tapisoides* is used to relieve stomachache and as abortifacient (Ahmad et al., 2010). Therefore, it is necessary that the behaviour of goniothalamin upon hydrolysis in alkaline and acidic condition be studied. Hydrolysis is a chemical reaction that always occur upon consumption of a change in human body.

Complete degradation of the drug in solution as a function of temperature and buffer concentration should be determined before a specific drug can be evaluated for its potential use. Chemical kinetic studies constitute the study of chemical transformation occurs in time to a certain mechanism with regularities characteristics (Denisov et al., 2003). It has valuable potential to break down complex mechanisms of chemical reactions into sequences of simple reactions. The study of reaction mechanism is major application of chemical kinetics. It includes four components: (a) experimental kinetics, (b) determination of the rate laws, (c) writing the kinetic scheme / reaction mechanism, and (d) proposal of product structures.

The parameters of interest in kinetics are the effect of pH, temperature and buffer on the rate of reactions. In kinetics, reactants which disappear and the amount of products

which increase in reactions are always being measured with respect to the reaction time. The method used to monitor kinetics depends on the species involved and the rapidity of which their concentrations change during the course of reactions. Spectrophotometry, the measurement of intensity of absorption in a particular spectral region, is widely applicable. It is especially useful when one substance in the reaction mixture has a strong characteristic absorption in a conveniently accessible region of the electromagnet spectrum. The generally employed experimental techniques are the quenching method, the flow method and the stopped – flow technique. Other methods in determining composition include mass spectrometry, gas chromatography, nuclear magnetic resonance, and electron spin resonance (for reaction involving radicals).

An experimentally determined reaction equation is called the rate law of the reaction. A rate law is an equation that expresses the rate of reaction as a function of the concentrations of all the species present in the overall chemical equation for the reaction at some time. Kinetic order is defined as the sum of the exponents of the concentrations of reactants in the rate law. Each individual exponent is called the order with respect to that component.

Several methods can be used in the determination of order of reactions (zero-order, first-order, second-order, third-order and n^{th}-order). (a) The half-life method; the time required for one – half of the initial concentration of a given reactant to be consumed is called the half-life, $t_{1/2}$. (b) Substitution method; applicable to reactions that are not complex and the rate constant, k, should stay constant throughout the course of the reaction. (c) The reaction rate method; this rate is measured at the beginning of the reaction for several different initial concentrations of reactants which is particularly useful for obtaining the rate constants of slow reaction. (d) The isolation method, also called pseudo-order reactions method. The concentration of species not of interest presents in

large excess will remain virtually constant during the course of the chemical reaction, and the overall order of the reaction will be apparently reduced. The reaction following pseudo-first-order reaction kinetics will have a half-life which is independent of the initial concentration of reactant.

The rates of most chemical reactions are sensitive to the temperature, so in conventional experiments the temperature of the reaction mixture must be held constant throughout the course of the reaction. Our interest is in solution kinetics, so we will concern only with homogeneous solution phase reactions. Pseudo-first-order rate law is applied throughout the studies, for it often permits the simplification of the reaction kinetics. It may even allow a complicated rate law equation to be transformed into a simple rate law equation. Secondly, it is not necessary to know the exact concentration of the reactant or product which disappears or appears in a first-order reaction. In terms of products characterization of a particular kinetic run, one can compare the observed extinction coefficients with that of the authentic expected products, or with authentic products using other techniques such as LCMS and NMR spectroscopy.

In general, if one wishes to demonstrate the existence of a particular kinetic term in a reaction, it is desirable to choose experimental conditions such that at least a 50% change in observed rate is brought about by the variable which is being examined. It is important to be certain that changes in absorbance caused by factors other than the reaction under consideration are not taking place during the experiment. The most convincing way to plot and present kinetic data is often in the form of uncorrected experimental rate constants, with theoretical lines showing the calculated rate constants.

To the knowledge of the author, according to literature, the first natural product underwent kinetic and mechanism study was an alkaloid named securinine. The compound was isolated from the genus *Securinega*, and it was reported to be effective in

the treatment of paralysis and physical disorders. The study has shown plausible mechanisms for alkaline hydrolysis and acid cyclization reactions. (Lajis et al., 1995)

Another study was done on lithospermic acid B (LAB) degradation in aqueous solution. This is the most abundant and common compound found in one of the Chinese traditional medicine, "Danshen". Different buffer concentration, pH and temperature were tested to identify the stability of the compound. The degradation products were separated and detected by HPLC, followed by characterization using LC-MS. (Guo et al., 2007)

Zahari et al. reported on the acid-base equilibria of several aporphine alkaloids isolated from genus *Alseodaphne* and *Dehaasia*. From this study, the pK_a value of those alkaloids were determined. And it has been shown that those alkaloids are also stable at physiological pH which is about pH 7 – 9. (Zahari et al., 2016)

5.2　Simple First-Order Kinetics

Kinetic studies were performed under pseudo-first-order reaction conditions. For example, alkaline hydrolysis of goniothalamin **1** (A) is found to follow a simple first-order rate law for the formation of goniomicin A **147** (P) which can be represented by the equation below (with A = reactant and P = product):

$$A \xrightarrow{\ k_{OH}[HO^-]\ } P \tag{5.1}$$

The rate law of the reaction in Eq. (5.1) can be written as:

$$\text{Rate} = -\frac{d[A]}{dt} = -\frac{d[HO^-]}{dt} = +\frac{d[P]}{dt} = k_{OH}[A][HO^-] \tag{5.2}$$

Where [A] and [OH⁻] are the concentrations of A and hydroxide ion at reaction time, t, respectively, and k_{OH} is the second order rate constant for the alkaline hydrolysis of A. In order to maintain pseudo-first-order condition, $[HO^-]/[A] \geq 25$ and the pseudo-first order rate law for the cleavage of A follows Eq. (5.3).

$$\text{Rate} = k_{obs}[A] \tag{5.3}$$

Where k_{obs} is the observed pseudo-first-order rate constant and $k_{obs} = k_{OH}[HO^-]$.

From Eqs. (5.2) and (5.3),

$$\text{Rate} = -\frac{d[A]}{dt} = k_{obs}[A] \tag{5.4}$$

Integration of Eq. (5.4) gives

$$[A] = [A_0]\exp(-k_{obs}t) \tag{5.5}$$

Where $[A_0]$ is the initial concentration of A and [A] is the concentration of A at any reaction time *t*. if A_{obs} is the observed absorbance of the reaction following Eq. (5.1), then

$$A_{obs} = \delta_A[A] + \delta_P[P] \tag{5.6}$$

Where δ represents molar extinction coefficient of a particular species.

From Eq. (5.1), it can be shown that

$$[A_0] = [A] + [P] \tag{5.7}$$

and

$$[P] = [A_0] - [A] \tag{5.8}$$

Combining Eqs. (5.7) and (5.8), give

$$A_{obs} = \delta_A[A] + \delta_P([A_0] - [A]) \tag{5.9}$$
$$= (\delta_A - \delta_P)[A] + \delta_P[A_0]$$

If $\delta_P[A_0] = A_\infty$ and $\delta_A - \delta_P = \delta_{app}$, Eq. (5.9) can be simplified to

$$A_{obs} = \delta_{app}[A] + A_\infty \tag{5.10}$$

Substitution of Eq. (5.5) into (5.10), one gets

$$A_{obs} = \delta_{app}[X_0]\exp(-k_{obs}t) + A_\infty \tag{5.11}$$

Eq. (5.11) is applied to reaction conditions where the disappearance of reactant is monitored as a function of reaction time, t. When the appearance of product is monitored as a function of t, then Eq. (5.11) will be converted to Eq. (5.12) as follow:

$$A_{obs} = \delta_{app}[A_0][1 - \exp(-k_{obs}t)] + A_0 \tag{5.12}$$

where $A_0 = \delta_{app}[A_0] + A_\infty$. In both Eqs. (5.11) and (5.12), k_{obs}, δ_{app}, A_∞, and A_0 are the unknown parameters.

The observed data (A_{obs} versus t), obtained for alkaline hydrolysis kinetic runs obeying pseudo-first-order rate law, were found to fit to Eq. (5.12).

5.3   Experimental Details on Kinetic measurements

Kinetic measurements were carried out using Shimadzu UV-1650 PC and Shimadzu UV-1800. The kinetic study was carried out under pseudo-first-order reaction conditions and the temperature used are 50ºC, 60ºC, 70ºC and 80ºC, respectively. The temperature of the cell compartment was maintained at 50ºC to reduce the temperature differences as small as possible. The total volume of the reaction mixture was kept constant at 5.0 ml to 40.0 ml (for slow reactions which involve sampling technique). After adding all the reaction components except substrate into a conical flask, the reaction mixture was subsequently put into a thermostatic oil bath at specific experimental temperature (50-80ºC) for about 15 minutes. The spectrophotometer was standardized with distilled water both as reference and blank samples. The reaction was initiated by adding an appropriate amount of substrate with a microsyringe to the temperature equilibrated reaction mixture. The reaction mixture was then mixed well and quickly transferred to a quartz cuvette which was subsequently placed into the cell compartment of the spectrophotometer. Once after the reaction is initiated, the process of transfer the sample into the cuvette and placed into the cell compartment need to be done within 30 seconds.

The reactions were generally carried out for up to 6 – 10 half-lives. Sampling technique was utilized if the reaction was too slow and needed to be kept overnight to obtain more data of A_{obs} versus t. This technique is applied to all the kinetic runs with observed rate constant, $k_{obs} \leq 1.0 \times 10^{-4}$ s^{-1}.

The values of pH for all kinetic runs at pH > 3 were measured using WITEG digital pH meter, Model: W – 500, at 50-80ºC. The pH meter was calibrated just before the pH measurements with standard pH buffers. The standard pH buffer solutions with pH accuracy of ± 0.02 were supplied by Mettler Toledo. The pH readings for reaction mixtures were taken before and after each kinetic run when buffer solution is used.

In order to determine the wavelength and optimal concentration of **1** for the spectrophotometric kinetic measurement on the alkaline and acidic hydrolysis of **1**, a few trial run of spectral study for typical kinetic runs was carried out. The observed data was inserted into BASICA software in order to acquire the calculated data.

5.4 Hydrolysis of Goniothalamin 1

5.4.1 Effects of NaOH on Alkaline Hydrolysis of 1

To study alkaline hydrolysis for 0.1 M NaOH as a first trial, a reaction mixture with a total volume of 10.0 ml which contained 1.0 ml of 1.0 M NaOH at 1.0 M ionic strength was prepared by adding 1.8 ml of 5.0 M NaCl and 6.95 ml H_2O. The reaction mixture was allowed to temperature – equilibrate for ~15 minutes at 50ºC. The reaction was then initiated by adding 0.25 ml of 4.0×10^{-3} M of **1** (prepared in CH_3CN) to the temperature – equilibrated reaction mixture. The progress of alkaline hydrolysis of **1** was quickly scanned at different time intervals until the completion of the reaction. The UV spectra at different reaction time for alkaline hydrolysis of **1** are shown in **Figure 5.1**. It is evident from **Figure 5.1** that the absorbance at wavelength 230 nm increases as the reaction going-on.
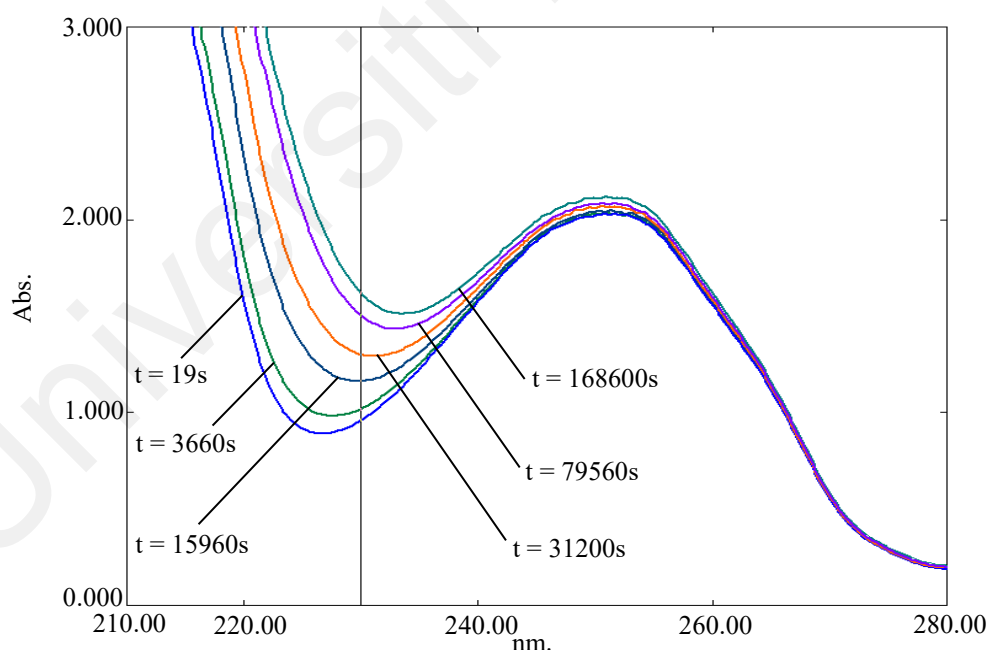
Figure 5.1: UV spectra of alkaline reaction mixture of **1** at 80°C in aqueous solvent containing 1.0×10^{-4} M of **1** and 0.1 M of NaOH.

After the first trial, it shown that the wavelength 250 nm has very close absorbance at 2.000. Therefore, the concentration of **1** at 1.0×10^{-4} M is not suitable for this study and reduced to 6×10^{-5} M in the following alkaline hydrolysis reaction.

5.4.1.1 Effect of Concentration of NaOH

Concentration within the range 0.1 to 1.0 M of NaOH were used to run alkaline hydrolysis for goniothalamin **1**. The data (time and absorbance at 230 nm) recorded for 0.1 M alkaline hydrolysis, together with the calculated absorbance and percentage of relative error acquired from BASICA software was tabulated in **Table 5.1**. The data in **Table 5.1** was then plotted into graph as shown in **Figure 5.2**.

Table 5.1: Observed data, time and absorbance at 230 nm, for alkaline hydrolysis of **1** at 0.1 M NaOH[a] .

Time (s)	A_{obs}	A_{calcd}[b]	%RE[c]
35	0.777	0.779	-0.23
348	0.811	0.804	0.87
744	0.836	0.834	0.26
1218	0.868	0.867	0.12
1821	0.904	0.905	-0.13
2822	0.951	0.960	-0.97
4320	1.016	1.026	-1.02
6660	1.104	1.100	0.36
9660	1.169	1.159	0.86
14100	1.215	1.205	0.86
18180	1.224	1.224	-0.01
21660	1.229	1.233	-0.29
25500	1.229	1.237	-0.69

[a] $[1] = 6 \times 10^{-5}$ M, $[NaOH] = 0.1$ M, 1.0 M ionic strength, $\lambda = 230$ nm, 80ºC.
[b] Calculated from Eq. (5.12) with $k_{obs} = 1.78 \times 10^{-4}$ s^{-1}, $\delta_{app} = 7750$ M^{-1} cm^{-1} and $A_0 = 0.908$
[c] Percent relative error, RE$=100(A_{obs} - A_{calcd})/A_{obs}$.
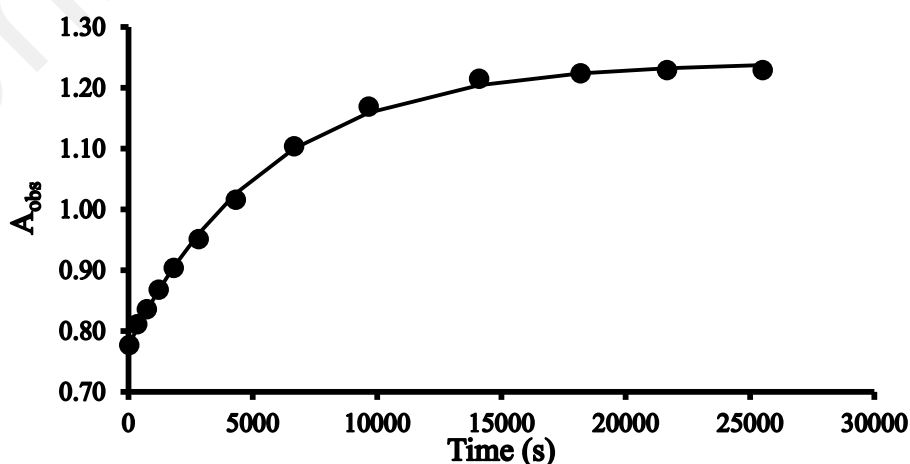
Figure 5.2: Plots showing the absorbance versus time dependence for alkaline hydrolysis of **1** at 0.1 M NaOH, experimental data points (●). The solid lines are drawn through the calculated data points.

The observed data (A_{obs} versus time, t) summarised in **Table 5.1** or **Figure 5.2** were found to fit to Eq. (5.12) where δ_{app}, k_{obs} and A_0 represent apparent molar extinction coefficient of the reaction mixture, pseudo first-order rate constant and initial absorbance, respectively. The nonlinear least square technique has been used to calculate the values of k_{obs}, δ_{app} and A_0, and such calculated values are $(1.78 \pm 0.07) \times 10^{-4}$ s^{-1}, $(7.75 \pm 0.07) \times 10^3$ $M^{-1}cm^{-1}$ and 0.908 ± 0.003, respectively. **Table 5.2** contains the values of k_{obs}, δ_{app} and A_0 at different values of [NaOH] within its range $0.1 – 1.0$ M.

Table 5.2: Values of k_{obs}, A_0 and δ_{app} for alkaline hydrolysis of **1** at different [NaOH][a].

[NaOH] (M)	$10^4 k_{obs}$ (s^{-1})	A_0	$10^{-3} \delta_{app}$ ($M^{-1}cm^{-1}$)
0.1	1.78 ± 0.07[b]	0.776 ± 0.005[b]	7.77 ± 0.10[b]
0.3	4.86 ± 0.20	0.955 ± 0.008	8.40 ± 0.16
0.4	6.74 ± 0.40	0.95 ± 0.01	7.20 ± 0.17
0.5	7.30 ± 0.40	0.95 ± 0.01	8.94 ± 0.20
0.6	8.99 ± 0.50	1.02 ± 0.01	7.98 ± 0.19
0.7	11.00 ± 0.07	1.04 ± 0.01	7.59 ± 0.19
0.8	13.10 ± 1.00	1.11 ± 0.01	8.67 ± 0.27
0.9	12.50 ± 1.00	1.20 ± 0.02	9.48 ± 0.37
1.0	14.10 ± 1.00	1.18 ± 0.02	8.95 ± 0.26

[a] $[1] = 6 \times 10^{-5}$ M, 1.0 M ionic strength, $\lambda = 230$ nm, 80ºC, the aqueous solvent for each kinetic run contained 2% v/v CH_3CN and 98% v/v H_2O.
[b] Error limits are standard deviations.

Figure 5.1 shows that the reaction is a monotonic reaction (one-step reaction) as there is only one changes were observed from the figure, which is the absorbance at wavelength 230 nm was increasing. The experiment was then repeated with concentration 0.3 to 1.0 M NaOH. The time and absorbance were recorded, and the curves of absorbance against time were plotted for each reaction. **Figure 5.3** and **Figure 5.4** contain the combined plots of $0.1 – 0.5$ M and $0.6 – 1.0$ M NaOH, respectively. It shows that the rate of reaction increases as the concentration of NaOH increases.

Figure 5.3: Plots showing the absorbance at 230 nm versus time of 0.1 M (●), 0.3 M (□), 0.4 M (▲) and 0.5 M (✕) NaOH for alkaline hydrolysis of **1**. The solid lines are drawn through the calculated data points.

Figure 5.4: Plots showing the absorbance at 230 nm versus time of 0.6 M (●), 0.7 M (Δ), 0.8 M (■), 0.9 M (✕) and 1.0 M (♦) NaOH for alkaline hydrolysis of **1**. The solid lines are drawn through the calculated data points.

Pseudo-first-order rate constants (k_{obs}) for rates of alkaline hydrolysis of **1** at different [NaOH] are shown in **Table 5.3**. These data are also shown graphically in **Figure 5.5**. The linear plot of **Figure 5.5** shows that k_{obs} versus [NaOH] data fit to an equation of straight line in the form: $y = mx + c$.

Table 5.3: Pseudo-first-order rate constants (k_{obs}) for alkaline hydrolysis of **1** at 0.1-1.0 M NaOH[a].

[NaOH] (M)	$10^4 k_{obs}$ (s⁻¹)	$10^4 k_{calc}$ (s⁻¹)	%RE
0.1	1.78 ± 0.07[b]	2.133[c]	-19.86
0.3	4.86 ± 0.20	4.913	-1.11
0.4	6.74 ± 0.40	6.304	6.47
0.5	7.30 ± 0.40	7.694	-5.40
0.6	8.99 ± 0.50	9.084	-1.05
0.7	11.00 ± 0.07	10.475	4.78
0.8	13.10 ± 1.00	11.865	9.43
0.9	12.50 ± 1.00	13.255	-6.04
1.0	14.10 ± 1.00	14.645	-3.87

[a][**1**] = 6×10^{-5} M, [NaOH] = 0.1-1.0 M, 1.0 M ionic strength, λ = 230 nm, 80°C.
[b] Error limits are standard deviations.
[c] Calculated from equation: $y = mx + c$ with $m = 1.39 \times 10^{-3}$ M⁻¹s⁻¹ and $c = 7.43 \times 10^{-5}$ s⁻¹
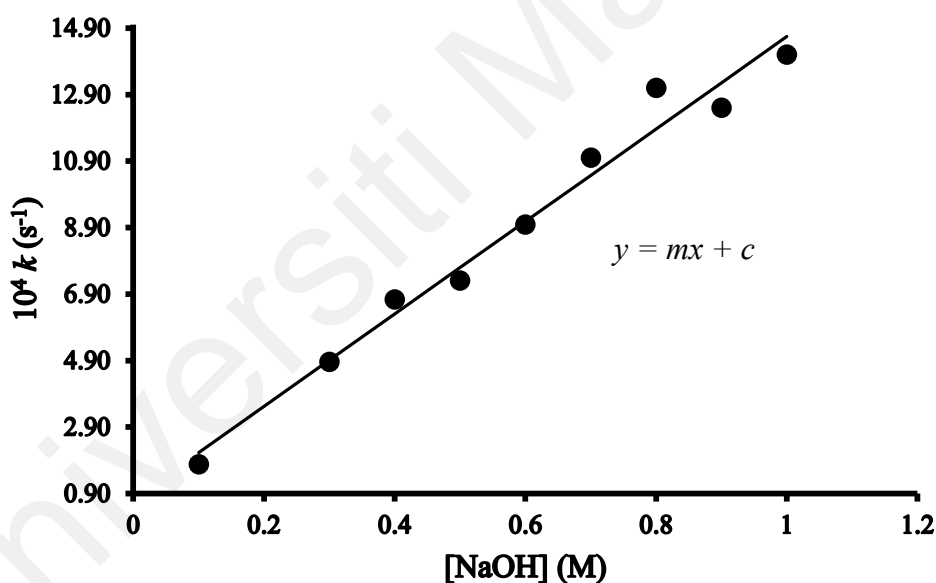
Figure 5.5: Plots showing the dependence of k_{obs} and k_{calc} versus [NaOH] for the reaction of **1** with HO⁻ at of 0.1-1.0 M NaOH. The solid line is drawn through the calculated data points.

The gradient (m) and y-intercept (c) acquired from plots in **Figure 5.5** are $(1.39 \pm 0.08) \times 10^{-3}$ M⁻¹s⁻¹ and $(7.43 \pm 5.26) \times 10^{-5}$ s⁻¹, respectively.

5.4.1.2 Effects of Temperature on k_{obs} for Alkaline Hydrolysis of 1

The kinetic study of **1** was performed as a function of temperature where the previous procedure was applied at 1.0 M NaOH by using five different thermostatically controlled oil baths set at 40, 50, 60, 70 and 80°C. The influence of temperature on the reaction rate constant was given by Arrhenius equation as follows:

$$\ln k_{obs} = \ln A - E_a / RT \tag{5.13}$$

where k_{obs} is the reaction rate constant, A is the frequency factor, E_a is the activation energy, R is the universal gas constant and T is the absolute temperature. **Table 5.4** shows that increasing the temperature leading to increasing of the reaction rate constant. The activation energy of alkaline hydrolysis of **1** is 102 kJ mol⁻¹. This amount is acquired by inserting data from plotted graph (**Figure 5.6**) into Arrhenius equation (5.13) that equivalent to $y = mx + c$.

$$y = \ln k \; ; \; m = -\frac{E_a}{R} \; ; \; x = \frac{1}{T} \; ; \; c = \ln A$$

From the plots in **Figure 5.6**, gradient (m) acquired is $(-12.2 \pm 1.5) \times 10^3$ K and y-intercept (c) is 28.4 ± 4.5. The gas constant, R is 8.314 J K⁻¹ mol⁻¹. Activation energy of the reaction can be calculated by substitute the values into the equation. The calculation is shown below:

$$E_a = -mR = -(-12241 \times 8.314) = 101781 \text{ J mol}^{-1} = 102 \text{ kJ mol}^{-1}$$

Table 5.4: Effect of temperature on the observed pseudo-first-order rate constants for alkaline hydrolysis of **1** in 1.0 M NaOH.

T (°C)	10^3 1/T (K⁻¹)	10^4 k_{obs} (s⁻¹)	ln k_{obs}	ln k_{calc}[a]	%RE[b]
40	3.183	0.19 ± 0.03[c]	-10.87	-10.547	2.97
50	3.085	1.04 ± 0.10	-9.17	-9.32	-1.66
60	2.993	3.44 ± 0.30	-7.97	-8.22	-3.15
70	2.906	10.50 ± 1.00	-6.86	-7.24	-5.56
80	2.824	14.10 ± 1.00	-6.56	-6.14	6.97

[a] Calculated from Eq. (5.13).

[b] Percentage relative error, difference between ln k_{obs} and ln k_{calc}.

[c] Error limits are standard deviations.
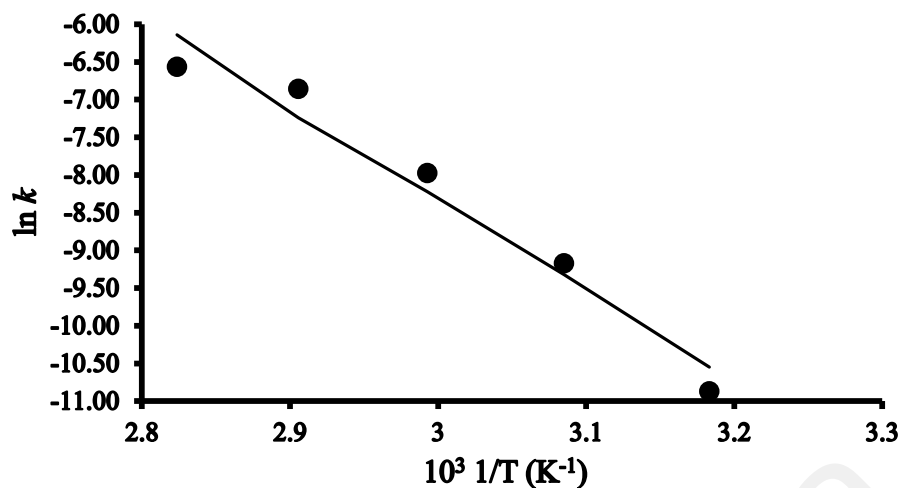
Figure 5.6: Arrhenius plots of alkaline hydrolysis of **1** where solid line is drawn through the calculated rate constants ln k_{calc}.

5.4.2 Effects of HCl on Acid Hydrolysis of 1

To study acidic hydrolysis for 0.1 M HCl, a reaction mixture with a total volume of 10.0 ml which contained 0.21 ml of 4.775 M HCl at 1.0 M ionic strength was prepared by adding 1.8 ml of 5.0 M NaCl and 7.89 ml H_2O. The reaction mixture was allowed to temperature – equilibrate for ~15 minutes at 80ºC. The reaction was then initiated by adding 0.10 ml of 4.0×10^{-3} M of **1** (prepared in CH_3CN) to the temperature – equilibrated reaction mixture.
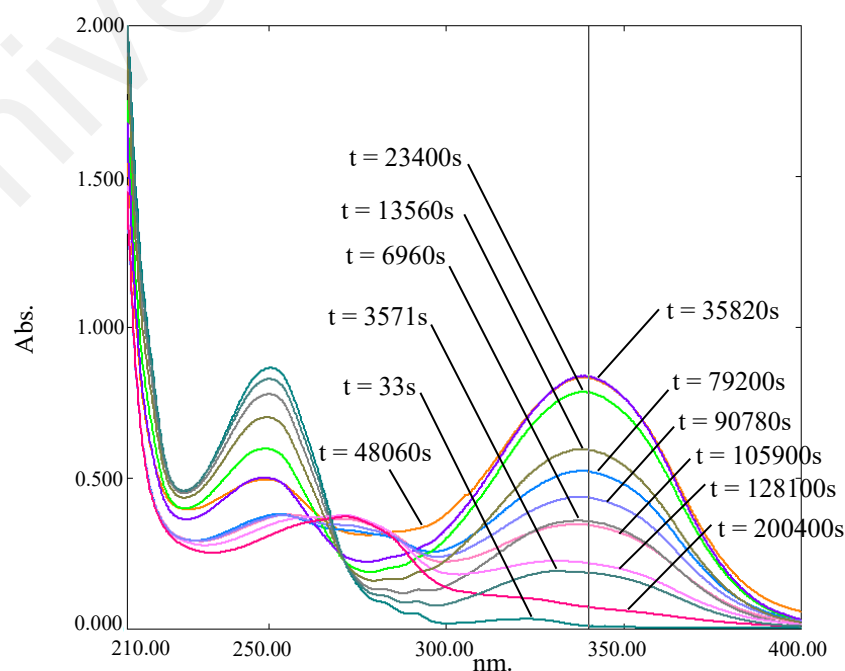
Figure 5.7: UV spectra of acidic reaction mixture of containing 4.0×10^{-5} M of **1** at 80°C in aqueous solvent for 0.1 M HCl.

The progress of acidic hydrolysis of **1** was quickly scanned at different time intervals until the completion of the reaction. The UV spectra at different reaction time for acidic hydrolysis of **1** are shown in **Figure 5.7**. From this figure, it appears that the absorbance at wavelength 340 nm increases until it reaches a highest value, and then decreases until it reach as a lowest constant value.

5.4.2.1 Effect of Concentration of HCl

Kinetic runs were carried out for acidic hydrolysis of **1** at 1.0 M ionic strength and within [HCl] range of 0.1 to 1.0 M. The observed data (A_{obs} versus reaction time, t) recorded for 0.1 M acidic hydrolysis, together with the calculated absorbance and percentage of relative error acquired from BASICA software was tabulated in **Table 5.5**. The data in **Table 5.5** was then plotted into graph as shown in **Figure 5.8**, together with other three curves of absorbance against time at concentration 0.3 – 0.5 M HCl. Another five plots with concentration of HCl in between 0.6 to 1.0 M was shown in **Figure 5.9**.

Table 5.5: Observed data, time versus absorbance at 340 nm, for acidic hydrolysis of **1** at 0.1 M HCl[a].

Time (s)	A_{obs}	A_{calcd}[b]	%RE[c]
33	0.009	0.009	4.87
3571	0.186	0.213	-14.64
6960	0.356	0.371	-4.30
9840	0.467	0.481	-2.89
13560	0.593	0.592	0.10
18840	0.726	0.704	2.98
27900	0.815	0.801	1.73
35820	0.837	0.818	2.27
48060	0.824	0.773	-6.75
64860	0.679	0.648	4.54
79200	0.521	0.530	-1.71
90780	0.436	0.441	-1.09
105900	0.344	0.340	1.21
128100	0.218	0.226	-3.73
165660	0.102	0.110	-7.74
200400	0.072	0.056	21.54
259200	0.049	0.021	57.88

[a] [**1**] = 4 ×10^{-5} M, [HCl] = 0.1 M, 1.0 M ionic strength, λ = 340 nm, 80°C.
[b] Calculated from Eq. (5.12) with $k_{1\,obs}$ = 3.70 × 10^{-5} s^{-1}, δ_{app} = 43500 M^{-1} cm^{-1} and A_0 = 0.0064
[c] Percentage of relative error, difference between observed and calculated absorbance.

The plots in **Figure 5.8** and **Figure 5.9** shows that acidic hydrolysis reaction is consecutive reaction (multi-step reaction), there is an intermediate stage before it become the final product. It shows that the rate of reaction increases as the concentration of HCl increases.
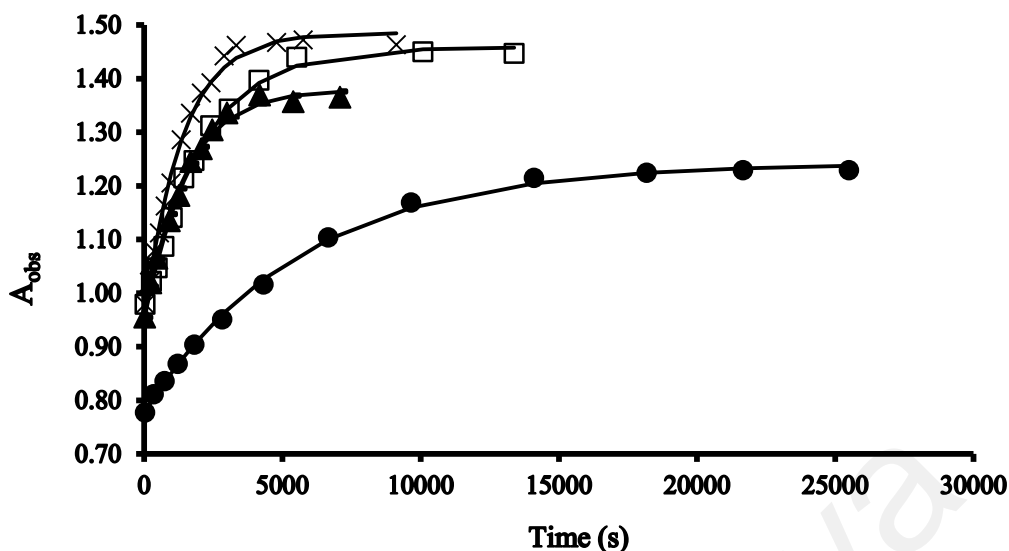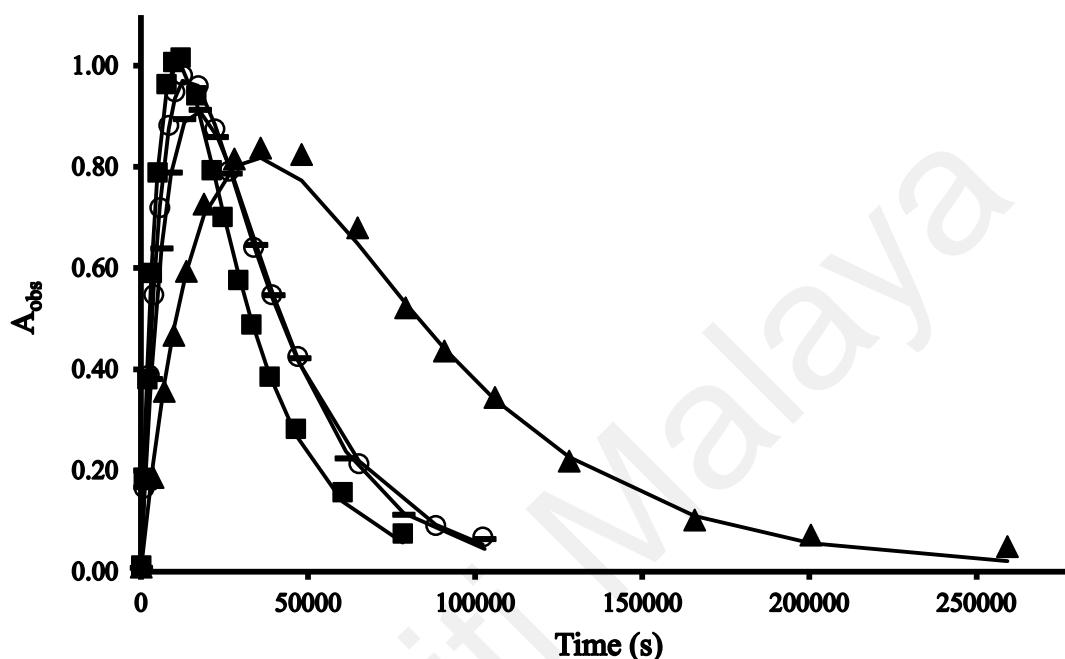

Figure 5.8: Plots showing the absorbance at 340 nm versus time of 0.1 M (▲), 0.3 M (─), 0.4 M (○) and 0.5 M (■) HCl for acidic hydrolysis of **1**. The solid lines are drawn through the calculated data points.
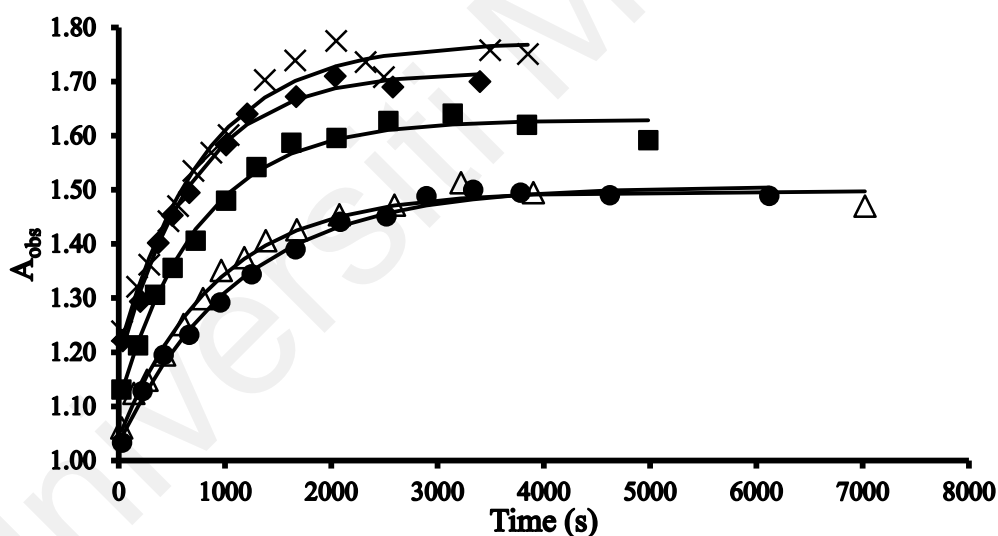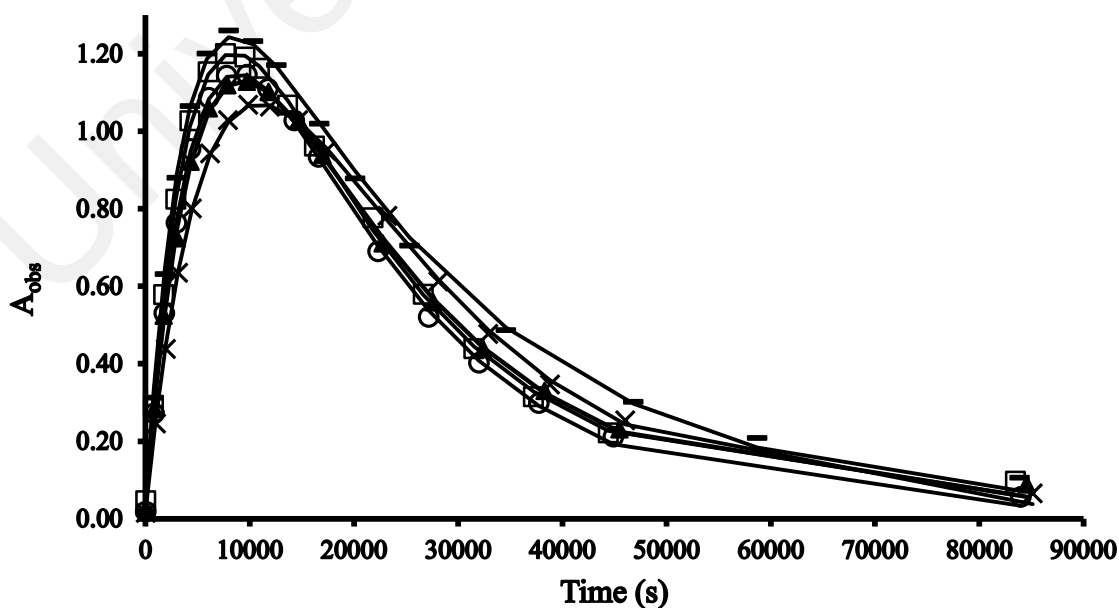

Figure 5.9: Plots showing the absorbance at 340 nm versus time of 0.6 M (✕), 0.7 M (▲), 0.8 M (○), 0.9M (□) and 1.0 M (─) HCl for acidic hydrolysis of **1**. The solid lines are drawn through the calculated data points.

The observed data (observed absorbance, A_{obs} versus time, t) summarised in **Table 5.5** or **Figure 5.8**, **Figure 5.9** were found to fit to Eq. (5.14) as shown below.

$$A_{obs} = \frac{A_3 A_1}{A_2 - A_1}(e^{-A_1 t} - e^{-A_2 t}) + A_4 \qquad (5.14)$$

Where $A_1 = k_1$ (rate of reaction when absorbance increases), $A_2 = k_2$ (rate of reaction when absorbance decreases), $A_3 = \delta_{ap}[A_0]$ and $A_4 = A_0$ (initial absorbance at $t = 0$), all of these are empirical constant. $[A_0]$ represents initial concentration **1**.

Eq. (5.14) can be derived from a simple reaction scheme shown by **Scheme 5.1**.

$$\mathbf{1} \xrightarrow{\ k_1\ } \text{Int} \xrightarrow{\ k_2\ } \text{P}$$
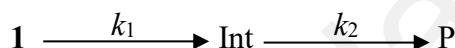
Scheme 5.1: Hydronium ion-catalysed hydrolysis of **1** where Int and P represent intermediate product and final product, respectively. Symbols k_1 and k_2 represent pseudo-first-order rate constants for first and second reaction steps.

Table 5.6 contains all A_1, A_2, A_3 and A_4 data obtained within [HCl] range 0.1 M to 1.0 M HCl. The nonlinear least square technique has been used to calculate the values of A_1, A_2, A_3, and A_4. And such calculated values of A_1, A_2, A_3, and A_4 at 0.1 M HCl are 0.37 ± 0.09 s^{-1}, 2.19 ± 0.51 s^{-1}, 1.738 ± 0.895 and 0.0064 ± 0.0167, respectively.

Table 5.6: Values of k_{obs}, A_0 and $\delta_{ap}[A_0]$ for acidic hydrolysis of **1** at different [HCl][a].

[HCl] (M)	$10^4 k_{1obs}$ (s^{-1})	$10^5 k_{2obs}$ (s^{-1})	$\delta_{ap}[A_0]$ (cm^{-1})	A_0	$10^{-4}\, \delta_{ap}$ (M^{-1}cm^{-1})
0.1	0.37 ± 0.09^b	2.19 ± 0.51^b	1.738 ± 0.895^b	0.0064 ± 0.0167^b	4.35
0.3	0.71 ± 0.10	5.18 ± 0.73	2.111 ± 1.076	0.0117 ± 0.0069	5.28
0.4	1.25 ± 0.47	3.52 ± 0.14	1.618 ± 0.055	-0.0074 ± 0.0074	4.05
0.5	1.48 ± 0.09	3.33 ± 0.20	1.584 ± 0.067	0.0053 ± 0.0129	3.96
0.6	1.31 ± 0.08	6.01 ± 0.38	2.043 ± 0.194	0.0152 ± 0.0087	5.11
0.7	1.74 ± 0.10	6.07 ± 0.34	1.920 ± 0.119	0.0391 ± 0.0107	4.80
0.8	1.81 ± 0.08	6.40 ± 0.29	1.994 ± 0.102	0.0192 ± 0.0090	4.99
0.9	2.00 ± 0.11	6.18 ± 0.33	1.957 ± 0.102	0.0455 ± 0.0119	4.89
1.0	2.51 ± 0.11	4.34 ± 0.21	1.773 ± 0.047	0.0161 ± 0.0145	4.43

[a] $[A_0] = 4 \times 10^{-5}$ M, 1.0 M ionic strength, $\lambda = 340$ nm, 80°C, the aqueous solvent for each kinetic run contained 2% v/v CH$_3$CN and 98% v/v H$_2$O.
[b] Error limits are standard deviations.

Rate constants (k_{1obs} and k_{2obs}) for acidic hydrolysis of **1** within [HCl] range $0.1 - 1.0$ M were calculated and listed in **Table 5.7**. The plots of **Figure 5.10** were plotted based on the data k_{1obs} and k_{2obs} versus [HCl]. The plot of k_{1obs} versus [HCl] reveals a linear straight line. But k_{2obs} values fluctuated between 2.19×10^{-5} s^{-1} to 6.40×10^{-5} s^{-1}. Therefore, it is concluded that k_{1obs} is pseudo-first-order reaction, while k_{2obs} values are independent of [HCl]. Linear least-squares technique gave slope and intercept of linear plot of k_{1obs} versus [HCl] of **1** as $(2.2 \pm 0.2) \times 10^{-4}$ M^{-1}s^{-1} and $(1.93 \pm 1.27) \times 10^{-5}$ s^{-1}, respectively.

Table 5.7: Rate of acidic hydrolysis of **1** at 0.1-1.0 M HCl[a].

[HCl] (M)	$10^4 k_{1obs}$ (s^{-1})	$10^4 k_{calc}$ (s^{-1})	$10^5 k_{2obs}$ (s^{-1})	%RE
0.1	0.37 ± 0.09[b]	0.409	2.19 ± 0.51[b]	-10.41
0.3	0.71 ± 0.10	0.840	5.18 ± 0.73	-18.31
0.4	1.25 ± 0.47	1.056	3.52 ± 0.14	15.54
0.5	1.48 ± 0.09	1.272	3.33 ± 0.20	14.08
0.6	1.31 ± 0.08	1.487	6.01 ± 0.38	-13.53
0.7	1.74 ± 0.10	1.703	6.07 ± 0.34	2.12
0.8	1.81 ± 0.08	1.919	6.40 ± 0.29	-6.01
0.9	2.00 ± 0.11	2.135	6.18 ± 0.33	-6.73
1.0	2.51 ± 0.11	2.350	4.34 ± 0.21	5.99

[a] [**1**] = 4×10^{-5} M, [HCl] = 0.1-1.0 M, 1.0 M ionic strength, λ = 340 nm, 80ºC.
[b] Error limits are standard deviations.

Figure 5.10: Plots showing the dependence of k_{1obs} (●) and independence k_{2obs} (✗) versus [HCl] for the reaction of 1 at 0.1-1.0 M HCl. The solid line is drawn through the calculated data points.

5.4.2.2 Effects of Temperature

Kinetic runs were carried out for acidic hydrolysis of **1** in the temperature range of 40-80 ℃ at 1.0 M HCl. The hydrolysis kinetics and its observed rate constant (k_{obs}) were determined at 40, 50, 60, 70 and 80°C. Arrhenius plots is used to determine the activation energy (E_a) of acidic degradation of **1**.

The influence of temperature on the reaction rate constant was given by Eq. (5.13) (Arrhenius equation: $\ln k_{obs} = \ln A - E_a / RT$). Where k_{obs} is the reaction rate constant, A is the frequency factor, E_a is the activation energy, R is the universal gas constant and T is the absolute temperature.

Table 5.8 shows that the increase of the temperature increased the values of reaction rate constant. The activation energy is calculated by inserting data from **Table 5.8** into Arrhenius equation (5.13) that equivalent to $y = mx + c$.

$$y = \ln k_{1obs} \; ; \; m = -\frac{E_a}{R} \; ; \; x = \frac{1}{T} \; ; \; c = \ln A$$

From the plot of **Figure 5.11**, gradient (m) turned out to be $(-11.01 \pm 0.48) \times 10^3 K$ and intercept (c) is 22.7 ± 1.4. The gas constant, R is 8.314 J K^{-1} mol^{-1}. Activation energy of the reaction can be calculated by substitute the values into the equation:

$E_a = - mR = - (-11014 \times 8.314) = 91570$ J mol^{-1} = 91.6 kJ mol^{-1}

Therefore, the activation energy of acidic hydrolysis of **1** to the first intermediate product is 91.6 kJ mol^{-1}. But the activation energy of the sequential process is unable to identified from the collected data as the rate constant (k_2) are fluctuated.

Table 5.8: Effect of temperature on the observed pseudo-first-order rate constants (k_1) for acidic hydrolysis of **1** in 1.0 M HCl.

T (°C)	10^3 1/T (K^{-1})	10^5 k_{1obs} (s^{-1})	ln k_{1obs}	ln k_{1calc}[a]	%RE[b]
40	3.183	0.48 ± 0.04[c]	-12.24	-12.32	-0.68
50	3.085	1.13 ± 0.02	-11.39	-11.24	1.28
60	2.993	3.99 ± 0.16	-10.13	-10.23	-1.00
70	2.906	8.43 ± 0.30	-9.38	-9.27	-1.14
80	2.824	25.10 ± 1.10	-8.29	-8.37	-0.84

[a] Calculated from Eq. (5.13).

[b] Percentage relative error, difference between ln k_{1obs} and ln k_{1calc}.

[c] Error limits are standard deviations.
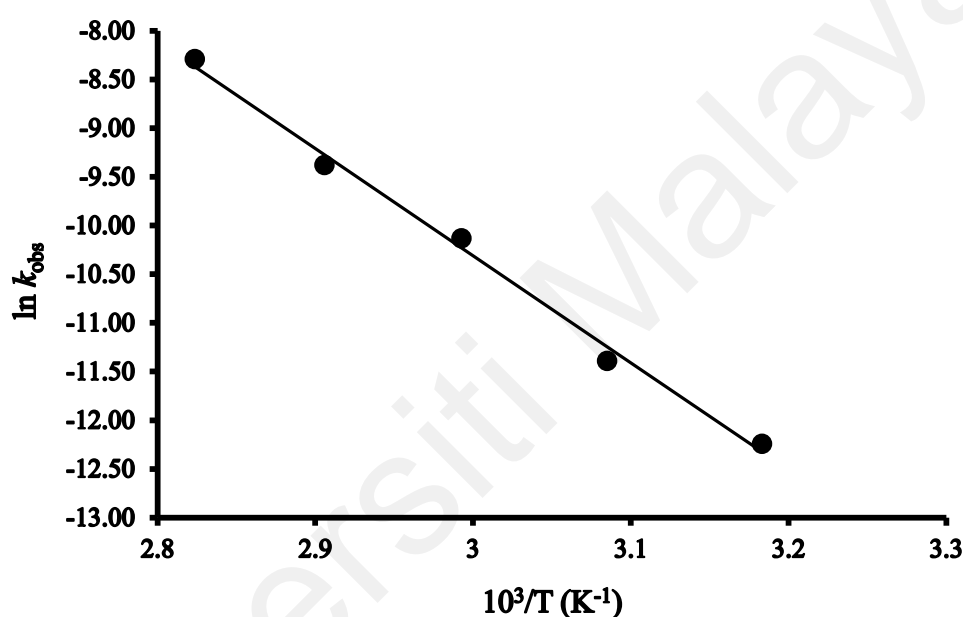
Figure 5.11: Arrhenius plots of acidic hydrolysis of **1** where solid line is drawn through the calculated rate constants ln k_{1calc}.

5.4.3 Effects of Sodium Acetate Buffer on k_{obs} for the Hydrolysis of 1

In order to discover the buffer effect on the hydrolysis reaction of **1**, kinetic runs were carried out in buffer solutions of sodium acetate (pH 3.97-5.12). The UV spectra at different reaction time for buffer hydrolysis of **1** is similar to the acidic hydrolysis. From

Figure **5.12**, it shows that the absorbance at wavelength 328 nm increases until a maximum is reached, then decreases. The pH values of the reaction mixture is measured

and recorded before the reaction started and after the reaction ended. This is to ensure sodium acetate buffer do not decompose during the reaction.

Concentration within the range 0.1 to 0.9 M of sodium acetate buffer solution were used to run hydrolysis for goniothalamin **1**. The plots in **Figure 5.13**, **Figure 5.14** and Figure 5.15 shows that sodium acetate buffer hydrolysis reaction is consecutive reaction, which is similar to acidic hydrolysis.
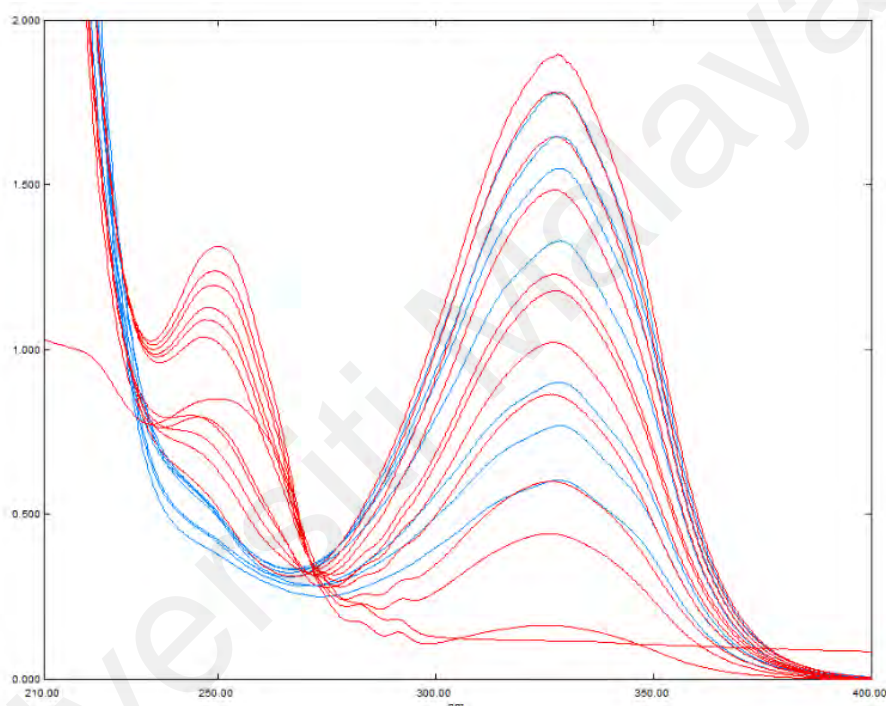
Figure 5.12: UV spectra of sodium acetate buffer reaction mixture of **1** at 80°C in aqueous solvent containing 6.0×10^{-3} M **1** and 0.1 M 25% f_b CH$_3$COONa. The red and blue colour lines indicate the increase and decrease of absorbance at 340 nm, respectively.

The observed data (**Figure 5.13**-**Figure 5.15**) were found to fit to Eq. (5.14). The values of k_{1obs}, k_{2obs}, δ_{ap} [X$_0$] and A$_0$ are summarized in **Table 5.9** for sodium acetate buffer.

The plot of k_{1obs} and k_{2obs} versus [CH$_3$COONa] in **Figure 5.16** and **Figure 5.17**, respectively, reveals a non-linear shape. Both k_{1obs} and k_{2obs} values fluctuated between 1.80×10^{-6} s^{-1} to 3.51×10^{-6} s^{-1} and 3.06×10^{-7} s^{-1} to 5.01×10^{-7} s^{-1}, respectively. Therefore, it is concluded that there is no buffer catalysis of sodium acetate with **1**.
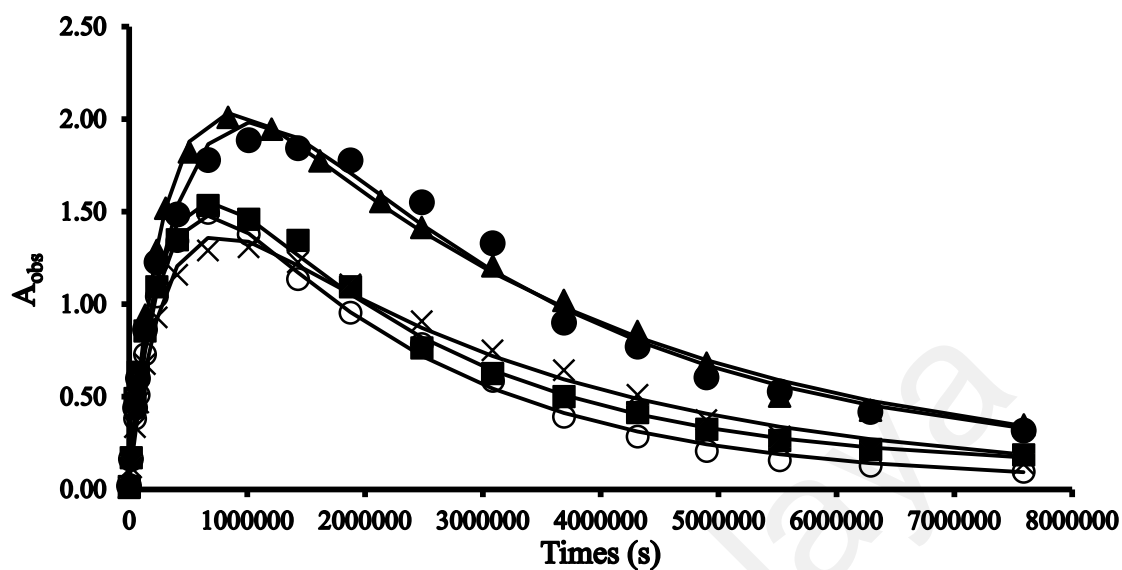
Figure 5.13: Plots showing the absorbance at 328 nm versus time of 0.1 M (●), 0.3 M (▲), 0.5 M (○), 0.7 M (■) and 0.9 M (✕) 25% f_b CH$_3$COONa for hydrolysis of **1**. The solid lines are drawn through the calculated data points.
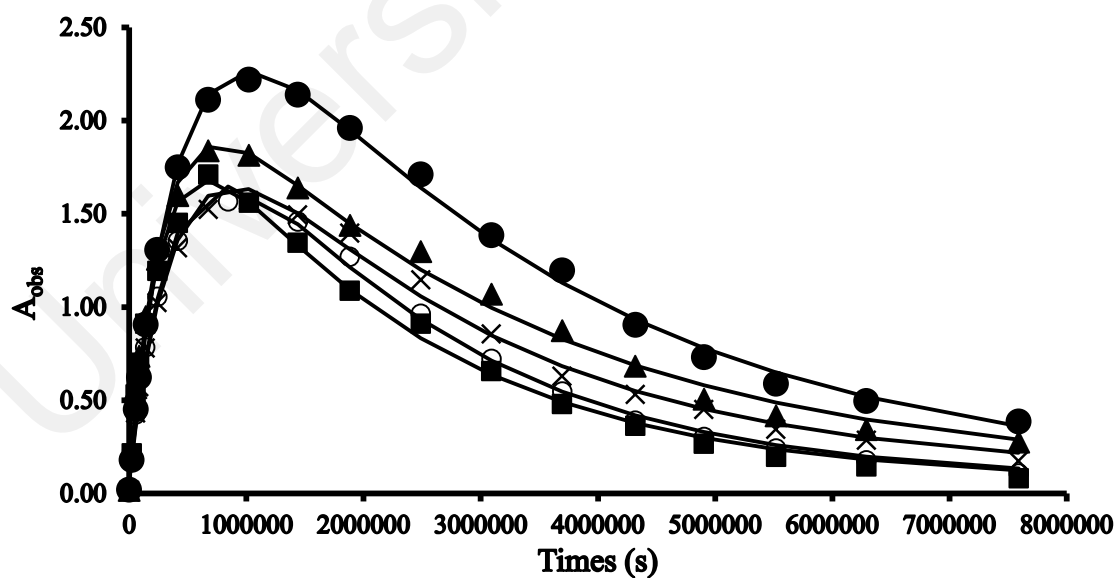
Figure 5.14: Plots showing the absorbance at 328 nm versus time of 0.1 M (●), 0.3 M (▲), 0.5 M (○), 0.7 M (■) and 0.9 M (✕) 50% f_b CH$_3$COONa for hydrolysis of **1**. The solid lines are drawn through the calculated data points.
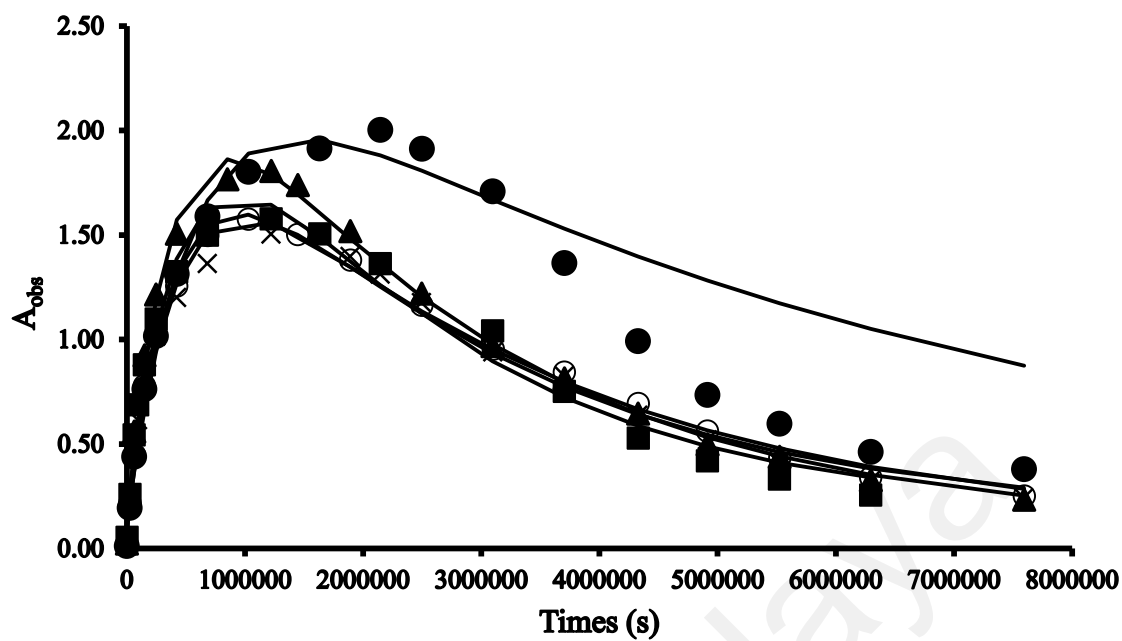
Figure 5.15: Plots showing the absorbance at 328 nm versus time of 0.1 M (●), 0.3 M (▲), 0.5 M (○), 0.7 M (■) and 0.9 M (✗) 75% f_b CH$_3$COONa for hydrolysis of **1**. The solid lines are drawn through the calculated data points.

.

Table 5.9: Observed data (k_{1obs} and k_{2obs} versus $[Buf]_T$) .

25% f_b CH$_3$COONa

$[Buf]_T{}^a$ (M)	$10^6\,k_{1obs}$ (s^{-1})	$10^7\,k_{2obs}$ (s^{-1})	$\delta_{ap}\,[X_0]$ (cm^{-1})	A_0	$10^{-4}\,\delta_{ap}$ (M^{-1}cm^{-1})	pH (before reaction)	pH (after reaction)
0.1	2.04 ± 0.29 [b]	3.69 ± 0.46 [b]	2.703 ± 0.233 [b]	0.1290	4.51	5.158	5.196
0.3	3.00 ± 0.18	3.06 ± 0.17	2.555 ± 0.063	0.0629	4.26	5.184	5.215
0.5	3.37 ± 0.22	5.01 ± 0.29	2.006 ± 0.070	0.0402	3.34	5.217	5.176
0.7	3.38 ± 0.37	4.77 ± 0.47	1.994 ± 0.114	0.1096	3.32	5.226	5.248
0.9	3.27 ± 0.31	3.37 ± 0.27	1.726 ± 0.0693	0.0395	2.88	5.284	5.209

[a] $[Buf]_T$ represents total buffer concentration.
[b] Error limits are standard deviations.

50% f_b CH$_3$COONa

$[Buf]_T{}^a$ (M)	$10^6\,k_{1obs}$ (s^{-1})	$10^7\,k_{2obs}$ (s^{-1})	$\delta_{ap}\,[X_0]$ (cm^{-1})	A_0	$10^{-4}\,\delta_{ap}$ (M^{-1}cm^{-1})	pH (before reaction)	pH (after reaction)
0.1	2.20 ± 0.12 [b]	3.32 ± 0.16 [b]	3.073 ± 0.091 [b]	0.0697	5.12	5.380	5.411
0.3	3.27 ± 0.31	3.40 ± 0.28	2.311 ± 0.093	0.0927	3.85	5.411	5.429
0.5	2.41 ± 0.23	4.94 ± 0.42	2.383 ± 0.155	0.0640	3.97	5.449	5.486
0.7	3.51 ± 0.35	4.84 ± 0.44	2.225 ± 0.113	0.0589	3.71	5.475	5.515
0.9	2.33 ± 0.28	4.22 ± 0.45	2.241 ± 0.164	0.1068	3.74	5.512	5.573

[a] $[Buf]_T$ represents total buffer concentration.
[b] Error limits are standard deviations.

Table 5.9, continued.

75% f_b CH$_3$COONa

[Buf]$_T{}^a$ (M)	$10^6\, k_{1obs}$ (s^{-1})	$10^7\, k_{2obs}$ (s^{-1})	δ_{ap} [X$_0$] (cm^{-1})	A$_0$	$10^{-4}\, \delta_{ap}$ (M^{-1}cm^{-1})	pH (before reaction)	pH (after reaction)
0.1	$1.80 \pm 0.45\,^b$	$1.61 \pm 0.40\,^b$	2.337 ± 0.270^b	0.1178	3.90	5.763	5.814
0.3	2.50 ± 0.21	3.92 ± 0.31	2.482 ± 0.112	0.1033	4.14	5.782	5.829
0.5	2.49 ± 0.22	3.23 ± 0.25	2.061 ± 0.087	0.0813	3.44	5.814	5.896
0.7	2.06 ± 0.44	4.56 ± 0.88	2.333 ± 0.356	0.1704	3.89	5.848	5.913
0.9	2.50 ± 0.21	3.92 ± 0.31	2.482 ± 0.112	0.1033	4.14	5.855	5.922

^{a} [Buf]$_T$ represents total buffer concentration.

^{b} Error limits are standard deviations.
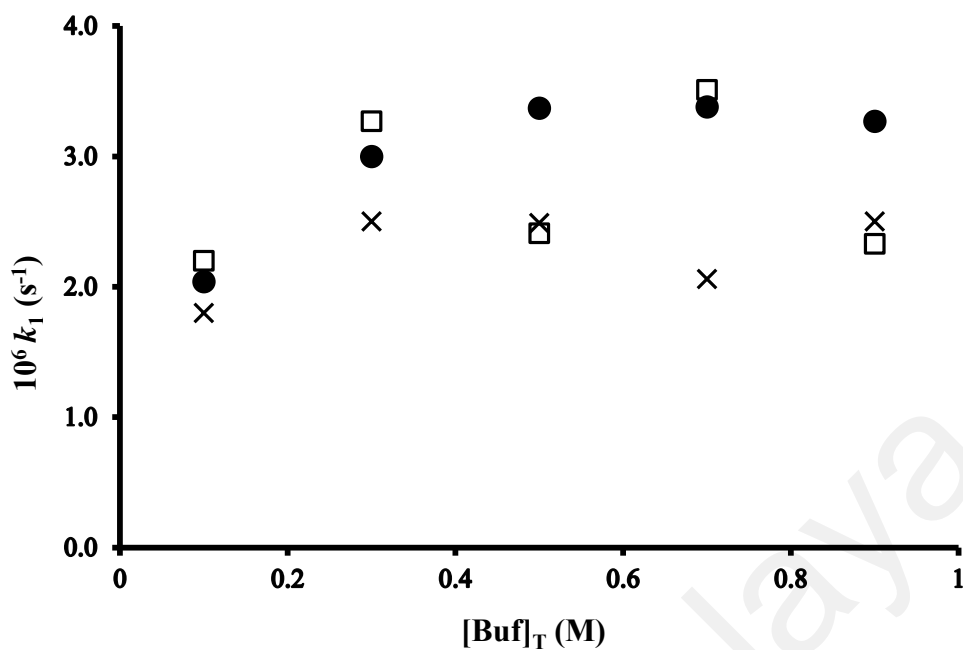
Figure 5.16: Plots showing the independence of k_{1obs} versus [CH$_3$COONa] for reaction 25% f_b CH$_3$COONa (●), 50% f_b CH$_3$COONa (□) and 75% f_b CH$_3$COONa (✗).
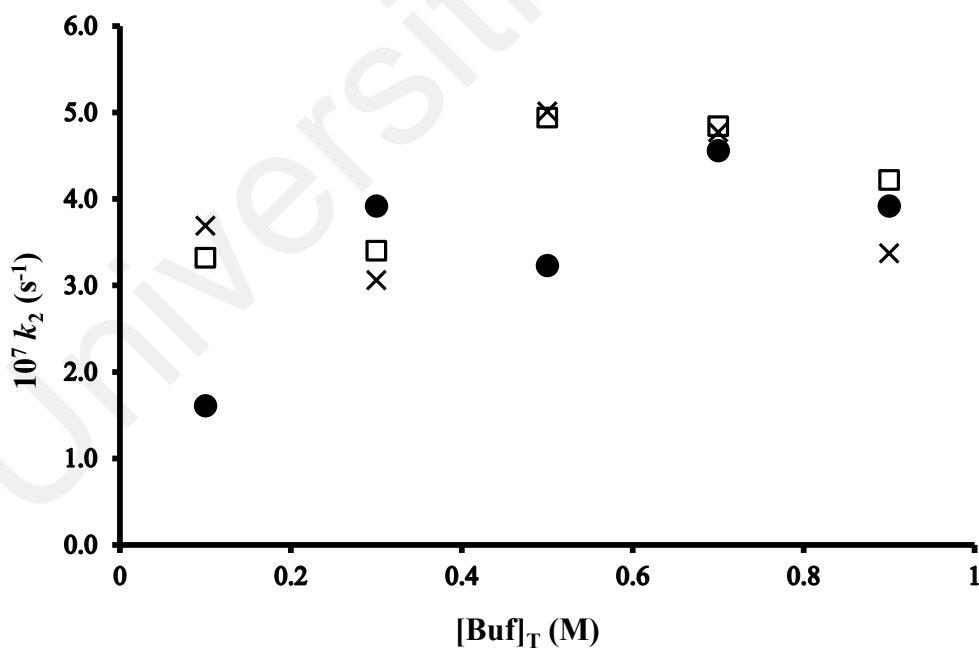
Figure 5.17: Plots showing the independence of k_{2obs} versus [CH$_3$COONa] for reaction 25% f_b CH$_3$COONa (●), 50% f_b CH$_3$COONa (□) and 75% f_b CH$_3$COONa (✗).

5.5 Product Characterization and Proposed Reaction Mechanism

In order to identify the structure of the products of acidic and alkaline hydrolysis of **1**, a minimum amount of 2 mg of products were required in order to run NMR experiments. In this case, a larger scale of hydrolysis experiment was prepared in order to yield sufficient amount of products.

5.5.1 Product from Alkaline Hydrolysis

5.5.1.1 Experimental Details

A reaction is initiated by adding 0.05 M of **1** into 2.0 M NaOH at 50ºC. The total volume of reaction was kept constant at 20 ml. After allowing the reaction to carry out for reaction period of more than 10 half-lives, the product was extracted by using liquid-liquid (water – ethyl acetate) extraction. The product acquired was then elucidated through NMR spectra analysis. The NMR spectra (^{1}H, ^{13}C, COSY and HMBC) data were summarized in **Table 5.10**.

5.5.1.2 Structural Elucidation of Product from Alkaline Hydrolysis
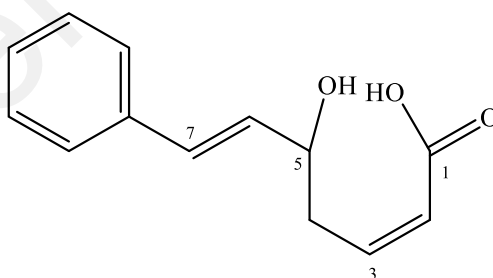
The product was acquired as light yellow amorphous. The molecular formula was established as $C_{13}H_{14}O_3$ by LCMS-IT-TOF analysis (**Figure 5.23**), with $[M+H]^+$ ion peak at m/z 219.1736 (calcd. for $C_{13}H_{15}O_3$, 219.1734).

The complete assignments of ^{1}H NMR and ^{13}C NMR spectroscopic data of the product were achieved from the results of 2D correlation measurement, including HSQC, COSY and HMBC experiments.

The ^{1}H NMR spectrum showed the aromatic protons at δ 7.19-7.35 referring to five aromatic protons (H-9 to H-13) of a *mono*-substituted phenyl ring. Four olefinic protons peaks at δ 6.59, δ 6.33, δ 6.22 and δ 5.93 were assigned to H-7, H-3, H-6 and H-, respectively. H-7 and H-6 were in *trans* configuration, while H-3 and H-2 were in *cis* configuration. The others configurations were determined by a proton signal at δ 4.33 (*q*, *J*=6.2 Hz) was indicative of oxygen bearing methine proton H-5. Two allylic protons resonated at δ 2.92 (*m*) belonged to H-4.

The ^{13}C and DEPT-135 spectra confirmed the presence of thirteen carbons; one methylene, ten methines and two quaternary carbon peaks appeared at δ 170.2 and δ 137.0 which were most probably belonged to C-1 and C-8 respectively. Four olefinic carbons; C-2, C-3, C-6 and C-7, resonated at δ123.6, δ 140.9, δ 131.8 and δ 129.8 respectively. C-3 resonated most downfield compared to the other olefinic carbons due to the α-β unsaturated resonance effect of carbonyl group at position C-1. The methylene carbon C-4 gave a peak at δ 36.2 meanwhile C-5 showed a peak at δ 71.5 which were due to the deshielding effect by the neighbouring oxygen atom. Finally the five aromatic protons gave signals centred at δ 126.1-128.2 (C-9 to C-13).

The HMBC correlations of H-2, H-3 to C-1 suggested that the double bond was linked to C-1. The correlations of the two olefinic protons H-6, H-7 to C-5 and C-8 indicated the aromatic ring was connected to C-7.

The assignments of the ^{1}H NMR and ^{13}C NMR spectroscopic data were achieved from the results of the 2D correlation measurements, including the COSY, HSQC and HMBC experiments. The COSY and HMBC correlations were summarised in **Table 5.10**. It was observed that the spectroscopic data of product were in accordance with those reported for goniomicin A **147** (**Table 5.11**). Therefore, the product was characterized as **147**, an ring-opening styryl-lactones of goniothalamin **1**.

Table 5.10: ^1H, ^{13}C, COSY and HMBC spectral data of product from alkaline hydrolysis in CDCl$_3$.

Position	δ$_H$, J (Hz)	δ$_C$	COSY	HMBC (H→ C)
1	-	170.3	-	-
2	5.93 (1H, *d*) *J*=11.4	123.1	3	C1, C4
3	6.34 (1H, *m*)	145.0	2, 4	C1, C4, C5
4	2.92 (2H, *m*)	36.8	3, 5	C2, C3, C5, C6
5	4.42 (1H, *dd*) *J*=11.6, 5.8	71.8	4, 6	C3, C4, C7
6	6.22 (1H, *dd*) *J*=16.5, 5.8	131.8	5, 7	C4, C5, C8
7	6.58 (1H, *d*) *J*=16.5	130.3	6	C5, C9, C13
1-OH	6.13 (OH, *br s*)	-	-	-
5-OH	5.85 (OH, *br s*)	-	-	-
8	-	136.7	-	-
9		126.6	10	C7
10		128.6	9, 11	C8
11	7.19-7.35 (5H, *m*)	127.6	10, 12	C9, C13
12		128.6	11, 13	C8
13		126.6	12	C7

Table 5.11: ^1H, ^{13}C NMR spectroscopic data (in CDCl$_3$, 400 MHz) of product from alkaline hydrolysis and goniomicin A **147**.

Position	^1H-NMR δ$_H$ (ppm), J (Hz)		^{13}C-NMR δ$_C$ (ppm)	
	Experimental	Literature	Experimental	Literature
1	-	-	170.3	169.6
2	5.93 (1H, *d*) *J*=11.4	5.96 (1H, *d*) *J*=11.9	123.1	125.3
3	6.34 (1H, *m*)	6.12 (1H, *ddd*) *J*=11.9, 8.5, 3.5	145.0	140.6
4	2.92 (2H, *m*)	2.76 (1H, *m*) 2.81 (1H, *m*)	36.8	36.6
5	4.42 (1H, *dd*) *J*=11.6, 5.8	4.41 (1H, *q*) *J*=6.6	71.8	71.5
6	6.22 (1H, *dd*) *J*=16.5, 5.8	6.20 (1H, *dd*) *J*=16.0, 6.6	131.8	131.9
7	6.58 (1H, *d*) *J*=16.5	6.59 (1H, *d*) *J*=16.0	130.3	129.9
8	-	-	136.7	136.7

Table 5.11, continued.

				126.6	126.5
9, 13					
10, 12	7.19-7.35 (5H, *m*)	7.19-7.34 (5H, *m*)		128.6	128.6
11				127.6	127.6
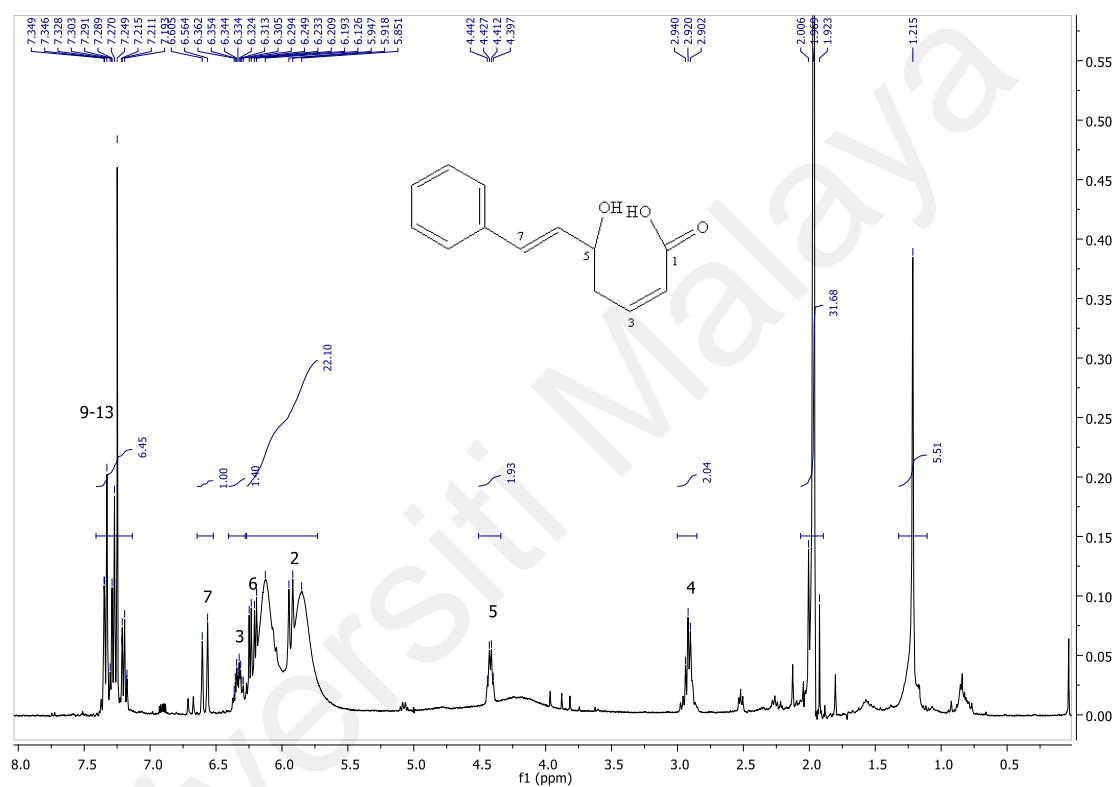
Figure 5.18: ^{1}H NMR spectrum of product from alkaline hydrolysis.
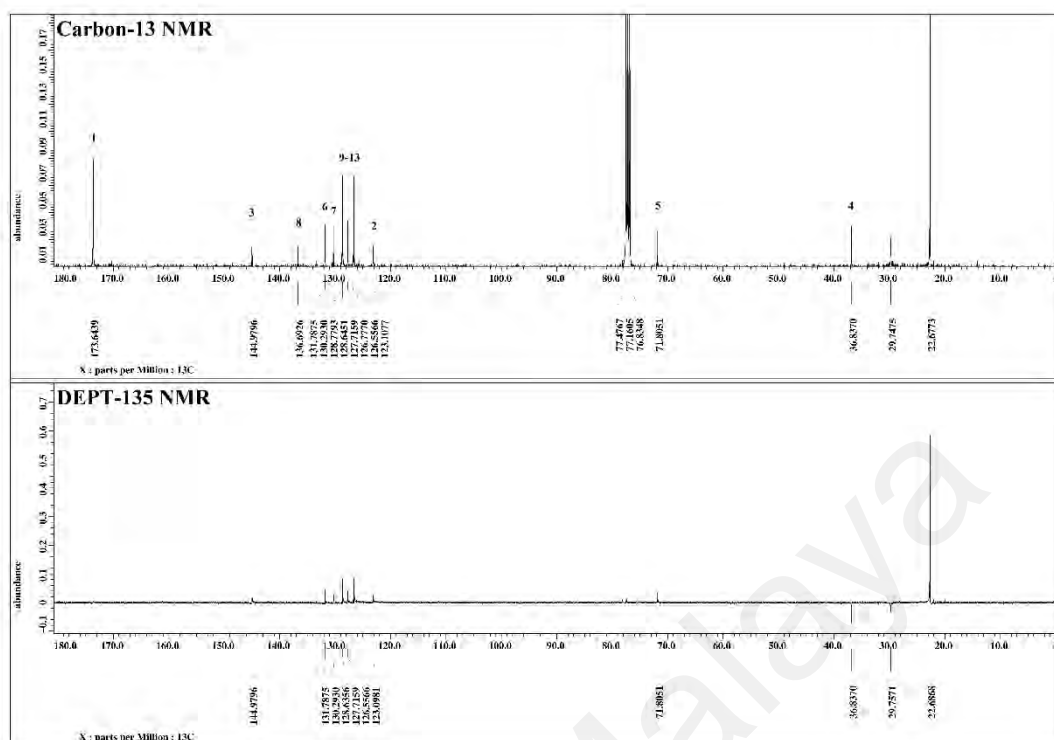
Figure 5.19: ^{13}C and DEPT-135 NMR spectra of product from alkaline hydrolysis.
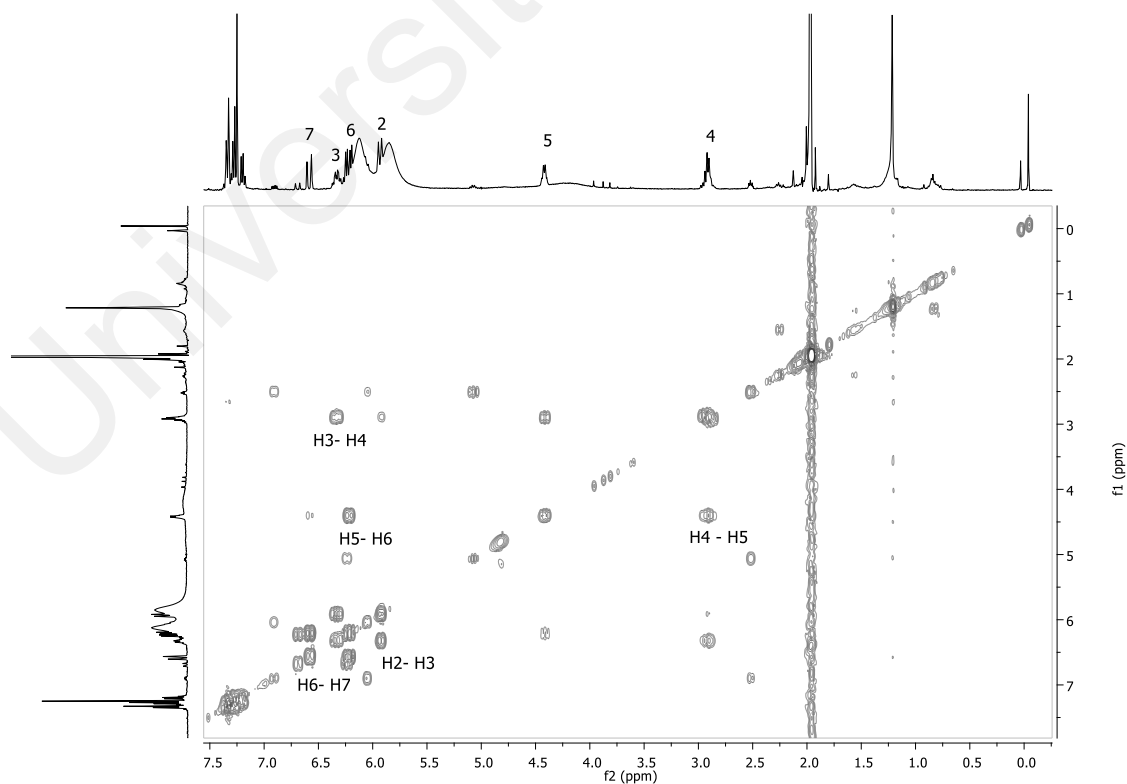
Figure 5.20: COSY spectrum of product from alkaline hydrolysis.
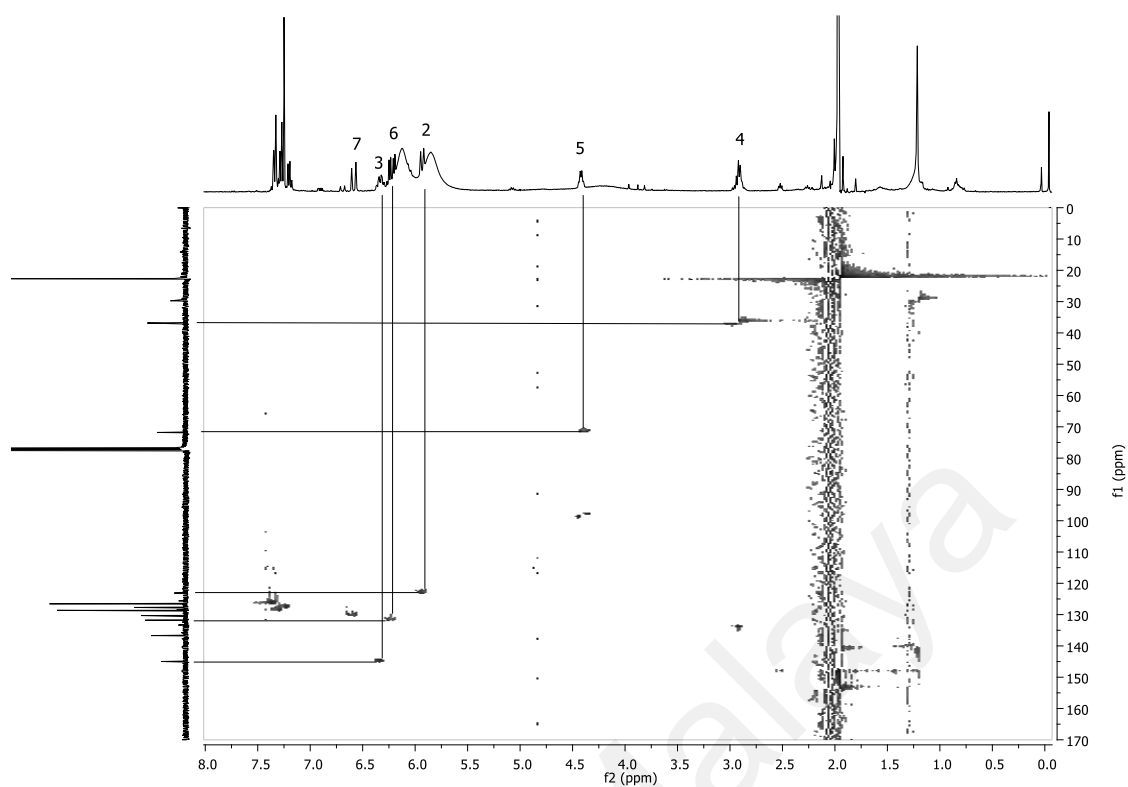
Figure 5.21: HSQC spectrum of product from alkaline hydrolysis.
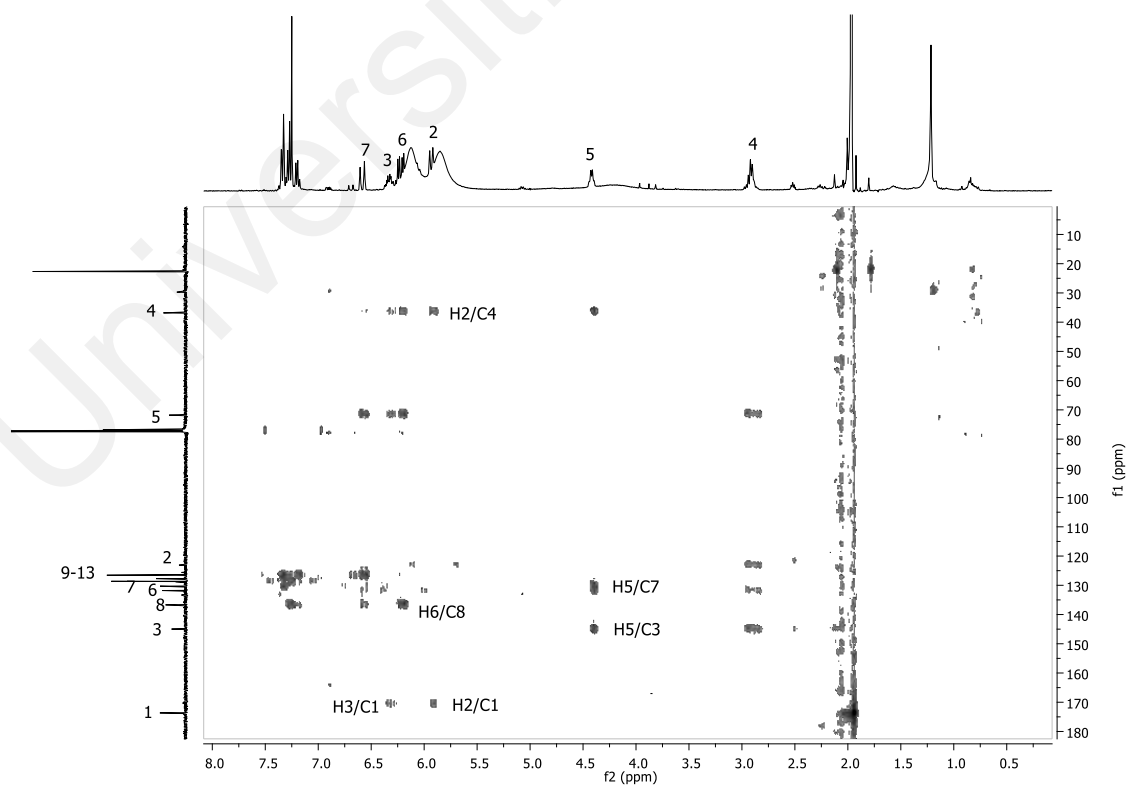
Figure 5.22: HMBC spectrum of product from alkaline hydrolysis.
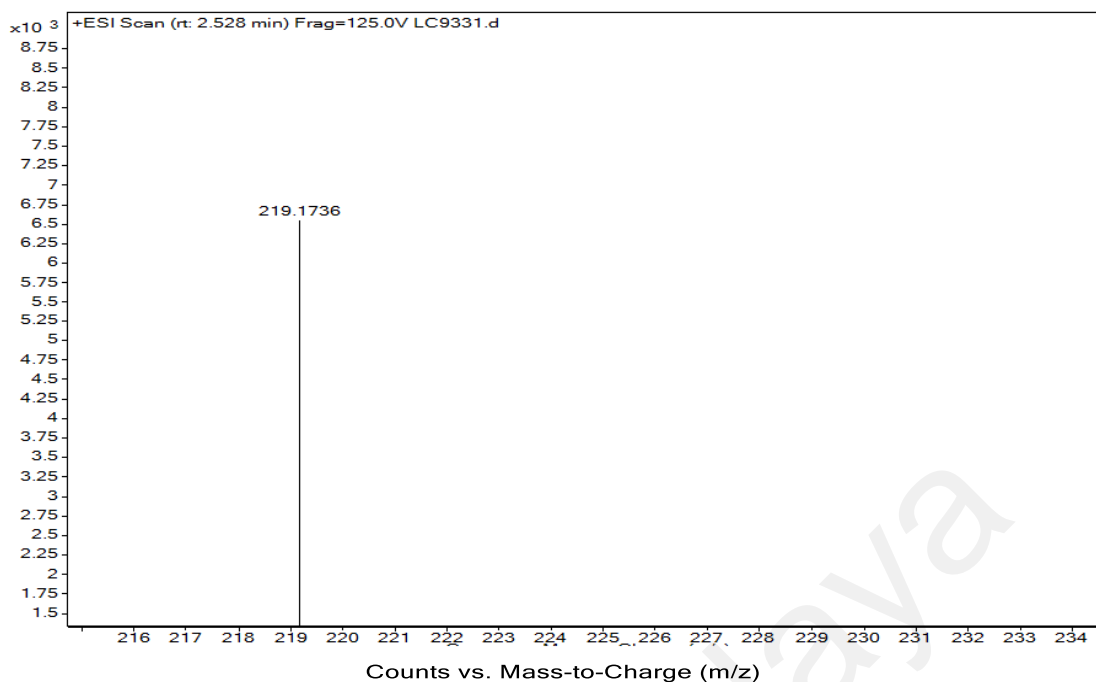
Figure 5.23: LCMS spectrum of product from alkaline hydrolysis.

5.5.1.3 Proposed Reaction Mechanism of Alkaline Hydrolysis

After the identification of the product of alkaline hydrolysis, a tentative pathway was proposed in **Figure 5.24**. In this mechanism, the cleavage of lactone ring occur due to catalysation of hydroxide ions. An intermediate complex is formed, and almost immediately, it react with water, forming the product and hydroxide ions. The necleophilic addition – elimination mechanism at the carbonyl carbon of esters and other related compounds is well-establishes (Jencks, 1969).
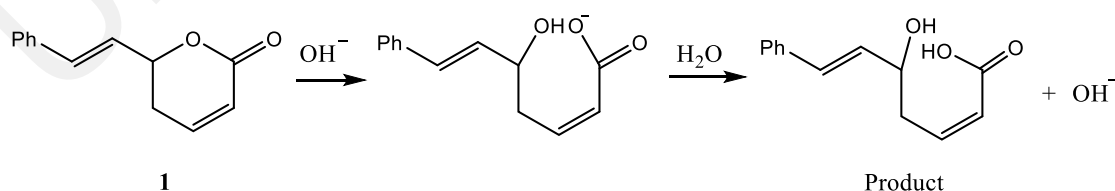
Figure 5.24: Hydroxide ion-catalysed opening of the lactone ring.

Rate determining step is the slowest step of a chemical reaction that determines the rate of overall reactions (Hahn, 1968). The reaction was initiated by binding of hydroxide ions (OH^-) on the carbon of carbonyl group. Subsequently, the electrons pair will move

163

to the oxygen binded to the next carbon, and the bond of C– O is broken (Lajis et al., 1995). The intermediate product will then react with water to form the product **147**.

The reactant **1** is more stable compared to the intermediate complex. Under such condition, hydroxide ion binding on the carbon will be slower step. Therefore, it is proposed that the rate determining step for the alkaline hydrolysis reaction is the step from **1** to convert to the intermediate complex.

The results from UV study is compatible to the proposed product in alkaline study. As the reaction going-on, increasing of UV absorbance at wavelength 230 nm is probably due to the opening of lactone ring.

5.5.2 Product from Acidic Hydrolysis

5.5.2.1 Experimental Details

A reaction is initiated by adding 0.05 M **1** to 2.0 M HCl at 50ºC. The total volume of reaction was kept constant at 40 ml. After allowing the reaction to carry out for reaction period of more than 10 half-lives, the product was extracted by using liquid-liquid (water – ethyl acetate) extraction. The product acquired was then elucidated through NMR spectra analysis. The NMR spectra (^{1}H, ^{13}C, COSY and HMBC) data were summarized in **Table 5.12** and **Table 5.13**.

5.5.2.2 Structural Elucidation of Product Acidic Hydrolysis

Through NMR spectra data analysis, mixture of two products were found in the extract of acidic hydrolysis of **1**. Although these two products appeared as mixture in NMR spectra, but the integration value in 1H NMR spectrum could be used to differentiate the minor and major products. Product 1 was assigned as a minor product, because it have smaller integration value compared to product 2.
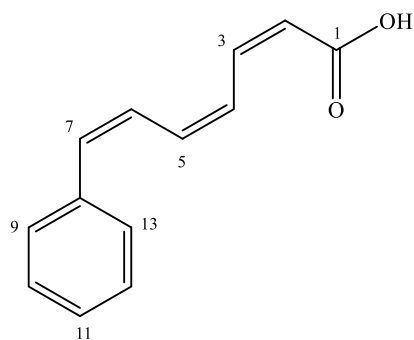
Minor Product (1)   Major Product (2)
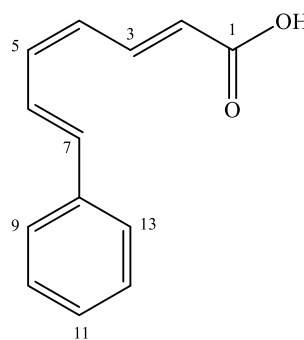
156   **157**

The product was acquired as yellow amorphous. The molecular formula was established as $C_{13}H_{12}O_2$ by LCMS-IT-TOF analysis (**Figure 5.31**), with [M] peak at m/z 200.1229 (calcd. for $C_{13}H_{12}O_2$, 200.1224).

The complete assignments of ^1H NMR and ^{13}C NMR spectroscopic data of both products were achieved with the aid of the HSQC, COSY and HMBC experiments. The peaks of minor product were circled in **Figure 5.25** and those details were summarised in **Table 5.12**. Meanwhile, the peaks of minor product were circled in **Figure 5.26** and the details were summarised in **Table 5.13**.

These two products are diastereomers with different *cis-trans* configuration at double bond C2 and C3. The olefinic protons split into doublet at δ 5.68 have coupling constant of 11.0 Hz. This indicated *cis* configuration of C2 and C3 in minor product **156**. The major product **157** shows *trans* configuration with coupling constant of 15.6 Hz.

Table 5.12: ^{1}H, ^{13}C, COSY and HMBC spectral data of minor product (1) **156** from acidic hydrolysis in CDCl$_3$.

Position	δ_H, J (Hz)	δ_C	COSY	HMBC (H $\rightarrow$ C)
1	-	172.3	-	-
2	5.68 (1H, *d*) *J*=11.0	116.1	3	C-4
3	6.75 (1H, *m*)	146.9	2, 4	C-1
4	6.87 (1H, *dd*) *J*=15.6, 11.0	127.9	3, 5	-
5	6.73 (1H, *m*)	137.4	4, 6	-
6	6.68 (1H, *dd*) *J*=15.4, 11.0	142.8	5, 7	-
7	6.94 (1H, *dd*) *J*=15.4, 11.0	128.6	6	C-8
8	-	136.7	-	-
9		127.0	10	-
10		128.9	9, 11	-
11	7.16-7.35 (5H, *m*)	128.6	10, 12	-
12		128.9	11, 13	-
13		127.0	12	-

Table 5.13: ^{1}H, ^{13}C, COSY and HMBC spectral data of major product (2) **157** from acidic hydrolysis in CDCl$_3$.

Position	δ_H, J (Hz)	δ_C	COSY	HMBC
1	-	171.8	-	-
2	5.91 (1H, *d*) *J*=15.6	119.8	3	C-1, C-4
3	7.45 (1H, *m*)	146.9	2, 4	C-1
4	6.46 (1H, *dd*) *J*=15.1, 11.2	130.0	3, 5	C-2
5	6.77 (1H, *dd*) *J*=11.2, 6.9	137.6	4, 6	-
6	6.75 (1H, *m*)	142.1	-	-
7	7.62 (1H, *dd*) *J*=14.6, 11.9	129.1	6	C-9, C-13
8	-	136.6	-	-
9		127.0	-	-
10		128.9	9, 11	-
11	7.16-7.35 (5H, *m*)	128.7	10, 12	-
12		128.9	11, 13	-
13		127.0	12	-
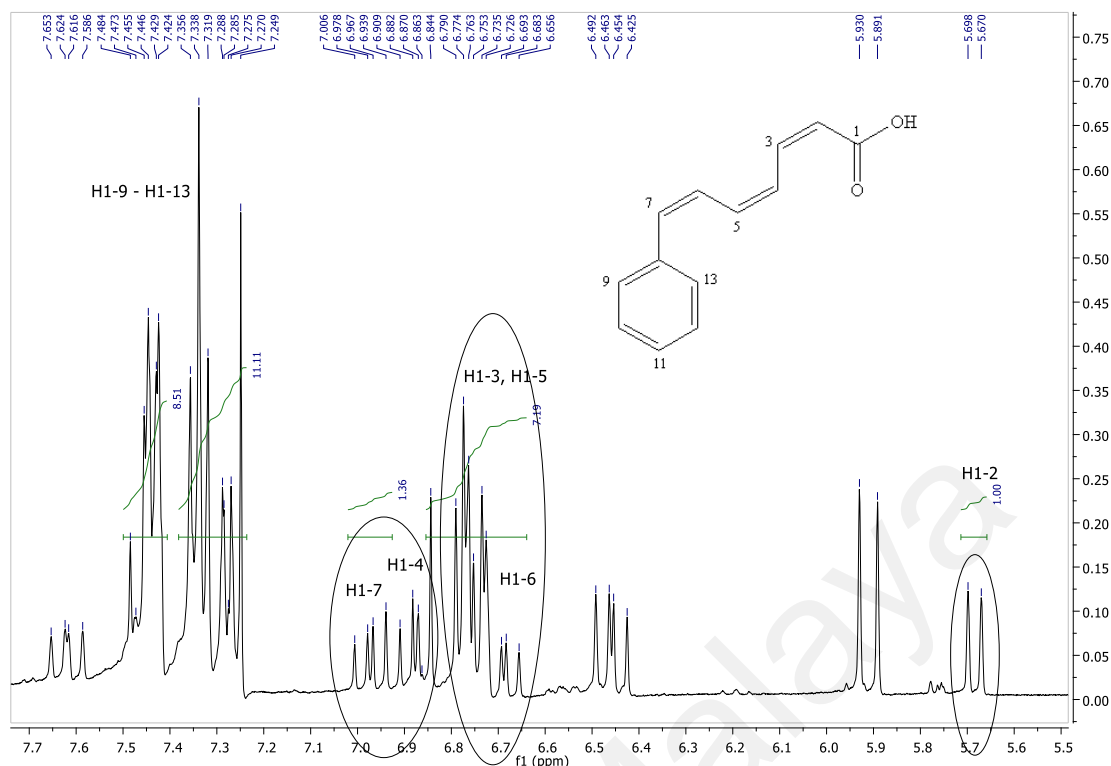
Figure 5.25: ^{1}H NMR spectrum of the two product mixtures. Circles are drawn on the peaks of minor product **156**.
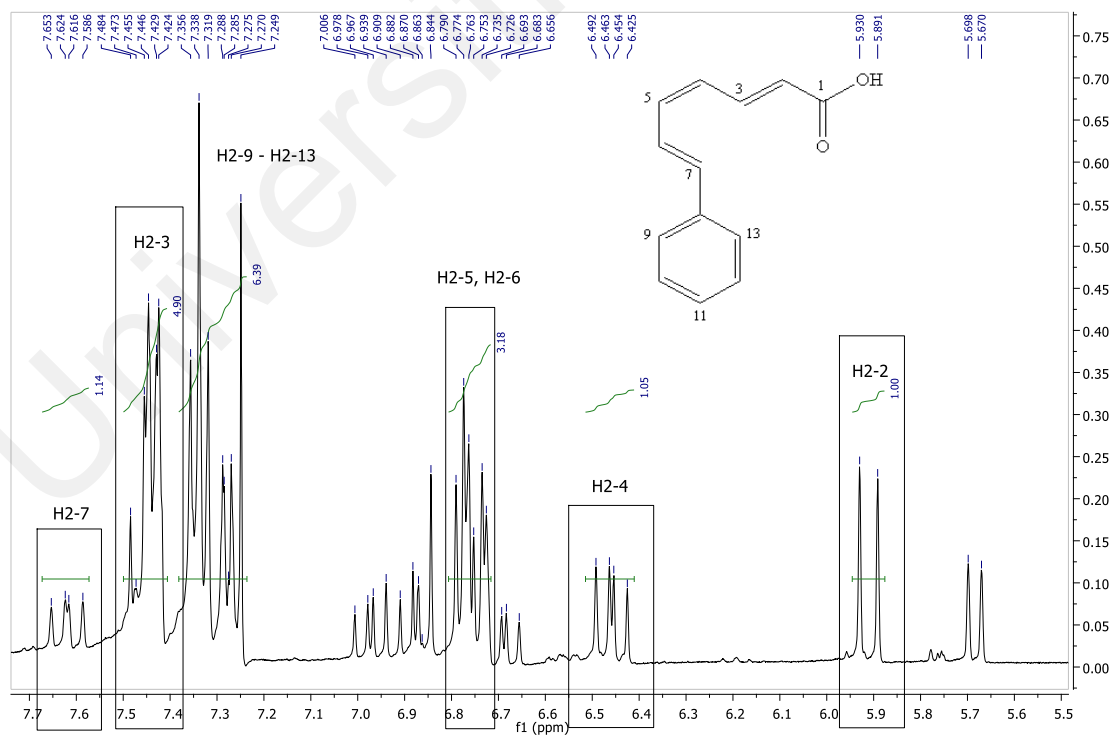
Figure 5.26: ^{1}H NMR spectrum of the two product mixtures. Rectangels are drawn on the peaks of major product **157**.
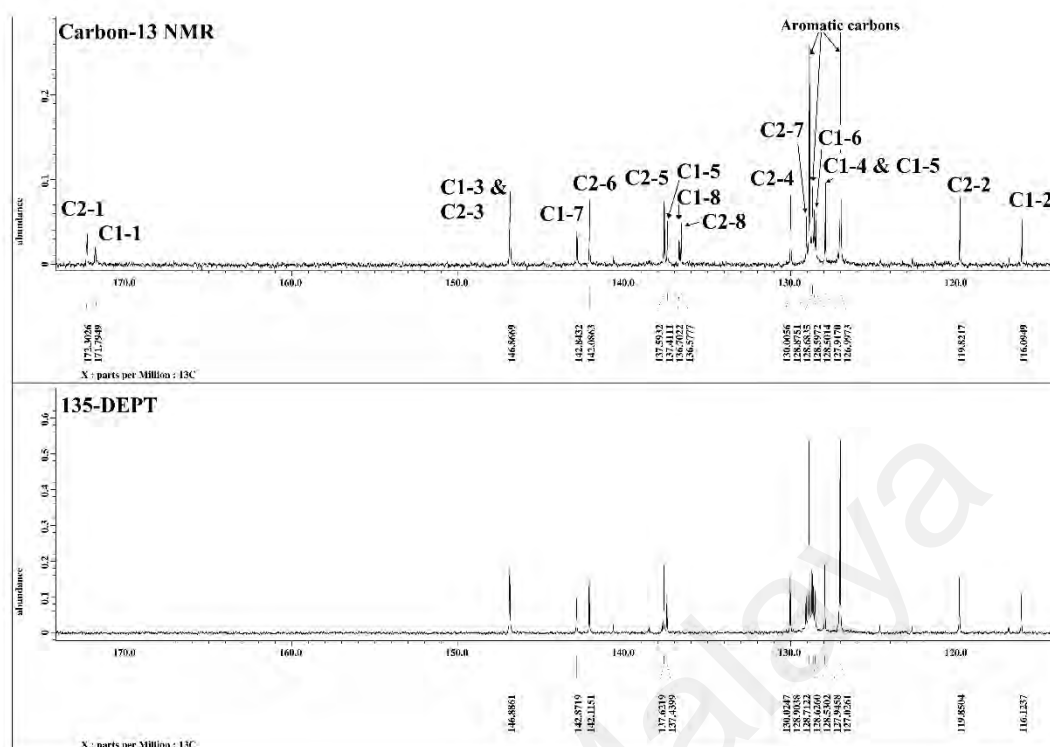
Figure 5.27: ^{13}C and DEPT-135 NMR spectrum of mixture of products from acidic hydrolysis.
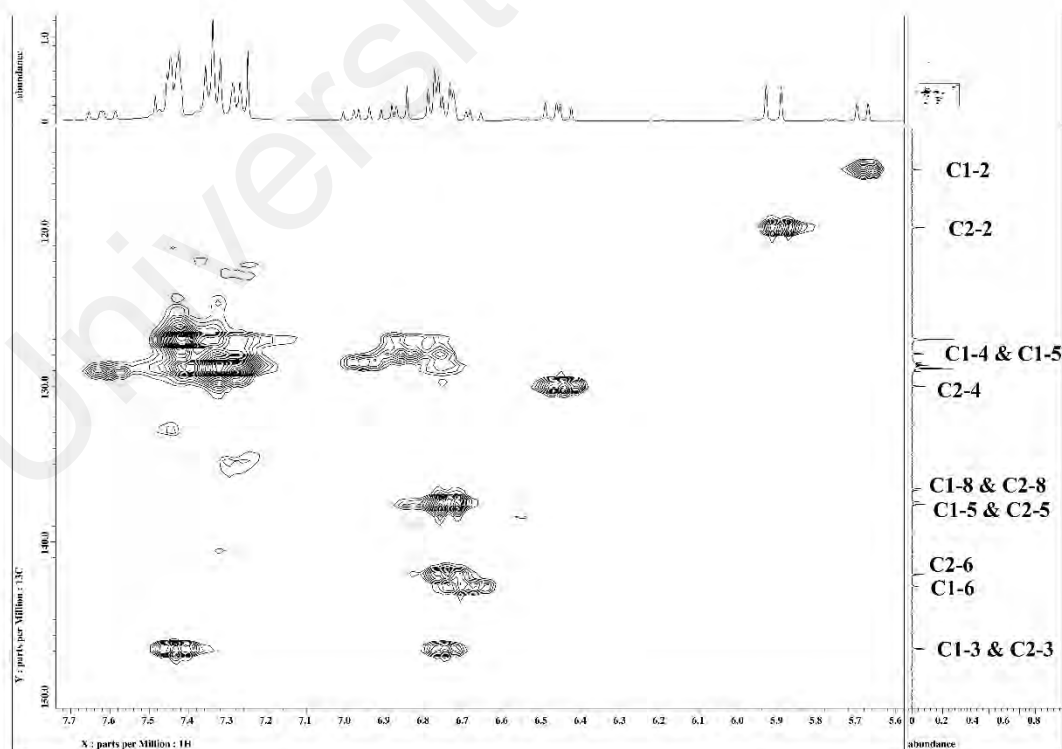
Figure 5.28: HSQC spectrum of products from acidic hydrolysis.

168
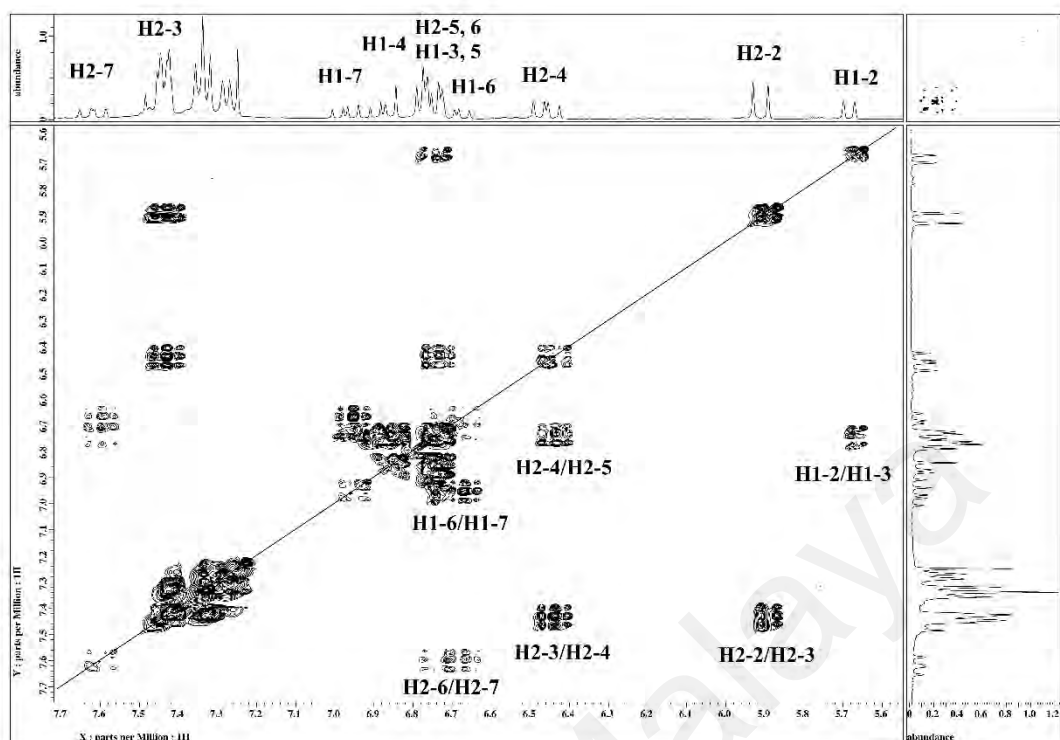
Figure 5.29: COSY spectrum of mixture of products from acidic hydrolysis.
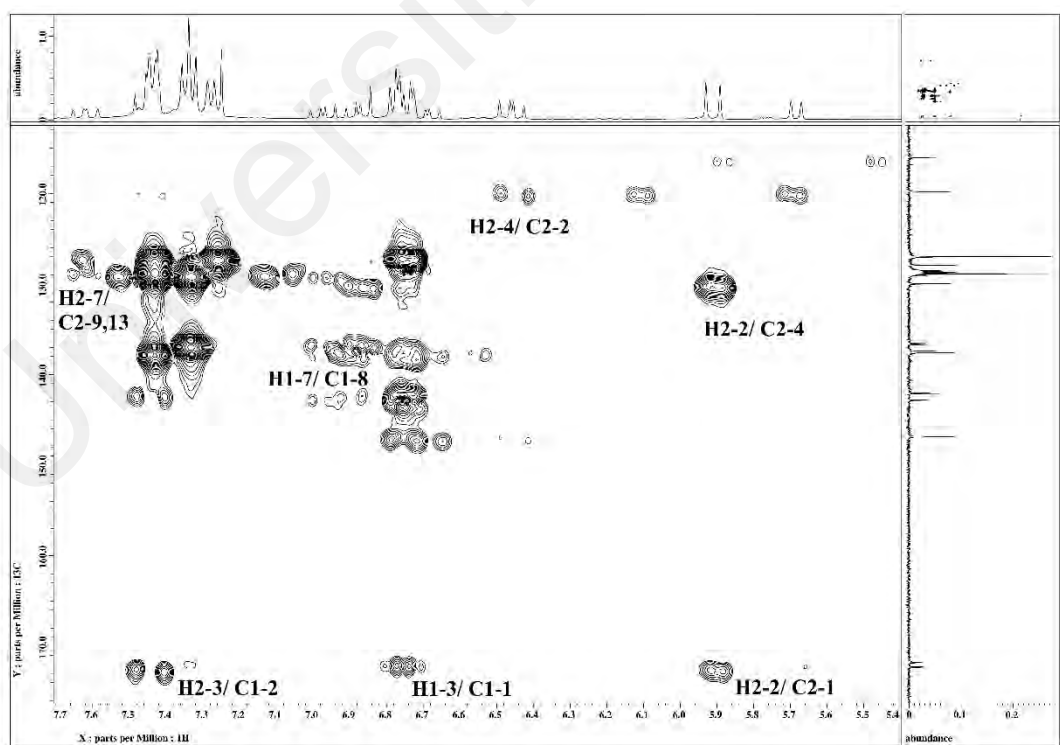
Figure 5.30: HMBC spectrum of mixture of products from acidic hydrolysis.
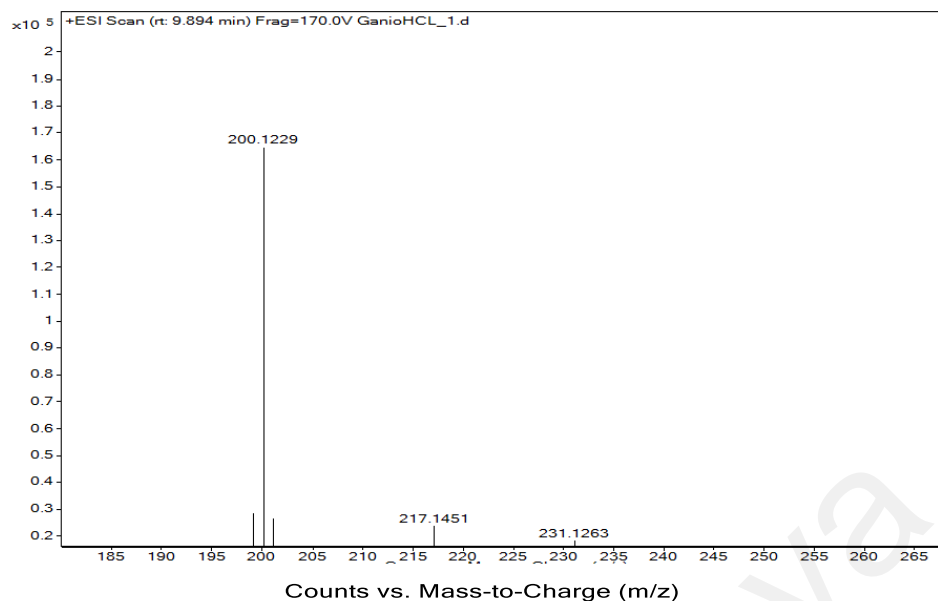
Figure 5.31: LCMS of products from acidic hydrolysis.

5.5.2.3 Proposed Reaction Mechanism of Acidic Hydrolysis

Based on the spectra analysis of the product of acidic hydrolysis of **1**, the mechanism of reaction was proposed as illustrated in **Figure 5.32**. It is suggested that the cleavage of lactone ring occur due to the catalysation of hydroxonium ions. An intermediate product is formed and it react with hydrogen ions and followed by the formation of two diastereomers product.
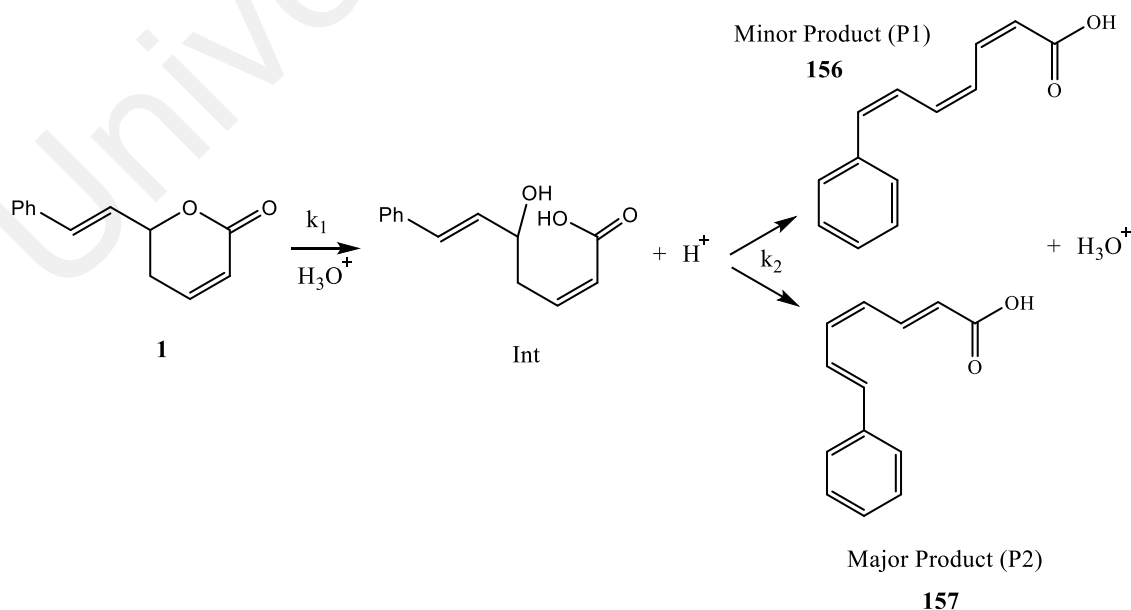
Figure 5.32: Hydronium ion-catalysed opening of the lactone ring and dehydration reaction.

The UV spectra of acidic hydrolysis in **Figure 5.7** shows that UV absorbance appearing at wavelength 350 nm, and keep increasing as reaction going-on. The UV spectrum is compatible with the structure of products formed in acidic hydrolysis. Because the products with three conjugated double bond contribute to UV absorbance at higher wavelength.

5.6   Results and Discussion

The hydrolysis reaction of goniothalamin **1** in alkaline and acidic medium were analysed by spectrophotometric techniques. During alkaline hydrolysis, the UV spectra shows gradual increase at 230 nm, with rate constant of 1.78×10^{-4} s^{-1} at 0.1 M NaOH (80ºC). The rate constant of the reaction obeyed pseudo-first-order kinetics which fitted equation (5.12). **Figure 5.3**, **Figure 5.4** and **Table 5.3** showed that as concentration of NaOH increases, the rate of product formation increases which can be deduced that the rate of cleavage of lactone ring ia also increasing. From the NMR experiments, the structure of product were identified as goniomicin A **147**. Therefore, it is concluded that alkaline hydrolysis exhibits monotonic reaction that involve ring-opening of lactone ring.

However, acidic hydrolysis of **1** is a multi-step reaction (consecutive reaction), as there is an intermediate stage before final product was formed. The UV spectra demonstrated increases of wavelength absorption at 340 nm, followed by decreases in wavelength absorption. Two varied rate constants were obtained from the absorbance data. The first rate constant, k_{1obs}, is the rate of acidic hydrolysis forming intermediate product. This k_{1obs} is was calculated from the increase of absorbance value, and it obeyed pseudo-first-order reaction with rate constant of 0.37×10^{-4} s^{-1} at 0.1 M of HCl (80ºC). While the second rate constant, k_{2obs}, is evaluated from the decrease of absorbance value, when the intermediate product is converting to final product. The k_{2obs} values do not increase or decrease constantly as concentration of HCl increases. Therefore, it is concluded that k_{2obs} (second rate constant) are independent on the concentration of hydrochloric acid.

From the **Figure 5.8**, **Figure 5.9** and **Table 5.6** showed that as concentration of HCl increases, the rate of intermediate complex formation increased which can be deduced that the rate of cleavage of lactone ring also increased. But the rate of dehydration will not be affected by the increase of concentration in HCl.

NMR spectra data analysis showed that final product acquired from acidic hydrolysis of **1** appeared to be diastereomers with *cis-trans* configuration. From the integration data in ^{1}H NMR, it was suggested that minor product **156** have *cis* configuration, while major product **157** have *trans* configuration. Based on the structure of the final product, the probable mechanism of acidic hydrolysis may be shown in **Figure 5.32**. Firstly, the hydronium ion catalyses the opening of lactone ring, and led to formation of intermediate product, goniomicin A **147**. Followed by dehydration and formation of double bond at C-4 and C-5. The results of kinetic study in both alkaline and acidic medium were compatible with the proposed mechanism.

CHAPTER 6 CONCLUSION

Phytochemical analysis on the bark of two species of *Goniothalamus*; *G. tapis* and *G. tapisoides* were carried out. *G. tapis* was collected from Kelantan while *G. tapisoides* was collected from Sarawak.

Chemical investigation of these two plants yielded seventeen compounds including five new styryl-lactones; 3-acetylisoaltholactone **151**, goniomicin E **152**, goniomicin F **153**, goniomicin G **154** and goniomicin H **155**, along with ten known styryl-lactones; goniothalamin **1**, isoaltholactone **41**, cheliensisin A **22**, goniodiol **3**, 7-*epi*-goniodiol **10**, garvensintriol **4**, goniopyyprone **26**, 8-*epi*-9-deoxygoniopypyrone **24**, 7-*epi*-goniofufurone **49** and goniomicin A **147**, as well as two steroids; stigmasterol **133** and β-sitosterol **134**. Previous phytochemical investigation on *G. tapis* collected from Indonesia and Malaysia demonstrated the presence of difference secondary metabolites. Diverse types of compounds such as alkaloids, sesquiterpenes and lignin were reported for *G. tapis* from West Sumatran, Indonesia, however, none were styryl-lactones. Meanwhile, a styryl-lactone was isolated from the leaves and roots of same species collected from Kelantan, Malaysia. Collaterally, the same styryl-lactone appeared to be major compound in the present study, namely isoaltholactone **41**.

Goniothalamin, the major compound isolated from *G. tapisoides,* is recognised as a highly potent compound that provides promising activity against wide range of cancer cell lines. Kinetic spectrophotometric methods is widely used in pharmaceutical analysis. Therefore, this studies were attempted in the move to better understand the mechanism of goniothalamin **1** undergoes hydrolysis in alkaline and acidic medium.

These are the first kinetic spectrophotometric studies examine on the the rate of alkaline and acidic hydrolysis reaction of **1**. Alkaline hydrolysis established a monotonic

reaction with pseudo-first-order rate constant of 1.78×10^{-4} s^{-1}, obtained for kinetic runs carried out at 0.1 M of NaOH and 80°C. As for acidic hydrolysis, it is a consecutive reaction with existence of intermediate product before forming final product. The first rate constant, k_{1obs}, is the rate of acidic hydrolysis forming intermediate product. It obeyed pseudo-first-order reaction with rate constant of 0.37×10^{-4} s^{-1} at 0.1 M of HCl and 80°C. While the second rate constant, k_{2obs}, is evaluated when intermediate was converted to final product. These k_{2obs} values are independent on the concentration of hydrochloric acid. The rate constant of 0.1 M of HCl and 80°C is 2.19×10^{-5} s^{-1}.

Comparing all the rate constants of acidic and alkaline hydrolysis, it reveals the progress of hydroxide ion-catalysed is more rapid than hydronium ion-catalysed. During acidic hydrolysis, the latter part of reaction forming the final product is ten times slower than the initial step.

From the NMR experiments, the products of alkaline hydrolysis was identified as goniomicin A **147**. A mechanism is proposed, suggesting there is a cleavage of lactone ring occur in **1**, forming the product **147**. As for acidic hydrolysis, a mixture of two products appeared in the NMR spectra. From the coupling constant of carbon 2, these two products were identified as diastereomers. The minor product **156** having *trans* configuration while the major product **157** having cis configuration. It was proposed that hydronium ion catalyses the opening of lactone ring, led to formation of intermediate product **147**. Dehydration was then occurred, removal of hydroxyl group turns **147** into final products; **156** and **157** with three consecutive double bond.

The current findings reveals the plausible mechanism and the rate of alkali and acidic hydrolysis for **1**. Therefore, one may suggest to run the kinetic spectrophotometric analysis on others styryl-lactones with cytotoxic activity. In order to uncover the rate and mechanism of chemical reactions on potent drugs.

REFERENCES

Abdullah, A., Zakaria, Z., Ahmad, F. B., Mat-Salleh, K., & Din, L. B. (2009). Chemical constituents from the fruit peel of *Goniothalamus scortechinii*. *Sains Malaysiana, 38*(3), 365-369.

Abdullah, N., Sahibul-Anwar, H., Ideris, S., Hasuda, T., Hitotsuyanagi, Y., Takeya, K., Diederich, M., & Choo, C. (2013). Goniolandrene A and B from *Goniothalamus macrophyllus*. *Fitoterapia, 88C*, 1-6.

Ahmad, F. B., & Din, L. B. (2002). Isolation and characterization of dehydrogoniothalamin from *Goniothalamus umbrosus*. *Indian Journal of Chemistry, Section B: Organic Chemistry Including Medicinal Chemistry, 41B*(7), 1540-1541.

Ahmad, F. B., Jusoh, S., Zakaria, Z., & Din, L. B. (2015). Isolation and characterization of styryllactone of *Goniothalamus ridleyi*. *Sains Malaysiana, 44(3)*, 365-370.

Ahmad, F. B., Moharm, B. A., & Jantan, I. (2010). A comparative study of the constituents of the essential oils of *Goniothalamus tapis* Miq. and *G. tapisoides* Mat Salleh from Borneo. *Journal of Essential Oil Research, 22*(6), 499-502.

Ahmad, F. B., Tukol, W. A., Omar, S., & Sharif, A. M. (1991). 5-Acetylgoniothalamin, a styryldihydropyrone from *Goniothalamus uvaroides*. *Phytochemistry, 30*(7), 2430-2431.

Ajithabai, M. D., Rameshkumar, B., Jayakumar, G., Varma, L., & Nair, M. S. (2011). Molecular and crystal structure of 8-acetoxy goniofufurone from *Goniothalamus wyanaadensis*, Bedd. *Indian Journal of Chemistry, Section B: Organic Chemistry Including Medicinal Chemistry, 50B*(12), 1786-1793.

Alkofahi, A., Ma, W. W., McKenzie, A. T., Byrn, S. R., & McLaughlin, J. L. (1989). Goniotriol from *Goniothalamus giganteus*. *Journal of Natural Products, 52*(6), 1371-1373.

Bermejo, A. (1997). *Aislamiento, Sintesis y Actividad Farmacologica de Estiril-lactonas de Goniothalamus arvensis. Bencilisoquinoleinas y Aporfinas da Xylopia papuana.* (Ph.D. Thesis), University of Valencia, Spain.

Bermejo, A., Blazquez, M. A., Rao, K. S., & Cortes, D. (1998). Styryl-pyrones from *Goniothalamus arvensis*. *Phytochemistry, 47*(7), 1375-1380.

Bermejo, A., Blázquez, M. A., Rao, K. S., & Cortes, D. (1999). Styryl-lactones from the stem bark of *Goniothalamus arvensis*. *Phytochemical Analysis, 10*(3), 127-131.

Bermejo, A., Blázquez, M. A., Serrano, A., Zafra-Polo, M. C., & Cortes, D. (1997). Preparation of 7-Alkoxylated Furanopyrones: Semisynthesis of (−)-Etharvensin, a New Styryl-Lactone from *Goniothalamus arvensis*. *Journal of Natural Products, 60*(12), 1338-1340.

Bermejo, A., Lora, M. J., Blazquez, M. A., Rao, K. S., Cortes, D., & Zafra-Polo, M. C. (1995). (+)-Goniotharvensin, a novel styryl-lactone from the stem bark of *Goniothalamus arvensis*. *Natural Product Letters, 7*(2), 117-122.

Bin Din, L., Colegate, S. M., & Razak, D. A. (1990). Scorazanone, a 1-aza-anthraquinone from *Goniothalamus scortechinii*. *Phytochemistry, 29*(1), 346-348.

Blazquez, M. A., Bermejo, A., Zafra-Polo, M. C., & Cortes, D. (1999). Styryl-lactones from *Goniothalamus* species-a review. *Phytochemical Analysis, 10*(4), 161-170.

Bourgaud, F., Gravot, A., Milesi, S., & Gontier, E. (2001). Production of plant secondary metabolites: a historical perspective. *Plant Science, 161*(5), 839-851.

Cao, S. G., Wu, X. H., Sim, K. Y., Tan, B. K. H., Pereira, J. T., & Goh, S. H. (1998). Styryl-lactone derivatives and alkaloids from *Goniothalamus borneensis* (Annonaceae). *Tetrahedron, 54*(10), 2143-2148.

Chatrou, L. W., Pirie, M. D., Erkens, R. H. J., Couvreur, T. L. P., Neubig, K. M., Abbott, J. R., Mols, J. B., Maas, J. W., Saunders, R. M. K., & Chase, M. W. (2012). A new subfamilial and tribal classification of the pantropical flowering plant family Annonaceae informed by molecular phylogenetics. *Botanical Journal of the Linnean Society, 169*(1), 5-40.

Chaturvedula, V. S. P., & Prakash, I. (2012). Isolation of stigmasterol and *β*-sitosterol from the dichloromethane extract of *Rubus suavissimus*. *International Current Pharmaceutical Journal, 1*(9), 239-242.

Chen, R., Yu, D., Ma, L., Wu, F., & Song, W. (1998). The chemical constituents of *Goniothalamus howii* Merr. *Yao Xue Xue Bao, 33*(6), 453-456.

Chen, S. B., & Yu, J. G. (1999). The chemical constituents in the stem of *Goniothalamus griffithii*. *Zhiwu Xuebao, 41*(3), 330-333.

Chen, W. C. (1995). The Geographical Distribution of The Annonaceae. *Journal of Tropical and Subtropical Botany, 3*(2), 19-35.

Chiu, C. C., Liu, P. L., Huang, K. J., Wang, H. M., Chang, K. F., Chou, C. K., Chang, F. R., Chong, I. W., Fang, K., Chen, J. S., Chang, H. W., & Wu, Y. C. (2011). Goniothalamin inhibits growth of human lung cancer cells through DNA damage, apoptosis, and reduced migration ability. *Journal of Agricultural and Food Chemistry, 59*(8), 4288-4293.

Colegate, S. M., Din, L. B., Latiff, A., Salleh, K. M., Samsudin, M. W., Skelton, B. W., Tadano, K., White, A. H., & Zakaria, Z. (1990). (+)-Isoaltholactone: a furanopyrone isolated from *Goniothalamus* species. *Phytochemistry, 29*(5), 1701-1704.

Cragg, G. M., Kingston, D. G. I., & Newman, D. J. (2005) *Anticancer Agents from Natural Products, Second Edition*: CRC Press, Taylor & Francis Group.

de Fatima, A., Kohn, L. K., Antonio, M. A., de Carvalho, J. E., & Pilli, R. A. (2005). (R)-Goniothalamin: total syntheses and cytotoxic activity against cancer cell lines. *Bioorganic & Medicinal Chemistry, 13*(8), 2927-2933.

de Fatima, A., Modolo, L. V., Conegero, L. S., Pilli, R. A., Ferreira, C. V., Kohn, L. K., & de Carvalho, J. E. (2006). Styryl lactones and their derivatives: biological activities, mechanisms of action and potential leads for drug design. *Current Medicinal Chemistry, 13*(28), 3371-3384.

Demain, A. L., & Fang, A. (2000). The natural functions of secondary metabolites. *History of Modern Biotechnology I* (pp. 1-39): Springer.

Demain, A. L., & Vaishnav, P. (2011). Natural products for cancer chemotherapy. *Microbial Biotechnology, 4*(6), 687-699.

Denisov, E. T., Sarkisov, O. M., & Likhtenshteĭn, G. I. (2003). *Chemical Kinetics: Fundamentals and New Developments*: Elsevier.

Duc, L. V., Thanh, T. B., Thanh, H. N., & Tien, V. N. (2016). Chemical constituents and cytotoxic effect from the barks of *Goniothalamus chinensis* Merr. & Chun. growing in Vietnam. *Journal of Applied Pharmaceutical Science, 6*(4), 1-5.

Ee, G. C. L. (1998). Larvicidal principles from *Goniothalamus velutinus* (Annonacea). *Oriental Journal of Chemistry, 14*(1), 41-46.

Ee, G. C. L., Chew, L. P., Sukari, M. A., & Rahmani, M. (1999). Sesquiterpenes and styryl-lactones from *Goniothalamus ridleyi* (Annonaceae). *Oriental Journal of Chemistry, 15*(2), 233-236.

Ee, G. C. L., Ng, K. N., Rahmani, M., & Taufiq-Yap, Y. H. (2001). Larvicidal flavanone and sesquiterpenes from *Goniothalamus macrophyllus* (Annonaceae). *Asian Journal of Chemistry, 13*(2), 550-554.

Ee, G. C. L., Pang, Y. S., Rahmani, M., & Taufig-Yap, Y. H. (2000). Bioactive styryllactones from *Goniothalamus tapis*. *Research Journal of Chemistry and Environment, 4*(3), 7-9.

Efdi, M., Fujita, S., Inuzuka, T., & Koketsu, M. (2010). Chemical studies on *Goniothalamus tapis* Miq. *Natural Product Research, 24*(7), 657-662.

El-Zayat, A. A. E., Ferrigni, N. R., McCloud, T. G., McKenzie, A. T., Byrn, S. R., Cassady, J. M., Chang, C.-j., & McLaughlin, J. L. (1985). Goniothalenol: a novel, bioactive, tetrahydrofurano-2-pyrone from *Goniothalamus giganteus* (Annonaceae). *Tetrahedron Letters, 26*(8), 955-956.

Fang, X.-P., Anderson, J. E., Chang, C.-J., McLaughlin, J. L., & Fanwick, P. E. (1991). Two New Styryl Lactones, 9-Deoxygoniopypyrone and 7-epi-Goniofufurone, from *Goniothalamus giganteus*. *Journal of Natural Products, 54*(4), 1034-1043.

Fang, X. P., Anderson, J. E., Chang, C. J., Fanwick, P. E., & McLaughlin, J. L. (1990). Novel bioactive styryl-lactones: goniofufurone, goniopypyrone, and 8-acetylgoniotriol from *Goniothalamus giganteus* (Annonaceae). X-ray molecular

structure of goniofufurone and of goniopypyrone. *Journal of Chemical Society, Perkin Transactions 1*(6), 1655-1661.

Fang, X. P., Anderson, J. E., Chang, C. J., & McLaughlin, J. L. (1991a). Three new bioactive styryllactones from *Goniothalamus giganteus* (Annonaceae). *Tetrahedron, 47*(47), 9751-9758.

Fang, X. P., Anderson, J. E., Chang, C. J., McLaughlin, J. L., & Fanwick, P. E. (1991b). Two new styryl lactones, 9-deoxygoniopypyrone and 7-epi-goniofufurone, from *Goniothalamus giganteus*. *Journal of Natural Products, 54*(4), 1034-1043.

Fang, X. P., Anderson, J. E., Qiu, X. X., Kozlowski, J. F., Chang, C. J., & McLaughlin, J. L. (1993). Gonioheptolides A and B: novel eight-membered-ring lactones from *Goniothalamus giganteus* (Annonaceae). *Tetrahedron, 49*(8), 1563-1570.

Fun, H. K., Chantrapromma, S., Prawat, U., Boonnak, N., & Razak, I. A. (2012). 8-*O*-Acetyl-8-*epi*-9-deoxygoniopypyrone. *Acta Crystallographica Section E: Structure Reports Online, 68*(Pt 4), 1072-1073.

Goh, S. H., Ee, G. C. L., Chuah, C. H., & Mak, T. C. W. (1995). 5*β*-Hydroxygoniothalamin, a styrylpyrone derivative from *Goniothalamus dolichocarpus* (Annonaceae). *Natural Product Letters, 5*(4), 255-259.

Gordaliza, M. (2009). Terpenyl-Purines from the Sea. *Marine Drugs, 7*(4), 833.

Guo, Y.-X., Xiu, Z.-L., Zhang, D.-J., Wang, H., Wang, L.-X., & Xiao, H.-B. (2007). Kinetics and mechanism of degradation of lithospermic acid B in aqueous solution. *Journal of Pharmaceutical and Biomedical Analysis, 43*(4), 1249-1255.

Gurib-Fakim, A. (2006). Medicinal plants: traditions of yesterday and drugs of tomorrow. *Molecular Aspects of Medicine, 27*(1), 1-93.

Hahn, H. H. S., W. (1968). Kinetics of coagualtion with hydrolyzed Al (III): the rate determining step. *Journal of Colloid and Interface Science, 28*, 134-144.

Harikumar, B., Varghese, H. T., Panicker, C. Y., & Jayakumar, G. (2008). Vibrational spectroscopic studies and ab initio calculations of Goniothalamin, a natural

product. *Spectrochimica Acta Part A: Molecular and Biomolecular Spectroscopy, 71*(2), 731-738.

Hasan, C. M., Hussain, M. A., Mia, M. Y., & Rashid, M. A. (1995). Goniothalamin from *Goniothalamus sesquipedalis*. *Fitoterapia, 66*(4), 378-379.

Hasan, C. M., Mia, M. Y., Rashid, M. A., & Connolly, J. D. (1994). 5-Acetoxyisogoniothalamin oxide, an epoxystyryl lactone from *Goniothalamus sesquipedalis*. *Phytochemistry, 37*(6), 1763-1764.

Hisham, A., Harassi, A., Shuaily, W., Echigo, S., & Fujimoto, Y. (2000). Cardiopetalolactone: a novel styryllactone from *Goniothalamus cardiopetalus*. *Tetrahedron, 56*(51), 9985-9989.

Hisham, A., Toubi, M., Shuaily, W., Bai, M. D., & Fujimoto, Y. (2003). Cardiobutanolide, a styryllactone from *Goniothalamus cardiopetalus*. *Phytochemistry, 62*(4), 597-600.

Hlubucek, J., & Robertson, A. (1967). (+)-(5S)-δ-Lactone of 5-hydroxy-7-phenylhepta-2,6-dienoic acid, a natural product from *Cryptocarya caloneura* (Scheff.) Kostermans. *Australian Journal of Chemistry, 20*(10), 2199-2206.

Holland, H. D. (1997). Evidence for life on Earth more than 3850 million years ago. *Science, 275*(5296), 38-39.

Hu, Z. B., Liao, S. X., Mao, S. L., & Zhu, H. P. (2000). Structural elucidation of gonioffithine I from *Goniothalamus griffithii* Hook.f.et Thoms. *Yaoxue Xuebao, 35*(4), 277-278.

Izaddin, S., Ee, G., & Rahmani, M. (2008). Bioactive compound from *Goniothalamus andersonii*. *Proceeding International Seminar on Chemistry 2008,* 495-497.

Jaidee, W., Andersen, R. J., Patrick, B. O., Pyne, S. G., Muanprasat, C., Borwornpinyo, S., & Laphookhieo, S. (2019). Alkaloids and styryllactones from *Goniothalamus cheliensis*. *Phytochemistry, 157*, 8-20.

Jencks, W. P. (1969). *Catalysis in Chemistry and Enzymology*: McGraw-Hill.

Jewers, K., Davis, J. B., Dougan, J., Manchanda, A. H., Blunden, G., Kyi, A., & Wetchapinan, S. (1972). Goniothalamin and its distribution in four *Goniothalamus* species. *Phytochemistry, 11*(6), 2025-2030.

Jiang, M. M., Feng, Y. F., Gao, H., Zhang, X., Tang, J. S., & Yao, X. S. (2011). Three new bis-styryllactones from *Goniothalamus cheliensis*. *Fitoterapia, 82*(4), 524-527.

Jiang, M. M., Feng, Y. F., Zhang, X., Dai, Y., & Yao, X. S. (2011). Chemical constituents from the roots of *Goniothalamus cheliensis*. *Chinese Traditional and Herbal Drugs, 42*(2), 214-216.

Jiang, M. M., Feng, Y. F., Zhang, X., & Yao, X. S. (2011). Chemical constituents from roots of *Goniothalamus cheliensis* (II). *Zhongcaoyao, 42*(12), 2386-2388.

Jiang, M. M., Zhang, X., Dai, Y., Gao, H., Liu, H. W., Wang, N. L., Ye, W. C., & Yao, X. S. (2008). Alkaloids from the root barks of *Goniothalamus cheliensis*. *Chinese Chemical Letters, 19*(3), 302-304.

Kabir, K. E., Khan, A. R., & Mosaddik, M. A. (2003). Goniothalamin: A potent mosquito larvicide from *Bryonopsis laciniosa* L. *Journal of Applied Entomology, 127*(2), 112-115.

Kampong, R., Pompimon, W., Meepowpan, P., Sukdee, S., Sombutsiri, P., Nantasaen, N., & Krachodnok, S. (2013). (-)-7-O-Acetylgoniodiol as cancer chemopreventive agent from *Goniothalamus griffithii*. *International Journal of Chemical Sciences, 11*(3), 1234-1246.

Khan, M. R., Komine, K., & Kamano, Y. (1998). (+)-Isoaltholactone from the leaves of *Goniothalamus grandiflorus*. *Fitoterapia, 69*(3), 279.

Kim, R. P. T., Bihud, V., Bin Mohamad, K., Leong, K. H., Bin Mohamad, J., Bin Ahmad, F., Hazni, H., Kasim, N., Halim, S. N., & Awang, K. (2012). Cytotoxic and antioxidant compounds from the stem bark of *Goniothalamus tapisoides* Mat Salleh. *Molecules, 18*(1), 128-139.

Krause, J., & Tobin, G. (2013). *Discovery, Development, and Regulation of Natural Products*.

Kumaraswamy, G., & Satish Kumar, R. (2013). Highly Diastereoselective Total Syntheses of (+)-7-Epigoniodiol, (−)-8-Epigoniodiol, and (+)-9-Deoxygoniopypyrone. *Helvetica Chimica Acta, 96*(7), 1366-1375.

Lajis, N. H., Khan, M. N., & Noor, H. M. (1995). Kinetics and mechanism of the alkaline hydrolysis of securinine. *Journal of Pharmaceutical Sciences, 84*(1), 126-130.

Lan, Y. H., Chang, F. R., Yang, Y. L., & Wu, Y. C. (2006). New constituents from stems of *Goniothalamus amuyon*. *Chemical and Pharmaceutical Bulletin (Tokyo), 54*(7), 1040-1043.

Lan, Y. H., Chang, F. R., Yu, J. H., Yang, Y. L., Chang, Y. L., Lee, S. J., & Wu, Y. C. (2003). Cytotoxic styrylpyrones from *Goniothalamus amuyon*. *Journal of Natural Products, 66*(4), 487-490.

Lekphrom, R., Kanokmedhakul, S., & Kanokmedhakul, K. (2009). Bioactive styryllactones and alkaloid from flowers of *Goniothalamus laoticus*. *Journal of Ethnopharmacology, 125*(1), 47-50.

Levrier, C., Balastrier, M., Beattie, K. D., Carroll, A. R., Martin, F., Choomuenwai, V., & Davis, R. A. (2013). Pyridocoumarin, aristolactam and aporphine alkaloids from the Australian rainforest plant *Goniothalamus australis*. *Phytochemistry, 86*, 121-126.

Li, C. M., Liu, Z. L., Mu, Q., Sun, H. D., Zheng, H. L., & Tao, G. D. (1997). Studies on chemical constituents from leaves of *Goniothalamus griffithii*. *Yunnan Zhiwu Yanjiu, 19*(3), 321-323.

Li, C. M., Mu, Q., Sun, H. D., Xu, B., Tang, W. D., Zheng, H. L., & Tao, G. D. (1998). A new anti-cancer constituent of *Goniothalamus cheliensis*. *Acta Botanica Yunnanica, 20*(1), 102-104.

Likhitwitayawuid, K., Klongsiriwet, C., Jongbunprasert, V., Sritularak, B., & Wongseripipatana, S. (2006). Flavones with free radical scavenging activity from *Goniothalamus tenuifolius*. *Archives of Pharmacal Research, 29*(3), 199-202.

Likhitwitayawuid, K., Wirasathien, L., Jongboonprasert, V., Krungkrai, J., Aimi, N., Takayama, H., & Kitajima, M. (1997). Antimalarial alkaloids from

Goniothalamus tenuifolius. *Pharmaceutical and Pharmacological Letters, 7*(2/3), 99-102.

Limpipatwattana, Y., & Khumkratok, S. (2008). Chemical constituents from the stems of *Goniothalamus laoticus*. *Biochemical Systematics and Ecology, 36*(10), 3-3.

Loder, J. W., & Nearn, R. H. (1977). Altholactone, a novel tetrahydrofuro [3,2b] pyran-5-one from a *Polyalthia* species (Annonaceae). *Heterocycles, 7*, 113-118.

Macabeo, A. P. G., Lopez, A. D. A., Schmidt, S., Heilmann, J., Dahse, H.-M., Alejandro, G. J. D., & Franzblau, S. G. (2014). Antitubercular and cytotoxic constituents from *Goniothalamus gitingensis*. *Records of Natural Products, 8*(1), 41-45.

Mahiwan, C., Buayairaksa, M., Nuntasaen, N., Meepowpan, P., & Pompimon, W. (2013). Potential cancer chemopreventive activity of styryllactones from *Goniothalamus marcanii*. *American Journal of Applied Sciences, 10*(1), 112-116.

Martins, C. V. B., de Resende, M. A., da Silva, D. L., Magalhães, T. F. F., Modolo, L. V., Pilli, R. A., & de Fátima, Â. (2009). In vitro studies of anticandidal activity of goniothalamin enantiomers. *Journal of Applied Microbiology, 107*(4), 1279-1286.

McChesney, J. D., Venkataraman, S. K., & Henri, J. T. (2007). Plant natural products: Back to the future or into extinction? *Phytochemistry, 68*(14), 2015-2022.

Mendelsohn, R., & Balick, M. J. (1995). The value of undiscovered pharmaceuticals in tropical forests. *Economic Botany, 49*(2), 223-228.

Mosaddik, M. A., & Haque, M. E. (2003). Cytotoxicity and antimicrobial activity of goniothalamin isolated from *Bryonopsis laciniosa*. *Phytotherapy Research, 17*(10), 1155-1157.

Mu, Q., He, Y. N., Tang, W. D., Li, C. M., Lou, L. G., Sun, H. D., Xu, B., Yang, G. X., & Hu, C. Q. (2004). A styrylpyrone dimer from the bark of *Goniothalamus leiocarpus*. *Chinese Chemical Letters, 15*(2), 191-193.

Mu, Q., Tang, W., Li, C., Lu, Y., Sun, H., Zheng, H., Hao, X., Zheng, Q., Wu, N., & Lou, L. (1999). Four new styryllactones from *Goniothalamus leiocarpus*. *Heterocycles, 51*(12), 2969-2976.

Mu, Q., Tang, W. D., Liu, R. Y., Li, C. M., Lou, L. G., Sun, H. D., & Hu, C. Q. (2003). Constituents from the stems of *Goniothalamus griffithii*. *Planta Medica, 69*(9), 826-830.

National Policy on Biological Diversity. (1998).

Newman, D. J., Cragg, G. M., & Snader, K. M. (2003). Natural products as sources of new drugs over the period 1981-2002. *Journal of Natural Products, 66*(7), 1022-1037.

Omar, S., Chee, C. L., Ahmad, F., Ni, J. X., Jaber, H., Huang, J., & Nakatsu, T. (1992). Phenanthrene lactams from *Goniothalamus velutinus*. *Phytochemistry, 31*(12), 4395-4397.

Ong, H. C., Faezah, A. W., & Milow, P. (2012). Medicinal Plants Used by the Jah Hut Orang Asli at Kampung Pos Penderas, Pahang, Malaysia. *Studies on Ethno Medicine, 6*(1), 11-15.

Pan, S.-Y., Zhou, S.-F., Gao, S.-H., Yu, Z.-L., Zhang, S.-F., Tang, M.-K., Sun, J.-N., Ma, D.-L., Han, Y.-F., Fong, W.-F., & Ko, K.-M. (2013). New Perspectives on How to Discover Drugs from Herbal Medicines: CAM's Outstanding Contribution to Modern Therapeutics. *Evidence-Based Complementary and Alternative Medicine,2013,* Article#627375.

Peris, E., Estornell, E., Cabedo, N., Cortes, D., & Bermejo, A. (2000). 3-acetylaltholactone and related styryl-lactones, mitochondrial respiratory chain inhibitors. *Phytochemistry, 54*(3), 311-315.

Prawat, U., Chaimanee, S., Butsuri, A., Salae, A.-W., & Tuntiwachwuttikul, P. (2012). Bioactive styryllactones, two new naphthoquinones and one new styryllactone, and other constituents from *Goniothalamus scortechinii*. *Phytochemistry Letters, 5*(3), 529-534.

Rasol, N. E., Ahmad, F. B., Lim, X.-Y., Chung, F. F.-L., Leong, C.-O., Mai, C.-W., Bihud, N. V., Zaki, H. M., & Ismail, N. H. (2018). Cytotoxic lactam and naphthoquinone alkaloids from roots of *Goniothalamus lanceolatus* Miq. *Phytochemistry Letters, 24*, 51-55.

Rout, S. P., Choudary, K. A., Kar, D. M., Das, L., & Jain, A. (2009 July-Sep). Plants in Traditional Medicinal System-Future Source of New Drugs. *International Journal of Pharmacy and Pharmaceutical Sciences, 1*(1).

Sajise, P. E., Ticsay, M. V., & Saguiguit, G. C. J. (2010). Moving Forward: Southeast Asian Perspectives on Climate Change and Biodiversity.

Sam, T. W., Chew, S. Y., Matsjeh, S., Gan, E. K., Razak, D., & Mohamed, A. L. (1987). Goniothalamin oxide: an embryotoxic compound from *Goniothalamus macrophyllus* (Annonaceae). *Tetrahedron Letters, 28*(22), 2541-2544.

Saunders, R. M. K. (2002). The genus *Goniothalamus* (Annonaceae) in Sumatra. *Botanical Journal of the Linnean Society, 139*(3), 225-254.

Saunders, R. M. K. (2003). A synopsis of *Goniothalamus* species (Annonaceae) in Peninsular Malaysia, with a description of a new species. *Botanical Journal of the Linnean Society, 142*(3), 321-339.

Schwartsmann, G. (2000). Marine organisms and other novel natural sources of new cancer drugs. *Annals of Oncology, 11 Suppl 3*, 235-243.

Seidel, V., Bailleul, F., & Waterman, P. G. (2000). (Rel)-1beta,2alpha-di-(2,4-dihydroxy-6-methoxybenzoyl)-3beta, 4alpha-di-(4-methoxyphenyl)-cyclobutane and other flavonoids from the aerial parts of *Goniothalamus gardneri* and *Goniothalamus thwaitesii*. *Phytochemistry, 55*(5), 439-446.

Senthil-Nathan, S., Choi, M.-Y., Paik, C.-H., & Kalaivani, K. (2008). The toxicity and physiological effect of goniothalamin, a styryl-pyrone, on the generalist herbivore, *Spodoptera exigua* Huebner. *Chemosphere, 72*(9), 1393-1400.

Seyed, M. A., Jantan, I., & Bukhari, S. N. A. (2014). Emerging Anticancer Potentials of Goniothalamin and Its Molecular Mechanisms. *BioMed Research International, 2014*, 10.

Siddig Ibrahim, A.-W., Ahmad Bustamam, A., Fong, H., Syam, M., Manal Mohamed, E., Adel Sharaf, A.-Z., & Mariod, A. A. (2009). Antimicrobial and free radical scavenging activities of the dichloromethane extract of *Goniothalamus umbrosus*. *International Journal of Tropical Medicine, 4*(1), 32-36.

Smith, E., & Dent, G. (2005). Modern Raman Spectroscopy–A Practical Approach.

Soonthornchareonnon, N., Suwanborirux, K., Bavovada, R., Patarapanich, C., & Cassady, J. M. (1999). New cytotoxic 1-azaanthraquinones and 3-aminonaphthoquinone from the stem bark of *Goniothalamus marcanii*. *Journal of Natural Products, 62*(10), 1390-1394.

Suchaichit, N., Kanokmedhakul, K., Panthama, N., Poopasit, K., Moosophon, P., & Kanokmedhakul, S. (2015). A 2H-tetrahydropyran derivative and bioactive constituents from the bark of *Goniothalamus elegants* Ast. *Fitoterapia, 103*, Ahead of Print.

Tai, B. H., Huyen, V. T., Huong, T. T., Nhiem, N. X., Choi, E. M., Kim, J. A., Long, P. Q., Cuong, N. M., & Kim, Y. H. (2010). New pyrano-pyrone from *Goniothalamus tamirensis* enhances the proliferation and differentiation of osteoblastic MC3T3-E1 cells. *Chemical and Pharmaceutical Bulletin (Tokyo), 58*(4), 521-525.

Talapatra, S. K., Basu, D., Chattopadhyay, P., & Talapatra, B. (1988). Aristololactams of *Goniothalamus sesquipedalis* Wall. Revised structures of the 2-oxygenated aristololactams. *Phytochemistry, 27*(3), 903-906.

Talapatra, S. K., Basu, K., & Goswami, T. D. (1985). Structure and stereochemistry of four new 5,6-dihydro-2-pyrones from *Goniothalamus sesquipedalis* and *Goniothalamus griffithii*. *Indian Journal of Chemistry, 24B*, 29-34.

Tanaka, S., Yoichi, S., Ao, L., Matumoto, M., Morimoto, K., Akimoto, N., Honda, G., Tabata, M., Oshima, T., Masuda, T., bin Asmawi, M. Z., Ismail, Z., Yusof, S. M., Din, L. B., & Said, I. M. (2001). Potential immunosuppressive and antiinflammatory activities of Malaysian medicinal plants characterized by reduced cell surface expression of cell adhesion molecules. *Phytotherapy Research, 15*(8), 681-686.

Tantithanaporn, S., Wattanapiromsakul, C., Itharat, A., & Keawpradub, N. (2011). Cytotoxic activity of acetogenins and styryl lactones isolated from *Goniothalamus undulatus* Ridl. root extracts against a lung cancer cell line (COR-L23). *Phytomedicine, 18*(6), 486-490.

Tian, Z., Chen, S., Zhang, Y., Huang, M., Shi, L., Huang, F., Fong, C., Yang, M., & Xiao, P. (2006). The cytotoxicity of naturally occurring styryl lactones. *Phytomedicine, 13*(3), 181-186.

Tip-pyang, S., Limpipatwattana, Y., Khumkratok, S., Siripong, P., & Sichaem, J. (2010). A new cytotoxic 1-azaanthraquinone from the stems of *Goniothalamus laoticus*. *Fitoterapia, 81*(7), 894-896.

Tran, D. T., Mai, H. D. T., Pham, V. C., Nguyen, V. H., Litaudon, M., Guéritte, F., Nguyen, Q. V., Tran, T. A., & Chau, V. M. (2013). Alkaloids and styryllactones from the leaves of *Goniothalamus tamirensis*. *Phytochemistry Letters, 6*(1), 79-83.

Trieu, Q. H., Mai, H. D., Pham, V. C., Litaudon, M., Gueritte, F., Retailleau, P., Schmitz-Afonso, I., Gimello, O., Nguyen, V. H., & Chau, V. M. (2014). Styryllactones and acetogenins from the fruits of *Goniothalamus macrocalyx*. *Natural Product Communications, 9*(4), 495-498.

Tulp, M., & Bohlin, L. (2005). Rediscovery of known natural compounds: Nuisance or goldmine? *Bioorganic & Medicinal Chemistry, 13*(17), 5274-5282.

Verdine, G. L. (1996). The combinatorial chemistry of nature. *Nature (London), 384*(6604, Suppl.), 11-13.

Wach, J. Y., Guttinger, S., Kutay, U., & Gademann, K. (2010). The cytotoxic styryl lactone goniothalamin is an inhibitor of nucleocytoplasmic transport. *Bioorganic & Medicinal Chemistry Letters, 20*(9), 2843-2846.

Wang, S., Dai, S. J., Chen, R. Y., Yu, S. S., & Yu, D. Q. (2003). Two New Styryllactones from *Goniothalamus cheliensis*. *Chinese Chemical Letters, 14*(5), 487-488.

Wang, S., Zhang, P. C., Chen, R. Y., & Yu, D. Q. (2001). Two new compounds from *Goniothalamus cheliensis* Hu. *Chinese Chemical Letters, 12*(9), 787-790.

Wang, S., Zhang, Y. J., Chen, R. Y., & Yu, D. Q. (2002). Goniolactones A-F, six new styrylpyrone derivatives from the roots of *Goniothalamus cheliensis*. *Journal of Natural Products, 65*(6), 835-841.

Wiart, C. (2007). *Goniothalamus* species: a source of drugs for the treatment of cancers and bacterial infections? *Evidence-Based Complementary and Alternative Medicine, 4*(3), 299-311.

Wu, Y. C., Chang, F. R., Duh, C. Y., Wang, S. K., & Wu, T. S. (1992). Cytotoxic styrylpyrones of *Goniothalamus amuyon*. *Phytochemistry, 31*(8), 2851-2853.

Wu, Y. C., Duh, C. Y., Chang, F. R., Chang, G. Y., Wang, S. K., Chang, J. J., McPhail, D. R., McPhail, A. T., & Lee, K. H. (1991). The crystal structure and cytotoxicity of goniodiol-7-monoacetate from *Goniothalamus amuyon*. *Journal of Natural Products, 54*(4), 1077-1081.

Zahari, A., Ablat, A., Omer, N., Nafiah, M. A., Sivasothy, Y., Mohamad, J., Khan, M. N., & Awang, K. (2016). Ultraviolet-visible study on acid-base equilibria of aporphine alkaloids with antiplasmodial and antioxidant activities from *Alseodaphne corneri* and *Dehaasia longipedicellata*. *Scientific Reports, 6*, Article#21517.

Zakaria, Z., Din, L. B., Ahmad, F. B., San, C. H., & Mat-Salleh, K. (2002). Styrylpyrone derivatives from *Goniothalamus kinabaluensis* (Annonaceae). *ACGC Chemical Research Communications, 15*, 72-77.

Zhang, L., & Demain, A. L. (2005). *Natural Products: Drug Discovery and Therapeutic Medicine*: Humana Press.

Zhang, L. L., Yang, R. Z., & Wu, X. J. (1993). Chemical compositions of *Goniothalamus howii* (I). *Zhiwu Xuebao, 35*(5), 390-396.

Zhang, Y. J., Kong, M., Chen, R. Y., & Yu, D. Q. (1998). New alkaloids from the rhizomes of *Goniothalamus griffithii*. *Chinese Chemical Letters, 9*(11), 1029-1032.

Zhang, Y. J., Kong, M., Chen, R. Y., & Yu, D. Q. (1999). Alkaloids from the roots of *Goniothalamus griffithii*. *Journal of Natural Products, 62*(7), 1050-1052.

Zhang, Y. J., Zhou, G. X., Chen, R. Y., & Yu, D. Q. (1999). Styryllactones from the rhizomes of *Goniothalamus griffithii*. *Journal of Asian Natural Products Research, 1*(3), 189-197.

Zhong, L., Li, C. M., Hao, X. J., & Lou, L. G. (2005). Induction of leukemia cell apoptosis by cheliensisin A involves down-regulation of Bcl-2 expression. *Acta Pharmacologica Sinica, 26*(5), 623-628.

Zhu, G. J., Yu, J. G., Luo, X. Z., Sun, L., Li, D. Y., & Yang, S. L. (2000). Alkaloids from leaves of *Goniothalamus cheliensis*. *Zhongcaoyao, 31*(11), 813-814.

Zhu, J. X., Yu, D. L., Huang, W. H., Sun, L., Lv, Y., Zheng, Q. T., Lee, K. H., & Yu, J. G. (2012). Goniodilactone and gonioheptenolactone, two novel cytotoxic styryllactones from the leaves of *Goniothalamus cheliensis*. *Chinese Chemical Letters, 23*(5), 583-586.

Zhu, J. X., Yu, J. G., Sun, L., Li, S. J., & Huang, W. H. (2006). Styryllactones in leaves of *Goniothalamus cheliensis*. *Zhongguo Tianran Yaowu, 4*(2), 91-93.